ORAL DELIVERY OF PROTEIN ANTIGENS TO ATLANTIC SALMON

Thesis submitted for the degree of

Doctor of Philosophy

at the University College London

by

Goran Klaric

Department of Mechanical Engineering

University College London

December 2015

Declaration

I Goran Klaric confirm that the work presented in this thesis is my own. Where information has been derived from other sources, I confirm that this has been indicated in the thesis.

17. December 2015

_____ _____

Signature **Date**

Abstract

During recent years, the use of functional ingredients in aquaculture industry has increased dramatically. Accordingly, there are a broad range of functional feeds available for use in fish farming. As a result, there is ongoing research which focuses on developing oral delivery systems for fish. Variety of products can be incorporated into alginate matrices to avoid damage from the low pH and proteolytic enzymes encountered in the digestive tract of fish. However, there has been very little research reported on the effectiveness of those oral delivery systems with respect to performance within fish feed and fish. Furthermore, the reported particle sizes used within alginate delivery systems require further reduction to be suitable for effective association within feed pellets. Additionally, it is essential that active compounds are released at the right place in fish.

In this study, encapsulation technology capable of providing an economical and high throughput method for producing fine alginate beads (≤10 μm) was assessed. Post-coating examination with the micro-tomography (micro-CT) equipment confirmed the presence of alginate particles inside the pellet in large numbers. According to our observations in an enzyme assay, the active compounds are released at the most favourable site in Atlantic salmon which is the distal intestine. There is also evidence to suggest that alginate-encapsulated protein antigens when released in the intestine are capable of crossing the intestinal epithelial layer. Similarly, in the assessment of intraperitoneal priming/oral boosting strategy against infectious pancreatic necrosis (IPN), alginate-encapsulated IPN antigens boosted immune

response in salmon. This could be seen in significant up-regulation of relevant genes measured by quantitative PCR and specific antibody response detected in an ELISA assay.

The results of these investigative studies significantly improve understanding of the issues regarding incorporation of delivery systems into fish feed in the current manufacturing process leading to a novel approach for functionalizing fish feed.

Keywords

Aerodynamically assisted jetting, alginate, antigen uptake, Atlantic salmon dissolution test, electro-spraying, encapsulation efficiency, encapsulation, feed extrusion, fish feed, immune response, IPNV antigen, oral vaccine and vacuum coating.

Acknowledgements

This study is supported by joint grant from Norwegian Research Council and EWOS Innovation AS (grant number: 202089/O30), as a part of industrial PhD programme.

First and foremost, I would like to thank all employee of EWOS Innovation who provided me with useful and helpful assistance. I am especially thankful to Elisabeth Eie for her help in conducting fish trials as well as Joar U. Horpestad and his staff with in the lead for producing all experimental fish feed. A very special recognition needs to be given to Dr Kari Ruohonen for his contribution in statistical analysis. I would also like to acknowledge Dr Stephen Mutoliki and Lihan Chan from Norwegian School of Veterinary Science (Oslo) for their outstanding ELISA and qPCR work. I owe my deepest gratitude to my mentor at EWOS Innovation, Dr Simon Wadsworth for his guidance and input throughout the process of this research.

Finally, I would like to express my sincere gratitude to my supervisor Dr Suwan Jayasinghe (UCL) for his support, encouragement and motivation during this project.

Contents

List of Figures

List of Tables

List of Equations

Abbreviations

AAJ	Aerodynamically assisted jetting
APAEJ	Air pressure-assisted energised jetting
API	Active pharmaceutical ingredient
AROC	Average rate of change
Ba-alginate	Barium alginate
BD	Blue dextran
BD-Ca-alg	Calcium alginate beads loaded with blue dextran
BD-EDA-alg	Ethylenediammonium alginate beads loaded with blue dextran
BCS	Biopharmaceutics Classification System
BP	Base pellet
Ca-alginate	Calcium alginate
CAP	Cellulose acetate phthalates
CCD	Central composite design
CG	Cardiogreen
CF	Control feed
CI	Confidence interval
CMS	Cardiomyopathy Syndrome
DC	Direct current
DI	Deionized water
DS	Daily serving
DSP	Disodium phosphate
EA	Encapsulated antigen

EC	Encapsulated control
EE	Encapsulation efficiency
EDA·2H_2O	Ethylenediamine dihydrochloride
EDA	Ethylenediammonium dication
EDA-alg	Ethylenediammonium alginate
EFI	EWOS feed index
EncForm	Encapsulation formulation
Encap 1	Calcium alginate beads loaded with IPNV antigen
Encap 2	Ethylenediammonium alginate beads loaded with IPNV antigen
ELISA	Enzyme-linked immunosorbent assay
FAO	Food and Agriculture Organization of the United Nations
FCR	Feed conversion ratio
FDA	U.S. Food and Drug Administration
FITC	Fluorescein isothiocyanate
FW	Fish weight
G	Guluronic acid
GI	Gastrointestinal
HPLC	High-performance liquid chromatography
HRP-Ca-alg	Calcium alginate beads loaded with horseradish peroxidase
HRP-EDA-alg	Ethylenediammonium alginate beads loaded with horseradish peroxidase
HRP	Horseradish peroxidase

HSMI	Heart and skeleton muscle inflammation
ID	Inner diameter
IHN	Infectious hematopoietic necrosis
i.p.	Intraperitoneal injection
IPN	Infectious pancreatic necrosis
IPNV	Infectious pancreatic necrosis virus
IR|	Immediate release
ISA	Infectious salmon anaemia
IVIVC	*In vitro-in vivo* correlation
KPH	Potassium hydrogen phthalate
LRT	Likelihood ratio test
LoQ	Limit of quantification
M	Mannuronic acid
MAA	Methacrylates
Micro-CT	Micro-computed tomography
MM	MicroMatrix®
MMA	Methyl methacrylates
MSP	Monosodium phosphate
Na-alginate	Sodium alginate
OB	Oral boost
OBF	Oral boost feeds
NMR	Nuclear magnetic resonance
NSS	Not statistically significant
OD	Optical density
PBS	Phosphate-buffered saline

PD	Pancreas disease
p.i.	Post intubation
PLG	Polylactide-co-glycolide
qPCR	Quantitative real-time polymerase chain reaction
QTL	Quantitative trait loci
ROC	Rate of change
RNA	Ribonucleic acid
RPS	Relative survival
SEM	Scanning electron microscope
SFR	Specific feeding rate
SGR	Specific growth rate
SODF	Solid oral dosage forms
SME	Specific mechanical energy
SMZ	Stereo microscope zoom
$TCID_{50}$	50% Tissue culture infective dose
TMB	3,3’,5,5’-Tetramethylbenzidine substrate
UA	Un-encapsulated antigen
UC	Un-encapsulated control
Unencap	Un-encapsulated/free IPNV antigen
USP	United States Pharmacopoeia
VP	Viral protein
XlinkSol	cross-linking solutions

Chapter One: General Introduction

1.1 Lay summary

Intensification of aquaculture has led to an increasing frequency of outbreaks of infectious viral disease, resulting in high economic losses and fish mortality. Infectious Pancreatic Necrosis (IPN) emerged as a very important disease with large impact on salmon production in the European Union and Norway. It is primarily an acute, clinical disease in young salmonid fish. The IPN virus is a good model virus to work with because of being very well characterised and understood while other viruses are less well documented. Equally, the experience and technology acquired working with IPN could easily be applied to other viral disease.

The common scientific view in aquaculture is that some viral vaccines are not effective enough in the field and may not exert sufficient long-lasting protective effects. For this reason, there is a growing demand from fish farmers for an effective oral vaccine against the viral diseases. At present there are few, if any, effective oral vaccines in the market.

For sensitive antigens, various delivery options involving polymeric coatings and encapsulation are being evaluated and tested. These various options involve synthetic and naturally occurring polymers such as alginate. The advantages of using natural polymers include their low cost, biocompatibility and aqueous solubility.

Despite the fact that an extensive research on alginate is going on, there are several factors that remain to be explored before adopting alginates as an

oral delivery system for viral antigens to salmonid fish. For instance, many oral vaccines have been found ineffective as a result of insufficient uptake of antigen due to degradation in the digestive tract. Furthermore, size of alginate beads needs further reduction in order to be suitable for an effective incorporation into fish feed pellets. At the same time, there are no scientific reports about assessing *in vitro* release of macromolecular drugs from alginates at test conditions relevant for A. salmon. Similarly, very few studies provide evidence of macromolecular drug release in the intestinal region of salmonid fish. Currently unexplored as well is the ability of alginate to protect protein antigens throughout the entire fish feed production process.

The aforementioned issues are addressed in four chapters (Ch. 3, 4, 5 and 6) of this thesis. Thus, Chapter 3 deals with the uptake of IPNV antigen and the ability of antigen to immunise salmon. Chapter 4 addresses issues related to the release from alginate matrices. Size of alginate microbeads was adapted for better integration with fish feed in Chapter 5. Ultimately, stability of antigens in fish feed production process was assessed in Chapter 6.

Before modifying and improving, exploring the full potential of IPNV antigen with frequently tested alginate technology was the most sensible assessment to start with. Hence, the assessment of uptake and immunogenicity of IPNV antigen were selected as the initial trails (Chapter 3). Previous to these trails, adverse effects and efficiency of the encapsulation method were studied (Section 3.2). It was necessary to check whether the encapsulation process (electrospraying) was damaging to the antigen. Additionally, the encapsulation efficiency of IPNV antigen in alginate matrix/microbeads had to be determined. This was necessary to know for determining the

concentration of antigen in microbeads as accurately as possible. These two experiments are described in Section 3.2.1 while Section 3.2.2 presents the results and Section 3.5 discusses them. In fact, all results obtained in Chapter 3 are discussed in Section 3.5.

In the next instance, the uptake of free antigen was compared to the uptake of encapsulated antigen (Section 3.3). The encapsulated antigen was entrapped in calcium alginate matrix. The uptake study, which was carried out by oral intubation, is described in Section 3.3.1 while Section 3.3.2 presents the results.

In the final instance, the ability of both encapsulated and free antigen to immunise A. salmon was investigated in a feeding study (Section 3.4). In this study, ethylenediammonium alginate was introduced as a novel oral delivery system for fish. The immune response study by feeding is described in Section 3.4.1 while Section 3.4.2 presents the results.

To develop a fast-dissolving and temperature-independent oral delivery system within the temperature range of seawater in which A. salmon habituate, a series of dissolution tests were conducted. Firstly, it was necessary to determine encapsulation efficiency of blue dextran which served as a model compound in the dissolution testing. Secondly, it was also necessary to develop a new dissolution test. The new test was required to be more representative for the mechanisms of alginate disintegration in the gastrointestinal tract of A. salmon. Dissolution testing is described and the results are discussed in Section 4.2.

To check whether the *in vitro* dissolution tests are consistent with the actual release from alginate matrices in fish, two *in vivo* tests were carried out. The first *in vivo* experiment was performed with the aim of visualising dissolution of alginate microbeads loaded with cardiogreen by an *in vivo* imagining technique. The second *in vivo* experiment was conducted with the purpose of localising the site where most of the release from alginate matrices occurred. The first trial is detailed in Section 4.3 while the second trial is elaborated in Section 4.4.

After all, the main vehicle for an oral delivery system intended for farmed fish is the feed pellet. Fish feed pellets are extruded in a process which involves high temperature, pressure and shear force. Optionally, alginate microbeads can be incorporated into feed pellets before extrusion in a vacuum coater and after extrusion in a meal mixer. Thus, Chapter 5 deals with the issues related to the post-extrusion addition, while the pre-extrusion addition is addressed in Chapter 6. The main problem related to the post-extrusion addition is the low ability of microbeads to fuse with the feed pellets. This issue is linked to the size of pellet pores along with the size of microbeads.

For this reason, the feed pellet pores were characterised by mercury intrusion porosimetry and scanning electron microscopy. In addition, feed pellets, which were infused with alginate microbeads in a vacuum coater, were scanned by micro–computed tomography. These experiments are described in Section 5.2 while Section 5.2.2 presents and discuss the results.

Nevertheless, it was preferred to further reduce the size of microbeads. Therefore, the encapsulation process, namely air pressure-assisted

energised jetting (APAEJ) was optimised to produce the smallest attainable alginate microbeads. This experiment is described in Section 5.3 while the results are presented and discussed in its subsections.

Finally, the morphology of the obtained alginate microbeads were characterised by using an imaging particle analysis system in Section 5.4. The results were discussed as they were presented in Section 5.4.2. At the end, an overall conclusion for Chapter 5 was drawn in Section 5.5.

The major issue related to the pre-extrusion addition is the survival of protein antigens throughout the fish feed production process. In order to learn whether IPNV antigen is able to get undamaged through an entire feed production process, a stability test was performed in Chapter 6. The test is described in Section 6.2 while the results are discussed in Section 6.3.

Chapter 7 concludes the thesis. It discusses the major findings, provides guidelines for future directions and draws a general conclusion

1.2 General overview

In the mid-60s Norwegian fish farmers started cultivating Atlantic salmon (*Salmo salar*) (Tilseth et al., 1991). The growth of the industry has been particularly rapid from 1980 onwards (Liu et al., 2011). Since then, salmon aquaculture has experienced remarkable growth. In slightly less than 30 years, global salmon production increased from 5,288 tonnes in 1980 to more than 1.7 million tonnes in 2012 with a farm gate value of over $ 7 billion. Norway dominates this production, accounting for 60% by volume and 50% by value (FAO, 2012).

Intensification of aquaculture has led to an increasing number and frequency of infectious viral disease outbreaks, resulting in high economic losses and fish mortality. The most important contagious and loss-making viral diseases are infectious pancreatic necrosis (IPN) (Cepeda et al., 2011), infectious salmon anemia (ISA) (Toennessen et al., 2010), pancreas disease (PD) (Jansen et al., 2014), cardiomyopathy syndrome (CMS) (Haugland et al., 2011) and heart and skeleton muscle inflammation (HSMI) (Kristoffersen et al., 2013).

IPN is very important disease with large impact on salmon production in the European Union and Norway (Skjelstad et al., 2003). It is primarily an acute, clinical disease in young freshwater salmonids (Pedersen, 2007). For that reason, IPN is a cause of high morality in first feeding fry (Roberts and Pearson, 2005). However, the number of outbreaks is also high during the first months after transferring salmon smolt to seawater (Jarp et al., 1995; Smail et al., 1995). Generally, IPN virus attacks salmon in its very critical

stages of development. It is usually the first viral infection affecting these fish. Consequently, the disease can influence the outcome of the secondary infections as well (Johansen and Sommer, 2001; Johansen et al., 2009). Therefore, there is a common wish in aquaculture industry to gain control of the disease. By doing so, vulnerable smolts would become more resistant to the other diseases.

From the Figure 1.1 it can be seen that fish mostly at risk of succumbing to PD in early summer (May and June) or early autumn (September and October) (Rodger and Mitchell, 2007). The observed period of clinical HSMI and mortality was from June to August (Kongtorp et al., 2006). HSMI is normally observed five to nine months after transfer to sea water while clinical CMS first occurs after 12 to 18 months (Palacios et al., 2010). The ISA outbreaks occur in all seasons with a peak during spring (April–June) and autumn (October–December) (Lyngstad et al., 2008).

IPN virus belongs to the genus *Aquabirnavirus* within the family *Birnaviridae*. A brinavirus has double stranded RNA which codes for the five viral proteins VP1-VP5 (Bain et al., 2008). The proteins are arranged into a non-enveloped T=13 icosahedral structure with an average diameter of 70 nm. The capsid is composed of 260 trimeric spikes formed by VP2 (Coulibaly et al., 2010). In particular, VP2 is assumed to be major carriers of IPN virus virulence properties (Song et al., 2005). IPNV is a good model virus to work with because of being well characterised and VP2 being very well understood while other viruses are less well documented (Rodrguez Saint-Jean et al., 2010).

Development of an effective IPN vaccine is important as well for a sustained control of the disease in salmon farming. There are three major modes for the application of vaccines: injection, immersion and oral. According to the Norwegian Medicines Agency, there are currently four commercial injection vaccines (Pentium Forte Plus vet, Novartis; Norvax Minova 6 vet, Intervet; Alpha Ject 6-2 and Alpha Ject Micro 6, Pharmaq). These vaccines are based on both killed virus particles and recombinant VP2 capsid protein.

Good protective effect of the IPN vaccine based on recombinant VP2 has been obtained in laboratory and field experiments (Ramstad et al., 2007). Although the number of IPN outbreaks in Norway shows a decreasing trend from 2010 (198 outbreaks) to 2012 (119 outbreaks), it is still very high (Johansen, 2013). However, the actual losses due to IPN appear to have declined in recent years. This decline could be attributed to the extensive vaccination programme (Munang'andu et al., 2014; Robertsen, 2011), improved husbandry and gene typing by quantitative trait loci (QTL) technique for resistant individuals (Moen et al., 2009).

Accidentally, salmon, which have pulled through an IPNV infection, may become an asymptomatic carrier of the virus for a long time. As a consequence, production of the virus may resume in the stressed carriers anytime in the future. In that case, the re-infected fish can spread the virus to the surrounding fish and thus cause a new outbreak (Gadan et al., 2013; Skjesol et al., 2011). There are indications that the effect of IPN is pro-inflammatory and may lead to some immune suppression in the carriers (Collet, 2014; Ellis et al., 2010). This may increase risk from subsequent diseases such as HSMI (Kongtorp et al., 2006).

The common scientific view in aquaculture is that some viral vaccines are not effective enough in the field and may not exert sufficient long-lasting protective effects (Robertsen, 2011). Generally, viral vaccines are short lived. For this reason, there is a growing demand from fish farmers for an effective oral vaccine against the viral diseases. Delivery of oral vaccines would allow a booster immunisation to occur after some months in seawater (Villumsen et al., 2014).

According to current practice, after injection with oil based vaccines, subsequent vaccinations are not usually carried out. The only known exception is the vaccination against piscirickettsiosis in Chile where injection is followed by oral booster vaccination (Brudeseth et al., 2013). The reason for this is the lack of effective oral vaccines in the market although the oral vaccination is the most feasible method from the perspective of a fish farmer.

Some of the beneficial characteristics assigned to the oral vaccination are described as labour-saving, non-stressful and large-scale applicable to fish in the seawater cages (Adelmann et al., 2008). There are also some negative characteristics related to the oral vaccination. For example, administration of an exact antigen dose is challenging due to variable feed consumption among fish. Moreover, delivery of intact antigens through the acidic part of the gut is problematic in gastric fish (Dhar, 2013; Quentel and Vigneulle, 1997). All this leads to another issue with the oral vaccination which is the high dosage requirement. Consequently, the economic viability of an oral vaccine project is always challenged. Additionally, ineffective uptake, short term protection and high dosage requirement are factors that prevent oral vaccines from being favoured as the primary choice in treating diseased fish.

It has always been a challenge to deliver medicines and functional ingredients to farmed fish. The only available oral delivery system to farmed salmon is the fish feed pellet produced by extrusion cooking. The extrusion cooking is often called the high temperature short time (HTST) process. This kind of processes tends to maximise the beneficial effects of heating feeds while minimising the detrimental effects (Harper, 1978).

According to current knowledge, most biological proteins will lose their higher-order structure after being exposed to heat treatment. As a result, they become denatured and may coagulate. Loss of three-dimensional structure usually produces a loss of biological activity (Privalle et al., 2011).

For sensitive antigens, various approaches involving polymeric coatings or encapsulation are being evaluated and tested (Bruno et al., 2013; Pinto Reis et al., 2013; Singh and O'Hagan, 1998). These various approaches include naturally occurring polymers: starch, gelatine, alginates and synthetic polymers: polylactide-co-glycolide (PLG), proteinoid microspheres, cellulose acetate phthalates (CAP), methacrylates (MAA), methyl methacrylates (MMA), polyanhydrides (Singh and O'Hagan, 1998). Furthermore, mesoporous silica nanoparticles (MSN) are another synthetic approach. This material have recently been investigated for its potential as drug delivery system (Urabe et al., 2007).

The advantages of using natural polymers include their low cost, biocompatibility and aqueous solubility. In contrast, synthetic polymers can be prepared with a desired degradation rate.

With annual production of 6,700 tonnes, Norway is the world's leading producer of alginate. This ensures good availability and makes this raw material very interesting in this context (Bixler and Porse, 2011). Marine alginate is an ideal polymer for oral delivery systems exhibiting protective features (Augst et al., 2006). Alginate encapsulation may protect bioactive compounds from acidic and proteolytic degradation in the gastrointestinal tract of the fish. Cross-linked alginate is characterised by being stable at low pH and soluble in the alkaline environment (Maurice et al., 2004; Tian et al., 2008). As a result, antigens entrapped in an alginate matrix are protected throughout the stomach, and then released in the intestinal region of the gut where their chances for uptake are maximized (Rombout et al., 2011).

Despite the fact that extensive research on alginate is going on, there are several factors that remain to be explored before adopting alginates as an oral delivery system for salmonid fish. For instance, particle size of the delivery systems based on alginates needs further reduction in order to be suitable for an effective incorporation into fish feed pellets. At the same time, there are no scientific reports about assessing release of macromolecular drugs from alginates at test conditions relevant for A. salmon. Similarly, very few studies provide evidence of macromolecular drug release in the intestinal region of salmonid fish. In addition, ability of alginate to protect protein antigens throughout fish feed production process and fish itself is currently unexplored.

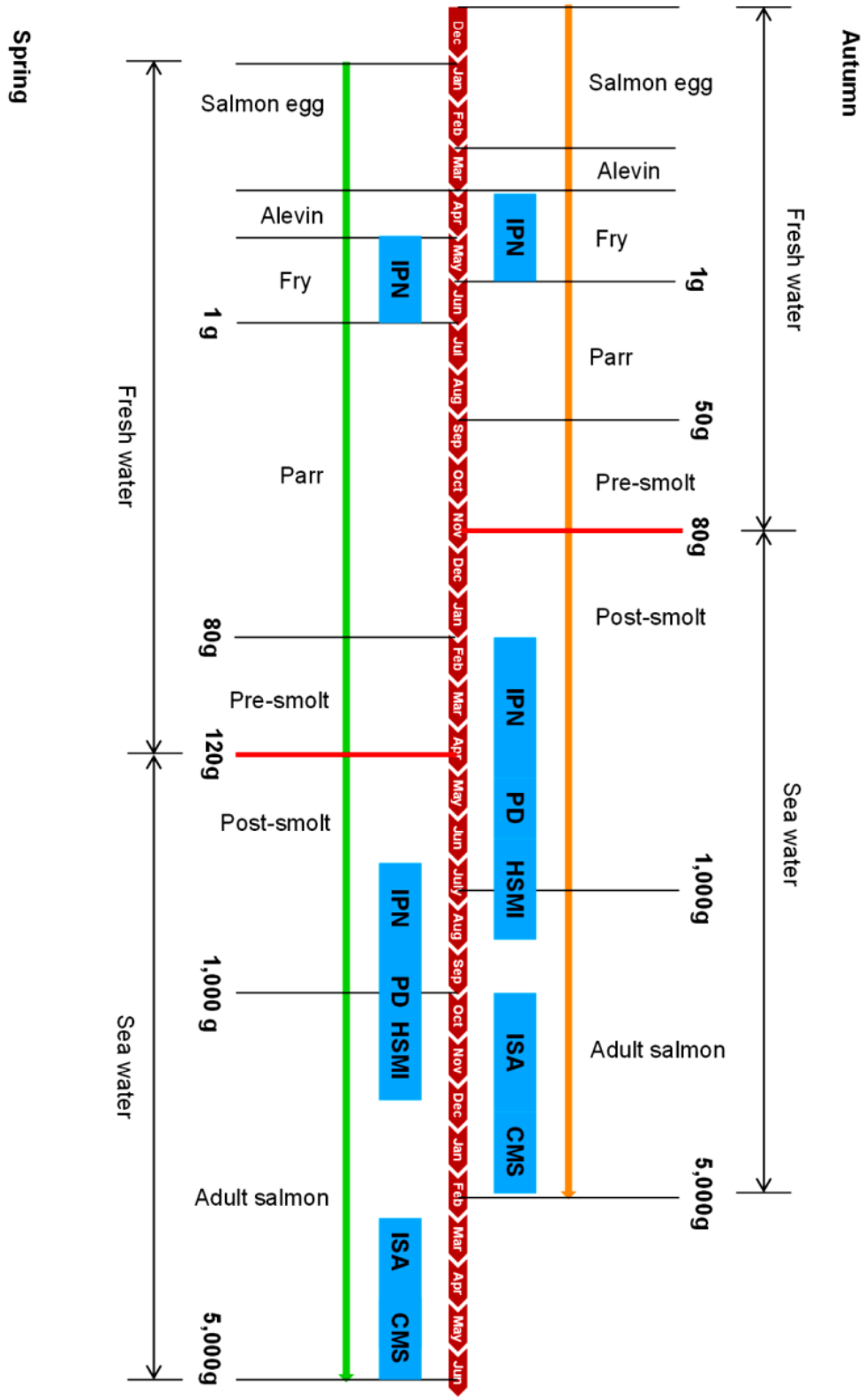

Figure 1.1: Life cycle of farmed A. salmon with potential outbreaks of viral diseases. Orange arrow represents autumn smolt cycle while green arrow represents spring smolt. The most important contagious and loss-making viral diseases are mapped: infectious pancreatic necrosis (IPN), infectious salmon anaemia (ISA), pancreas disease (PD), cardiomyopathy syndrome (CMS) and heart and skeleton muscle inflammation (HSMI).

1.3 Immune response

From the previous section it becomes evident that the ability to help antigens immunise the host is one of the key criteria for a promising oral delivery system to A. salmon. In order to be able to measure the effects of immunisation, it is important to understand how the immune system can respond to a delivered antigen. This understanding is crucial for selecting useful markers that can reveal which immune pathways are induced by the ingested antigen.

For clarity reasons, only the basic immune factors, which are relevant for the immune response study described in Chapter 3, are reviewed in this Section. Since immunology is a complex matter, the immune system here is depicted as simply as possible.

Firstly, the ingested antigens are processed by antigen presenting cells (APC). After processing antigens, APCs present their fragments to T cells, particularly naïve $CD4^+$ T cells (T_h0 cells). From this point, immune response can go in at least two main directions (Figure 1.2). One direction is the T_h1 response which induces the cell-mediated immune system. Second direction is the T_h2 response which induces the humoral immunity (Collet, 2014; Romagnani, 2000). Furthermore, there is a third response (T_h3) which is balancing T_h1 and T_h2 cytokines to prevent serious cell-mediated inflammatory reactions. This mechanism mainly acts in mucosal tissue (Strober et al., 1997). However, T cells can also differentiate into regulatory T cells (T_{reg}). As a result, immune functions can be suppressed by induced T_{reg} (Kumari et al., 2013). Consequently, fish may develop immune tolerance

(Sakaguchi et al., 2008). It is considered that both very high and very low dose of the same antigen may induce immune tolerance (Möbs et al., 2008; Zouali, 2014).

In the cell-mediated immune response, T_h0 cells are activated and developed into effector T_h1 cells against intracellular bacteria, virus and protozoa. The major effectors of the cellular immunity are macrophages and cytotoxic T cells. The differentiation into T_h1 cells is activated by IL-12 and INF-γ cytokines (Wang and Husain, 2014). The rate of transcription is controlled by T-bet and STAT4 transcription factors (Whitmire, 2014).

In the humoral immune response, the naïve T cells develop into effector T cells against extracellular microorganisms including helminths. This development is activated by IL-4 and IL-10 among others interleukins (McKenzie et al., 1998). On the other hand, transcription is controlled by GATA-3 and STAT6 transcription factors (Kumari et al., 2009; Urban et al., 1998). The major effector cells of the humoral immunity are eosinophils (Damask, 2015), basophils (Schwartz et al., 2015), mast cells (Gregory et al., 2005) and B cells. Eventually, B cells are transformed into immunoglobulins (Ig) or antibodies (Marrella et al., 2015). According to the present knowledge, there are only three major Ig isotypes in A. salmon. These are: IgM that is systemic antibody and IgD along with IgT that are mucosal antibodies (Hordvik, 2015; Rombout et al., 2011).

Unlike T_h cells, T_{reg} cells generally suppress induction and proliferation of effector T cells (Möbs et al., 2008). This is an important feature of the immune system when an infection is eliminated. In addition, T_{regs} can limit

inflammatory responses and prevent autoimmunity (Gol-Ara et al., 2012). Production of T_{reg} cells is triggered by TGF-β and IL-6 cytokines (Li and Flavell, 2008). Factors such as FoxP3 and STAT5 control the rate of transcription (Chen et al., 2003; Hori et al., 2003).

In this thesis, IPNV antigen was used with the purpose of inducing the humoral or adaptive immunity. Adaptive immunity involves activation of T cells and B cells that can initiate a tailored immune response to a specific pathogen (Rote, 2007). For this reason, gene expression of IgM, IgT, CD4, GATA-3 and IL-10 was of special interest. The cytokine IL-10 was selected because of its ability to both activate T_h2 and inhibit the T_h1 pathway (Tec and Morita, 2015; Zhou et al., 2007). IL-10 has a potent immunosuppressive capacity towards T_h1 route (Akdis and Akdis, 2014; Weiner et al., 2011). It also enhances B cell survival and antibody production (Trifunović et al., 2015). In addition, it is common that IL-10 along with IL-4 act together with TGF-β in down-regulating inflammatory T_h responses (Gonnella et al., 1998; Skugor et al., 2008). The status of T_{reg} cells is interested due to possible development of immune tolerance against the oral antigen (Chen et al., 1996). For that purpose, level of the IL-10 and FoxP3 (T_{reg} markers) expression is important to determine.

An interesting subset of T_{reg} cells is T_h3 cells. Although T_h3 cells are considered as antigen non-specific, their response is associated with microbial antigens (Belkaid, 2007; Weiner et al., 2011). These cells can differentiate from T_h0 cells under influence of IL-10 and TGF-β. Therefore, these two cytokines are good markers for T_h3 response (Sonmez et al., 2004). It is also suggested that orally ingested antigen can initiate the T_h3

response with the oral tolerance as an outcome (Castro-Sánchez and Martín-Villa, 2013; Wan and Flavell, 2008). In fact, the oral tolerance is mediated by TGF-β which is produced by T_h3 cells (Carrier et al., 2007; Letterio and Roberts, 1998). However, all details related to the mechanisms of T_h3 action are unexplored.

Finally, T_h17-cells act at epithelial barrier driving pro-inflammatory responses. Development of autoimmunity is also attributed to induction of T_h17 pathway. Differentiation from T_h0 cells is initiated by activators such as RORγ and STAT3. This transcription factors induce the expression of TGF-β, IL-17, IL-6 among other cytokines (Wilson et al., 2009).

In summary, induced INF-γ, and STAT4 together with IL-12 refers to the T_h1 immune response. On the other hand, the induced GATA3, STAT6, IL-4 along with IL-10 witnesses of T_h2 response. Furthermore, the up-regulated IL-10 together with FoxP3 indicates that the T_h1 related immunity is in the process of being down-regulated. However, the up-regulated IL-10 together with TGF-β is a sign of suppression of both T_h1 and T_h2 immunity (Cecere et al., 2012). This condition is linked to immune tolerance (T_h3 response). Finally, pro-inflammatory pathway, T_h17 is recognised by IL-17, RORγ and STAT3 among other markers.

There are many more markers and pathways than those mentioned here. The reason these markers were selected is that they are very well documented and understood.

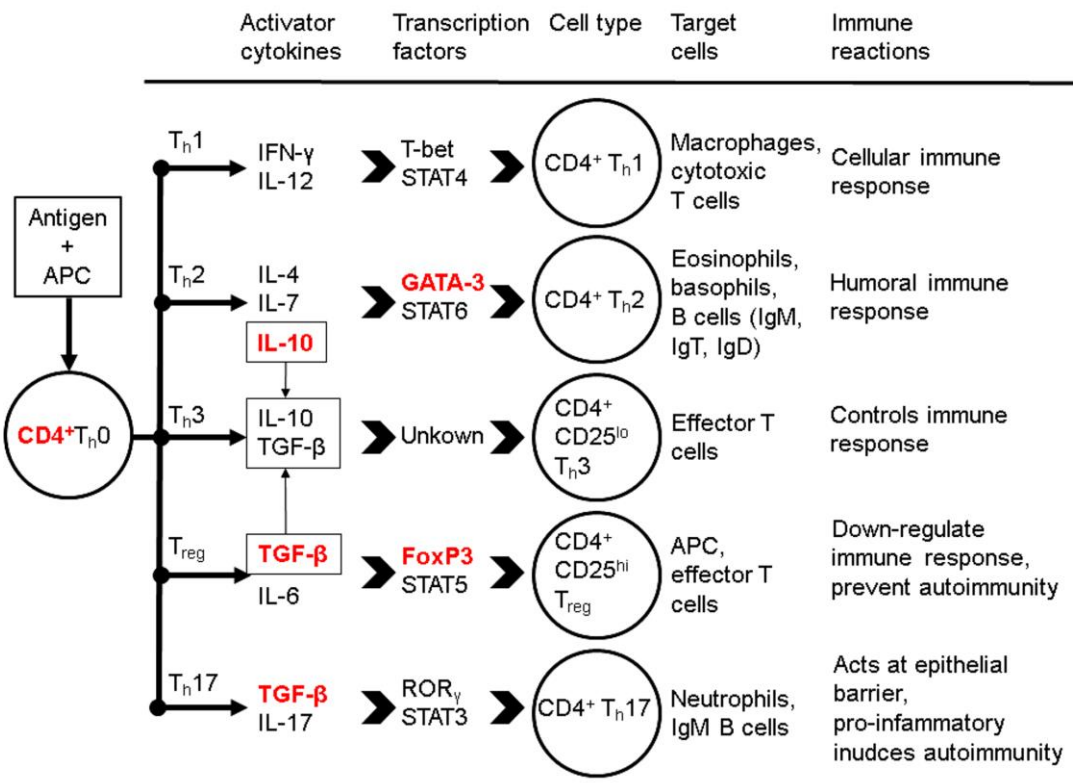

Figure 1.2: An overview of the most likely immune responses to the ingested antigen. Immune system can respond to an ingested antigen in two different ways: 1) cellular immune response (T_h1 cells) activated by IFN-γ and IL-12 cytokines in combination with T-bet and STAT4 transcription factors and 2) humoral immune response (T_h2 cells) triggered by IL-4 and IL-10 among others cytokines with support of GATA-3 and STAT6 transcription factors. These two responses are balanced by Th3 cells secreting IL-10 and TGF-β cytokines. As a consequence, immune system can start self-limiting its own response. This is done by inducing T_{reg} cells with the aid of TGF-β & IL-6 activator cytokines and FoxP3 & STAT5 transcription factors. In addition, immune system can also overreact and cause sustained inflammation which can turn into autoimmune disease. This reaction is a main characteristic of T_h17 response.

1.4 Alginate encapsulation

The most likely immune responses of A. salmon to ingested antigens were reviewed in the preceding section. Some useful markers for different immune pathways were highlighted. To generate an effective oral delivery system based on alginate, it is important to get an overview of encapsulation methods and their capabilities as well. Equally important, it is to gain an insight into the relations between crosslinking properties and chemical composition of alginate. The mentioned overview and insight are also essential for the reason that the alginate encapsulation is the key element in all experiments conducted in this thesis.

Alginates are polysaccharides isolated from brown algae such as *Ascophyllum nodosum, Durvillaea sp., Ecklonia sp., Laminaria sp., Lessonia sp., Sargassum sp.* and *Macrocystis pyrifera* found in coastal waters around the globe. *Laminaria digitata* and *Laminaria hyperborea* are the major raw materials for Norwegian alginate industry (McHugh et al., 2003). The first characterisation of alginic acid was carried out by Stanford who extracted it with sodium carbonate and then precipitated the alginate out of solution at low pH (Stanford, 1886).

Marine alginates are composed of two forms of uronic acid: mannuronic (M) and guluronic (G) (Figure 1.3). Some of the first analytical methods applied to obtain the M/G ratio included partial acid hydrolysis of the alginates followed by separation and detection using paper chromatography. It was shown that the M/G ratio varies between sources and that alginates are block polymers (Haug et al., 1966). Nowadays, more advance analytical methods such as

Nuclear magnetic resonance (NMR) are used to study that matter (Salomonsen et al., 2009; Sperger et al., 2011). Two blocks of adjacent polymer chains can be cross-linked with multivalent cations (e.g., Ca^{2+}, Ba^{2+}, etc.) through interactions with the carboxylic groups in the uronic acid, which leads to the formation of a gel network as shown in the Figure 1.4 (Augst et al., 2006). From light-scattering and viscosity experiments, it was found that stiffness of the chain blocks increased in order MG<MM<GG (Smidsrød et al., 1973). The arrangement of M and G bocks in a polymer chain is the major differences between alginate products (Minghou et al., 1984).

In this thesis, two very different cations were used to crosslink sodium alginate, namely calcium cation ($Ca^{2+)}$ and ethylenediammonium dication (EDA^{2+} or $C_2H_4(NH_3)_2^{2+}$). The former ($Ca^{2+)}$ is most commonly used to crosslink sodium alginates, and therefore, it is a good benchmark for every new cross-linker (Lee et al., 2012; Pathak et al., 2010). However, it seems that the letter (EDA^{2+}) has been very rarely studied in combination with alginates since Cooper et al. described it in 1962. Consequently, the application of EDA-alginate as an oral delivery system for protein antigens to animals and humans is currently unexplored and novel.

According to Cooper et al., (1962) EDA-alginate is superior to Ca-alginate in the rate of dissolution under alkaline conditions. For this reason, EDA-alginate was compared to Ca-alginate in terms of encapsulation efficiency and immune response in Chapter 3. Thus, the encapsulation efficiency was assessed in Section 3.2. The ability of EDA-alginate to improve the specific immune response to IPNV antigen in salmon was investigated in Section 3.4.

These two alginate matrices were also compared to each other in terms of the *in vitro* and *in vivo* dissolution in Chapter 4. The need for a fast-dissolving alginate matrix is pointed out in Section 4.1. The performed experiments are described in Sections 4.2.1 and 4.4.1. On the other hand, the results are presented in Sections 4.2.2 and 4.4.2 while Section 4.5 discusses them. Finally, the major implications regarding EDA-alginate are stressed again in the concluding chapter, namely Chapter 7 (Section 7.1.2).

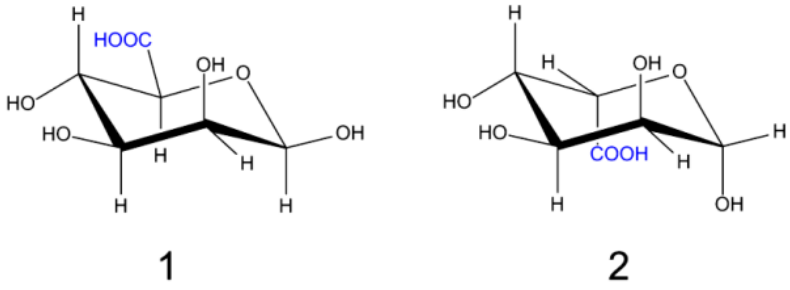

Figure 1.3: Monomer molecules of the alginate building blocks: β-D-mannuronate (M) and α-L-guluronate (G). 1) M and 2) G residues are covalently (1-4)-linked together in consecutive M-blocks, G-blocks and alternating MG-blocks forming a linear copolymer called alginate.

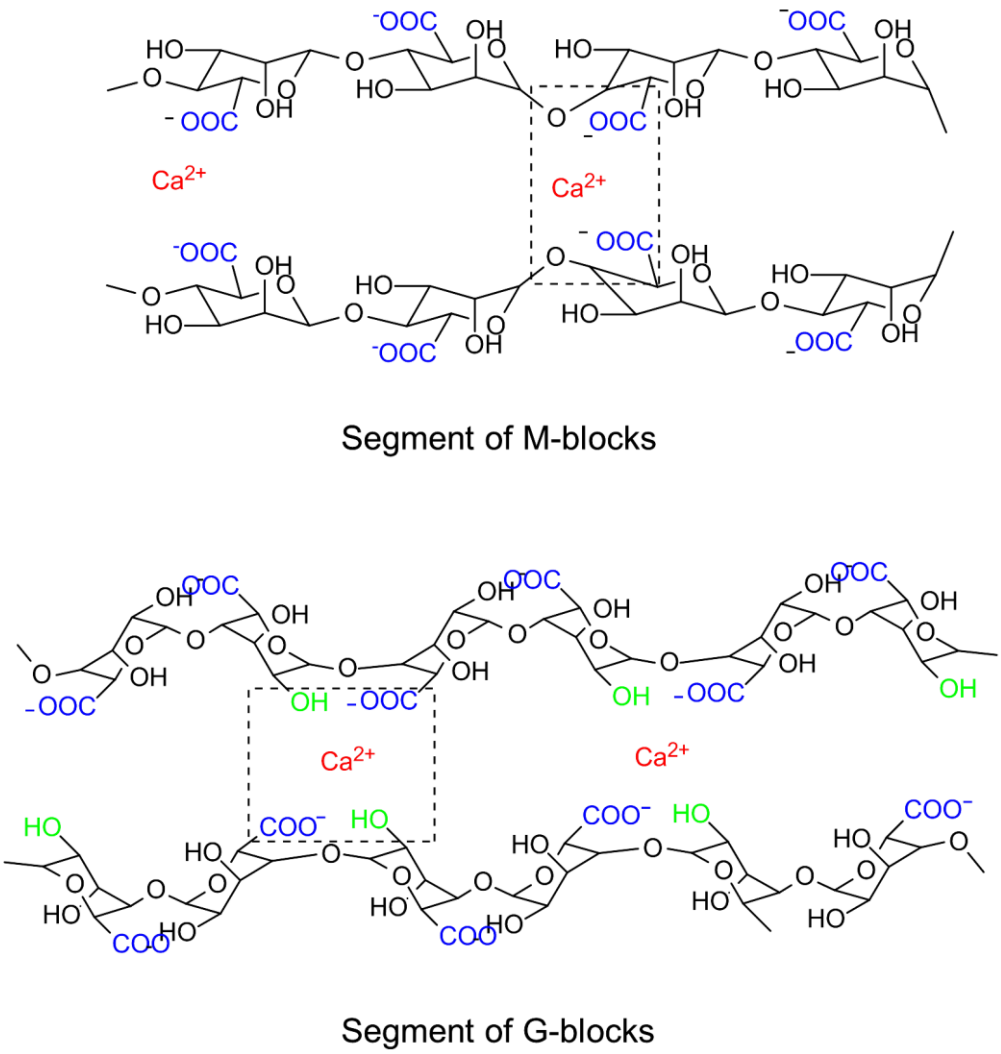

Figure 1.4: Crosslinking pattern of M and G blocks in the presence of calcium cations.

The crosslinking properties of alginate form the basis for various encapsulation techniques including both electrostatic driven and non-electric driven methods. For instance, aerodynamically assisted bio-jetting/-threading is a good representative for non-electric driven methods (Arumuganathar and Jayasinghe, 2008; Jayasinghe, 2011). On the other hand, electrospraying is a typical example of an electrostatic driven process. Electrospraying was conceived through the theory established by Lord Rayleigh. He anticipated that droplets would disrupt and throw out fine jets of liquid if the total charge

on the droplet surface would reach a limiting value. This limiting value is now known as the "Rayleigh limit" (Rayleigh, 1882). This theory has been confirmed experimentally by many researchers since that time (Gomez and Tang, 1994).

As a result, there are various electrostatic microbead generators in the market today. These generators use an electric potential to pull the droplets from a needle tip (Moyer et al., 2010). Consequently, motion and size of the droplets can be controlled by the electrostatic potential. The electrostatic potential is established between the needle feeding the mixture of alginate and hardening solution. Spherical microbeads are formed by electrostatic extrusion of the alginate solution through a needle using a syringe pump and a plastic syringe. The generated droplets fall into a hardening solution through the centre of a ring electrode. The ring electrode is grounded while the needle is charged. The opposite is possible as well. Potential difference is controlled by a high voltage DC unit. Droplet size may be controlled by adjusting the magnitude of the voltage. Size of the microbeads depends on the distance between the needle tip and the hardening solution. Diameter of the needle and flow rate of the alginate solution along with the viscosity are important factors as well (Figure 1.5) (Jaworek and Sobczyk, 2008).

The generated droplets are rather uniform in size. Compared to the other encapsulation techniques, electrospraying allows for better regulation of morphology and particle size distribution (Bock et al., 2012). Moreover, electrospraying is frequently used technique and very well documented in the scientific literature (Bock et al., 2014; Jaworek, 2007). The advantages of using electrospraying are: monodispersed particles, even morphology, high

encapsulation efficiencies and undamaged bioactive compounds. On the other hand, disadvantageous aspects are: low throughput and high sensitivity to the viscosity of polymer solutions. Since electrospraying offers high control over the generation of microbeads, it is an obvious first choice for encapsulating protein antigens. However, an area that electrospraying could be improved in is the particle size. Generally, size of the alginate microbeads needs further reduction to be suitable for incorporation into feed pellets.

For this reason, another encapsulation technique, namely aerodynamically assisted jetting (AAJ) was modified in this thesis. The new technique was named air pressure-assisted energised jetting (APAEJ). APAEJ is a further development of AAJ and it is basically fusion of AAJ with electrospraying (Figure 1.6). AAJ offers relatively high throughput and the possibility of producing very small microbeads (Jayasinghe and Suter, 2006). For this reason, the focus was eventually directed towards this encapsulation process.

In this process, a jet of alginate microdroplets is generated by extruding alginate solution through a nozzle into an air-pressurised chamber. The chamber is fitted with a narrow exit orifice. Through the orifice, the expanding air is dispersing the incoming solution into a jet of fine alginate micro-droplets. Hovering aerosols and very fine micro-droplets are attracted to cross-linking solution by creating electric potential difference between the jetting head and the solution. Along the way, a high precision syringe pump regulates the flow rate of alginate solution while a pressure regulator controls the air flow (Griessinger et al., 2012). This encapsulation process is further explained and discussed in details in Chapter 5.

For the reason that encapsulation herein is based on the entrapment of a bioactive compound in an alginate matrix, the term “encapsulation” is interchangeable with the term “entrapment”. However, the word “encapsulation” is most commonly used of the two in the scientific literature. Therefore, “encapsulation” meaning “entrapment” will be mostly used in this thesis as well.

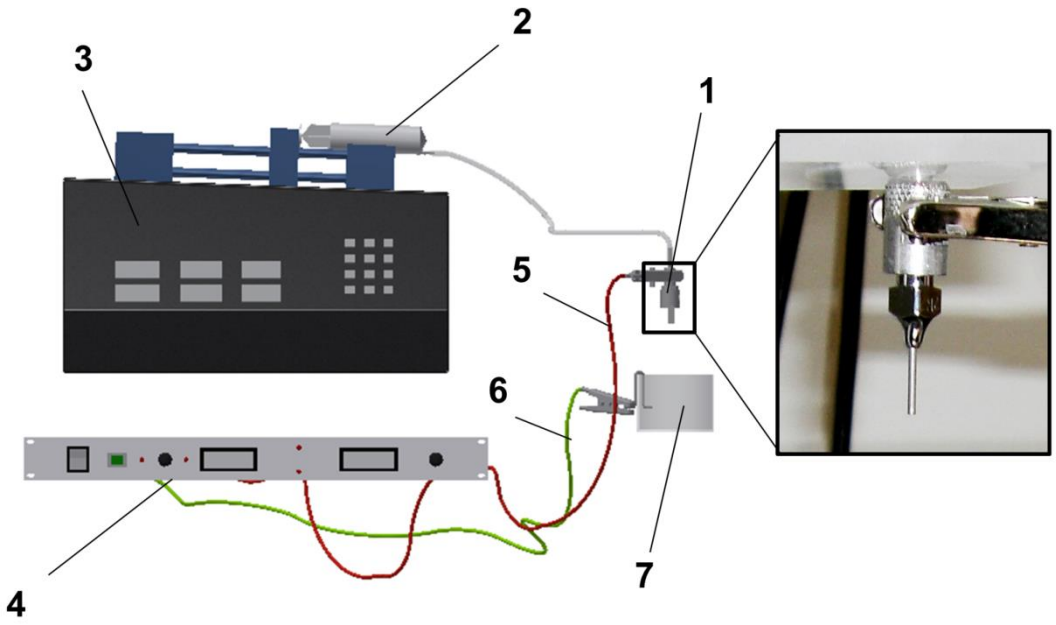

Figure 1.5: Architecture of the electrospraying apparatus**.** The apparatus consist of a needle (1), syringe (2), syringe pump (3), high voltage DC power supply (4) and a vessel (7). Needle (1) is wired to positive voltage (5) while vessel is grounded (6).

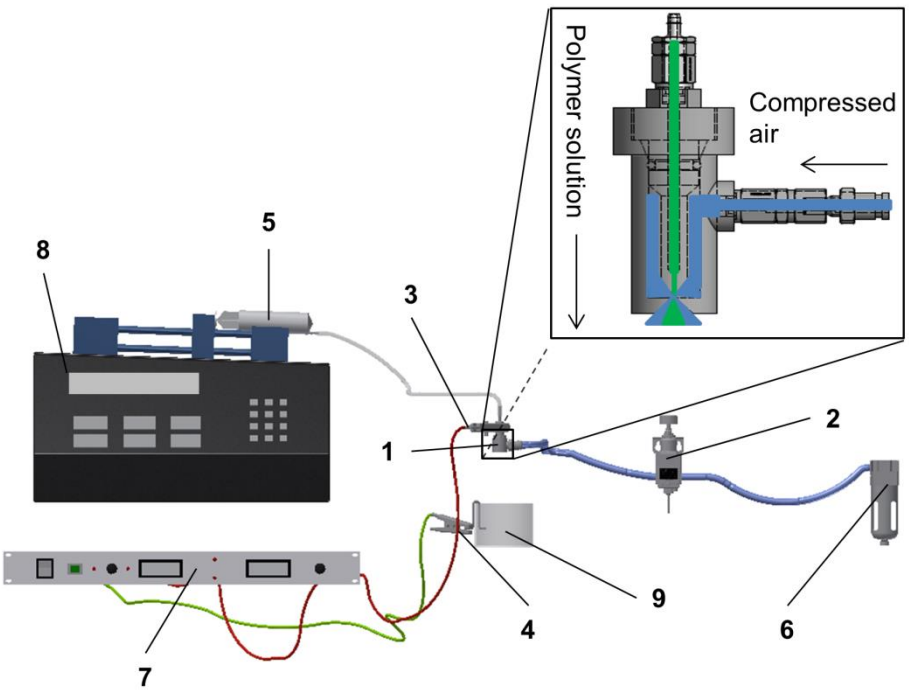

Figure 1.6: Architecture of the air pressure-assisted energised jetting apparatus. The apparatus consists of a jetting head (1), pressure regulator (2), syringe (5), syringe pump (8), air filter (6), high voltage DC power supply (7) and a vessel (9). Jetting head is wired to positive voltage (3) while vessel is grounded (4). Air filter connects to a source of compressed air.

Reported average size of alginate particle using aforementioned methods and other available methods varies a lot. For instance, Park et al., 2012 demonstrate that the encapsulation of adenovirus in alginate beads smaller than 150 µm using electrospraying is feasible. Though the alginate beads with d_{avg} = 170 ±100 µm (Bugarski et al., 1994) and 50 > d_{avg} < 200 µm (Sugiura et al., 2005) were reported successfully fabricated, generation of smaller beads than 200 µm with an electrostatic droplet generator has been rather impractical to date. In a study by Arumuganathar et al., 2007, the average droplets size observed in the jet formed by an aerodynamically assisted jetting device were between 55 and 87µm.

When it comes to other methods, Sahu and Prusty (2010) provide evidence for successful generations of polymeric (alginate and chitosan) nanoparticles by a complex coacervation process. In his study, the minimum achieved average size (d_{avg} ±SD) of empty and bovine serum albumin (BSA) loaded nanoparticles were d_{avg} = 339.8 ±0.2 nm and d_{avg} = 474 ±19 nm respectively. On the other hand, Shinde and Nagarsenker (2011a) report that eugenol was micro-capsulated in a gelatine sodium alginate complex coacervate system yielding microbeads of d_{avg} = 425 µm.

Paques et al. (2013) shows that emulsification/external gelation approach is capable of yielding alginate beads in the range of 0.2 - 5 µm with an average of d_{avg} = 1 µm. Similarly, in a study by Ciofani et al. (2008), the average size of polymeric (alginate and chitosan) particles was d_{avg} = 1.2 µm using an analogous approach. Silva et al. (2006) show that it is possible to produce insulin loaded alginate microspheres with d_{avg} = 60 µm using the emulsification/internal gelation method. However, the investigation of Song et al. (2013) show that the size of microbeads produced by emulsification/external and emulsification/internal gelation were d_{avg} = 325 ± 202 µm and d_{avg} = 151 ±77 µm respectively.

Del Gaudio et al. (2005) affirm that most of the alginate beads were below 750 µm in his study by using electromagnetic laminar jet breakup process. In another study involving the same process, Rodríguez-Rivero et al. (2011) describe the formation of alginate micro-particles, ranging from 300 to 700 µm with a mean size of d_{avg} = 490 µm.

Work by Ribeiro et al. (2004) demonstrate fabrication of uniform-sized microspheres of approximately d_{avg} = 1000 µm using pure alginate in the coaxial air flow induced dripping process. Semyonov et al. (2010) observe that particle sizes are distributed between 400 and 1800 µm in a study that combines the coaxial air flow induced dripping process and spray freeze drying technique for collecting beads.

Iwanaga et al. (2013a) describe successful production of alginate beads (d_{avg}= 13 µm) loaded FITC-labelled nanoparticles by using inkjet printing technology. In recent years, there has been increased activity in the field of printing technologies where various printing techniques of use for development of drug delivery systems have been explored (Kolakovic et al., 2013). Lian et al. (2012) report that a three-dimensional microfluidic droplet generator which is rather unconventional technique, is able to produce mono-disperse alginate microbeads with d_{avg} = 14.55 ±1.13 µm.

The resulting alginate microbeads have excellent biocompatibility within host tissues and are able to biodegrade in a controlled manner. This attributes make them interesting for use as oral delivery systems (Adelmann et al., 2008; Joosten et al., 1997; Maurice et al., 2004; Polk et al., 1994). A variety of products can be combined with alginate matrices to avoid damage from the low pH and proteolytic enzymes encountered in the digestive system. Incorporation of products can be conducted under mild conditions, allowing sensitive proteins to remain intact within the matrix. Alginate is an anionic polymer, with carboxyl end groups. This allows it to attach more readily to mucosal surfaces (George and Abraham, 2006). Moreover, alginate microbeads are stable at low pH while they dissolve at high pH. As a result,

faster release occurs at a higher pH, after microbeads have passed through the stomach (Yu et al., 2008). These properties have important implications for the oral delivery of macromolecular drug, particularly protein antigens.

1.5 Comparative dissolution testing

In the previous section, crosslinking properties of alginate and the available encapsulation methods were reviewed. In this section, the focus is aimed at dissolution testing. Dissolution testing is useful for comparing dissolution profiles of different alginate formulations assessed in this thesis. To be released at the right place in fish is essential for an antigen to be able to trigger off an adequate immune response. The issues related to the release of bioactive compounds from alginate matrices are addressed in Chapter 4.

1.5.1 Application of dissolution tests

In 1897, Noyes and Whitney published the work “The rate of solution of solid substances in their own solutions”, in which, for the first time, the process of dissolution of solids was described (Noyes and Whitney, 1897). Nowadays, *in vitro* dissolution test is an essential analytical tool necessary for understanding delivery systems. For clarity reasons, further in the text, the terms “pharmaceutical product” and “solid oral dosage form (SODF)” correspond to “oral delivery system plus an active pharmaceutical ingredient (API)”. Oral delivery system is herein identified with alginate while API can refer to IPNV antigen, blue dextran or HRP.

In vitro dissolution testing is a main analytical test for determining the *in vitro* release profile of an API. The test information can be used for both optimising API release from SODFs and evaluating batch-to-batch uniformity of SODFs as a part of quality control (QC) procedure. Dissolution tests can also be used to identify the effect of important manufacturing variables on dissolution rate of SODFs. Additionally, *in vitro* dissolution testing is one of the tools

recommended by the FDA guidance for determining the level of *in vitro-in vivo* correlation (IVIVC) (Kytariolos et al., 2010), and verifying the level of scale-up and post-approval changes (SUPAC) (Van Buskirk et al., 2014). In this thesis, dissolution tests were used to develop a fast-dissolving and temperature-independent alginate matrix within the temperature range of seawater in which A. salmon habituate.

In the Biopharmaceutics Classification System (BCS) guidelines for classifying APIs on the basis of their solubility, permeability and dissolution, *in vitro* dissolution test is a main method for determining dissolution class boundaries (Anand et al., 2011). In line with the BCS, APIs are classified in four classes with respect to their solubility and permeability (Table 1.1). Regarding dissolution boundaries, an immediate release (IR) product is considered rapidly dissolving when ≥85% of API dissolves within 30 minutes in dissolution medium (≤900 ml) using USP apparatus 1 or 2.

Table 1.1: Classification of the active pharmaceutical ingredients (APIs) on the basis of their solubility and permeability.

Class	Permeability[i]	Solubility[ii]
1	High	High
2	High	Low
3	Low	High
4	Low	Low

[i]Highly permeable: the extent of absorption in humans is determined to be ≥90% of an administered dose, based on mass-balance or in comparison to an intravenous reference dose.
[ii]Highly soluble: the highest dose strength of is soluble in ≤250 ml water over a pH range of 1 to 7.5.

The widespread application of dissolution tests has resulted in several dissolution apparatus which are standardized and specified by the United

States Pharmacopoeia (USP). The following apparatus are described in the USP General Chapters: 1) the USP Apparatus 1 (basket), 2) USP Apparatus 2 (paddle) (Gray et al., 2009), USP Apparatus 3 (reciprocating cylinders) (Joshi et al., 2008), USP Apparatus 4 (flow-through-cell) (D'Arcy et al., 2010), USP Apparatus 5 (paddle-over-disk) (Prodduturi et al., 2009), USP Apparatus 6 (cylinder) and USP Apparatus 7 (reciprocating holders) (Zhou et al., 2007). Which dissolution test will be applied depends on the intended route of administration and characteristics of API and dosage form. For evaluation of SODFs, the most relevant dissolution test apparatus and methods are USP 1-4. On the other hand, USP 5-7 are recommended for *in vitro* release testing of topical and transdermal drug products (Chang et al., 2013). The USP 1-4 and USP 5-7 including corresponding test methodologies are described in the USP General Chapters <711> and 725 respectively (USP, 2012a, 2012b).

1.5.2 Development of dissolution method

Development of a successful dissolution test procedure involves choosing factors like dissolution medium, volume, agitation rate, temperature, sampling time points, sampling volume and method of analysis suitable for the pharmaceutical product of interest (USP, 2012c). This overview will concentrate on the USP 1 and 2 because these two systems constitute the majority of dissolution testing in the pharmaceutical industry (Figure 1.7), (Gray et al., 2009).

1.5.2.1 Volume

The common volumes of dissolution media are between 500 – 1000 ml with 900 ml as the most frequent volume. With proper justification, the volume could also be below 500 ml and above 1000 ml.

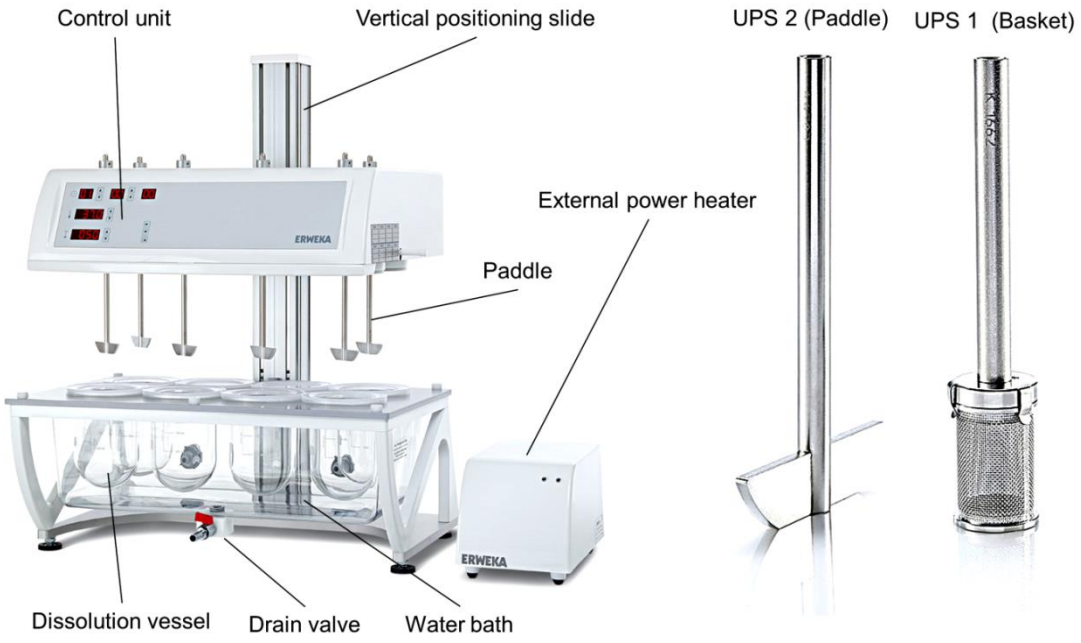

Figure 1.7: Example of a dissolution tester (ERWEKA DT 626 series, www.erweka.com), UPS apparatus 1 and 2.

1.5.2.2 Dissolution medium

An ideal dissolution medium gradually dissolves SODF resulting in complete release (100%) of API within one hour. These qualities are preferable due to an increased possibility of observing variations in a formulation or process parameters. Therefore, screening with buffer solutions in the range of pH 1.2 – 6.8 is performed before everything else. In a case of low solubility within the selected pH range, addition of surfactants is suggested.

Typical dissolution media are 0.1- 0.001M HCl buffer pH 1.2, 0.05M Acetate buffer pH 4.1 – 5.5, and 0.05M phosphate buffer pH 5.8 – 8.0. In addition, there are simulated gastric and intestinal fluids available in both fed and fasted variant.

1.5.2.3 Agitation rate and temperature

Agitation speed is normally between 25 – 150 rpm. The typical speed of rotating baskets is from 50 – 100 rpm in the USP 1 method. On the other hand, the routinely used speed of rotating paddles is 50 or 75 rpm in the USP 2 method. Other speeds could be applied with justification but rates below 25 rpm and above 150 rpm are usually unacceptable in both methods. Generally, dissolution tests are performed at 37 ± 0.5°C.

1.5.2.4 Sampling points

Selection of sampling procedure depends on release technology used in designing the SODF. For immediate-release SODFs (IR – SODFs), the test time is normally 30 – 60 min with sufficient number of sampling time points to properly characterize the ascending and plateau phases of the dissolution curve. However, for the APIs –class 1 (according to BSC: highly soluble and permeable drug,) which are formulated with fast-dissolving products and showing 85% release within 15 min, one-point test is sufficient. For slower-dissolving APIs, an infinity point may be obtained by increasing the speed of rotating device to 150 rpm for another 30 – 60 min at the end of the run after which an additional sample is taken. The infinity point, which is not mandatory for the pharmacopeial purpose, can provide useful information about formulation in the initial phases of the drug development.

For extended-release SODFs (ER – SODFs), a three-point test is sufficient to characterise the *in vitro* API release profile for the pharmacopeial purpose. The first sample is usually taken after 1 – 2 hours, while the third sample is taken when release of the API is completed. The second sampling point is chosen somewhere between these two points. More on method development for modified-release dosage forms could be found in the USP General Chapter <1088> (USP, 2012d).

1.5.2.5 Sampling volume and analysis

At set time points, aliquots of filtered medium (eppendorf tubes: 3 - 5 ml or HPLC vials: 1.5 ml) are removed and analyzed for API content by HPLC or UV-Vis. During development, HPLC is most commonly used. It has the advantage of being able to separate the API from potential interferences from the formulation matrix or dissolution medium and can detect API degradation. Furthermore, large variations in sample concentration can often be accommodated by adjusting injection volume.

1.5.2.6 Observation of dissolution behaviour

Visual observation of all vessels and documentation of dissolution behaviour is very important part of the testing. Some of the observations that could be made are: distribution of particles throughout the vessels, adhering of particles to the vessel, floating of particles, coning, mounding, swelling, air bubbles etc.

1.5.3 Dissolution profiles

Cumulative dissolution profiles represent the total amount of drug dissolved from the formulation over time. When cumulative dissolution is measured in a constant-volume system, no correction for the amount lost in sampling needs to be made. If sample is removed from the system, the amount consumed in analysis must be replaced or accounted for in the calculation (USP, 2012c).

There are many approaches used for comparing dissolution profiles of SODFs. They can be divided into two main groups: 1) model independent methods and 2) model dependent methods. Model independent methods, which are also recommended by Food and Drug Administration (FDA), use f_1 and f_2 factors. The difference factor (f_1) directly compares the difference between percent drug dissolved per unit time for a test and a reference product. Two dissolution profiles are similar when f_1 value is between 0 and 15. The similarity factor (f_2) is also a simple measure for the comparison of two dissolution profiles. When two profiles are identical, $f_2 = 100$. An average difference of 10% at all measured time points results in a f_2 value of 50 (Moore and Flanner, 1996). FDA has set a public standard of f_2 value between 50 and 100 to indicate similarity between two dissolution profiles (Shah et al., 1998). In other words, $f_2 \geq 50$ should be a reliable estimate to assure product consistency and performance. There are several model dependent methods that can be used to compare dissolution profiles. Some of them are: First-order model, Hixson-Crowell, Weibull, Higuchi and Logistic model (Yuksel et al., 2000).

1.6 Fish feed production process

When dissolution profiles are good and the alginate-encapsulated antigen is ready to be administered to fish, the final formulation eventually needs to be incorporated into feed pellets. Ultimately, a feed pellet is the main delivery vehicle for orally administering bioactive compounds to fish. For this reason, the fish feed production process with different inclusion options is reviewed here. Thus, this section serves as a prelude to Chapter 6 where stability of antigen in fish feed production process is addressed.

In short, fish feed production process consists of four steps or sub-processes: 1) formulation of meal mix by grinding and mixing the required ingredients, 2) generation of extrudate by extruding the meal mix, 3) preparation of base pellet by drying the extrudate, and 4) production of the finished product by infusing an appropriate oil mix into the base pellets. Of all the above mentioned steps, extrusion is the most important sub-process of the production process.

The verb ”to extrude” derives from Latin words *ex* (out) and *trudere* (to thrust), and means to force something through a small opening. Extrusion cooking can be described as a process whereby moistened starch and proteinous material are cooked and transformed into viscous, plastic-like dough which is forced through a die opening of desired cross-section (Singh et al., 2007). This processing technique has long been used for the preparation of human foods and animal feed products (Harper, 1989). Process of extrusion has been known for over 200 years. The early extruders were ram-type extruders for processing metals such as lead, copper and

brass. The first extruder of such type was patented by Joseph Bramah in England in 1797 (Pugh and Watkins, 1961). Since then, it had been more than 80 years before Gray (1879) patenting the first screw extruder which served for wire coating. Furthermore, the end of the 1800s is also the time period when the first extruders were adopted for food production. This early use of the screw extrudes was intended for producing sausages (Karwe, 2003). Later on, in the 1930's extruders were developed to manufacture pasta products (Akdogan, 1999). Shortly afterwards, in the 1940's, extruders were used to produce expanded corn products. In the 1950's this equipment was tailored to manufacture dry expanded pet food pellets.

However, there are other technologies that can convert feed mash into a compact, cylindrical form, called a pellet. For instance, such a one technology is pelleting by pellet press that was introduced in the 1920's (Schoeff, 1994). A pellet press, when used alone, is adequate for producing poultry, swine and shrimp feed. On the other hand, since the late 1980's, pellet press has been coupled with an expander in order to produce suitable feed for ruminants. An expander could be briefly described as a pre-pelleting conditioner where the feed material is subjected to high temperatures for a short period of time (Pipa and Frank, 1989).The first fish feed pellets were introduced to farmed trout at the Red River Hatchery near Taos (USA) in the 1950's (Sigler and Sigler, 1986). These early fish feed pellets were produced by using a pellet press. First in the late 1980's fish feed producers started replacing simple pelleting by extrusion. Since recently, twin-screw extruders are being introduced into fish feed factories. It should be mentioned that the twin-screw extruders were developed for commercial use first in the 1950's,

although the ground-breaking work came 20 years earlier. Other forms of extrusion, which have found application in human and pet food industry but not yet in the fish feed industry, are co-extrusion and co-injection. Co-injection employs a primary system, which is an extruder, to create the outer texture of a product. Inner texture is injected into the centre of a product by using a secondary system, which is normally a filling pump. Products containing multiple layers of texturally different materials are also attainable with this technique. Co-extrusion involves the use of two extruders connected together to simultaneously extrude two products which fuse into one final product.

The extruders, which were originally designed for producing pasta and cereal pellets, are now considered a high temperature-short time bioreactors which transform raw materials into semi-finished and finished products (Alam et al., 2015). Increased use of the extrusion technology in human food and animal feed production has advanced the technology into a versatile and very productive processing technique. As a result, there is plenty of inexpensive, mass-produced food available in the market today (Dunn, 2011).

Extrusion cooking is preferable to other feed-processing methods in terms of high throughput and continuous process retaining nutritional quality (Makki, 2002). In addition, the extrusion process achieves high degree of gelatinisation of starch, denatures undesirable enzymes, inactivates some antinutritional factors (trypsin inhibitors, haemagglutinins, tannins and phytates), retains natural colours and flavours of foods, sterilises and expends the finished product (Fellows, 2000; Mukhopadhyay et al., 2007; Romarheim et al., 2005).

In this study, fish feed production process based on a single screw extruder was applied. Such a production process consists of a grinder, mixer, supply bin, conditioner, extruder barrel, dryer and a vacuum coater. The mixer is a place where all the ground raw ingredients are mixed into homogenous mixture, so called dry mix. The conditioner has a body with an inlet, an outlet, and rotating mixing elements within the body. The inlet of the conditioner is connected to a screw conveyer for transport of a dry mix from the supply bin to the conditioner. Dry mix is preconditioned to a moisture content of 28-38% at temperature from 70°C to 110°C (Tumuluru, 2014). The conditioner is the place where most of the starch is gelatinised (Zimonja and Svihus, 2009). Furthermore, the outlet of pre-conditioner is operatively coupled with the inlet of an extruder barrel for passage of preconditioned material from the conditioner into the extruder.

The extruder barrel has a body with an inlet, and one or two elongated, axially rotatable, helically flighted extruder screws within the barrel. The barrel is fitted with restricted orifice die at the downstream end (Kartika et al., 2006). In typical processing, the feed ingredients are fed through the extruder barrel where they are subjected to increasing levels of heat, pressure and shear (Oke et al., 2012). As the material moves through the extruder the pressure within the barrel increases due to a restriction at the outlet of the barrel. The restriction is caused by one or more shaped openings called a die. Discharge pressure is typically around 20 bar (Kraugerud et al., 2011). The feed dough is subjected to high shear rates as it is conveyed through the extruder by the action of a screw. Heat is added to the feed dough as it passes through the screw by one or more of three mechanisms: 1) viscous

dissipation of mechanical energy 2) heat transfer from electrical heaters surrounding the barrel and 3) direct injection of steam (Mukhopadhyay et al., 2007).

Temperatures in an extruder can reach >150°C but the residence time at this elevated temperatures is very short (10 – 15 s) (Köksel et al., 2004). When material reaches the end of the barrel it is squeezed out through a die openings, where it experiences a sudden drop in pressure, resulting in the characteristic puffed product also called the extrudate (Harper, 1978). The extrudate may be cut or otherwise subdivided into pellets at the extruder die.

A typical extrusion system is illustrated in the Figure 1.8. The resulting pellets are subjected to post-extrusion treatments such as drying and application of fat/oil. Oil is applied to fish feed in a vacuum coater which is an enclosed chamber with rotating shafts. While oil and dry feed (base pellet) is mixed together, the air is evacuated from the chamber and so from the feed pellet pores. After reaching sufficient pressure (<100 mbar), the air is released back into the chamber. On its way back, the air is pushing oil into the evacuated pellet pores. In this way, possible particles suspended in oil will be incorporated into fish feed provided that they are of appropriate size.

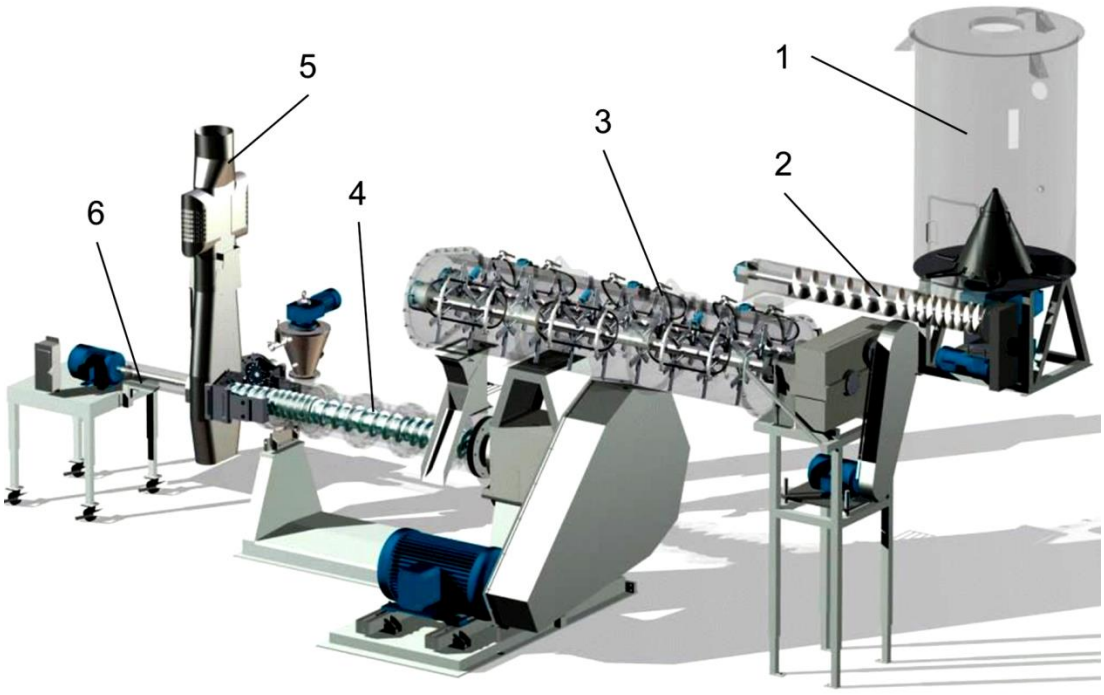

Figure 1.8: Example of an extrusion system consisting of a supply bin (1), screw conveyer (2), pre-conditioner (3), extruder barrel (4), outlet for continuation of pellets to a dryer (5) and a knife mechanism (6). This is an OPTIMA extruder illustrated by Wenger Manufacturing, Inc.

Extrusion is a complex multivariate process that requires careful control if product quality is to be maintained (Samuelsen et al., 2014). This process is defined by several input, system and output parameters (Figure 1.9). Input parameters, which can modify the extrusion process, are screw speed, flow rate, moisture content and hardware setup such as die diameter, screw configuration, shear lock position etc. System parameters, which depend on input parameters, are known while process is running. These parameters include specific mechanical energy (SME), retention time, pressure and temperature. Output parameters are defining quality of the fish feed pellet. Quality of the fish feed pellet could be defined by physical properties (durability, hardness, water stability, fat seepage etc.), chemical properties

(nutritional content, content of negative components such as anti-nutrients, toxic compounds etc.), biological properties (specific growth rate of the fish, feed conversion ratio, health status of the fish etc.) and sensory properties (odour, appearance, texture and taste of the fish). The above mentioned parameters are used in the modelling, system design and system exploitation with a purpose of producing high quality fish feed (Ganjyal et al., 2003).

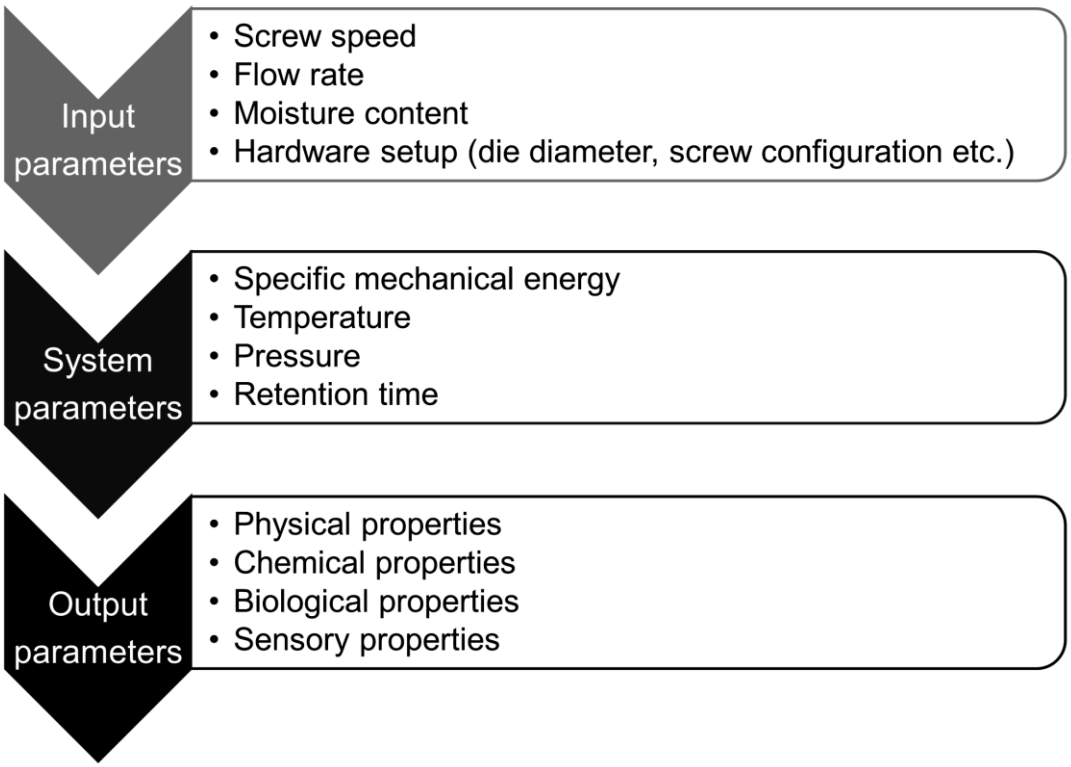

Figure 1.9: An overview of the extrusion process parameters

In the fish farming industry, the feed pellet is the major vehicle for delivery of bioactive compounds including microencapsulated antigens. Microbeads can be added to the extruded feed in two ways. One way is the pre-extrusion addition together with dry mix and water (high temperature). The other way is

post-extrusion addition together with oil in a vacuum coater (low temperature) (Ljungqvist et al., 2013). The latter can effectively be done only if the size of microbeads is small enough to fit into the pores of a feed pellet. Therefore, it can be concluded that success of coating depends both on size of microbeads and size of the feed pellet's pore. Though the alginate beads with diameters of 170 µm (Bugarski *et al.*, 1994) and 50–200 µm (Sugiura *et al.*, 2005) were reported successfully prepared, preparation of smaller beads of less than 200 µm with a narrow size distribution has been impractical to date.

It is difficult to determine pore size of an extruded pellet due to the variability in the size and shape of the pores. The pores have properties depending on size, shape and manner of the constituent particles packing (Draganovic et al., 2013). Too large alginate beads will not be able to enter into the pellet pores and thus remain on the surface of pellet. This in turn may lead to considerable loss of alginate beads causing reduced efficacy of the active compound.

1.7 Thesis objectives

The main objective of this study was to develop an oral delivery system based on alginate with the following characteristics: 1) easy to incorporate into feed pellets via a vacuum infusion coating process, 2) effectively protects antigens throughout fish feed production process 3) protects protein antigens from thermal, acidic and proteolytic degradation in gastrointestinal tract of A. salmon, 4) delivers antigens in the intact form to the distal intestine of salmon and 5) releases antigens *in vivo,* independent of the seasonal temperature changes in the natural habitat of salmon.

In addition, this study aims to assess antigen absorption and immune response as a result of feeding salmon with encapsulated antigens.

1.8 Summary of contribution

This study will increase knowledge on processing of protein antigens and advance alginate encapsulation systems with emphasis on fish health and environmentally friendly solutions. Outcome of this study may lead to a commercial diet for farmed salmon with functional protein antigen protected in alginate matrix. Over the longer term the effective control of aquatic diseases would significantly reduce risks and economically benefit the salmon farming industry. Effective control of pathogens will increase the environmental sustainability of the industry as well. This will reduce mortality, improve welfare of cultured animals as well as reduce transmission to wild stocks.

Chapter Two: Materials and Methods

In this thesis, a great number of chemicals, stock solutions, tools and analytical instruments were used. To get a good overview, four main tables have been created each of which contains information on a specific group of materials. To make it easier to find information on these materials, all used items were tabulated under their unique numbers. Accordingly, the materials used in the experiments are referred to with item number and table number further in the thesis.

In the methods section, only common methods are described. Methods which are specific to only one study are described in their respective chapters. Parameters that vary between experiments are expressed only with symbol and unit in this chapter. Values of the parameters are given in the methods sections of the chapters which are referring to these common methods.

2.1 Materials

All chemicals, raw material and different products which were used in this thesis are listed in the Table 2.1. In the Table 2.2, information on the applied tools is condensed while the used instruments are summarised in the Table 2.3. Type/model, grade, manufacturer and supplier data are declared. In addition, stock solutions are listed in the Table 2.4. The items have been assigned a specific numbers in the first column. These numbers are used as reference numbers further in the thesis.

Table 2.1: Chemicals and raw materials

Item no	Name	Type/grade	Manufacturer	Supplier
C001	Sodium alginate	Na-alginate, Protanal LF 20/40, food grade	FMC BioPolymer AS, Norway	FMC BioPolymer AS, Norway
C002	Calcium chloride dihydrate	$CaCl_2 \cdot 2H_2O$, ≥99 AnalaR NORMAPUR®	VWR International LLC, USA	VWR Ltd., UK
C003	IPNV antigen[i] suspension	IPNV Ag susp., 10^9 $TCID_{50}$ ml^{-1}	NSVS[ii], Norway	NSVS, Norway
C004	Ethylenediamine dihydrochloride	EDA·2HCl, $C_2H_4(NH_2)_2 \cdot 2HCl$, ≥98%	Aldrich Chemical Co. Inc., USA	Sigma-Aldrich Ltd., UK
C004	Sodium bicarbonate	$NaHCO_3$, ≥99 ACS analytical reagent	Alfa Aesar Inc., USA	VWR Ltd., UK
C005	Phosphate buffered saline	1X Dulbecco's PBS without Ca^{2+} and Mg^{2+}, $\kappa=1.6\times10^4$ µS cm^{-1}	Sigma International Inc., USA	Sigma-Aldrich Ltd., UK

Item no	Name	Type/grade	Manufacturer	Supplier
C006	RNA stabilisation solution	RNA*later*®	Sigma International Inc., USA	Sigma-Aldrich AS, Norway
C007	Base pellet	BP, EWOS Opal 200	EWOS Innovation AS, Norway	EWOS Innovation AS, Norway
C008	Commercial feed	EWOS Opal 200	EWOS AS, Norway	EWOS AS, Norway
C009	Commercial feed	EWOS Opal 500	EWOS AS, Norway	EWOS AS, Norway
C010	Horseradish Peroxidase	HRP, P/N 31491	Thermo Fisher Scientific Inc., USA	Perbio Science Ltd., UK
C011	Sodium hydroxide	NaOH flakes, ≥98%,	Alfa Aesar Inc., USA	VWR Ltd., UK
C012	Potassium hydrogen phthalate	KPH, $C_8H_5KO_4$, ≥99%	Alfa Aesar Inc., USA	VWR Ltd., UK
C013	Hydrochloric acid fuming	HCl, 37%, AnalaR NORMAPUR®	VWR International LLC, USA	VWR Ltd., UK
C014	Glycine	Gly, $C_2H_5NO_2$, ≥99%, ReagentPlus®	Sigma International Inc., USA	Sigma-Aldrich Ltd., UK
C015	Disodium phosphate dihydrate	$Na_2HPO_4 \cdot 2H_2O$, ≥99%, analytical reagent	Aldrich Chemical Co. Inc., USA	Sigma-Aldrich Ltd., UK
C016	Monosodium phosphate dihydrate	$NaH_2PO_4 \cdot 2H_2O$, ≥98%, analytical reagent	Aldrich Chemical Co. Inc., USA	Sigma-Aldrich Ltd., UK
C017	Blue dextran	BD, P/N D5751 MW_{avg}=2,000,000	Sigma International Inc., USA	Sigma-Aldrich Ltd., UK
C018	3,3′,5,5′-Tetramethylbenzidine	TMB, Ready-to-use, P/N T8665,	Sigma International	Sigma-Aldrich Ltd., UK

Item no	Name	Type/grade	Manufacturer	Supplier
	liquid substrate system	Premium quality	Inc., USA	
C019	Fish oil	EWOS ID: 20180	Egersund Sildoljefabrikk AS, Norway	Egersund Sildoljefabrikk AS, Norway
C020	Sodium chloride	NaCl, halite ≥99%, ACS analytical reagent	Sigma International Inc., USA	Sigma-Aldrich Ltd., UK
C021	Barium chloride dihydrate	$BaCl_2 \cdot 2H_2O$ ≥99%, ACS analytical reagent	Sigma International Inc., USA	Sigma-Aldrich Ltd., UK
C022	DI water	Deionised water, H_2O, analytical reagent	Fisher Chemical Ltd., UK	Fisher Scientific Ltd, UK
C023	DI water	Deionised water, AnalaR Normapur, $\kappa \leq 0.05\ \mu S\ cm^{-1}$	VWR International LLC, USA	VWR Ltd., UK
C024	Cardiogreen	I2633, dye content, ~90%	Sigma International Inc., USA	Sigma-Aldrich Ltd., UK
C025	Anaesthetic	Finquel vet. tricain mesilate	Scanvacc AS, Norway	Scanvacc AS, Norway
C026	Meal-mix	EWOS OPAL 50	EWOS Innovation AS	EWOS Innovation AS
C026	Multivalent vaccine	ALPHA JECT® micro 6	Pharmaq AS	Pharmaq AS

[i]IPNV antigen – Infectious pancreatic necrosis viral antigen was produced by growing virus (a recombinant Sp strain of IPNV, rNVI-15PTA) as previously reported by (Chen et al., 2013).

[ii]NSVS – Norwegian School of Veterinary Science, Oslo, Norway

Table 2.2: Tools

Item no	Name	Type	Manufacturer	Supplier
T001	Plastic syringe	1 ml BD™	Dickinson and Company Ltd, UK	VWR International AS, Norway
T002	Plastic syringe	60 ml BD™	Dickinson and Company Ltd, UK	VWR International AS, Norway
T003	Syringe pump	PHD4400	Harvard Apparatus Ltd, UK	Harvard Apparatus Ltd, UK
T004	High voltage DC unit	FP-30	Glassman Europe Ltd, UK	Glassman Europe Ltd, UK
T005	High-performance disperser	T-25	IKA® Werke GmbH & Co., Germany	n.a.
T006	96-well plate	Assay plates, round-bottom	Nunc AS, Denmark	Sigma-Aldrich Ltd., UK
T007	Freeze dry system	FreeZone 6	Labconco, USA	Nerliens Meszansky AS, Norway
T008	Pressure regulator	IR1000	SMC Corporation, Japan	n.a.
T009	Sterile syringe filter	0.2 µm, Polyethersulfone (PES) membrane, PN 514-0073	VWR International LLC, USA	VWR Ltd., UK
T010	Coffee filter	Ali number 4	Joh. Johannson Kaffe AS, Norway	Local supermarket, Norway

Item no	Name	Type	Manufacturer	Supplier
T011	Qualitative filter paper	Whatman™, grade 1, d = 125 mm, Particle retention ≥11 µm	Whatman part of GE Healthcare, USA	VWR International AS, Norway
T012	Qualitative filter paper	Whatman™, grade 6, d = 125 mm, Particle retention ≥3 µm	Whatman part of GE Healthcare, USA	VWR International AS, Norway
T013	Needle	ID = 700 µm	Nisco Engineering AG, Switzerland	Nisco Engineering AG, Switzerland
T014	Needle	ID = 2000 µm	Nisco Engineering AG, Switzerland	Nisco Engineering AG, Switzerland
T015	Vacuum coater	VC-6, No 1870	Halvor Forberg AS, Norway	Halvor Forberg AS, Norway
T016	Dissolution tester	Caleva 8ST	Caleva International Ltd., UK	Caleva International Ltd., UK
T017	Extruder	X85	Wenger Inc., USA	Wenger Inc., USA
T018	Spray/jetting head	n.a	Nisco Engineering AG, Switzerland	Nisco Engineering AG, Switzerland
T019	Needle	ID = 1200 µm	Nisco Engineering AG, Switzerland	Nisco Engineering AG, Switzerland
T020	Multivalent vaccine	ALPHA JECT® micro 6	Pharmaq AS	Pharmaq AS

Table 2.3: Analytical instruments

Item no	Name	Model	Manufacturer	Supplier
I001	Stereo microscope	Leica MZ10 F	Leica Microsystems GmbH, Germany	Leica Microsystems, Germany
I002	Microplate reader	GENios, XFLUOR4 Version: V 4.40	Tecan Group Ltd, Switzerland	n.a.
I003	Microplate reader	VERSAmax	Molecular Devices LLC, USA	n.a.
I004	Porosimeter	PoreMaster 60	Quantachrome Corporation, USA	
I005	SEM	Field emission scanning electron microscope, JSM-7401F	Joel Ltd., Japan	Joel Ltd., UK
I006	High-resolution micro-CT scanner	SkyScan 1172	Bruker – MicroCT Ltd., Belgium	RJL Micro and Analytic GmbH, Germany
I007	Laser diffraction system	HELOS BR CUVETTE, CUV-50ML/US, optical module R5	Sympatec GmbH, Germany	Sympatec Ltd., UK
I008	Imaging-based particle analysis system	FlowCAM® PV-100	Fluid Imaging Technologies Inc., USA	Fluid Imaging Technologies Inc., USA
I009	*In vivo* imaging system	IVIS Spectrum	PerkinElmer Inc., USA	Caliper Life Sciences Ltd., UK

Table 2.4: Stock solutions

Item no	Name	Description
S001	EncForm 1	Encapsulation formulation 1 was prepared by dissolving Na-alginate (2.0% w/w, Item C001, Table 2.1) in an IPNV Ag susp. (Item C003, Table 2.1) derived from viral culture with titre of 10^9 $TCID_{50}$ ml^{-1}.
S002	EncForm 2	Encapsulation formulation 2 was prepared by dissolving Na-alginate (2.0% w/w, Item C001, Table 2.1) in ten-fold dilution of IPNV Ag susp. (Item C003, Table 2.1) to produce a formulation containing IPNV Ag 10^8 $TCID_{50}$ ml^{-1}
S003	XlinkSol $CaCl_2$	Calcium chloride cross-linking solution (XlinkSol $CaCl_2$) was prepared by dissolving $CaCl_2 \cdot 2H_2O$ (36.8 g, Item C002, Table 2.1) in DI water (1000 ml, Item C022, Table 2.1)
S004	XlinkSol EDA·2HCl	Ethylenediamine dihydrochloride cross-linking solution (XlinkSol EDA·2HCl) was prepared by dissolving EDA·2HCl (33.3 g, Item C004, Table 2.1) in DI water (1000 ml, Item C022, Table 2.1)
S005	Saturated $NaHCO_3$ solution	Sodium bicarbonate, $NaHCO_3$ (150 g, Item C004, Table 2.1) was mixed with DI water (1000 ml, Item C022, Table 2.1) to produce saturated $NaHCO_3$ solution. Any undissolved $NaHCO_3$ crystals were filtered off prior to use.
S006	BD solution	Blue dextran (BD) solution (50 mg ml^{-1}) was prepared by dissolving blue dextran (10.00 g, Item C017, Table 2.1) in DI water (200 ml, Item C022, Table 2.1)
S007	BD-EncForm	Blue dextran encapsulation formulation, BD-EncForm was generated by dissolving Na-alginate (2.0% w/v, Item C001, Table 2.1) in a BD solution (200 ml, Item S006 in this Table) at ambient temperature.
S008	0.4M NaCl solution	Sodium chloride, NaCl (23.38 g, Item C020, Table 2.1) was dissolved in DI water (1000 ml, Item C022, Table 2.1).
S009	0.4M HCl solution	Hydrochloric acid, HCl (33.33 ml, Item C013, Table 2.1) was mixed with DI water (1000 ml).
S010	0.4M KPH solution	Potassium hydrogen phthalate, KPH (81.69 g, Item C012, Table 2.1) was dissolved in DI water (1000 ml).

Item no	Name	Description
S011	0.4M MSP solution	Monosodium phosphate (MSP) dehydrate, $NaH_2PO_4 \cdot 2H_2O$ (62.40 g, Item C016, Table 2.1) was dissolved in DI water (1000 ml).
S012	0.4M DSP solution	Disodium phosphate (DSP) dehydrate, $Na_2HPO_4 \cdot 2H_2O$ (71.20 g, Item C015, Table 2.1) was dissolved in DI water (1000 ml)
S013	0.4M Glycine solution	Glycine (30.03 g, Item C014, Table 2.1) was dissolved in DI water (1000 ml).
S014	0.4M NaOH solution	Sodium hydroxide, NaOH (16.00 g) was dissolved in DI water (1000 ml).
S015	Buffer pH 1.2	Sodium chloride/hydrochloric acid (NaCl/HCl, pH 1.2) buffer was prepared by mixing 0.4M NaCl solution (250 ml, Item S008 in this Table) with 0.4M HCl solution (425 ml, Item S009 in this Table). Before making up the volume to 1000 ml with DI water, the pH of the buffer solution was adjusted to pH 1.2.
S016	Buffer pH 3.0	Potassium hydrogen phthalate/hydrochloric acid (KPH/HCl, pH 3.0) buffer was prepared by combining 0.4M KPH (500 ml, Item S010 in this Table) with 0.4M HCl (223 ml, Item S009 in this Table). The resulting buffer solution was adjusted to pH 3.0 before replenishing with DI water to give a total volume of 1000 ml.
S017	Buffer pH 6.8	Phosphate buffer (pH 6.8) was created by mixing 0.4M MSP solution (255 ml, Item S011 in this Table) with 0.4M DSP solution (245 ml, Item S012 in this Table). The resulting buffer was adjusted to pH 6.8 before levelling the volume to 1000 ml with DI water.
S018	Buffer pH 8.0	Phosphate buffer (pH 8.0) was created by combining 0.4M MSP (26.5 ml, Item S011 in this Table) with 0.4M DSP (473.5 ml, Item S012 in this Table). The resulting buffer solution was adjusted to pH 8.0 and then diluted with DI water to a final volume of 1000 ml.

Item no	Name	Description
S019	Buffer pH 8.6	Glycine/sodium hydroxide (Gly/NaOH, pH 8.6) buffer was produced by mixing 0.4M glycine solution (250 ml, Item S013 in this Table) with 0.4M NaOH (20 ml, Item S014 in this Table) to produce Gly/NaOH buffer. After fine-tuning the pH to 8.6, the generated buffer solution was diluted to a volume of 1000 ml with DI water (Item C022, Table 2.1).
S020	HRP solution (5000 ppm)	Horseradish peroxidase (HRP) solution (5 mg ml^{-1}) was prepared by dissolving HRP powder (10 mg; Item C10, Table 2.1) in DI water (2.0 ml, Item C022, Table 2.1) at 4°C. Aliquots of this HRP solution (20 µl) were stored at -20°C for application in constructing standard curves in the enzyme assay.
S021	HRP solution (400 ppm)	Horseradish peroxidase (HRP) solution (400 µg ml^{-1}) was prepared by dissolving HRP powder (200 mg; Item C10, Table 2.1) in DI water (500 ml, Item C022, Table 2.1) at 4°C.
S022	HRP-EncForm	Horseradish peroxidase (HRP) encapsulation formulation, HRP-EncForm was generated by dissolving sodium alginate (2.0% w/w, Item C001, Table 2.1) in the 5000 ppm HRP solution (500 ml, Item S021 in this Table) at 4°C.
S023	0.25M $BaCl_2$ solution	Barium chloride dehydrate, $BaCl_2 \cdot 2H_2O$ (61.1 g, Item C021, Table 2.1) was dissolved in DI water (1000 ml, Item C022, Table 2.1)
S024	Na-alginate solution (1.5% w/v)	Sodium alginate (1.50 g, Item C001, Table 2.1) was dissolved in DI water (100 ml, Item C023, Table 2.1).
S025	Na-alginate solution (2.25% w/v)	Sodium alginate (2.25 g, Item C001, Table 2.1) was dissolved in DI water (100 ml, Item C023, Table 2.1).
S026	Na-alginate solution (3.0% w/v)	Sodium alginate (3.00 g, Item C001, Table 2.1) was dissolved in DI water (100 ml, Item C023, Table 2.1).

Item no	Name	Description
S027	Na-alginate solution (2.0% w/v)	Sodium alginate (2.00 g, Item C001, Table 2.1) was dissolved in DI water (100 ml, Item C023, Table 2.1).
S028	Na-alginate solution (1.8% w/v)	Sodium alginate (1.80 g, Item C001, Table 2.1) was dissolved in PBS (100 ml, Item C005, Table 2.1).
S029	CG solution (1000 ppm)	Cardiogreen (CG) solution (1 mg ml^{-1}) was prepared by dissolving CG (15 mg; Item C024, Table 2.1) in DI water (15 ml, Item C022, Table 2.1).
S030	CG-EncForm	Cardiogreen (CG) encapsulation formulation, CG-EncForm was prepared by dissolving sodium alginate (2.0% w/w, Item C001, Table 2.1) in the 1000 ppm CG solution (15 ml, Item S029 in this Table).

2.2 Methods

In this section all common methods are described. Moreover, all important parameters and process variables are listed with their symbols and units. The parameters are assigned values in the methods sections of the chapters referring to the methods described here.

2.2.1 Encapsulation methods

2.2.1.1 Electrospraying

Spherical beads were formed by electrostatic extrusion of an encapsulation formulation (Item S001, S002 or S007; Table 2.4) through a positively charged needle (ID [µm]; Item T013, T014 or T019, Table 2.2) using a syringe pump (Item T003, Table 2.2) and a plastic syringe (Item T002, Table 2.2). The pump was working in the volume mode running at a flow rate of Q [cm^3 h^{-1}] until the target volume (V_{tv} [ml]) was delivered. The resulting jet of droplets was directed from a distance of x [mm] towards a vessel with cross-linking solution (V_{xls} [ml]) which was grounded. The potential difference was maintained at constant voltage (U [kV]) by a high voltage DC unit (Item T004, Table 2.2). Alginate droplets were collected and cured in a cross-linking solution (Item S003 or S004, Table 2.4) under stirring. Solution was removed 10 min after generating the last bead. Thereafter, the recovered alginate beads were washed three times with DI water (5 ml, Item C022, Table 2.1). Encapsulation process variables (ID, Q, V_{tv}, U, x, V_{xls}) are summarised in the Table 2.5. The encapsulation method (electrospraying) is illustrated in the Figure 1.5.

Table 2.5: Electrospraying - process variables with their respective symbols and units.

Internal diameter (needle)	Flow rate	Target volume	Voltage	Distance[i]	Volume[ii]
ID	Q	V_{tv}	U	x	V_{xls}
µm	$cm^3\ h^{-1}$	ml	kV	mm	ml

[i]Distance between the needle tip and the surface of crosslinking solution (x)
[ii]Volume of the cross-linking solution (V_{xls})

2.2.1.2 Aerodynamically assisted jetting/ aerodynamically assisted energised jetting

A jet of alginate droplets was generated by dispersing an encapsulation formulation (Item S022, S024, S025, S026, S027 or S028; Table 2.4) using a jetting/spray head (Figure 1.5; Item T018, Table 2.2). The created jet was directed from a predetermined distance (x [mm]) towards a vessel with cross-linking solution (V_{xls} [ml]; Item S003, S004, S023; Table 2.4). Hovering aerosols and very fine micro-droplets was attracted to the cross-linking solution by using a high voltage DC generator (Item T004, Table 2.2). The positive voltage output was connected to the jetting head (Item T018, Table 2.2) while the cross-linking solution was grounded. The applied voltage (U [kV]) was modified in accordance with the experimental design. Flow rate (Q [$cm^3\ h^{-1}$]) was controlled by high precision syringe pump (Item T003, Table 2.2) working in the volume mode (V_{tv} [ml]). The air pressure (P [bar]) was regulated by a pressure regulator (Item T008, Table 2.2) which was equipped with a digital pressure controller. Process variables x, V_{xls}, U, Q, V_{tv} and P are summarised in Table 2.6. The encapsulation method (aerodynamically

assisted energised jetting) is illustrated in the Figure 1.6. Method without any voltage applied is called aerodynamically assisted jetting.

Table 2.6: Air pressure-assisted energised jetting - process variables with their respective symbols and units.

Distance[i]	Volume[ii]	Voltage	Flow rate	Target volume	Pressure
x	V_{xls}	U	Q	V_{tv}	P
mm	ml	kV	$cm^3\ h^{-1}$	ml	bar

[i]Distance between the jetting head and the surface of crosslinking solution (x)
[ii]Volume of the cross-linking solution (V_{xls})

2.2.2 Dissolution test

Dissolution tester (Item T016, Table 2.2) equipped with dissolution vessels (V = 1000 ml) and rotating stainless steel baskets (40 mesh) was employed to assess release from alginate beads. This setup was in compliance with the standard requirements for Apparatus 1 set by United States Pharmacopoeia (USP) and described in General Chapter <711> (USP, 2012a). Dissolution medium (V [ml]; DM: Item S015, S016, S017, S018 or S019, Table 2.4) was added into each of the vessels (n_{vessel}) and then allowed to temperate overnight at the experimental temperature (t [°C]). The dissolution test started within two hours after producing alginate beads. The alginate beads (AB) were placed into rotating baskets (f [rpm]) and then submerged into dissolution medium.

Sample volume (V_{sample} [ml], n_{SP}) was taken from each vessel at five minutes intervals through an extent of 50 minutes (t_{SP} [min]). An equivalent volume of dissolution medium was then added back to keep the liquid level in the

vessels constant. All samples were filtered through a syringe filter (Item T009, Table 2.2) before applying aliquots of 100 µl onto a 96-well polystyrene plate (Item T006, Table 2.2). An endpoint assay was then performed using a microplate reader (Item I003, Table 2.3) at 610 nm and 24°C. Amount of blue dextran (BD) released was determined by applying standard curve approach. The standard curves were generated by plotting BD concentrations of nine two-fold serial dilutions of BD solution (1.0 mg ml^{-1}) versus absorbance in the range of 1.0 to 3.9×10^{-3} mg ml^{-1}. The BD solution (1.0 mg ml^{-1}) was derived from BD-EncForm (Item S007, Table 2.4) using the phosphate buffer (Item C005, Table 2.1) as a diluent. All of the above-mentioned dissolution parameters are listed in the Table 2.7.

Table 2.7: Dissolution parameters with their respective symbols and units.

Parameters	Symbol	Unit
Alginate beads loaded with blue dextran	AB	n.a
Apparatus	USP 1	n.a
Basket rotation	f	rpm
Type of dissolution media	DM	n.a
Volume of dissolution media	V	ml
Temperature of dissolution media	t	°C
Number of sampling points	n_{SP}	n.a.
Length of sampling time intervals calculated from the test start	t_{SP}	min
Number of vessels used in the test	n_{vessel}	n.a
Sample volume	V_{sample}	ml

2.2.3 Fish feed production

Fish feed production was conducted at Technology Centre (Ewos Innovation AS) in Dirdal (Norway).

Extruder runs were performed on the extruder (Item T017, Table 2.2) with single-screw volumetric feeder. The extruder barrel was not heated by using external devices. Experimental conditions and parameters for extruder runs including drying are listed in the Table 2.8. Feed rate, total liquid addition and temperature in the dryer were held constant. Temperature is monitored throughout the entire process. There are one measurement point in the supply bin and pre-conditioner, seven measurement points in extruder and three measurement points in the dryer. Pressure is only monitored in seven zones of the extruder. Furthermore, the process log contains information on flow rates of dry mix, water and steam. Mass flow through the extruder is recorded as well. System parameters such as specific mechanical energy, extruder screw speed, discharge rate and current are also specified.

This experimental facility for fish feed production is very well monitored which enables high degree of control in the experiments.

Table 2.8: The adjustable parameters of the applied extrusion process including drying.

Preconditioner		
Factor	Parameters	Unit
Meal	Feed rate (meal blend)	kg/h
	Temperature meal	^{o}C
Water	Water flow rate	kg/h
	Water flow rate (dry mixture)	%
	Water temperature	^{o}C
Steam	Steam flow rate	kg/h
	Steam flow rate (dry mixture)	%
Total	Total liquid addition	kg/h
	Total liquid addition	%
Extruder		
Engine	Extruder screw speed	rpm
	Extruder motor load	kW
	Current	A
	Specific mechanical energy (SME)	kW/tons/h
Temperature	Zone 1 (precond. outlet temp.)	^{o}C
	Zone 2	^{o}C
	Zone 3	^{o}C
	Zone 4	^{o}C
	Zone 5	^{o}C
	Zone 6	^{o}C
	Zone 7	^{o}C
	Spacer	^{o}C
Pressure (gauge)	Zone 1 (precond. outlet temp.)	^{o}C
	Zone 2	^{o}C
	Zone 3	^{o}C
	Zone 4	^{o}C
	Zone 5	^{o}C
	Zone 6	bar
	Zone 7	bar
	spacer	bar
Mass flow	Total die area	mm^2
	Total cylinder area	mm^2
	Extruder discharge rate	kg/h
Dryer		
Temp	Zone 1	^{o}C
	Zone 2	^{o}C
	Zone 3	^{o}C

2.2.4 Vacuum infusion coating

The final feed samples were produced by combining an oil mixture with the right amount of base pellet (BP; Item C007, Table 2.1) in a vacuum coater (Item T015, Table 2.2). Firstly, the air was evacuated from the mixing chamber and so from the feed pellet pores. Secondly, after reaching pressure of 88 mbar, the air was released back into the chamber. On its way back, the air was pushing oil into the empty pellet pores. In this way, the suitably-sized particles suspended in the oil mixture, were incorporated into feed pellets.

The major activities related to the coating process were described with three primary process variables: time, pressure and temperature. These activities and their variables are listed in the order of execution in the Table 2.9.

Table 2.9: The controllable variable related to the applied vacuum infusion coating process. The major activities are described by primary process variables (time, pressure and temperature) in the vacuum infusion coating process. These variables were kept constant for each activity in all trials.

Order	Activity name	Time [sec]		Pressure [mbar]		Temperature [°C]	
		Start	End	Start	End	Start	End
1	Adding BP to the mixing chamber[i]	0	10	ambient	ambient	ambient	ambient
2	Adding oil mixture to BP[ii]	11	20	ambient	ambient	ambient	ambient
3	Closing the chamber	21	35	ambient	ambient	ambient	ambient
4	Turning on the mixing gear	36	40	ambient	ambient	ambient	ambient
5	Evacuating the air from the chamber	41	100	ambient	88	ambient	ambient
6	Holding the reduced pressure	101	105	88	88	ambient	ambient
7	Letting the air back into the chamber	106	285	88	ambient	ambient	ambient
8	Turning off the mixing gear	286	290	ambient	ambient	ambient	ambient
9	Opening the chamber	291	305	ambient	ambient	ambient	ambient
10	Emptying the chamber	306	360	ambient	ambient	ambient	ambient

[i]Chamber – part of the coater where mixing of BP with oil takes place under reduced pressure

[ii]Oil mixture had temperature of 37°C prior to addition which took place at ambient temperature (18°C)

2.2.5 Fish trial designs

2.2.5.1 Voluntary feeding

A. salmon (m_{fish} [g]) was randomly distributed in circular tanks containing cold seawater (t [°C]) with constant oxygen level (O_2 [%]). The tanks were of the same size (d_{tanks} [m], V_{tanks} [m^3]) but could vary in numbers (n_{tanks}) between trials. Fish (n_{fish}) were randomly divided into groups (n_{groups}) with three tanks being assigned to each group. Prior to the start of each treatment fish were acclimatised for a certain number of weeks (t_{accl} [weeks]). The treatment usually lasted for one to two weeks (t_{treat} [weeks]) after which followed a sampling ($n_{sf/t}$, t_{SP} [weeks]). In the immune response trial, the treatments would be followed by an immune induction period, and sampling ($n_{sf/t}$, t_{SP} [weeks]) would take place at the end of each such period. There were two treatments so called oral boost (OB) periods (t_{OB} [weeks]), and thus two induction intervals [t_{induc} [weeks]). In accordance with the ordinary veterinary procedure, all sampled fish were anesthetised with tricain mesilate (100 mg l^{-1}; Item C025, Table 2.1). Furthermore, the individual weight of the fish was recorded for each sampled fish. In the end, it was noted that the health of the fish was relatively good during the trials.

All of the above-mentioned parameters are condensed in the Table 2.10. The applied values of parameters are specified in the method sections of the chapters referring to this fish trial design.

2.2.5.2 Oral intubation

A. salmon (m_{fish} [g]) were randomly selected from an acclimatisation tanks (pool of several hundred fish) for treatments (n_{treat}) carried out by oral intubation. The orally intubated fish (n_{fish}) which received the same treatment were placed in the same tank right after the intubation. As a consequence, the number of treatments corresponded to the number of tanks (n_{tanks}) and the number of groups (n_{groups}). The tanks, which were of the same size (d_{tanks} [m], V_{tanks} [m^3]), contained cold seawater (t [°C]). Level of oxygen (O_2 [%]) in the seawater was maintained constant during the trail. Fish ($n_{sf/t}$) were repeatedly sampled from each tank at certain time points (n_{SP}) scheduled few hours apart (t_{SP} [hours]). Each fish were anesthetised with tricain mesilate (100 mg l^{-1}; Item C025, Table 2.1) prior to both intubation and sampling. In the end, individual weight of the fish was recorded for each sampled fish.

The aforementioned parameters are listed in the Table 2.10. The applied values of parameters are declared in the method sections of the chapters referring to the fish trial by oral intubation

Table 2.10: Variable parameters of the fish trials based on voluntary feeding and oral intubation

Parameter	Symbol	Unit
Average weight of fish	m	g
Oxygen saturation in water	O_2	%
Water temperature	t	°C
Diameter of a tank	d	m
Volume of a tank	V	m^3
Number of tanks	n_{tanks}	n.a.
Number of fish per tank	n_{fish}	n.a.
Number of groups	n_{groups}	n.a.
Number of treatments	n_{treat}	n.a.
Number of sampled fish per tank	$n_{sf/t}$	n.a.
Number of sampling points	n_{SP}	n.a
Length of the acclimatisation period	t_{accl}	weeks
Length of the treatment period	t_{treat}	weeks
Length of the oral boost period	t_{OB}	weeks
Length of the immune induction period	t_{induc}	weeks
Length of the time intervals from the end of treatment to sampling	t_{SP}	hours/weeks

2.2.6 Statistical analysis

2.2.6.1 Statistical analysis of high voltage and encapsulation efficiency data

All statistical modeling of both high voltage and encapsulation efficiency data was conducted with the R language (version 3.0.2, released 25/09/2013) and its corresponding packages. The data structure of both experiments was multilevel with random variation related to replicated samples within the experiment that were split to multiple ELISA samples on the 96-well plate in the time of analysis. A multilevel model was fitted with the “lmer” function from the “lme4” package. Nested models with increasing complexity (null,

linear and nonlinear model based on cubic spline function) were compared to determine the most likely model in a likelihood ratio test (LRT). Significance level was set to $P < 0.01$.

2.2.6.2 Statistical analysis of antigen uptake and immunogenicity data

Statistical modeling of fish trial data was conducted with the R language (version 2.15.0, released 30/03/2012) and its corresponding packages. Data analysis was performed using regression and multilevel, hierarchical models with the “arm” package. This model was selected because multiple samples from each group had multiple ELISA values. The ELISA values were transformed to logarithms before statistical analysis to account for the constrained distribution. For estimation and prediction, linear mixed effect model was applied. For fitting of the model, the “lmer” function from the “lme4” package was used. Expected responses with 95% credible intervals for the respective treatments were generated by posterior simulations of fixed effects from the linear mixed effect model (n = 1500 random draws).

2.2.6.3 Statistical analysis of data obtained from dissolution and release studies

Dissolution profiles of BD shown as curves of the mean percentage of cumulative BD release with error bars (95% confidence intervals) over time were generated using Data analysis and Scatter plot functions in Microsoft Excel 2010. Mean HRP concentrations with error bars (95% confidence intervals) found in different compartments of gastrointestinal tract were calculated and represented in a graph using IBM SPSS Statistics for Windows, version 22.0.

2.2.6.4 Statistical analysis of data obtained from the study of antigen stability in fish feed production process

Experimental design was a 2^2 factorial with process (mild or standard/hot) and encapsulation (yes or no) as the factors. In addition, there were another two treatments described as “standard process with no antigen (Negative control)" and “no process with antigen (Positive control)". These two additional treatments were not part of the 2^2 factorial design and the following corresponding statistical analysis but are included in all raw data plots. Sampling was performed at five different stages in the production process: mixing (dry mix, dm), conditioning (wet mix, wm), extrusion (extrudate, ext), drying (base pellet, bp) and coating (final feed, ff). Five samples per treatment were taken for each step and analysed in duplicate with ELISA. An additional nuisance variable to consider in the statistical modeling was the position of the sample on the ELISA plate. The statistical model applied was a multilevel (mixed-effects) first degree model for the 2^2 factorial. A random effect of ELISA run was added to account for the variability between duplicates. All statistical modelling was conducted with the R language (version 2.15.1, released 22/06/2012) and its corresponding packages. Loading required “xtable” and “arm” packages and setup of “lmerSim” function.

Chapter Three: Uptake and Immunogenicity of IPNV antigens

Infectious pancreatic necrosis (IPN) is an acute, clinical disease with large impact on salmon production. IPN virus causes mortality in young freshwater salmonids with an increasing number of outbreaks during the first months after transferring to seawater. For this reason, the main focus of this chapter is a systemic priming/oral boost strategy in immunising A. salmon. Accordingly, the specific immune response was assessed in the fish which were treated with oral IPN vaccines 12 months after intraperitoneal vaccination. However, before conducting the immune response trial, the ability of A. salmon to absorb both alginate-encapsulated and free IPNV antigen was checked in a separate trial. Moreover, the quality of the oral IPNV antigen preparations was evaluated by two factors: 1) the encapsulation efficiency of alginate matrices, and 2) the effect of high voltage (an encapsulation process parameter) on antigen viability.

3.1 Introduction

Farmed salmonid fish are constantly challenged by various pathogens, especially during the sea water production phase (Collet, 2014). The common practice in the aquaculture industry has been to give an intraperitoneal (i.p.) injection to pre-smolt with a multivalent vaccine (e.g. ALPHA JECT® micro 4, 5-1 or 6 from Pharmaq). Following a short period of immunisation, full-grown smolt is transferred into seawater cages (Lillehaug, 1997). After this point, it is no longer practical to i.p. vaccinate fish.

In some experts' opinion, the bacterial i.p. vaccines appear to be more effective than the viral i.p. vaccines in the field. In their view, some of the viral vaccines may not exert sufficient long-lasting protective effects (Gudding and Van Muiswinkel, 2013; Robertsen, 2011). Delivery of an oral boost vaccine could re-immunise previously vaccinated fish and thus prolong the effect of an i.p. vaccine after some months in seawater (Lauterslager et al., 2003; Zhang et al., 2014).

There are currently several commercially available injection IPN vaccines, no immersion and only one oral subunit vaccine. Notably, this oral vaccine (AquaVac® IPN Oral, MSD Animal Health) has been given marketing authorisation only in Chile (Dhar et al., 2014). However, there are very few studies reporting successful development of an oral vaccine against the IPN.

Allnutt et al. (2007) observe the immune response specific for IPNV which is induced by an orally administered yeast-based recombinant DNA vaccine in rainbow trout (*Oncorhynchus mykiss*). The study also demonstrates the ability of immunised fish to reduce the IPN viral load in a challenge trial.

Rodriguez Saint-Jean et al. (2010) report that alginate microspheres loaded with a pDNA encoding for VP2 of the IPN virus, immunise rainbow trout obtaining 80% relative survival (RPS) in a challenge trial. Similarly, Ballesteros et al. (2012) suggest that alginate beads loaded with a pDNA encoding for VP2 immunize rainbow trout against IPN in a way resembling IPN virus. Work by Min et al. (2012) describes the mucosal and systemic immune responses specific for IPN virus. This immune response is induced by an orally administered *Lactobacilli*-based recombinant DNA vaccine in rainbow trout. In the same study, the orally immunised fish with this recombinant DNA vaccine reduced the IPN viral load in a challenge trial. However, there are several concerns associated with DNA vaccines which raise issues in terms of licensing and public acceptance of the technology (Evensen and Leong 2013, Hølvold et al. 2014). Some of the issues are the hypothetical integration of pDNA into fish genome (Nichols et al., 1995; Smith and Klinman, 2001) and the possible release of pDNA into the environment (Tonheim et al., 2008). Here, the potential consumption of fish meat contaminated with pDNA and the potential uptake of pDNA by intestinal bacteria are of particular concern (Hohlweg and Doerfler, 2001; Lorenzen and LaPatra, 2005). Despite these concerns there is a plasmid DNA-based vaccine that is gained marketing authorization from the Canadian Food Inspection Agency (CFIA) in 2005. This i.p. vaccine (Apex®-IHN, Novartis Animal Health) is used to prevent infectious hematopoietic necrosis (IHN) in salmon farmed in the Pacific Northwest.

There are also reports showing a successful assessment of oral vaccines against bacterial pathogens like *P. salmonis* (Tobar et al., 2011), *E. ictaluri*

(Thinh et al., 2009) and *L. garvieae* (Romalde et al., 2004). High RPSs (50-90%) were achieved when these vaccines were applied as a means of boosting the immune response in previously vaccinated fish. However, there are studies involving oral vaccines which are not equally successful. For instance, Santos et al., (2005) reported that delivering an oral boost vaccine after a primary vaccination by injection did not enhance protection of turbot (*Scophthalmus maximus*) against *A. salmonicida*.

Many oral vaccines turned out to be ineffective as a result of failing to 1) deliver sufficient dosage of antigen, 2) protect antigen from degradation in the digestive tract and 3) assist antigen in crossing the intestinal epithelium layer (Plant and Lapatra, 2011; Sommerset et al., 2005).

The present study addresses a systemic priming/oral boost strategy. This strategy involves i.p. priming of A. salmon with a combination vaccine (incl. IPNV antigens) followed by oral boosting with alginate-encapsulated IPNV antigens. These antigens are killed IPN viruses produced by growing virus (a recombinant Sp strain of IPNV, rNVI-15PTA) as previously reported by (Chen et al., 2013). The primary aim of this study was to examine whether the orally administered alginate-encapsulated IPNV antigens, could boost the specific immunity against IPN in the i.p. vaccinated A. salmon. A secondary aim of this study was to compare ethylenediammonium alginate- to calcium alginate-encapsulated IPNV antigen with respect to the specific immune response. To determine the quality of the oral antigen preparations, two additional factors were assessed: 1) the encapsulation efficiency of alginate matrices, and 2) the effect of high voltage (an encapsulation process parameter) on antigen viability.

3.2 Adverse effects and efficiency of the encapsulation

Electrospraying is a method that makes use of high voltage to create a jet of droplets for curing in crosslinking solution. Therefore, it is important to learn whether that high voltage is harmful for antigens. Moreover, it is also essential to know how much of the antigen added to an encapsulation formulation is actually encapsulated in alginate beads. This is determined by the encapsulation efficiency of alginate along with the encapsulation method.

3.2.1 Methods

3.2.1.1 Effect of high voltage on IPNV antigen viability

To assess the effect of high voltage on IPNV antigen viability, the encapsulation formulation (Item S001, Table 2.4) was electrosprayed into PBS (Item C005, Table 2.1) at different voltage levels. The electrospraying was conducted according to the general method described in the Section 2.2.1.1 (Chapter 2). The applied process variables are summarised in the Table 4.1. The exception was the use of PBS instead of a crosslinking solution. Consequently, no alginate beads were formed. In fact, crosslinking was an unnecessary action in this study. It would only introduce a need for an additional step to dissolve the created alginate beads.

Five samples were generated at each voltage level (0, 5, 10, 15, 20 and 25 kV) while the other parameters were kept constant. The samples (0 kV) produced without voltage, served as a reference samples (Figure 3.1). Concentration of IPNV Ag was determined in an ELISA assay at Norwegian School of Veterinary Science (Oslo, Norway). ELISA was performed in quadruplicate with minor modifications as previously described by

Munang'andu et al. (2012). On the other hand, statistical analysis was carried out according to the method described in the Section 2.2.6.1 (Chapter 2).

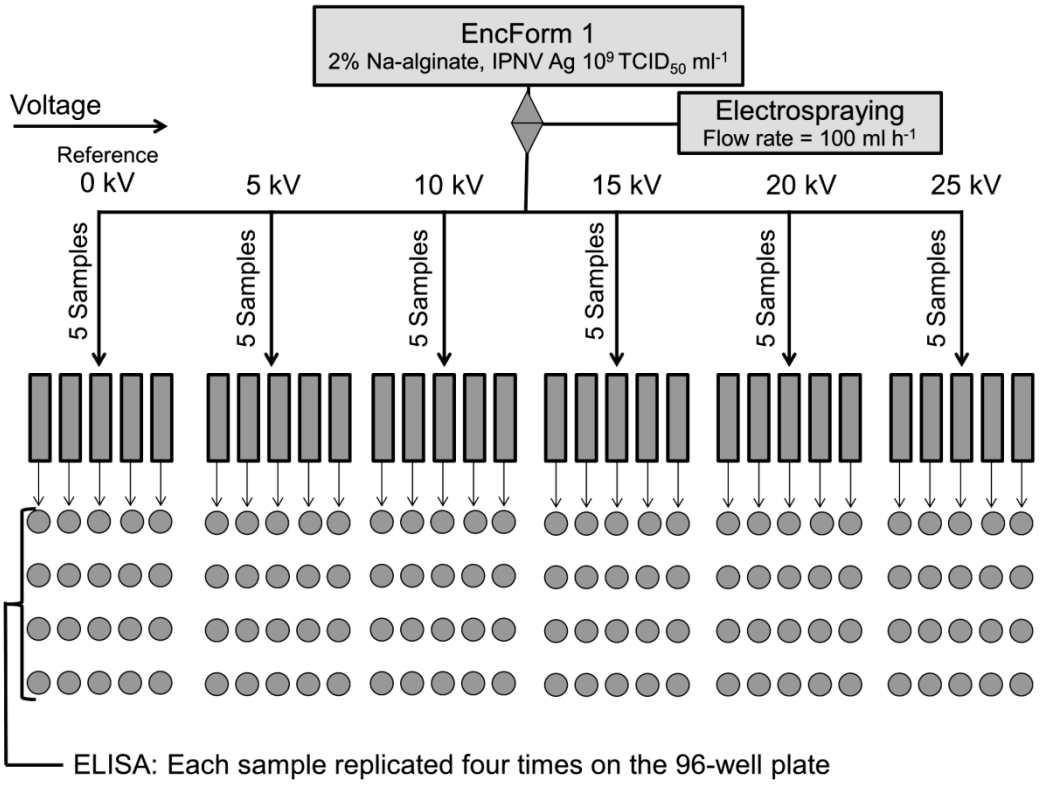

Figure 3.1: Experimental design of the high voltage test. Scheme for generating samples in the experiment assessing the effect of high voltage on IPNV Ag viability. Encapsulation formulation (EncForm 1: V = 1.0 ml, 2% sodium alginate, IPNV antigen 10^9 $TCID_{50}$ ml^{-1}) was extruded into PBS solution (9.0 ml) at constant flow rate (100.00 ml h^{-1}) with the assistance of voltage. Five samples were generated at each voltage level (0 kV, 5, 10, 15, 20 and 25 kV). The samples generated without voltage applied (0 kV) served as reference samples. Afterwards, each sample was replicated four times in an ELISA assay resulting in the total number of 120 samples on the 96-well plate.

Table 3.1: Process variables with their respective values for testing of the effect of high voltage on the antigen viability.

Internal diameter (needle)	Flow rate	Target volume	Voltage	Distance[i]	Volume[ii]
ID	Q	V_{tv}	U	x	V_{PBS}
µm	$cm^3\ h^{-1}$	ml	kV	mm	ml
2000	100	1.0	variable[iii]	100	9.0

[i]Distance between the needle tip and the surface of crosslinking solution (x)

[ii]Volume of PBS (V_{PBS})

[iii]Six levels of voltage were used: 0, 5, 10, 15, 20 and 25 kV

3.2.1.2 Encapsulation efficiency

Encapsulation efficiency of the IPNV antigen in alginate matrices was determined by using two different encapsulation formulations (Item S001 and S002, Table 2.4). Those two formulations were in turn combined with two types of crosslinking solution (Item S003 and S004). Samples of alginate beads (n_{sample} = 30) were produced according to the general method described in the Section 2.2.1.1 (Chapter 2). Notably, the non-use of voltage (U) was a deviation from the general method. For a better overview, the controlled variables of the encapsulation process are condensed in the Table 3.2. Moreover, the applied encapsulation formulations along with their corresponding crosslinking solutions are listed in the Table 3.3. In should also be noted that the needle (Item T014, Table 2.2) and the sodium bicarbonate solution (Item S005, Table 2.4) were utilised during the process of encapsulation. Ultimately, it was generated five of each of the following alginate samples: 10^8-Ca-alg, 10^9-Ca-alg, 10^8-EDA-alg and 10^9-EDA-alg. For

clarity reasons, the process of obtaining samples is schematically shown in the Figure 3.2. After preparation, the alginate beads were dissolved in the saturated sodium bicarbonate solution (9.0 ml). Dissolution was completed within an hour under stirring. To equalise all sample volumes, the level of the resulting solutions was adjusted to 10.0 ml before taking samples of 1.0 ml. Unlike the other samples, the reference samples (Ca-Ref and EDA-Ref) were produced by direct extrusion of encapsulation formulations (1.0 ml) into the saturated bicarbonate solution (9.0 ml). In the end, each sample was diluted with PBS (Item C005, Table 2.1) to an antigen level of 10^7 $TCID_{50}$ ml^{-1}.

Level of IPNV antigen in the samples was determined in an enzyme-linked immunosorbent assay (ELISA) at Norwegian School of Veterinary Science (Oslo, Norway). ELISA was performed in triplicate with minor modifications as previously described by Munang'andu et al. (2012).

Encapsulation efficiency was calculated on the basis of the data obtained from the ELISA test (Equation 3.1). Encapsulation efficiency was defined as the percent ratio of the total amount of encapsulated antigen (EncapAg) to the total amount of antigen in a reference sample (RefAg).

Finally, statistical analysis was performed according to the method described in the Section 2.2.6.1.

Table 3.2: Encapsulation efficiency test - process variables with their respective values.

Internal diameter (needle)	Flow rate	Target volume	Voltage	Distance[i]	Volume[ii]
ID	Q	V_{tv}	U	x	V_{xls}
µm	$cm^3\ h^{-1}$	ml	kV	mm	ml
2000	60	1.0	0	50	9.0

[i]Distance between the needle tip and the surface of crosslinking solution (x)
[ii]Volume of crosslinking solution (V_{xls})

Equation 3.1: Calculation of encapsulation efficiency (%EE)

$$EE = \frac{EncapAg}{\mathrm{Re}\ fAg} \cdot 100$$

EE – Encapsulation efficiency
EncapAg – Optical density (OD) of encapsulated antigen (ELISA value)
RefAg – OD of a reference sample (ELISA value

Table 3.3: Alginate beads generated in the encapsulation efficiency test. Generated alginate beads in relation to the type of alginate matrix (Ca-/EDA-alginate) and encapsulation formulation (EncForm 1 or 2) along with cross-linking solution (XlinkSol) applied in the encapsulation process.

	Ca-alginate beads			EDA-alginate beads		
	Ca-Ref	10^8-Ca	10^9-Ca	EDA-Ref	10^8-EDA	10^9-EDA
EncForm[i]	1	2	1	1	2	1
XlinkSol[ii]	NaHCO3[iii]	CaCl2	CaCl2	NaHCO3	EDA·2HCl	EDA·2HCl

[i]Encapsulation formulations – (EncForm) 1: IPNV Ag 10^9 $TCID_{50}$ ml^{-1} (Item S001, Table 2.4), EncForm 2: IPNV Ag 10^8 $TCID_{50}$ ml^{-1} (Item S002, Table 2.4)
[ii]Cross-linking solution (XlinkSol): calcium chloride ($CaCl_2$; Item S003, Table 2.4) and ethylenediamine dihydrochloride (EDA·2HCl; Item S004, Table 2.4)
[iii]Saturated sodium bicarbonate ($NaHCO_3$; tem S005, Table 2.4) does not cross-link but dissolves sodium alginate.

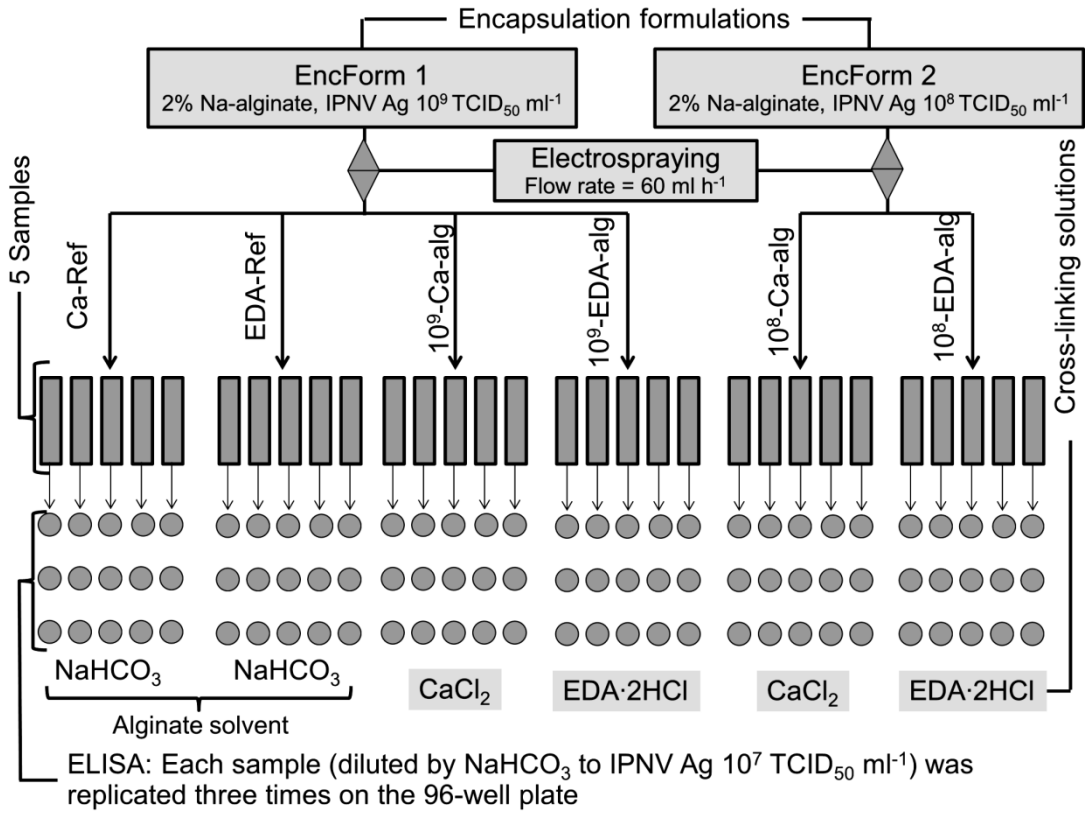

Figure 3.2: Experimental design of the encapsulation efficiency test. Scheme for generating samples in the experiment assessing encapsulation efficiency of two different IPNV antigen concentrations (10^8 and 10^9 $TCID_{50}$ ml^{-1}) in two types of alginate matrix (calcium alginate [Ca-alg] and ethylenediammonium alginate [EDA-alg]). Encapsulation formulation (EncForm 1) was electrostatically extruded to produce the reference samples (Ca-Ref and EDA-Ref, n = 5 samples each). Similarly, EncForm 1 was used to generate the Ca-alg (n = 5 samples) and EDA-alg beads (n = 5 samples) with high IPNV antigen concentration. Encapsulation formulation (EncForm 2) was utilised to produce Ca-alg (n = 5 samples) and EDA-alg beads (n = 5 samples) with low IPNV antigen concentration. Both of Ca-alg samples (high and low antigen level) were cross-linked with calcium chloride ($CaCl_2$) while both of EDA-alg were cross-linked with ethylenediamine dihydrochloride (EDA·2HCl). The reference samples were not cross-linked. Alternatively, they were directly extruded into sodium bicarbonate ($NaHCO_3$). Sodium bicarbonate was also applied in dissolving cross-linked alginate beads as well as in diluting the resulting alginate solutions to an antigen level (10^7 $TCID_{50}$ ml^{-1}) suitable for ELISA assay. Ultimately, each sample was replicated three times in an ELISA assay resulting in the total number of 90 samples on the 96-well plate.

3.2.2 Results

3.2.2.1 Effect of high voltage on IPNV Ag viability

According to the likelihood ratio test (LRT), the linear model does not produce significantly greater log-likelihood than the null model at 1% significance level ($p>0.3282$). Furthermore, the nonlinear model does not fit significantly better than the linear model at the same significance level ($p>0.8722$). It means that even nonlinear model cannot generate greater log-likelihood than null model at 1% level (Figure 3.4). In other words, there is no statistically significant difference between the reference samples (0 kV) and the electrostatically extruded samples (5-25 kV), (Figure 3.3).

Table 3.4: Likelihood ratio test statistic of the high voltage experiment. Likelihood ratio test statistic for the nested models (null, linear and nonlinear model). Neither linear ($p>0.3282$) nor nonlinear model ($p>0.8722$, versus linear model) fit significantly better than null model at the 5% significance level.

Model type	logLik[i]	Deviance[ii]	Chisq[iii]	Df[iv]	p(>chisq)[v]
Null	200.15	-400.30	n.a.	n.a.	n.a.
Linear	200.63	-401.26	0.9558	1	0.3282
Nonlinear	200.98	-401.96	0.7043	3	0.8722

[i]logLik – log-likelihood ratio statistic
[ii]Deviance – negative twice the log-likelihood
[iii]Chisq – Chi (X^2) square value
[iv]Df – Degrees of freedom – difference between number of free parameters in a "complex model" and a "simpler model".
[v]p(>chisq) – Probability of occurrence for an X^2 value depending on degrees of freedom (p-value).

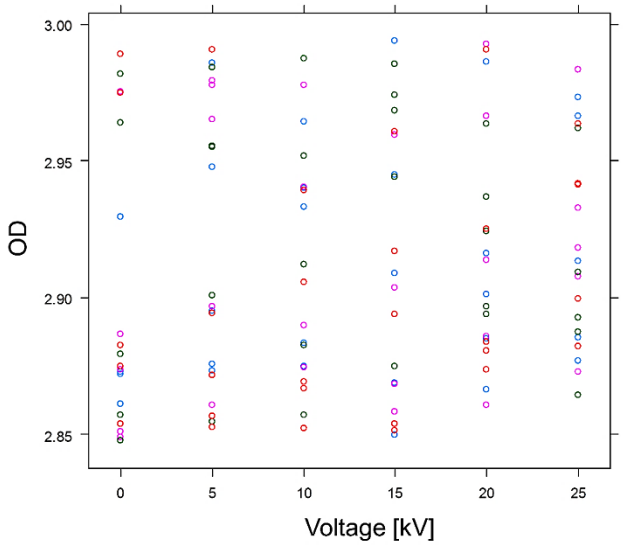

Figure 3.3: Observed OD values in relation to the voltage (kV) in the high voltage experiment. The ELISA samples (n = 20 per voltage level) are represented by a circlet. The samples taken at each voltage level (n = 5) are denoted by five different colours. The difference between the number of samples, which are taken and analysed, results from the fact that each sample taken was replicated four times on the 96-well plate. The likelihood ratio test (LRT) suggests there is no effect of voltage on the viability of IPNV antigen.

3.2.2.2 Encapsulation efficiency

The average encapsulation efficiency of 10^9-Ca-alg and 10^9-EDA-alg was 78% and 97% respectively. However, difference between the sample means of Ca-Ref and 10^8-Ca-alg cannot be considered as statistically significant at the 5% level (Figure 3.4). Equally, the ratio of 10^8-EDA-alg to EDA-Ref is not statistically significant at the same level. This suggests that IPNV antigen suspended at 10^8 $TCID_{50}$ ml^{-1} could be entrapped in an alginate matrix with negligible loss.

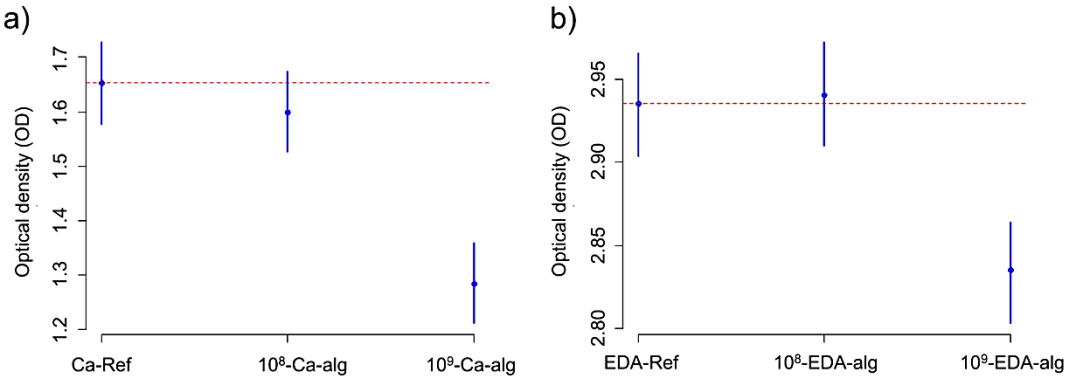

Figure 3.4: Results of the encapsulation efficiency test. Encapsulation efficiency (EE) of a) Calcium alginate at 10^8 (n.s. loss) and 10^9 (EE = 78%) $TCID_{50}$ ml^{-1} and b) Ethylenediammonium alginate at 10^8 (n.s. loss) and 10^9 (EE = 97%) $TCID_{50}$ ml^{-1} IPNV antigen. Error bars represent 95% confidence intervals. n.s. stands for “not significant”

3.3 Uptake of IPNV antigen in A. salmon

Uptake of IPNV antigen to blood plasma of A. salmon was assessed in this study. There were for treatments: 1) alginate-encapsulated antigen, 2) un-encapsulated antigen, 3) empty alginate beads and 4) PBS. The preparations were oral intubated into fish and the IgM level was determined in an ELISA assay.

3.3.1 Methods

3.3.1.1 Preparation of alginate beads loaded with antigen

Alginate beads loaded with IPNV antigen were prepared according to the general encapsulation method described in the Section 2.2.1.1. Controlled variables of the encapsulation process (electrospraying) are summarised in the Figure 4.5. In the process of encapsulation, the following items were used: encapsulation formulation (Item S001, Table 2.4), alginate solution (Item S028, Table 2.4), a needle (Item, T013, Table 2.2) and cross-linking solution (Item S003, Table 2.4). In order to reach the target dose (10^9 $TCID_{50}$ of IPNV antigen per fish), encapsulation efficiency (78%) of IPNV antigen (10^9 $TCID_{50}$ ml^{-1}) in calcium alginate was taken into consideration. As a result, 30 batches of encapsulation formulation (1.28 ml per batch) were processed into alginate beads for “Encapsulated Antigen (EA)” group of fish. Similarly, 30 batches of alginate solution (1.28 ml per batch) were turned into beads for “Encapsulated Control (EC)”. After preparation, alginate beads were dried under reduced pressure for 48 hours. Finally, approximately 100 mg of dry alginate powder per batch was recovered.

Table 3.5: Process parameters of the electrospraying method utilised in encapsulating IPNV antigen for the uptake study. These parameters apply to the production of one single batch (1.28 ml).

Internal diameter (needle)	Flow rate	Target volume	Voltage	Distance[i]	Volume[ii]
ID	Q	V_{tv}	U	x	V_{xls}
µm	$cm^3\ h^{-1}$	ml	kV	mm	ml
700	60	1.28	7.0	50	20

[i]Distance between the needle tip and the surface of crosslinking solution (x)
[ii]Volume of the cross-linking solution (V_{xls})

3.3.1.2 Oral intubation of A. salmon

The fish trial was performed according to the general method described in the section 2.2.5.2 (Chapter 2) at TempOx lab (EWOS Innovation AS, Dirdal, Norway). Parameters applied in this trial are listed in the Table 3.6. Moreover, fish was starved one day in advance of the treatment. The following groups were formed: “Unecapsulated Control (UC)”, “Un-encapsulated Antigen (UA)”, “Encapsulated Control (EC)” and “Encapsulated Antigen (EA)” (Figure 3.6). The UC group was intubated with PBS (Item C005, Table 2.1), the UA was intubated with un-encapsulated IPNV antigen while the EC and EA were given empty alginate beads and alginate-encapsulated IPNV antigen respectively (Figure 3.5). Both UA and EA received the same IPNV antigen dose (10^9 $TCID_{50}$ per fish).

Table 3.6: Parameters applied in the uptake study carried out by oral intubation with alginate beads loaded with IPNV antigen.

Parameter	Symbol	Quantity
Average weight of fish	m	172 g
Oxygen saturation in water	O_2	90%
Water temperature	t	12°C
Diameter of a tank	d	2.0 m
Volume of a tank	V	3.1 m^3
Number of tanks	n_{tanks}	4
Number of fish per tank	n_{fish}	30
Number of groups	n_{groups}	4
Length of the acclimatisation period	t_{accl}	1 week
Number of treatments	n_{treat}	4
Number of control fish	$n_{control}$	60
Number of control groups	$n_{ctrl-gr}$	2
Number of sampled fish per tank per sampling point	$n_{sf/t}$	10
Number of sampling points	n_{SP}	3
Length of sampling time intervals calculated from the end of treatment	t_{SP}	24, 72 and 168 h
Total number of sampled fish	$n_{sampled}$	120

Figure 3.5: Oral intubation of A. salmon. A) Plastic syringe (size: 1 ml) is inserted in the moth of a fish, B) Syringe with severed tip for intubating fish with empty alginate beads (Encapsulated control, EC group) and alginate beads loaded with IPNV antigen (Encapsulated antigen, EA group). C) Syringe with rubber tip for intubating fish with phosphate-buffered saline (Un-encapsulated control, UC group) and IPNV antigen suspension (Un-encapsulated antigen, UA group).

3.3.1.3 Sampling

Ten fish was sampled from each tank at 24, 72 and 168 hours post intubation. Prior to sampling, the fish were anaesthetised with tricain mesilate (100 mg l^{-1}; C025, Table 2.1). Weight of individual fish was recorded for every sampled fish. Blood was collected from the caudal artery with a heparinised blood collection tube (V = 4 ml) fitted with 0.8×38 mm disposable needles (Figure 3.6). The blood samples (approx. 4 ml $fish^{-1}$) were centrifuged at 4000 rpm for 10 min immediately after sampling. The plasma was then removed and kept frozen at -80^{o}C prior to ELISA test.

Level of IPNV antigen in the samples was determined in an ELISA assay at Norwegian School of Veterinary Science (Oslo, Norway). The assay was performed with minor modifications as previously described by Munang'andu et al. (2012). The plasma samples were diluted 40-fold with PBS before plating 100 µl per well.

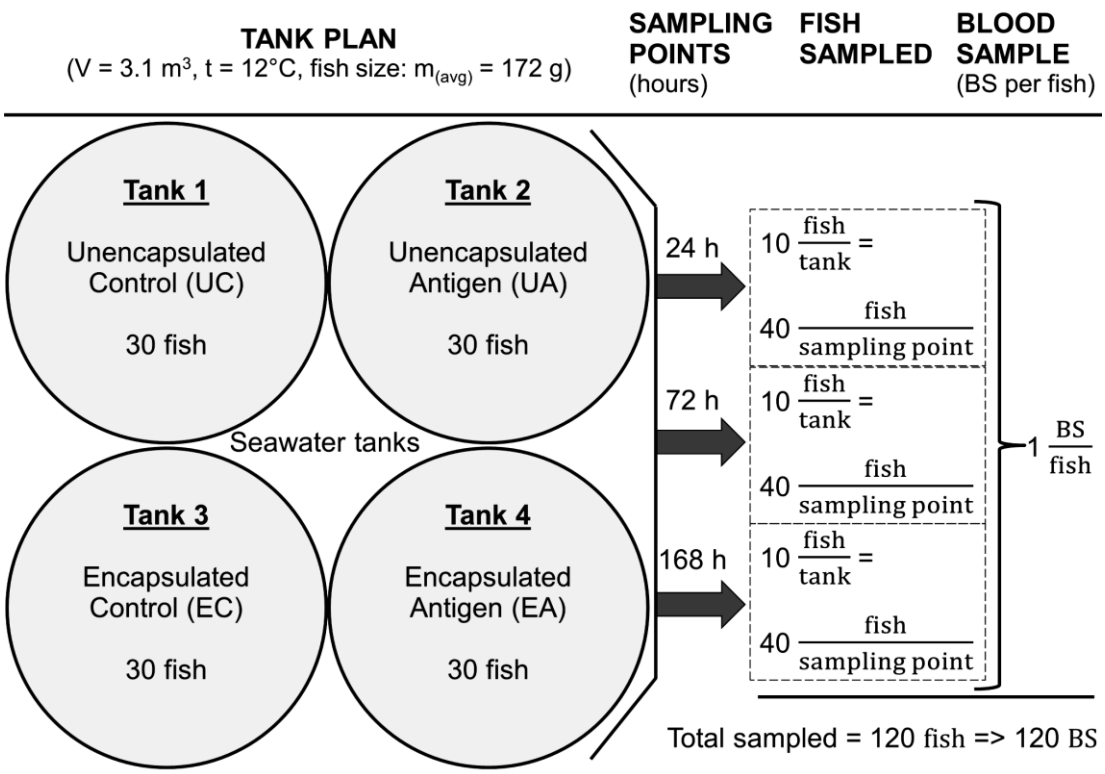

Figure 3.6: Tank and sampling plan of the IPNV antigen uptake study. The tank and sampling plan is illustrated in four vertical segments in this figure. Tank arrangement is shown in the first segment. It contains information on name of the treatments (UC – phosphate-buffered saline solution, UA – un-encapsulated IPNV antigen, EC – empty alginate beads and EA – alginate-encapsulated IPNV antigen), number of intubated fish (n = 30), fish size ($m_{(avg)}$ = 172 g), tank volume (3.1 m^3) and temperature (12°C). In the second segment, sampling points (24, 72 and 168 hours) are listed. Number of fish sampled per tank (10 fish/tank) at specified sampling points (40 fish/sampling point) is shown in the third segment. The last segment indicates the number of blood plasma samples (BS) taken per fish (1 BS/fish) at any sampling point resulting in the total of 120 samples.

3.3.2 Results

At 24 hours post intubation (p.i.), fish intubated with the un-encapsulated antigens (UA group) showed higher blood plasma concentrations of IPNV antigen than fish administered encapsulated antigens (EA group) (Figure 3.7). The EA group on the other hand showed a higher uptake than the UA group at 72 hours p.i. However, response of the encapsulated control group (EC) was surprisingly high. There was no statistical difference in uptake between all groups at 168 hours p.i..

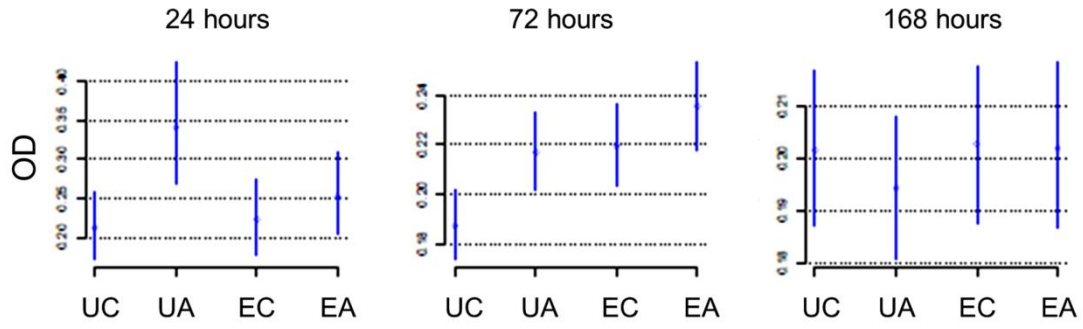

Figure 3.7: Uptake of IPNV antigen in blood plasma of A. salmon. Optical density (OD) responses for different oral treatments with IPNV antigen are shown. The responses were measured by an ELISA assay. Error bars shows 95% credible intervals. Four groups/treatments were: UC – un-encapsulated control (PBS solution), UA – unencapsulated antigen (IPNV antigen suspension), EC – encapsulated control (empty alginate beads) and EA – encapsulated antigen (alginate-encapsulated IPNV antigen). Blood plasma samples were taken at 24, 72 and 168 hours post intubation.

3.4 Immunogenicity of alginate-encapsulated antigen

Immune response of A. salmon to IPNV antigen was assessed in this study. Fish was treated with four different preparations. These preparations were: two oral vaccine formulations with alginate-encapsulated antigen, one formulation containing un-encapsulated antigen and one control preparation consisting of pure PBS. IgM antibody levels in blood plasma were measured by ELISA, The level of expression of IgM, IgT, CD4, GATA3, FOXP3, TGF-β and IL-10 genes in head kidney, spline and liver were determined by qPCR as well.

3.4.1 Methods

3.4.1.1 Fabrication and characterisation of alginate beads with IPNV antigen

Alginate beads loaded with IPNV antigen were produced according to the general method described in the section 2.2.1.1 (Chapter 2). Process parameters and their respective values are summarised in the Table 4.8. For the purpose of encapsulation, the encapsulation formulation (Item S001, Table 2.4) and the needle (Item T014, Table 2.2) were used as well.

Furthermore, the beads were cross-linked in two different ways using crosslinking solutions (Item S003 and S004, Table 2.4). As a result, two different alginate products labelled Encap 1 and Encap 2 were produced. The Encap 1 product was cross-linked with calcium (Item S003, Table 2.4). Seven batches a 60 ml were processed and then combined into one single batch totalling 420.0 g of wet calcium alginate beads. Regarding the production of Encap 2, five and a half batches were cross-linked with ethylenediammonium dication (Item S004, Table 2.4). Thereafter, the

resulting ethylenediammonium alginate beads were merged into one batch of 330.0 g.

The generated wet alginate beads were filtered off and then dried under reduced pressure (0.06 mbar; Item T007, Table 2.2) for 48 hours. The dry residue was crushed with mortar and pestle before being sieved through a 150 µm sieve. The particle size distribution and shape were determined by stereo microscope (Item I001, Table 2.3).

Table 3.7: Encapsulation process variables with their respective values applied in the study of encapsulation efficiency.

Internal diameter (needle)	Flow rate	Target volume	Voltage	Distance[i]	Volume[ii]
ID	Q	V_{tv}	U	x	V_{xls}
µm	$cm^3\ h^{-1}$	ml	kV	mm	ml
2000	100	60	7.0	30	150

[i]Distance between the needle tip and the surface of crosslinking solution (x)
[ii]Volume of crosslinking solution (V_{xls})

3.4.1.2 Preparation of oral boost feeds

Oral boost feeds (OBFs) were prepared by applying an oil mixture (OM) to base pellet (BP; Item C007, Table 2.1) in the vacuum infusion coating process. OMs were formulated by mixing IPNV Ag suspension (10^9 $TCID_{50}$ g^{-1}), phosphate buffered saline (PBS; Item C005, Table 2.1), Encap1 (2.70×10^{10} $TCID_{50}$ g^{-1}) or Encap2 (2.02×10^{10} $TCID_{50}$ g^{-1}) with fish oil (Item C019, Table 2.1). Mixing was performed by using high-performance disperser (Item T005, Table 2.2) at ambient temperature. The OBF-1, -2 and

-3 were composed with the aim of generating feeds containing an antigen level of 4.01×10^{7} $TCID_{50}$ g^{-1}. This level was selected due to an expected daily feed intake of 3.56 g $fish^{-1}$ during the first oral boost (1.OB) period. For the same reason, the targeted antigen level in the OBF-4, -5 and -6 was 2.99×10^{7} $TCID_{50}$ g^{-1}. It is because of the anticipated daily feed intake of 4.77 g $fish^{-1}$ in the second oral boost (2.OB) period. Feeding at these rates provides a weekly antigen dose of 1×10^{9} $TCID_{50}$ g^{-1} in both OB periods.

Table 3.8: Composition of the oral boost feeds (OBFs) and control feeds (CFs) in the immune response study. Base pellet (BP) was coated with an oil mixture consisting of fish oil and at most two other components to make 3900 g of CFs or OBFs. These other components are selected from the following group of additives: antigen suspension (Ag susp.), phosphate-buffered saline (PBS) and one of the encapsulation products (Encap 1 or 2).

	Oil mixture						
Feed name	Fish oil [g]	Ag susp[i] [g]	PBS [g]	Encap1[ii] [g]	Encap2[iii] [g]	BP[iv] [g]	Total [g]
CF-1	783.51	0.00	156.50	0.00	0.00	2959.99	3900.00
OBF-1	783.51	156.50	0.00	0.00	0.00	2959.99	3900.00
OBF-2	789.31	0.00	150.70	5.80	0.00	2954.19	3900.00
OBF-3	791.24	0.00	148.77	0.00	7.73	2952.26	3900.00
CF-2	783.51	0.00	156.50	0.00	0.00	2959.99	3900.00
OBF-4	783.51	116.80	39.70	0.00	0.00	2959.99	3900.00
OBF-5	788.00	0.00	152.17	4,33	0.00	2955.66	3900.00
OBF-6	789.28	0.00	150.73	0.00	5.77	2954.22	3900.00

[i]Ag susp – antigen suspension derived from IPN viral culture with titre of 10^{9} $TCID_{50}$ ml^{-1}

[ii]Encap 1 – product generated by encapsulating Ag suspension into Ca-alginate matrix

[iii]Encap 2 – product made by encapsulating Ag suspension into EDA-alginate matrix

[iv]BP – base pallet is a semi-finished fish feed product which is dry extrudate lacking oil mix

Control feeds (CF-1 and -2) were produced by mixing PBS with fish oil in advance of applying to BP in the vacuum infusion coating process. These two formulations were identical and IPNV Ag free. A detailed specification of the mixing ratios is shown in the Table 3.8.

3.4.1.3 Fish trial design

A. salmon (n = 540, m_{avg}=200g) was distributed randomly among 12 circular seawater tanks (d = 1 m, V = 500 l, t = 8°C) at EWOS Innovation AS (Dirdal, Norway) 10 weeks prior to the start of the 1.OB period. The tanks were randomly divided into four groups (Unecap, Encap 1, Encap 2 and Control), with three tanks being assigned to each group. All fish used in this trial were vaccinated with the multivalent vaccine (Item C026, Table 2.1) one year prior to the trial. For this reason circulating antibodies were expected to be present in the fish and the oral vaccinations were considered as immunity boosting treatments. Boosting was performed twice for a period of one week each time. After 10 weeks long acclimatisation stage, a weeklong 1.OB period took place. The 1.OB was succeeded by a seven week long induction period. After the end of that period, the first sampling was performed. The 2.OB commenced immediately upon completion of the first sampling. After the 2.OB interval, there was a four week long period of immune induction followed by the final sampling (Figure 3.9). The health status of the fish was very good during the 23 weeks long span of the trial.

3.4.1.4 Feeding plan and feed intake assessment

All groups were fed with EWOS commercial diets in excess in the periods outside the oral boost intervals. During the acclimatisation and the first immune induction period fish was provided with EWOS Opal 200 diet. In the time of the second induction period, feeding was conducted with EWOS Opal 500 due to the change in fish size. Throughout the oral boost intervals, fish received oral boost feeds (OBFs). Unencap group was fed with OBF-1 in the 1.OB period and then with the OBF-4 in the 2.OB period. Encap 1 group was fed with OBF-2 and OBF-5 in the 1.OB and 2.OB interval respectively. Encap 2 group was given OBF-3 in the 1.OB period and then OBF-6 in the 2.OB period. The Control group was provided with feed free of IPNV antigen in both of the OB periods. Each group contained 120 (3×40) fish in the time of the 1.OB period. In the 2.OB period, the groups were reduced to 75 (3×25) fish each. In order to predict feed intake as accurately as possible, feed consumption was measured over a course of seven days, one week ahead of the OB intervals. Therefore, the daily portions for all groups were set to 166 g and 147 g per tank during the 1.OB and 2.OB respectively (Figure 3.8). Unconsumed feed was collected during both boost periods to calculate feed intake. Uneaten pellets were spilled out of the tanks within 10 min post feeding and filtered off from the outlet water using an automatic collection system. Residual pellets were removed from the filters and put into a drying cabinet for 24 h at 70 °C. Amount of feed consumed was calculated as the difference between the dry weight of the feed served and the dry weight of unconsumed feed, expressed as the mass of feed per week per fish.

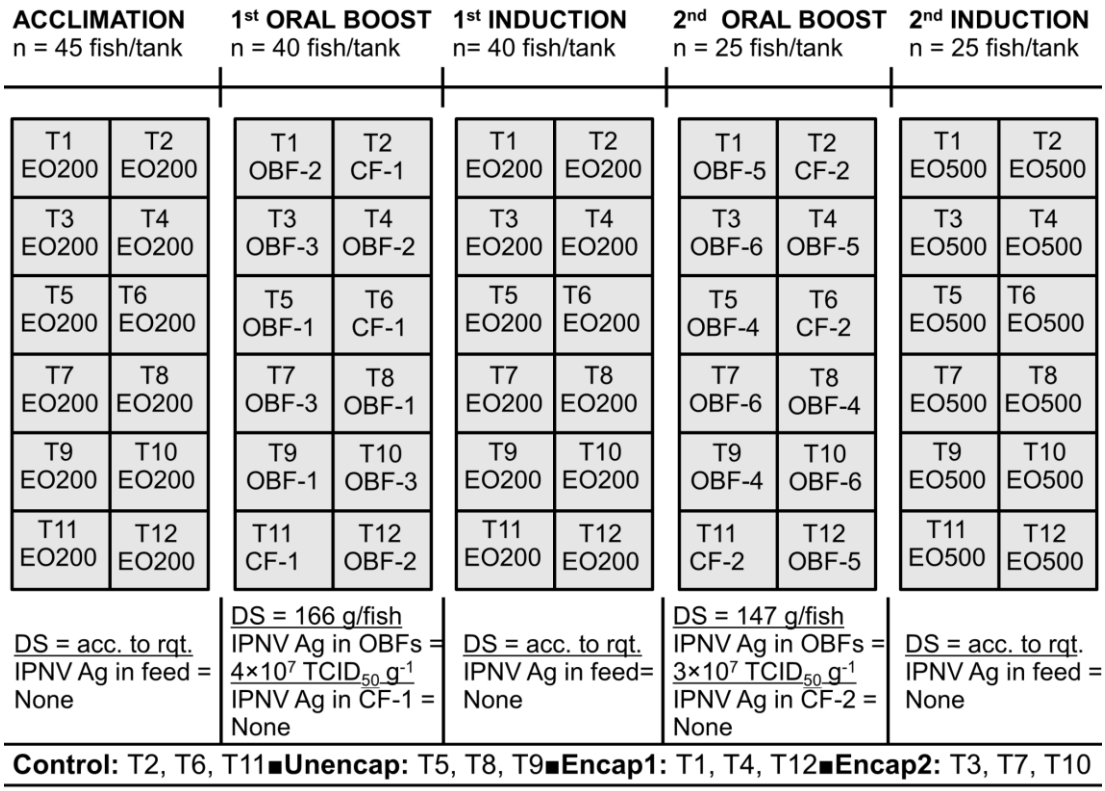

Figure 3.8: Tank arrangement and the corresponding feeding regime in the immune response study. Tank arrangement and corresponding feeding regime in the predefined trial intervals are outlined in four horizontal segments in this illustration. In the first segment of the figure, subsequent order of the intervals (from left to right) and number of fish in the tanks are denoted. Duration of the intervals is shown in the Figure 3.9. In the second segment, tank plan showing tank numbers (T1….T12) and diet codes are depicted. The following diet codes are used: EO200 – Ewos Opal 200 (commercial diet), EO500 – Ewos Opal 500 (commercial diet), OBFs – Oral boost feeds (OBF-1….OBF-6) and CF – Control feeds (CF-1 and CF-2) as detailed in the Table 2.2. Daily feed servings (DS) along with IPNV antigen content per gram feed in each interval are shown in the third segment. "DS = acc. to rqt" means that fish were fed according to requirement for the age, size and expressed appetite. In the last segment of the figure, the tanks assigned to the four treatments/groups (Control, Unencap, Encap1 and Encap2) are listed.

3.4.1.5 Sampling

Ten fish was sampled from each tank at each sampling point (Figure 3.9). Prior to sampling, the fish were anaesthetised with tricain mesilate (100 mg l^{-1}; C025, Table 2.1). The weight of individual fish was recorded for every sampled fish. Blood was collected from the caudal artery with a heparinised blood collection tube (V = 4 ml) fitted with 0.8×38 mm disposable needles. The blood samples (approx. 4 ml $fish^{-1}$) were centrifuged at 4000 rpm for 10 min immediately after sampling. The plasma was then collected and kept frozen at -80^{o}C until measuring antibody levels by ELISA. In addition, head kidney, spleen and hindgut were sampled and stabilised in RNA*later*® (Item C006, Table 2.1). These samples were kept frozen at -20°C until measuring the expression of selected genes by qPCR.

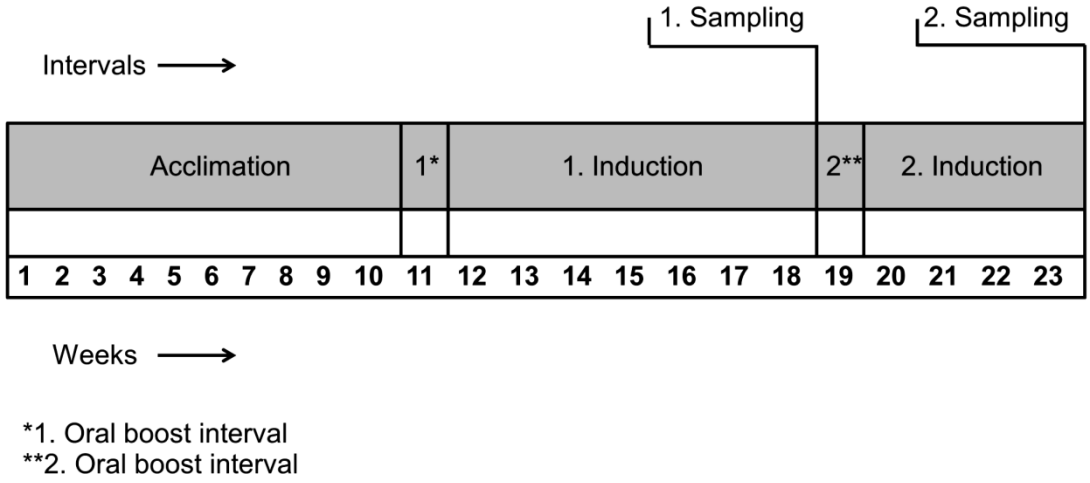

Figure 3.9: Immune response study shown in the subsequent order of events: 1) acclimation (ten weeks), 2) First oral boost (one week), 4) First immune induction (seven weeks), 5) First sampling, 6) Second oral boost (one week), 7) Second immune induction (four weeks), and 8) Second sampling. Altogether, the total length of the trial sums up to 23 weeks.

3.4.1.6 Sample analysis

Apart from measuring the antibody (IgM) levels in blood plasma by ELISA, the expression of IgM, IgT, CD4, GATA3, FOXP3, TGF-β and lL-10 genes were determined by qPCR. The selection of these genes is in line with the theory provided in the Section 1.3.

ELISA was performed with minor modifications as previously described by Munang'andu et al. (2012) at Norwegian School of Veterinary Science (Oslo, Norway). As distinct, these plasma samples were diluted 40-fold with PBS before plating 100 µl per well. Similarly, qPCR was carried out according to Chen at al. (2014) at the same institution. However, only samples from one encapsulated group (Encap 1) were examined by qPCR.

In the end, statistical analysis was conducted according to the method described in the Section 2.2.6.2.

3.4.2 Results

3.4.2.1 Characterisation of alginate beads loaded with IPNV antigen

Structure of wet alginate beads was spherical changing to irregularly shaped particles consequent to lyophilisation and subsequent grinding (Figure 3.10). The mean size of wet alginate beads was roughly 700-750 µm. After lyophilisation the average size decreased to 250-300 µm. The size was further scaled down to below 150 µm by sifting (150 µm screen) and grinding with mortar and pestle (Table 3.9). Theoretical concentration of IPNV Ag in the lyophilised alginate products Encap 1 and Encap 2 was 2.70×10^{10} and 2.02×10^{10} $TCID_{50}$ g^{-1} respectively.

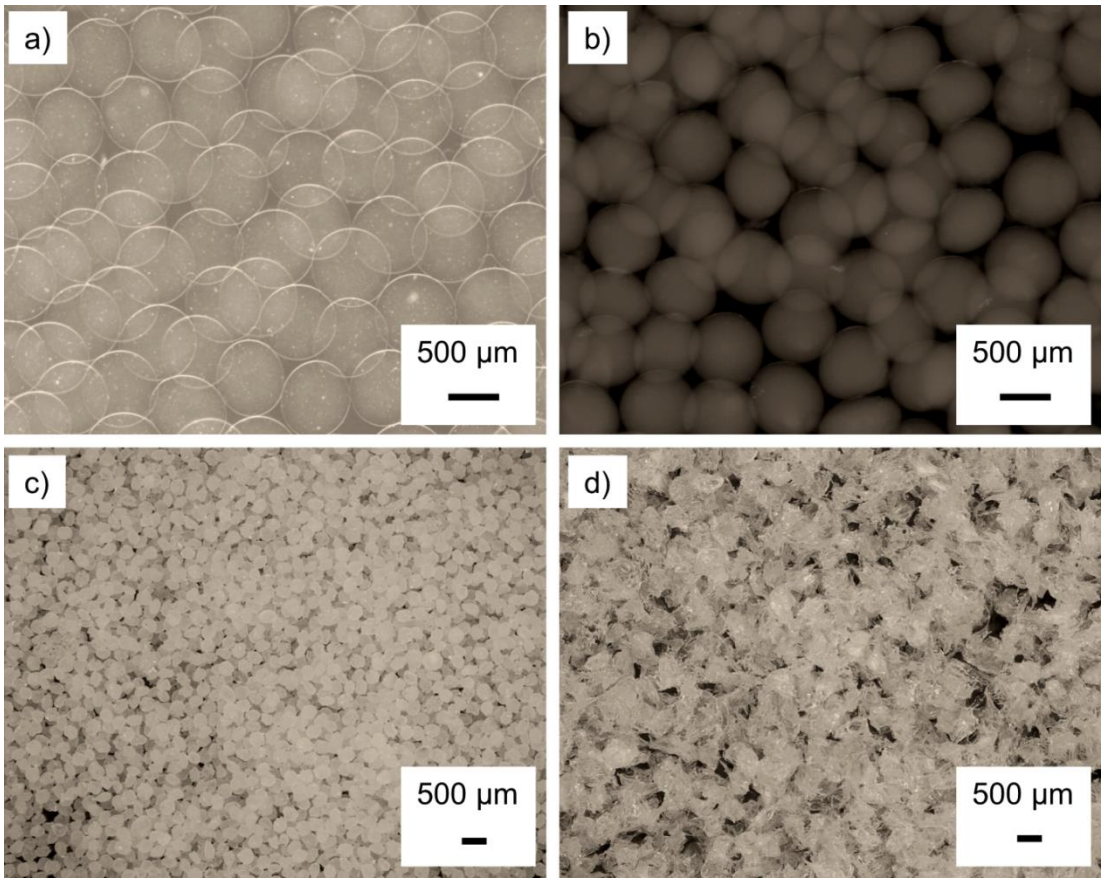

Figure 3.10: Stereo microscope zoom (SMZ) images of alginate beads. SMZ (Item I001, Table 2.3) images of a) Wet Ca-alginate beads loaded with IPNV Ag (Encap 1), b) Wet EDA-alginate beads loaded with IPNV Ag (Encap 2) c) Lyophilised Ca-alginate beads loaded with IPNV Ag (Encap 1: 2.70×10^{10} $TCID_{50}$ g^{-1}), d) Lyophilised EDA-alginate beads loaded with IPNV Ag (Encap 2: 2.02×10^{10} $TCID_{50}$ g^{-1}).

Table 3.9: Size of the alginate beads in the immune response trial.

	Wet size µm ±SD	Dry size µm ±SD	Post sifting size µm
Encap 1[i]	736±32	299±45	<150
Encap 2[ii]	712±28	268±37	<150

[i]Encap 1 – product generated by encapsulating Ag susp into Ca-alginate matrix
[ii]Encap 2 – product made by encapsulating Ag susp into EDA-alginate matrix

3.4.2.2 Feed intake of oral boost feeds (OBFs) and IPNV Ag dose

Theoretical concentration of IPNV Ag in the OBF-1,-2, and -3 was 4.01×10^{7} $TCID_{50}$ g^{-1} decreasing to 2.99×10^{7} $TCID_{50}$ g^{-1} in the OBF-4,-5 and -6. In the 1.OB period, the fish were served 29.1 g but consumed 23.9 ±1.3 g $fish^{-1}$ for the entire period while in the 2.OB period the weekly feed intake was around 38.4 ±2.2 g of 41.2 g $fish^{-1}$ offered. Average fish weight was 397 ±104 g in the 1.OB and then it doubled to 804 ±120 g in the 2.OB period. The attained average antigen dose in both OB periods was more or less 1×10^{9} $TCID_{50}$ $fish^{-1}$ which correspond the targeted weekly dose. However, due to the doubling of fish weight in the 2.OB period, the dose per unit of fish body weight was almost twice as low as the 1.OB dose. Control feeds (CFs) were IPNV antigen free (Table 3.10).

Table 3.10: Antigen dose related to the fish size in unit of mass and the weekly feed intake (FI) per fish. The dose is shown as a weekly IPNV antigen dose per fish ($TCID_{50}$ $fish^{-1}$) and a weekly IPNV antigen dose per unit of fish mass ($TCID_{50}$ kg^{-1}).

Period[i]	Group[ii]	Feed[iii]	Fish size (g) ±SD	FI (g $fish^{-1}$ $week^{-1}$) ±SD	IPNV Ag dose ($TCID_{50}$ $fish^{-1}$ $week^{-1}$) ±SD	IPNV Ag dose ($TCID_{50}$ kg^{-1} $week^{-1}$) ±SD
1.OB	Control	CF-1	395 ±92	24.7 ±0.4	0.00	0.00
	Unencap	OBF-1	375 ±82	23.9 ±2.4	9.6×10^{8} $\pm1\times10^{8}$	2.6×10^{9} $\pm6\times10^{8}$
	Encap 1	OBF-2	426 ±121	23.1 ±0.9	9.3×10^{8} $\pm4\times10^{7}$	2.2×10^{9} $\pm6\times10^{8}$
	Encap 2	OBF-3	395 ±115	24.1 ±0.8	9.7×10^{8} $\pm3\times10^{7}$	2.4×10^{9} $\pm7\times10^{8}$
2.OB	Control	CF-2	846 ±135	39.6 ±0.4	0.00	0.00
	Unencap	OBF-4	796 ±126	37.3 ±3.9	1.1×10^{9} $\pm1\times10^{8}$	1.4×10^{9} $\pm3\times10^{8}$
	Encap 1	OBF-5	782 ±105	38.0 ±1.3	1.1×10^{9} $\pm4\times10^{7}$	1.5×10^{9} $\pm2\times10^{8}$
	Encap 2	OBF-6	792 ±108	38.6 ±2.4	1.2×10^{9} $\pm7\times10^{7}$	1.5×10^{9} $\pm2\times10^{8}$

[i]Periods – two weeklong immunisation periods designated the first oral boost (1.OB) and the second oral boost (2.OB),

[ii]Groups – treated with PBS (Control), un-encapsulated IPNV Ag (Unencap), Ca-alginate-encapsulated IPNV Ag (Encap 1) and EDA-alginate-encapsulated IPNV Ag (Encap 2)

[iii]Feeds – oral boost feeds 1-6 (OBFs) associated with corresponding alginate products and control feeds 1 and 2 (CFs) added PBS.

3.4.2.3 Assessment of immune responses by ELISA

At seven weeks following the 1.OB, there was a significantly higher antibody response in fish fed with OBF-1/Encap1 feed than in fish fed with any other OBF (Figure 3.11). Fish fed with OBF-2/Encap 2 and OBF-3/Unencap had similar response to the un-boosted control. After the 2.OB, the antibody response of the Unencap group remained lower than the response of any other group. Although the OD values of the groups fed with OBFs (Encap1 and Encap 2) rose from the 1.OB to 2.OB, there was no significant difference between them and control feed. Particularly, OD value of the control group increased in the 2.OB. At the same time, possibility of the ELISA assay being more sensitive in the second run cannot be entirely excluded either. Notably, the fish received only half of the antigen dose per unit of fish mass in the 2.OB compared to the 1.OB period.

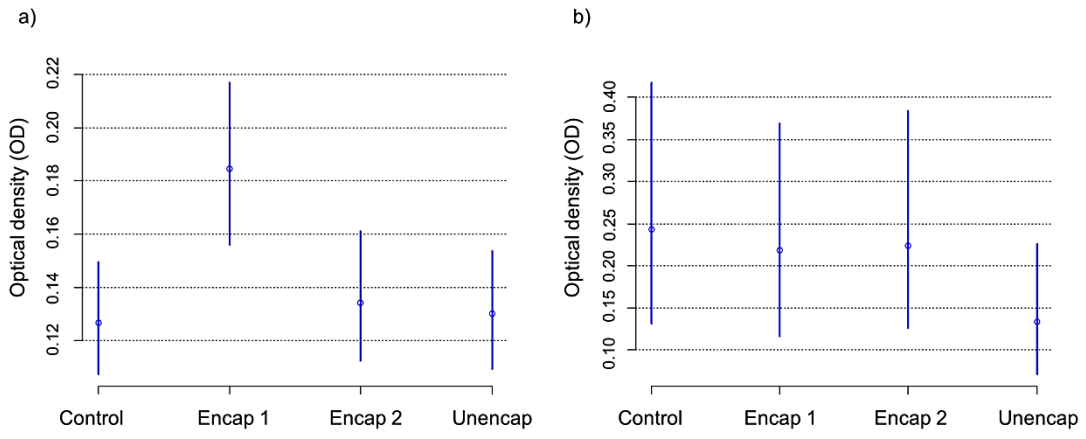

Figure 3.11: Antibody response in the immune response trial. Antibody response in plasma for different treatments in the 1.OB (a) and the 2.OB (b). Error bars show 95% credible interval. Fish treated with PBS (Control), un-encapsulated IPNV Ag (Unencap), Ca-alginate-encapsulated IPNV Ag (Encap 1) and EDA-alginate-encapsulated IPNV Ag (Encap 2).

3.4.2.4 Assessment of gene expression by qPCR

In order to verify whether antibody response was humoral, the expression of CD4 and GATA-3 genes was examined. These genes are known to be associated with T_h2 responses, especially in the head kidney and spleen.

Seven weeks after the 1.OB and four weeks after the 2.OB, the Encapsulated group had significantly higher CD4 expression ($p < 0.04$) in all three tissue samples (head kidney, spleen and hindgut) compared to the Un-encapsulated group (Figure 3.12). In this group, the CD4 gene was slightly suppressed although non-significantly. Similarly, the expression of GATA-3 in the Encapsulated group was significantly up-regulated ($p < 0.04$) at both sampling points in all three organs (Figure 3.13). On the other hand, GATA-3 was not induced in the Un-encapsulated group which is in accordance with the results of CD4.

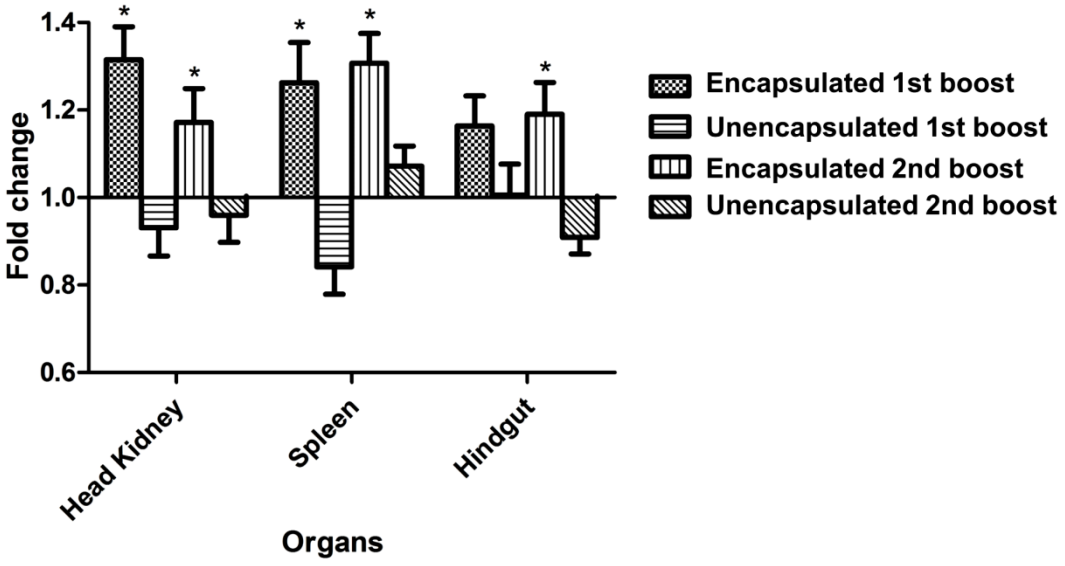

Figure 3.12: CD4 expression: Mean CD4 expression of boosted groups relative to un-boosted control. n = 30; *statistically significant $p < 0.05$. There was significant up-regulation of CD4 in all tissue samples of the Encapsulated group in both oral boost periods.

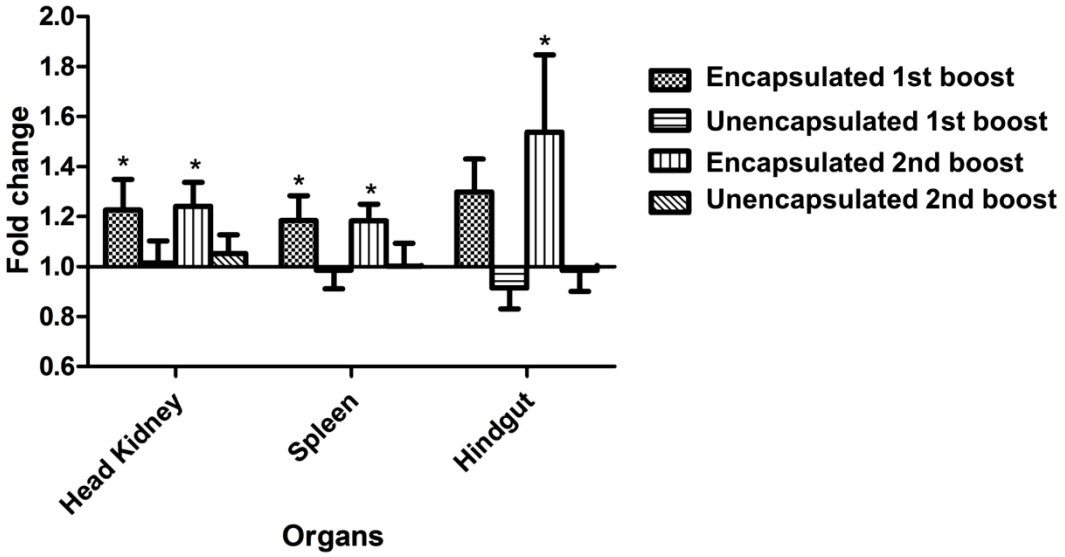

Figure 3.13: GATA-3 expression in different groups of A. salmon. Mean values of boosted relative to un-boosted controls, qPCR. n = 30; *statistically significant $p < 0.05$. There was significant up-regulation of GATA-3 in all tissue samples of the Encapsulated group in both oral boost periods.

In addition to CD4 and GATA-3, the expression of IgT and IgM genes was examined with the purpose of assessing the gut mucosal antibody response.

After the 1.OB, marginal but non-significant inductions of IgT were observed in both Encapsulated and Un-encapsulated group relative to the Control (Figure 3.14). After four weeks following the 2.OB, the expression significantly increased in the encapsulated group, particularly in the hindgut ($p < 0.01$). Interestingly, CD4 and GATA-3 expression in this organ had a similar pattern to IgT (Figure 3.12 and 3.13), especially for the encapsulated group. Conversely, CD4 and GATA-3 expression in the Un-encapsulated group were generally not induced in relation to the Control group. Additionally, the expression of IgM in the hindgut was not differentially expressed in all groups at all-time points examined (Figure 3.15).

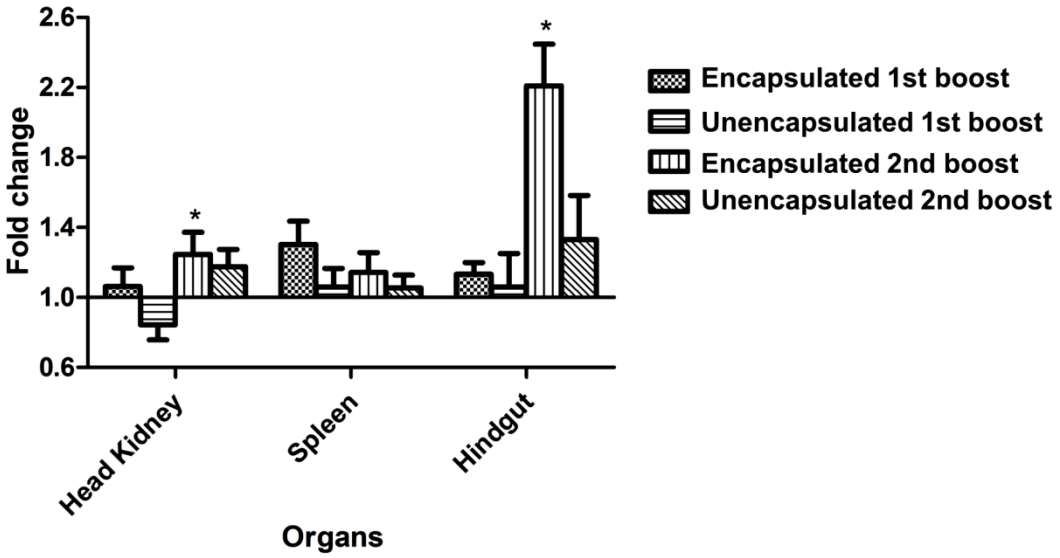

Figure 3.14: IgT expression in the different organs of A. salmon. Means of boosted groups relative to the un-boosted control, qPCR, n = 30; *statistically significant $p < 0.05$. IgT was significantly up-regulated in head kidney and hindgut of the Encapsulated group.

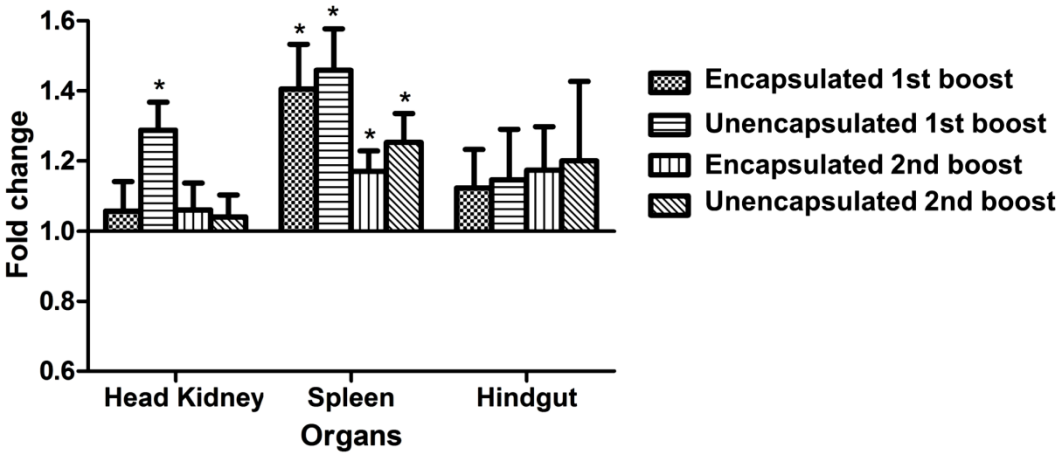

Figure 3.15: IgM expression in different groups of A. salmon. Mean values of boosted relative to un-boosted controls, qPCR, n = 30; *statistically significant $p < 0.05$. IgM was significantly expressed in spleen of both Encapsulated and Unencapsulated group at both sampling point. However, the level of expression was on a declining path from the 1st to 2nd oral boost. In addition, level of expression increased in head kidney of the Encapsulated group at the 2nd sampling point.

The assessment of IgT expression was extended to the head kidney and spleen where this gene was only differentially expressed in head kidney of the Encapsulated group, (Figure 3.14). More accurately, IgT was only significantly up-regulated in head kidney at the 2nd sampling point ($p < 0.03$).

The reduction in blood plasma antibodies following administration of antigens can be due to their consumption (Munang'Andu et al., 2013). Thus to check that the suppression in the present study was not due to consumption, we examined the transcript levels of IgM. Figure 3.15 shows significant down regulation of IgM transcripts both in the kidneys ($p < 0.01$) and spleen (0.001) of the Un-encapsulated group between the 1st to the 2nd sampling. A similar change was observed in the spleen of the Encapsulated group ($p<0.01$) but with no differential regulation in the kidneys.

In order to understand weak immune response of the Un-encapsulated group, expression of FoxP3, TGF-β and IL-10 was assessed. In higher vertebrates, FoxP3 is a key transcription factor of regulatory T cells (T_{regs}) while TGF-β is known to supress effector T cells except from T_{regs} (Li and Flavell, 2008). On the other hand, IL-10 is an anti-inflammatory cytokine that can induce immune tolerance (Weiner et al., 2011). These genes have also been described in fish although their functions related to immune tolerance remain to be characterised. Consistent with the suppression of antibodies in the Un-encapsulated group, the expression of FoxP3, TGF-β and IL-10 were significantly up-regulated ($p < 0.003$, 0.035 and 0.0048, respectively) in kidneys at the 1st sampling point (Figure 3.16, 3.17 and 3.18). In contrast, no differential expressions of either of these genes were observed in the spleen of any group at the same sampling point.

In the hindgut, FoxP3 was only induced in the Un-encapsulated group after the 2.OB (Figure 3.16) while both TGF-β ($p < 0.02$) and IL-10 ($p < 0.01$) were significantly induced in both Encapsulated and Un-encapsulated group.

In summary, immune response of the Encapsulated group was humoral in the 1.OB. This assumption is based on the fact that CD4, GATA-3 and IgM were up-regulated in both head kidney and spleen of the fish. However, in the 2.OB, the immune response was on decline. This conclusion is backed by the evidence of increasing levels of TGF-β and IL-10 in the hindgut. As it is known, TGF-β and IL-10 are associated with T_h3 response (Carrier et al., 2007). This type of response suggests that the Encapsulated group were eventually in the process of developing oral tolerance against IPNV antigen.

The immune system of the Un-encapsulated group did not respond to the oral vaccine treatment in the 1.OB. The elevated IgM levels most likely originated from the treatment with injectable vaccine one year prior to boosting with oral vaccine. In the 2.OB, all gens (TGF-β, FoxP3 and IL-10) related to the regulatory pathways (T_{reg} and T_h3) were induced. It indicates that small amount of antigen has passed through the stomach and reached the hindgut. Accordingly, the antigen dose was too low and thus the immune system probably responded by up-regulating T_{reg} and T_h3. Induction of these cells most likely led to down-regulation of the immune response with immune tolerance as a result. This theory is in line with numerous studies related to immune tolerance (Möbs et al., 2008; Sakaguchi et al., 2008; Weiner, 2001; Zouali, 2014).

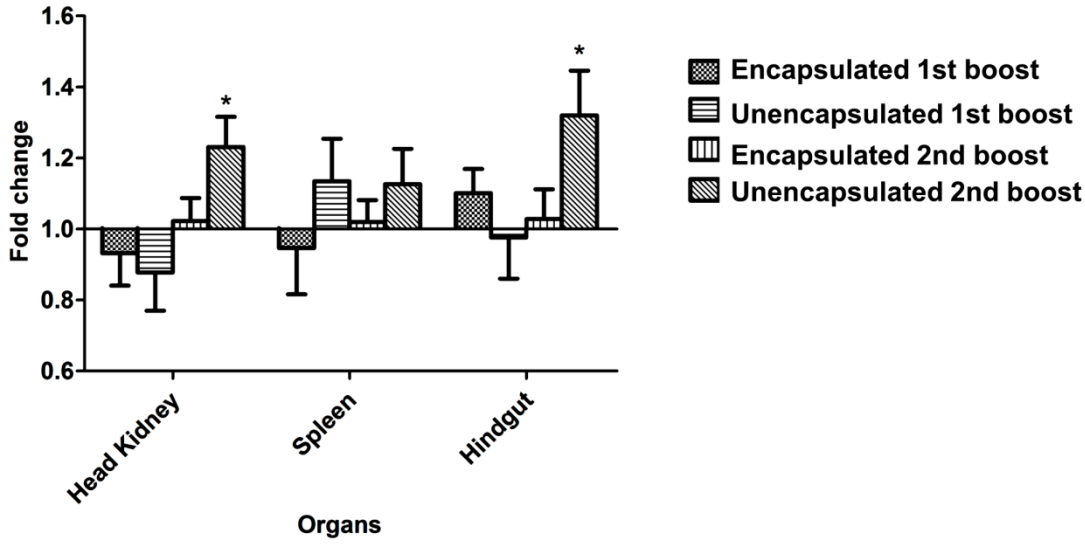

Figure 3.16: FoxP3 expression of boosted groups relative to the un-boosted control, n = 30; *statistically significant $p < 0.05$. FoxP3 was up-regulated in both head kidney and hindgut of only Un-encapsulated group.

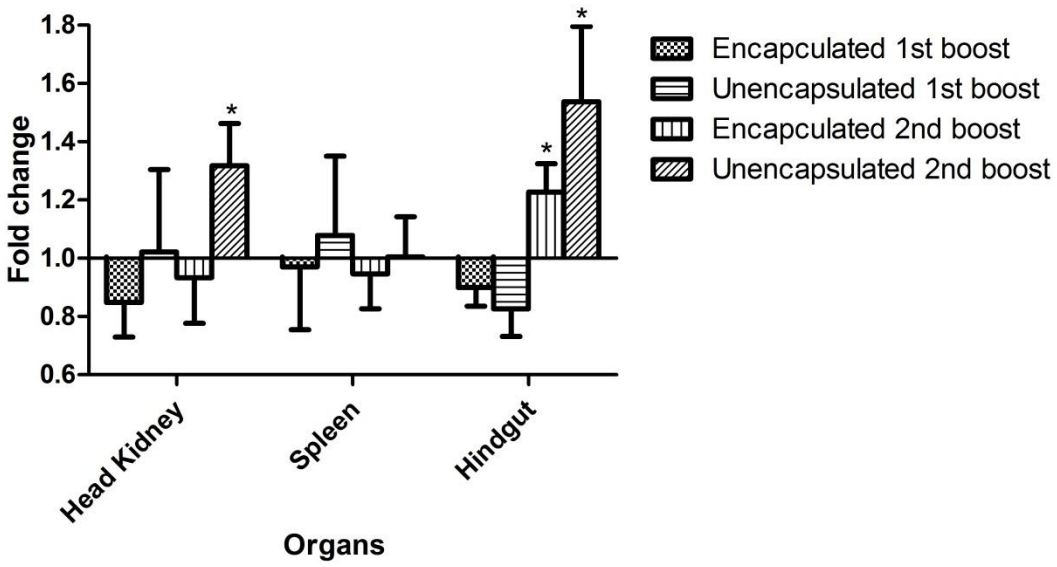

Figure 3.17: TGF-β expression in different organs of A. salmon. Means of boosted groups relative to un-boosted control, n = 30; *statistically significant $p < 0.05$. TGF-β was induced in both head kidney and hindgut of the Un-encapsulated group at both sampling points. However, TGF-β was only up-regulated in hindgut of the Encapsulated group at the 2nd sampling point.

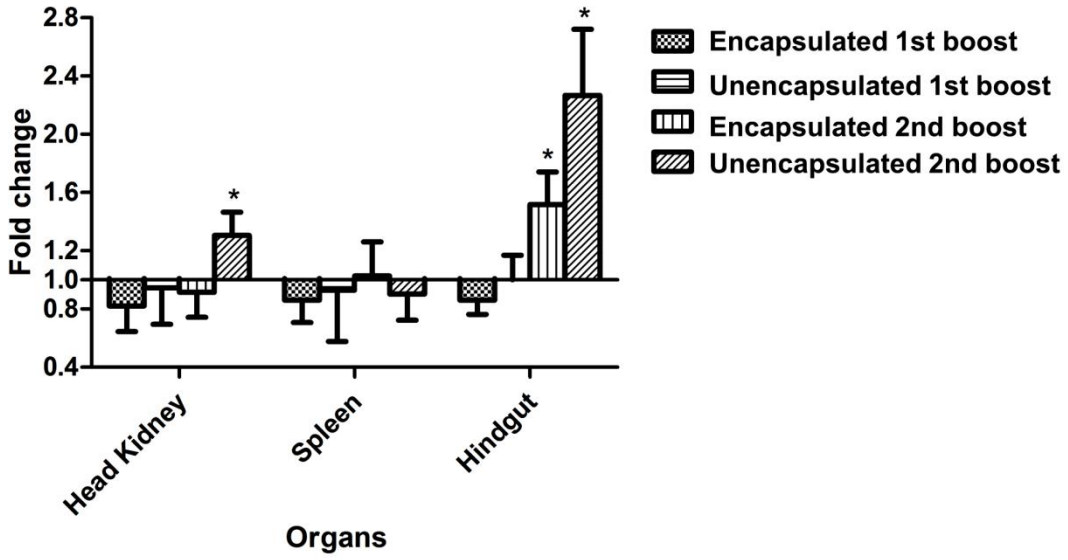

Figure 3.18: IL-10 expression in different organs of A. salmon. Means of boosted groups relative to un-boosted control, n = 30; *statistically significant $p < 0.05$. IL-10 was expressed in both head kidney and hindgut of the Un-encapsulated group at both sampling points. On the other hand, IL-10 was only induced in hindgut of the Encapsulated group at the 2nd sampling point.

3.5 Discussion

For an encapsulation process, being non-damaging towards active compounds is an important quality. This study shows that electrospraying utilizing high voltage up to 25.0 kV could be safely used as an encapsulation method for IPNV antigen. This is in accordance with a large number of studies that provide strong evidence for variety of cells and other agents retaining their viability when electrosprayed. For instance, electrospraying does not impair viability of cells such as the human brain astrocytoma cells (Eddaoudi et al., 2010), bone marrow derived mesenchymal stem cells (Braghirolli et al., 2013; Sahoo et al., 2010), embryonic stem cells (Abeyewickreme et al., 2009), neuroblastoma rat cells (Gasperini et al., 2013), microorganisms as lactobacilli (Jiménez-Pranteda et al., 2012) and virions like bacteriophage (Jung et al., 2009).

For an encapsulant, it is important to be highly efficient at entrapping the active compounds. Our results showed that EDA-alginate and Ca-alginate were characterised by high encapsulation efficiency of IPNV antigen. However, it can also be seen that differences existed between these two alginate matrices. Use of EDA·2HCl as a cross-linker could lead to higher encapsulation efficiency than use of $CaCl_2$. This difference is mostly expressed when encapsulating IPNV Ag suspensions approaching concentration of 10^9 $TCID_{50}$ ml^{-1}. According to previous reports (Ainsley Reid et al., 2005; Anjani et al., 2007; Dashevsky, 1998; Suksamran et al., 2009), encapsulation efficiency of large macromolecules in Ca-alginate is ranging from 50 to 96%. This is in agreement with our encapsulation efficiency results for Ca-alginate ranging from 78% to almost 100% or not statistically

significant (NSS) loss. On the other hand, the obtained encapsulation efficiency for EDA-alginate (97% to nearly 100% or NSS loss) makes this alginate matrix very interesting from the oral delivery point of view. However, the EDA-alginate as a potential oral delivery system is very little described in the literature.

From our study of antigen uptake it can be seen that the intubated fish carry IPNV antigen in blood plasma (Figure 3.7). Interestingly, the group intubated with un-encapsulated antigens (UA group) showed higher blood plasma levels than fish administered encapsulated antigens (EA group) at 24 hours post intubation (p.i.). The EA group on the other hand showed a higher antigen concentration than the UA group at 72 hours p.i. However, this result may be questionable due to the high response of the control group intubated with empty alginate beads (EC group). Nevertheless, it can be proposed that the alginate encapsulation is delaying uptake of protein antigens. These findings are in accordance with number of studies that have demonstrated antigen uptake from the intestine to the blood in the systemic circulation (Fuglem et al., 2010; Georgopoulou et al., 1988; Vandenberg, 2007; Villumsen et al., 2014).

Ultimately, there was not statistically significant difference in uptake between all groups at 168 hours p.i.. This indicates that the antigen could be neutralised and processed after one week post ingestion. One of the challenges faced in this study was the fact that the experimental fish had previously been i.p. vaccinated against IPN. Therefore, the fish could have circulating antibodies that neutralised the absorbed antigens (Boxus et al., 2014; El-Attar et al., 2013). Additionally, the wide natural variation, which is

inherent in fish as a living organism, could have made it difficult to discern differences in the current trial (Wang et al., 2014). For instance, it can be assumed that the applied trial design was not powerful enough to detect statistically significant differences in the model (Moher, 1994). In general, any increase in statistical power requires additional resources which are commonly in shortage (Fox, 1997). Even so, the current results may be encouraging to make a future trial large in order to increase sensitivity. As an alternative, the same trial could be performed with involving adjuvants. There are number of reported adjuvants with ability to induce antigen uptake across the gastrointestinal tract epithelium (Lavelle and O'Hagan, 2006). Some of the tested adjuvants are immune-stimulating complexes (ISCOM™) (Sjölander, 1998), bacterial toxins such as heat-labile enterotoxin (Douce et al., 1999) and cholera toxin (Bowen et al., 1994), bio-adhesives such as lectins (Lavelle et al., 2000) and chitosan (van der Lubben et al., 2002).

Furthermore, the immunogenicity of IPNV antigen (both encapsulated and un-encapsulated) was explored in a feeding study. At the moment, the knowledge of an i.p. priming and oral boost strategy involving inactivated IPN virus is limited. The outcome of the 1.OB suggests that the alginate-encapsulated IPNV antigen, which is orally administered via feed, could boost the immune response of A. salmon. The results also show that type of alginate matrix could have a great significance for the outcome of antibody response. At the same time, non-encapsulation would most likely result in a poor specific immune reaction.

From the results of second boosting phase (2.OB), it can be assumed that the applied antigen dose (10^9 $TCID_{50}$ $fish^{-1}$) is either insufficient or excessive

for A. salmon approaching size of one kilogram. This assumption is based on the theory of oral tolerance which was first described almost 70 years ago (Owen, 1945). Today, oral tolerance generated through ingestion of antigenic substances is very well known phenomena (Jump and Levine, 2004; Siewert et al., 2008; Weiner et al., 2011). Pabst and Mowat (2012) suggest that both high and low antigen dose may induce oral tolerance. According to their report, higher doses of antigen favour anergy/deletion while low doses favour the induction of regulatory T cells (T_{regs}) as a mechanism of tolerance. According to Chen et al. 1996, immune tolerance could be induced with either one single high dose or multiple low doses of antigen. Given this, it can be concluded that the provision of an appropriate boosting dose is essential for the success of an oral IPN preparation.

Following the lead of oral tolerance it can be assumed that the hypo-responsiveness to the IPNV Ag entrapped in Ca-alginate (Encap 1) was induced in the 2.OB rather than in the 1.OB interval. The opposite can be said about IPNV Ag entrapped in EDA-alginate (Encap 2). Apparently, the Encap 2 induced immune tolerance already in the 1.OB period. Therefore, it did not perform significantly different from the control in either of the two intervals. The main argument is essentially that EDA-alginate dissolves faster than Ca-alginate. As a consequence, the Encap 2 group of fish probably received a higher peak dose than Encap 1. Thus, the Encap 2 group might have developed the immune tolerance as early as in the 1.OB. Regarding the unprotected IPNV Ag (Unencap), it is unclear whether its inability to induce immune response is an issue of immune tolerance or antigen degradation in the gut.

Furthermore, the findings of the present study demonstrate that oral boosting of A. salmon with alginate encapsulated IPNV antigens induces both systemic and mucosal (gut) humoral responses. The significant up-regulation of CD4 ($p < 0.02$) and GATA-3 ($p < 0.04$) genes in the head kidneys and spleens of the Encapsulated group (Figure 3.12 – 3.15) fit very well with the induction of serum antibodies and point towards a predominantly T_h2 response. In higher vertebrates, the intestinal mucosa contains high basal levels of IL-4, IL-10 and TGFβ that are induced shortly after oral vaccination (Gonnella et al., 1998). This micro-environment is thought to tip responses of oral vaccines towards T_h2 (Weiner, 2001). Furthermore, the main mechanism of action of alginate encapsulated antigens has been proposed to be biased towards T_h2 responses (Maurice et al., 2004; Mutwiri et al., 2002; Salvador et al., 2012; Sarei et al., 2013). These findings are consistent with reports of others using different antigens (Thinh et al., 2009; Tobar et al., 2011), and suggest that oral boosting with alginate encapsulated antigens holds promise as a means of augmenting immune responses against IPN.

In conclusion it can be said that multi-boosting with high antigen doses is not advantageous for the purpose of inducing specific immune response. It is neither advantageous to apply unprotected antigens as well as high concentrated antigens entrapped in fast-dissolving alginate matrices. On the other hand, an oral vaccine with too low dose could also fail to induce the specific immune responses and succeed in inducing immune tolerance.

According to observations in this study and reviewed literature, short-term but adequate doses would be the optimum strategy for oral boost vaccination. Since the dose-response of the oral IPNV Ag in A. salmon is very little

known, additional research should address this issue. In the event that the dose represent limiting factor, testing of uptake-stimulating adjuvants should be seriously considered. There are also questions regarding duration of an oral IPNV Ag dose action which could be answered in a future study.

On the whole, this study shed light on the opportunities and issues related to i.p. priming/oral boost strategy involving an inactivated IPN virus.

Chapter Four: Release from alginate matrices

Difference between the endothermic animals like human and ectothermic animals like fish are evident with respect to body temperature at which digestion reactions occur. In most studies, release of an active pharmaceutical ingredient from a cross-linked alginate is assessed in a dual dissolution test at one acidic pH 1 – 2 and another nearly neutral pH 6.8 – 7.4. The test temperature, which is adapted to humans, is normally maintained constant at 37°C. Release from most cross-linked alginates is both pH- and temperature-responsive. Consequently, seasonal temperature changes could pose a risk of uneven release of alginate-encapsulated antigens in A. salmon.

Therefore, the main objective of this study was to develop a fast-dissolving and temperature-independent oral delivery system within the temperature range of seawater in which A. salmon habituate. In addition, this study assesses a new dissolution test strategy with respect to chemical properties of alginate and physiological conditions for A. salmon. The new strategy is based on one single dissolution test combining pH 3.0 for 15 min with pH 8.0 for 50 min. The test is performed at two different temperatures (4°C and 18°C). It is demonstrated that the results generated in the redesigned dissolution test are in strong correlation with the results produced in the *in vivo* study. However, an attempt to localise release from calcium alginate beads by *in vivo* imaging was not successful. In conclusion, ethylenediammonium alginate proved to be an excellent oral delivery system for macromolecular drugs to A. Salmon.

4.1 Introduction

A. salmon is a carnivorous fish with a rather short digestive system (Løkka et al., 2013). Insight into digestive physiology of salmonid fish is very important for delivering therapeutic proteins via oral route to A. salmon (Shaji and Patole, 2008). Digestion is a catabolic process of solubilising and degrading nutrients into smaller components that are more easily absorbed into a blood stream (Biology-Online.org, 2014). Digestive tract of salmon as a carnivorous fish can be subdivided into the foregut (mouth, oesophagus and stomach), midgut (pyloric ceca or proximal intestine and mid intestine) and hindgut or distal intestine terminating in the rectum (National Research Council, 2011). The major digestive components secreted in the stomach are pepsinogen and hydrochloric acid (HCl) and secretion of both of them are stimulated by feed intake (Volkoff, 2010). Study by Bucking and Wood (2009) shows that an average gastric pH of 2.7 increases to 4.9 when Rainbow trout (*Oncorhynchus mykiss*) goes from starved to fed state. The increased pH is maintained for eight hours post-feeding. However, most of the proteins are degraded by the action of HCl and pepsin in stomach (National Research Council, 2011). After processing in stomach, mixture of dissolved nutrients and partially digested feed material pass into the pyloric caeca. The pyloric caeca is a compartment where the other proteolytic enzymes like trypsin, chymotrypsin and aminopeptidase are completing peptide hydrolysis (Einarsson et al., 1996; Krogdahl and Bakke-McKellep, 2005). According to Krogdahl et al. (1999), most proteins are absorbed into the blood stream as free amino acids and short peptides in the pyloric region. When the acidic chime reaches the proximal intestine it becomes rapidly neutralised by

bicarbonate (HCO_3^-) in bile and pancreatic juice (Cooper, 2008). Bucking and Wood (2009) observe an average pH of 8.2 throughout the whole intestinal section before feed intake. After feeding, pH is decreasing to 7.5 in the proximal and mid intestine while it remains almost unchanged in the distal section. However, the pH increases again in the period after feeding, reaching its highest value after eight hours. At that point, the pH can be above 8.5 all along the intestinal tract with increasing trend toward the distal part.

However, despite the harsh proteolytic environment in the foregut and midgut, some proteins make it through to the distal intestine where they can be absorbed. Distal intestine is considered to be the most important place of absorption of large peptides including antigens used in oral vaccines (Hernandez-Blazquez and Silva, 1998; Valle et al., 2008). Additionally, the second segment of mid intestine and the distal intestine are the places with the highest levels of immune transcripts of immune-related genes in A. salmon (Løkka et al., 2014a). For instance, Petrie and Ellis (2006) provide evidence for uptake of particles (d <3 µm) by the hindgut of A. salmon following anal intubation of inert polystyrene microspheres. Løkka et al. (2014b) demonstrate uptake and possible transport of anally intubated yeast particles (5 – 10 µm) over the epithelium by macrophage-like cells in A. salmon.

Thamotharan et al. (1996) suggest that intestinal transport of peptides in herbivorous and carnivorous fishes is proton gradient dependent and resembles the peptide transport proposed for mammals. On the other hand, the passage time of feed material through the entire digestive system can be

very short. According to Storebakken (1985), intestinal transit time depends on meal size, feed composition and structure, and it could be anything from 5 to 35 hours after feed intake. Therefore, the main focus of this study is to assess an oral delivery system that protects at a low pH of the stomach and releases an active pharmaceutical ingredient (API) at an alkaline pH of the distal intestine. For the reasons that oral delivery of macromolecular drug is of special interest in the current study, blue dextran (BD) was selected as an appropriate model API. Additionally, bio-adhesive properties, fast release and temperature independency are preferable characteristics of an oral delivery system. These properties are useful in counteracting conditions occurred due to a possible short intestinal transit time and seasonal temperature effects. Taking these prerequisites into account, cross-linked alginates excel in an oral delivery systems exhibiting aforementioned properties (Augst et al., 2006; Maurice et al., 2004; Rombout et al., 2011; Tian et al., 2008). Moreover, considering the physical properties of cross-linked alginates, salts of calcium and ethylenediammonium alginate were investigated in this study. Ethylenediammonium alginate (EDA-alginate) is of particular interest due to better solubility than calcium alginate (Ca-alginate) (Cooper et al., 1962). However, design of an alginate matrix characterised with well-timed release is a typical challenge in delivering bioactive compounds to the distal intestine of A. salmon.

Most studies test dissolution of alginate matrices under conditions which are relevant for the human digestive system (pH = 1.1-2.0 and pH = 6.8-7.4 at 37°C)(Bashir et al., 2014; Ferreira Almeida and Almeida, 2004; Kaushik K. et al., 2011; Lee and Min, 1996). As previously mentioned it can be seen that

pH > 2.7 is most common in the stomach of salmonid fish. At the same time pH > 7.5 is prevalent in the intestinal sections, although pH > 8.5 is not an unusual condition either. Furthermore, winter temperature could be below 4°C while summer temperature could be at its most extreme above 18°C in Norwegian seawaters (Aldrin et al., 2013; Hevrøy et al., 2012). Despite these facts, there is no scientific study published evaluating *in vitro* dissolution of oral delivery systems based on alginates at test conditions relevant for A. Salmon. Therefore, this study is engaged in adapting the current dissolution test to the digestive conditions that are representative for salmonid fish as ectothermic animals.

The primary objective of this study was to develop an oral delivery system based on alginate with the following characteristics: 1) deliver antigens to the distal intestine of A. salmon in the intact form, and 2) releases the antigen *in vivo* independently of the seasonal temperature oscillations in the natural habitat of A. salmon.

The secondary objectives of this study were: 1) to develop a dissolution test that is representative for salmonid fish as ectothermic animals with alkaline pH in the intestine, and 2) to produce a test that is able to determine the release site of alginate-encapsulated antigens *in vivo*.

In order to meet the objectives of present study, several *in vitro* dissolution tests were assessed with the aim of comparing EDA-alginate to Ca-alginate. The tests were performed with BD as a model compound at relevant temperature and pH for A. salmon. Furthermore, an attempt was made to localise the site of Ca-alginate dissolution in A. salmon using an *in vivo*

imaging technique. The *in vivo* trial was based on the oral intubation of Ca-alginate-encapsulated cardiogreen as a model compound. In the end, another effort was made to localise the site of both Ca-alginate and EDA-alginate dissolution in A. salmon using an enzyme assay approach. The *in vivo* trial was based on feeding the fish with Ca-/EDA-alginate-encapsulated horseradish peroxidase (HRP) infused into feed.

4.2 *In vitro* study of blue dextran release from alginate matrices

In this section, release of BD from Ca-alginate and EDA-alginate beads was assessed in a standard dissolution test (pH 1.2 and 6.8 at 37°C). Thereafter, release from the same alginates was tested in alkaline dissolution media (pH 8.0 and 8.6) at 18°C. This was done in order to find an appropriate substitute for dissolution medium having pH 6.8. This medium is representative for conditions in duodenum of humans. However, conditions in the salmon intestine are alkaline (pH 8 – 8.6). Finally, based on the results from the previous tests, a new dissolution test strategy (pH 3.0/8.6 at 4°C/18°C) was assessed.

4.2.1 Methods

4.2.1.1 Preparation of alginate beads loaded with blue dextran

Alginate beads loaded with blue dextran (BD) were prepared according to the common encapsulation method described in the Section 2.2.1.1 (Chapter 2). The non-use of voltage (U) was the only variation to the general method. Process parameters and their respective values are listed in the Table 4.1. In the process of encapsulation, the following items were used: plastic syringe (Item T002, Table 2.2), needle (Item T014, Table 2.2), encapsulation formulation (Item S007, Table 2.4) and crosslinking solution (Item S003 and S004, Table 2.4).

By utilising this setup, 40 batches of BD-Ca-alg and 40 batches of BD-EDA-alg beads were produced. For the purpose of determining encapsulation efficiency, ten batches of each type of beads were used while the remaining

batches were used in dissolution tests (Table 5.1). The particle size distribution and shape were determined by stereo microscope (Item I001, Table 2.3). Electrospraying - process variables with their respective values

Table 4.1: Electrospraying process variables applied in encapsulating blue dextran by for dissolution testing.

Internal diameter (needle)	Flow rate	Target volume	Voltage	Distance[i]	Volume[ii]
ID	Q	V_{tv}	U	x	V_{xls}
µm	$cm^3\ h^{-1}$	ml	kV	mm	ml
2000	50	1.5	0	100	10

[i]Distance between the needle tip and the surface of crosslinking solution (x)
[ii]Volume of the cross-linking solution (V_{xls})

4.2.1.2 Encapsulation efficiency of blue dextran

BD-Ca-alg beads (10 batches) and BD-EDA-alg beads (10 batches) which preparation is previously described in the Section 4.2.1.1, were separately added to the saturated $NaHCO_3$ solution (380 ml per batch; pH 8.0; Item S005, Table 2.4). As a result, all beads were completely dissolved after two hours under stirring in glass beakers (Figure 4.1). An aliquot (10 ml) from each beaker was filtered through a syringe filter (Item T009, Table 2.2). The filtrates were then applied in the volume of 100 µl per well onto a 96-well polystyrene plate (Item T006, Table 2.2). An endpoint assay was carried out on a microplate reader (Item I003, Table 2.3). Absorbance of BD was measured at 610 nm and 24°C. Concentration of BD in the samples was determined by using standard curve in the range of 1.0 to 3.9×10^{-3} mg ml^{-1}. Standard curves were generated by plotting BD concentrations of nine two-

fold serial dilutions of BD solution (1.0 mg ml^{-1}) versus absorbance. The BD solution (1.0 mg ml^{-1}) was prepared by diluting BD-EncForm (Item S007, Table 2.4) with saturated $NaHCO_3$ solution (Item S005, Table 2.4).

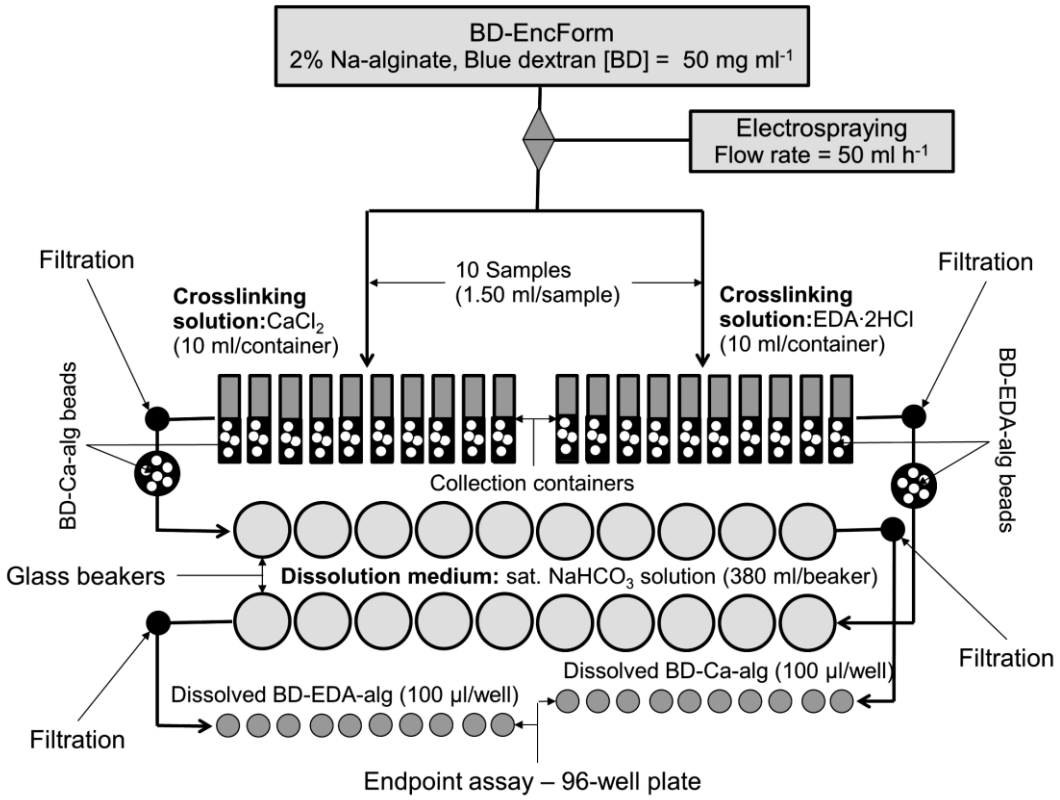

Figure 4.1: Execution of encapsulation efficiency test: BD-EncForm - encapsulation formulation containing sodium alginate [Na-alg] = 20 mg ml^{-1} and blue dextran [BD] = 50 mg ml^{-1}. BD-Ca-alg – calcium alginate beads loaded with blue dextran. BD-EDA-alg – ethylenediammonium alginate beads loaded with blue dextran. EDA▪2HCl – ethylenediamine dihydrochloride solution. CaCl2 – calcium chloride solution. Sat. $NaHCO_3$ – saturated sodium bicarbonate solution. Ten batches of BD-Ca-alg beads were generated by extruding BD-EncForm (1.5 ml per batch) into collection containers containing crosslinking solution ($CaCl_2$, 10 ml per container). Another ten batches of BD-EDA-alg beads were formed by extruding BD-EncForm (1.5 ml per batch) into collection containers containing crosslinking solution (EDA▪2HCl, 10 ml per container). The resulting alginate beads were removed from crosslinking solutions by filtration and then transferred into glass beakers containing sat. $NaHCO_3$ (380 ml per beaker). The beads were dissolved under stirring. Part of the solution (10 ml) from each beaker was filtered and then applied in the volume of 100 µl per well onto 96-well plate.

4.2.1.3 Standard dissolution test

This dissolution test is widely used to assess dissolution properties of oral dosage forms. For this reason, it was the first conducted test, although the test conditions were not representative for A. salmon.

Test alginate beads (10 batches of BD-Ca-alg and 10 batches BD-EDA-alg) loaded with BD were produced according to the method described in the Section 4.2.1.1. The following dissolution tests were performed in quintuplicate at 37°C: 1) BD-Ca-alg at pH 1.2, 2) BD-EDA-alg at pH 1.2, 3) BD-Ca-alg at pH 6.8 and 4) BD-EDA-alg at pH 6.8 (Table 4.2). Both dissolution tests and later sample analysis were carried out according to the method described in the section 2.2.2 (Chapter 2).

Table 4.2: Dissolution conditions applied in the standard dissolution test using UPS Apparatus 1. The dissolution conditions apart from pH were identical in all four tests.

Parameters	Test 1	Test 2	Test 3	Test 4
Alginate beads (AB)	BD-Ca-alg[i]	BD-EDA-alg[ii]	BD-Ca-alg	BD-EDA-alg
Apparatus	UPS 1	UPS 1	UPS 1	UPS 1
Basket rotation (f)	100 rpm	100 rpm	100 rpm	100 rpm
Dissolution media	NaCl/HCl[iii]	NaCl/HCl	PhB[iv]	PhB
(DM)	pH 1.2	pH 1.2	pH 6.8	pH 6.8
Volume of media (V)	380 ml	380 ml	380 ml	380 ml
Temperature (t)	37°C	37°C	37°C	37°C
Number of sampling points ($n_{SP)}$	10	10	10	10
Sampling points (t_{SP})	5,10,15,20, 25,…50 min	5,10,15,20, 25,…50 min	5,10,15,20, 25,…50 min	5,10,15,20, 25,…50 min
Number of vessels (n_{vessel})	5	5	5	5
Sample volume[v] (V_{sample})	1.0 ml	1.0 ml	1.0 ml	1.0 ml

[i]BD-Ca-alg – calcium alginate beads loaded with blue dextran
[ii]BD-EDA-alg – ethylenediammonium alginate beads loaded with blue dextran
[iii]NaCl/HCl – sodium chloride/hydrochloric acid buffer, pH 1.2 (Item S015, Table 2.4)
[iv]PhB – phosphate buffer, pH 6.8 (Item S017, Table 2.4)
[v]Sampled volume (1 ml per sampling point per vessel) was replaced by an equivalent amount of dissolution medium

4.2.1.4 Assessment of alkaline dissolution media

Four additional dissolution tests were performed in order to select an alkaline dissolution medium, which would be representative for the conditions found in A. salmon intestine. Test alginate beads (10 batches of BD-Ca-alg and 10 batches of BD-EDA-alg) loaded with BD were produced according to the method described in the Section 4.2.1.1. The same setup as the one described in the section 2.2.2 (Chapter 2) was applied in performing these new tests. The tests were carried out with five replications in two different

dissolution media: 1) phosphate buffer (pH 8.0; Item S018, Table 2.4) and 2) Gly/NaOH buffer (pH 8.6; Item S019, Table 2.4) at 18°C. Accordingly, the following tests were conducted: 5) BD-Ca-alg at pH 8.0, 6) BD-EDA-alg at pH 8.0, 7) BD-Ca-alg at pH 8.6 and 8) BD-EDA-alg at pH 8.6 (Table 4.3). The dissolution conditions other than pH were identical in all four tests. Concentration of BD in the samples was determined by using standard curve approach as previously described in the Section 2.2.2 (Chapter 2).

Table 4.3: Dissolution conditions applied in the four tests assessing alkaline dissolution media best suited for simulating intestinal conditions in A. salmon. The dissolution conditions other than pH were identical in all four tests.

Parameters	Test 5	Test 6	Test 7	Test 8
Alginate beads (AB)	BD-Ca-alg[i]	BD-EDA-alg[ii]	BD-Ca-alg	BD-EDA-alg
Apparatus	UPS 1	UPS 1	UPS 1	UPS 1
Basket rotation (f)	100 rpm	100 rpm	100 rpm	100 rpm
Dissolution media (DM)	PhB[iii] pH 8.0	PhB pH 8.0	Gly/NaOH[iv] pH 8.6	Gly/NaOH pH 8.6
Volume of media (V)	380 ml	380 ml	380 ml	380 ml
Temperature (t)	18°C	18°C	18°C	18°C
Number of sampling points ($n_{SP)}$	10	10	10	10
Sampling points (t_{SP})	5,10,15,20, 25,…50 min	5,10,15,20, 25,…50 min	5,10,15,20, 25,…50 min	5,10,15,20, 25,…50 min
Number of vessels (n_{vessel})	5	5	5	5
Sample volume[v] (V_{sample})	1.0 ml	1.0 ml	1.0 ml	1.0 ml

[i]BD-Ca-alg – calcium alginate beads loaded with blue dextran
[ii]BD-EDA-alg – ethylenediammonium alginate beads loaded with blue dextran
[iii]PhB – phosphate buffer, pH 8.0 (Item S018, Table 2.4)
[iv]Gly/NaOH – glycine/sodium hydroxide buffer, pH 8.6 (Item S019, Table 2.4)
[v]Sampled volume (1 ml per sampling point per vessel) was replaced by an equivalent amount of dissolution medium.

4.2.1.5 New dissolution test strategy

Conditions that alginate beads could be exposed to during their passage through gastrointestinal tract of A. salmon were simulated in another four dissolution tests. For that reason, alginate beads were first submerged into acidic dissolution medium (pH 3.0; Item S016, Table 2.4) to simulate the gastric conditions. After 15 minutes, the acidic medium was replaced with an alkaline medium (pH 8.0; Item S018, Table 2.4) to simulate the intestinal conditions in A. salmon. Test alginate beads (10 batches of BD-Ca-alg and 10 batches of BD-EDA-alg) loaded with BD were produced according to the method described in the Section 4.2.1.1. The tests were conducted using the UPS Apparatus 1 as shown in the Figure 4.2. In order to replicate the natural conditions in which A. salmon habituate as fully as possible, two different temperatures (4°C – winter and 18°C – summer) were applied in these tests. Consequently, the following four dissolution tests were carried out in quintuplicate: 9) BD-Ca-alg at pH 3.0 – 8.0 and 4°C, 10) BD-EDA-alg at pH 3.0 – 8.0 and 4°C, 11) BD-Ca-alg at pH 3.0 – 8.0 and 18°C, 12) BD-EDA-alg at pH 3.0 – 8.0 and 18°C (Table 4.4). The first sample was taken after 15 min in the KPH/HCl buffer (pH 3.0) or just before changing the dissolution medium. Further sampling, which started 5 min after replacing dissolution medium, were carried out according the general method described in the Section 2.2.2 (Chapter 2). Concentration of BD in the samples was determined by using standard curve approach along with an endpoint assay. The details regarding assay can be found in the Section 2.2.2 (Chapter 2) as well. The resulting dissolution profiles were compared by a model independent approach using both difference factor (f_1, Equation 4.1) and

similarity factor (f_2, Equation 4.2). Two dissolution profiles are similar when the f_1 value is between 0 and 15 and f_2 value between 50 and 100 (Costa and Sousa Lobo, 2001). It is important to note that encapsulation efficiency of BD was taken into consideration when designing the dissolutions tests.

Finally, statistical analysis of the obtained data was performed according to the description in the Section 2.2.6.3 (Chapter 2).

Equation 4.1: Difference factor (f_1) where, n is the number of observations, R_t is the average percentage of drug dissolved from a reference formulation at time t and T_t is the average percentage of drug dissolved from a test formulation at time t. Difference factor is defined as the percent (%) difference between two curves at different time points. It represents the measurement of relative error between two curves.

$$f_1 = 100\left[\frac{\sum_{t=1}^{n}|R_t - T_t|}{\sum_{t=1}^{n} R_t}\right]$$

Equation 4.2: Similarity factor (f_2) where, n is the number of observations, R_t is the average percentage of drug dissolved from a reference formulation at time t and T_t is the average percentage of drug dissolved from a test formulation at time t. Similarity factor is defined as a logarithmic reciprocal square root transformation of the sum of the squared error.

$$\boldsymbol{f_2 = 50\,\log\left\{\frac{100}{\sqrt{\left[1+\frac{1}{n}\sum_{t=1}^{n}(R_t - T_t)^2\right]}}\right\}}$$

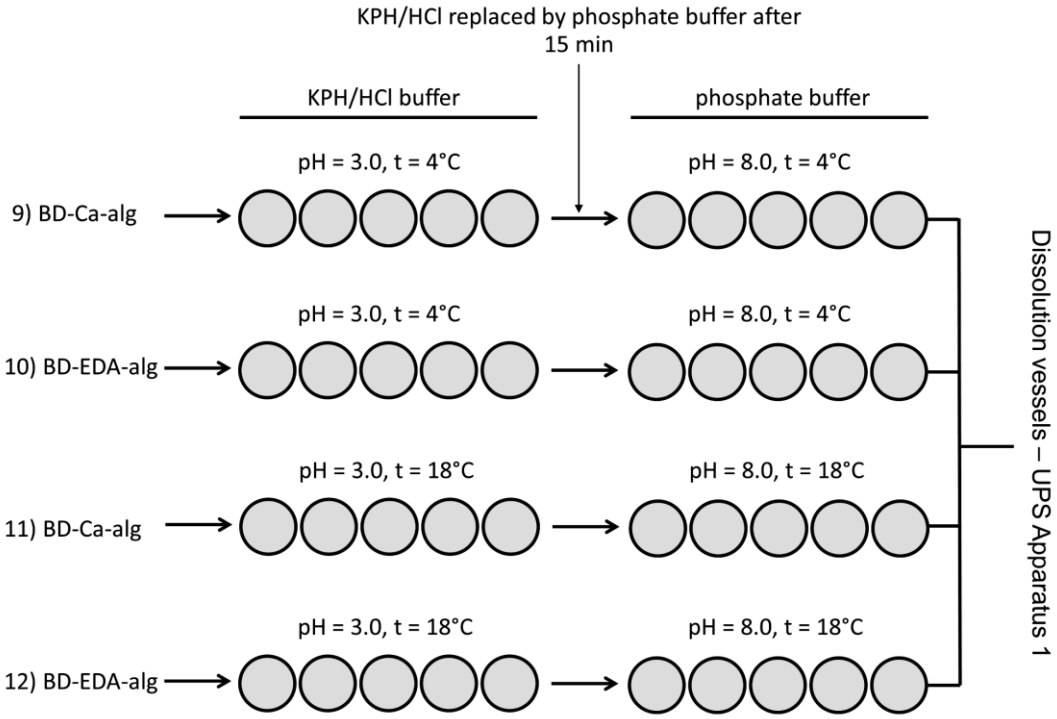

Figure 4.2: Assessment of a new dissolution test strategy using UPS Apparatus 1. BD-Ca-alg – calcium alginate beads loaded with blue dextran. BD-EDA-alg – ethylenediammonium alginate beads loaded with blue dextran. KPH/HCl – potassium hydrogen phthalate/hydrochloric acid buffer (pH 3.0). The tests were performed using two different dissolution media at 4°C and 18°C. Alginate beads were first submerged into KPH/HCl buffer (pH 3.0) for 15 min and then the acidic medium was replaced by phosphate buffer (pH 8.0). The first sample was taken after 15 min or just before changing the dissolution medium. Thereafter, one sample was taken with replacement from each vessel at five minutes intervals through an extent of 50 minutes totaling 10 samples per vessel.

Table 4.4: Dissolution conditions applied in the four tests assessing the new dissolution test strategy most suited for A. salmon. The dissolution conditions other than temperature were identical in all four tests.

Parameters	Test 9	Test 10	Test 11	Test 12
Alginate beads (AB)	BD-Ca-alg[i]	BD-EDA-alg[ii]	BD-Ca-alg	BD-EDA-alg
Apparatus	UPS 1	UPS 1	UPS 1	UPS 1
Basket rotation (f)	100 rpm	100 rpm	100 rpm	100 rpm
Dissolution media	1) KPH/HCl[iii]	1) KPH/HCl	1) KPH/HCl	1) KPH/HCl
(DM)	pH 3.0	pH 3.0	pH 3.0	pH 3.0
	2) PhB[iv]	2) PhB	2) PhB	2) PhB
	pH 8.0	pH 8.0	pH 8.0	pH 8.0
Volume of media (V)	380 ml	380 ml	380 ml	380 ml
Temperature (t)	4°C	4°C	18°C	18°C
Number of sampling points ($n_{SP)}$	10	10	10	10
Sampling points at pH 3.0 (t_{SP})	15 min	15 min	15 min	15 min
Sampling points at pH 8.0 (t_{SP})	5,10,15,20, 25,…50 min	5,10,15,20, 25,…50 min	5,10,15,20, 25,…50 min	5,10,15,20, 25,…50 min
Number of vessels (n_{vessel})	5	5	5	5
Sample volume[v] (V_{sample})	1.0 ml	1.0 ml	1.0 ml	1.0 ml

[i]BD-Ca-alg – calcium alginate beads loaded with blue dextran
[ii]BD-EDA-alg – ethylenediammonium alginate beads loaded with blue dextran
[iii]KPH/HCl – potassium hydrogen phthalate/hydrochloric acid buffer, pH 3.0 (Item S016, Table 2.4)
[iv]PhB – phosphate buffer, pH 8.0 (Item S018, Table 2.4)
[v]Sampled volume (1 ml per sampling point per vessel) was replaced by an equivalent amount of dissolution medium.

4.2.2 Results

4.2.2.1 Encapsulation efficiency of blue dextran

After encapsulating BD formulation (BD-EncForm, [BD] = 50 mg ml^{-1}; Item S007, Table 2.4), the actual average concentration (±SD) of BD in EDA-alginate and Ca-alginate beads dropped to 35 ±1.4 mg ml^{-1} and 45 ±1.8 mg ml^{-1} respectively (Table 4.5). From this, it can be derived that the average encapsulation efficiency (±SD) of BD in Ca-alginate and EDA-alginate was 90% (±4%) and 70% (±4%) respectively. Furthermore, the mean size (d_{mean} ±SD) of the Ca-alginate beads was 3.0 ±0.04 mm while the mean size (±SD) of the EDA-alginate beads reached 3.7 ±0.11 mm. From the Figure 4.3, it can be seen that shape of the beads was spherical for both type of the alginate beads.

Table 4.5: Encapsulation efficiencies of blue dextran (BD) in ethylenediammonium alginate (EDA-alg) and calcium alginate (Ca-alg). Variability of the data set is expressed by standard deviation (SD) based on ten replications of each formulation sample.

Formulation name	Theoretical BD concentration (mg ml^{-1})	Actual BD concentration (mg ml^{-1})	Encapsulation efficiency (%)	SD (%)
BD-EDA-alg[i]	50	35	70	4
BD-Ca-alg[ii]	50	45	90	4

[i]BD-Ca-alg – calcium alginate beads loaded with blue dextran
[ii]BD-EDA-alg – ethylenediammonium alginate beads loaded with blue dextran

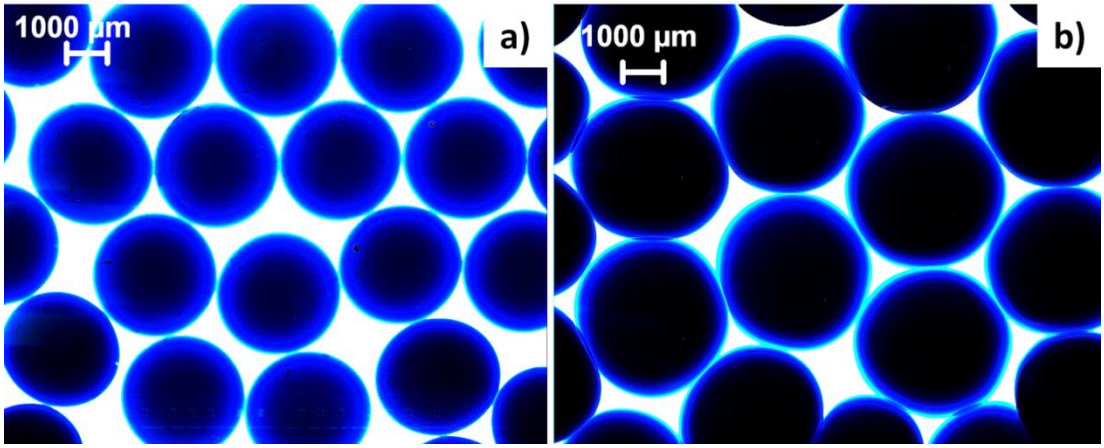

Figure 4.3: Stereo microscope zoom (SMZ) images of alginate beads loaded with blue dextran. SMZ (Item I001, Table 2.3) images of a) BD-Ca-alg beads, d_{mean} (±SD) = 3.0 (±0.04) mm, b) BD-EDA-alg beads, d_{mean} (±SD) = 3.7 (±0.11) mm. BD-Ca-alg – calcium alginate beads loaded with blue dextran, BD-EDA-alg – EDA-alginate beads loaded with blue dextran.

4.2.2.2 Dissolution tests

Release of BD from both Ca-alginate and EDA-alginate matrices was below the quantification limit (LoQ = 3.9×10^{-3} mg ml^{-1}) of the assay within the first hour in the standard dissolution tests. Similarly, the release of BD from both alginate matrices was below LoQ (3.9×10^{-3} mg ml^{-1}) at both pH 8.0 and pH 8.6 in the alkaline dissolution test.

In the dissolution tests adapted to the way in which salmonid fish process alginate, sufficient release of BD was observed in all four tests (Figure 4.4). So that the release, which was below LoQ (3.9×10^{-3} mg ml^{-1}) in pH 3.0 after 15 min, turned into a fairly rapid one in pH 8.0 during the following 50 minutes.

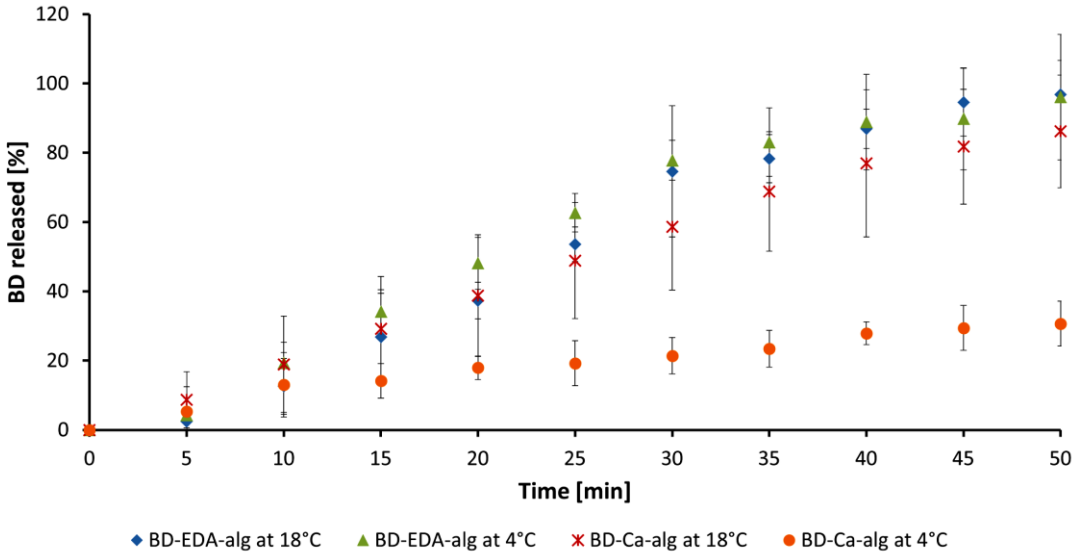

Figure 4.4: Dissolution profiles shown as curves of the mean percentage of cumulative blue dextran (BD) release from alginate beads over time. Dissolution tests performed in potassium hydrogen phthalate /HCl buffer (pH 3.0) for 15 min followed by phosphate buffer (pH 8.0) for the next 50 min. Release was below LoQ (3.9×10^{-3} mg ml^{-1}) in the acidic medium so the figure depicts only release in the alkaline dissolution medium. The error bars represent standard deviation (SD) based on five samples at each point. BD-EDA-alg denotes ethylenediammonium alginate beads loaded with BD while BD-Ca-alg means calcium alginate beads loaded with BD.

From the Table 4.6, it can be seen that the release rates of BD (ROC and AROC) from EDA-alginate beads were between 2.1% and 2.2% per minute. This release rate was very close to linear ($0.96 < R^2 > 0.97$) in the time interval (0, 50 min). Interestingly, the dissolution rates of EDA-alginate seemed to be unaffected by temperature in the interval (4, 18°C). On the other hand, the release rate of BD form Ca-alginate beads (ROC = 1.8% at 18°C and 0.6% at 4°C) seemed to be temperature dependent. In accordance with the dissolution profiles of EDA-alginate, the dissolution rates of Ca-alginate beads also followed the linear relationship ($0.95 < R^2 > 0.99$) in the same time interval (0, 50 min).

Table 4.6: Rates of blue dextran release (ROC[ii] and AROC[iii]) from calcium and ethylenediammonium alginate were determined at 4°C and 18°C. First- and second-order approximations of dissolution curves are shown with corresponding coefficients of determination (R^2). Data fits very well both linear and non-liner function in the time interval 0 to 50 minutes after changing dissolution medium.

Product	Order[i]	Dissolution curves	R^2	ROC[ii]	AROC[iii]
BD-EDA-alg[iv]	1st	y=2.2101x-3.9877	0.97	2.21	n.a.
at 18°C	2nd	$y=-0.0112x^2+2.7696x-8.1836$	0.98	n.a.	2.21
BD-EDA-alg	1st	y=2.1061x+2.251	0.96	2.11	n.a
at 4°C	2nd	$y=-0.0264x^2+3.4249x-7.6404$	0.99	n.a.	2.10
BD-Ca-alg[v]	1st	y=1.8109x+1.7095	0.99	1.81	n.a.
at 18°C	2nd	$y=-0.01x^2+2.3088x-2.0247$	1.00	n.a.	1.81
BD-Ca-alg	1st	y=0.5760x+4.0063	0.95	0.58	n.a.
at 4°C	2nd	$y=-0.0067x^2+0.91121x+1.4852$	0.98	n.a.	0.58

[i]orders of approximation: first- and second-order approximation applied here
[ii]ROC – rate of change or release of blue dextran (% per minute) derived from the 1st order approximation.
[iii]AROC – average rate of change or release of blue dextran (% per minute) derived from the 2nd order approximation.
[iv]BD-EDA-alg – ethylenediammonium alginate beads loaded with blue dextran
[v]BD-Ca-alg – calcium alginate beads loaded with blue dextran

From the Table 4.8, it can be seen that 85% of BD was released from EDA-alginate beads within 40 minutes in pH 8.0 regardless of temperature. Dissolution rate of Ca-alginate at 18°C was a little lower than that of EDA-alginate resulting in 85% release within 50 min. However, only 31% of BD was released from Ca-alginate beads after 50 min at 4°C. This was significantly lower compared to the dissolution rates in the other three tests. According to USP General Chapter <1092>, these dissolution results may be considered highly variable because of the RSD > 20% at time points below 10 min and RSD > 10% at the time points above 10 min (USP, 2012c).

Dissolution profile of Ca-alginate at 4°C was obviously different and therefore it was not mathematically compared with the other profiles.

The other three dissolution profiles were compared by calculating both difference factor (f_1) and similarity factor (f_2). In order to consider two dissolution profiles as similar, the f_1 value should be close to 0 and values f_2 should be close to 100. Generally, f_1 values lower than 15 and f_2 values higher than 50 indicate the similarity of the dissolution profiles. From the Table 4.7, it can be seen that the dissolution profiles excluding Ca-alginate at 4°C are quite similar. This may be argued even though the comparison of BD-Ca-alg at 18°C with BD-EDA-alg at 4°C resulted in the f_1 = 16 and f_2 = 48. These values as shown in the Table 4.7 are barely above ($f_1 \leq 15$) and below ($f_2 \geq 50$) the threshold.

Table 4.7: Similarity of dissolution profiles was determined by both difference factor (f1) and similarity factor (f2). Conventionally, f1 values lower than 15 and f2 values above 50 show the similarity of the dissolution profiles.

Compared formulations			f_1	f_2
BD-Ca-alg[i] at 18°C	vs	BD-EDA-alg[ii] at 18°C	14	52
		BD-EDA-alg at 4°C	16	48
BD-EDA-alg at 18°C	vs	BD-EDA-alg at 4°C	12	59

[i]BD-Ca-alg – calcium alginate beads loaded with blue dextran
[ii]BD-EDA-alg – ethylenediammonium alginate beads loaded with blue dextran

Table 4.8: The average value (Mean) and standard deviation (SD) of cumulative percentage drug dissolved for two different blue dextran (BD) formulations at two different temperatures (4°C and 18°C). Variability in the data set is expressed by relative standard deviation in terms of percentage (%RSD). It is obtained by dividing SD by Mean and then multiplying by 100.

	BD-Ca-alg[i] at 18°C				BD-EDA-alg[ii] at 18°C		
Time (min)	Mean	SD	%RSD	Time (min)	Mean	SD	%RSD
5	8.73	8.09	93	5	2.42	3.32	138
10	18.94	13.92	74	10	12.59	8.02	64
15	29.22	15.01	51	15	26.85	12.59	47
20	38.78	17.54	45	20	37.34	5.30	14
25	48.84	16.77	34	25	53.57	4.96	9
30	58.62	18.31	31	30	74.61	18.95	25
35	68.83	17.21	25	35	78.32	6.95	9
40	76.91	21,27	28	40	86.88	5.66	7
45	81.76	16.57	20	45	94.55	9.78	10
50	86.17	16.26	19	50	96.79	9.84	10
	BD-Ca-alg at 4°C				BD-EDA-alg at 4°C		
Time (min)	Mean	SD	%RSD	Time (min)	Mean	SD	%RSD
5	5.28	7.15	135	5	4.30	4.87	113
10	13.00	9.34	72	10	19.29	6.07	31
15	14.15	5.03	36	15	34.09	6.40	19
20	17.93	3.42	19	20	48.09	7.48	16
25	19.25	6.46	34	25	62.69	5.52	9
30	21.39	5.27	25	30	77.81	5.79	7
35	23.44	5.31	23	35	83.03	9.88	12
40	27.89	3.28	12	40	88.84	13.82	16
45	29.45	6.46	22	45	89.77	14.75	16
50	30.68	6.47	21	50	96.04	18.09	19

[i]BD-Ca-alg – calcium alginate beads loaded with blue dextran

[ii]BD-EDA-alg – ethylenediammonium alginate beads loaded with blue dextran

4.3 Dissolution of alginate beads visualised by the *in vivo* imaging technique

The aim of this study was to follow the *in vivo* displacement of one single alginate bead as a function of time. Eventually, the site of Ca-alginate dissolution in A. salmon would be localized by using an *in vivo* imaging technique. For this reason, fish was orally intubated with one Ca-alginate bead loaded with cardiogreen. Cardiogreen is a fluorescent marker which is used in medicine as an indicator compound.

4.3.1 Methods

4.3.1.1 Preparation of alginate beads loaded with cardiogreen

Alginate beads loaded with cardiogreen (CG) were prepared according to the common encapsulation method which is described in the Section 2.2.1.1 (Chapter 2). Disconnected voltage (U) was the only variation to the general method. Process parameters and their respective values are summarised in the Table 4.9. The following items were specific to this encapsulation process: needle (Item T014, Table 2.2), encapsulation formulation (Item S030, Table 2.4) and crosslinking solution (Item S003, Table 2.4).

Table 4.9: Electrospraying - process variables with their respective values in the *in vivo* imaging trial.

Internal diameter (needle)	Flow rate	Target volume	Voltage	Distance[i]	Volume[ii]
ID	Q	V_{tv}	U	x	V_{xls}
µm	$cm^3\ h^{-1}$	ml	kV	mm	ml
2000	50	10	0	100	50

[i]Distance between the needle tip and the surface of crosslinking solution (x)
[ii]Volume of the cross-linking solution (V_{xls})

4.3.1.2 Fish trial – oral intubation

The fish trial was performed according to the general method described in the section 2.2.5.2 (Chapter 2) at TempOx lab (EWOS Innovation AS, Dirdal, Norway). Parameters applied in this trial are listed in the Table 4.10. Moreover, fish was starved one day in advance of the treatment. Control fish ($n_{control}$ = 2) were sampled directly from the acclimatisation tank just before the intubation. Each fish (n_{fish} = 30) was orally intubated with one alginate bead loaded with cardiogreen (d_{avg} = 3.2 mm). Whole fish samples ($n_{sampled}$ = 18) were stored at -20^{o}C prior to the *in vivo* imaging. The *in vivo* imaging analysis of the fish was conducted by IVIS Spectrum (Item I009, Table 2.3) at Caliper Life Sciences Ltd. (Runcorn, UK). Trans-illumination (from the bottom) was used to illuminate the fluorescence source (alginate beads loaded with cardiogreen) in the fish. Excitation was induced at wavelength of 745 nm while the intensity of the emitted fluorescence was measured at 840 nm. The field of view was adjusted to 13.1 ˣ 13.1 cm. Images (2048 ˣ 2048

pixels) with pixel size of 13.5 µm were taken with read noise < 5 electrons for bin of 8 pixels at lens speed f/2

Table 4.10: Electrospraying – process parameters applied in the *in vivo* imaging trial carried out by oral intubation with alginate beads loaded with cardiogreen.

Parameter	Symbol	Quantity
Average weight of fish	m	157 g
Oxygen saturation in water	O_2	90%
Water temperature	t	10°C
Diameter of a tank	d	2.0 m
Volume of a tank	V	3.1 m^3
Number of tanks	n_{tanks}	1
Number of fish per tank	n_{fish}	30
Number of groups	n_{groups}	1
Length of the acclimatisation period	t_{accl}	1 week
Number of treatments	n_{treat}	1
Number of control fish	$n_{control}$	2
Number of sampled fish per tank per sampling point	$n_{sf/t}$	2
Number of sampling points	n_{SP}	8
Length of sampling time intervals calculated from the end of treatment	t_{SP}	0, 2, 4, 6, 8, 10, 24, 72 h
Total number of sampled fish	$n_{sampled}$	18

4.3.2 Results

The Figure 4.5 shows that the alginate bead did not change position considerably from the time of intubation (0 hours) to 72 hours post intubation (p.i.). It seems that cardiogreen was becoming systemic at 72 hours p.i. but the highest concentration was still at the same focal point. This suggests that cardiogreen was rather leaking from an unimpaired alginate bead than it was

spreading from leftovers of a degraded bead. This observation is also consistent with previous knowledge of alginate presence in acidic environment as it found in stomach. It is well known that alginate is poorly soluble at low pH. The reason for the alginate bead not migrating might be the fact that fish did not take in feed after intubation. Intake of some feed after intubation would obviously help to push the bead further down the gastrointestinal tract. Like this, it appears that the bead got stuck in the stomach as shown in the Figure 4.6. Therefore, the true place of dissolution could not be determined in this trial.

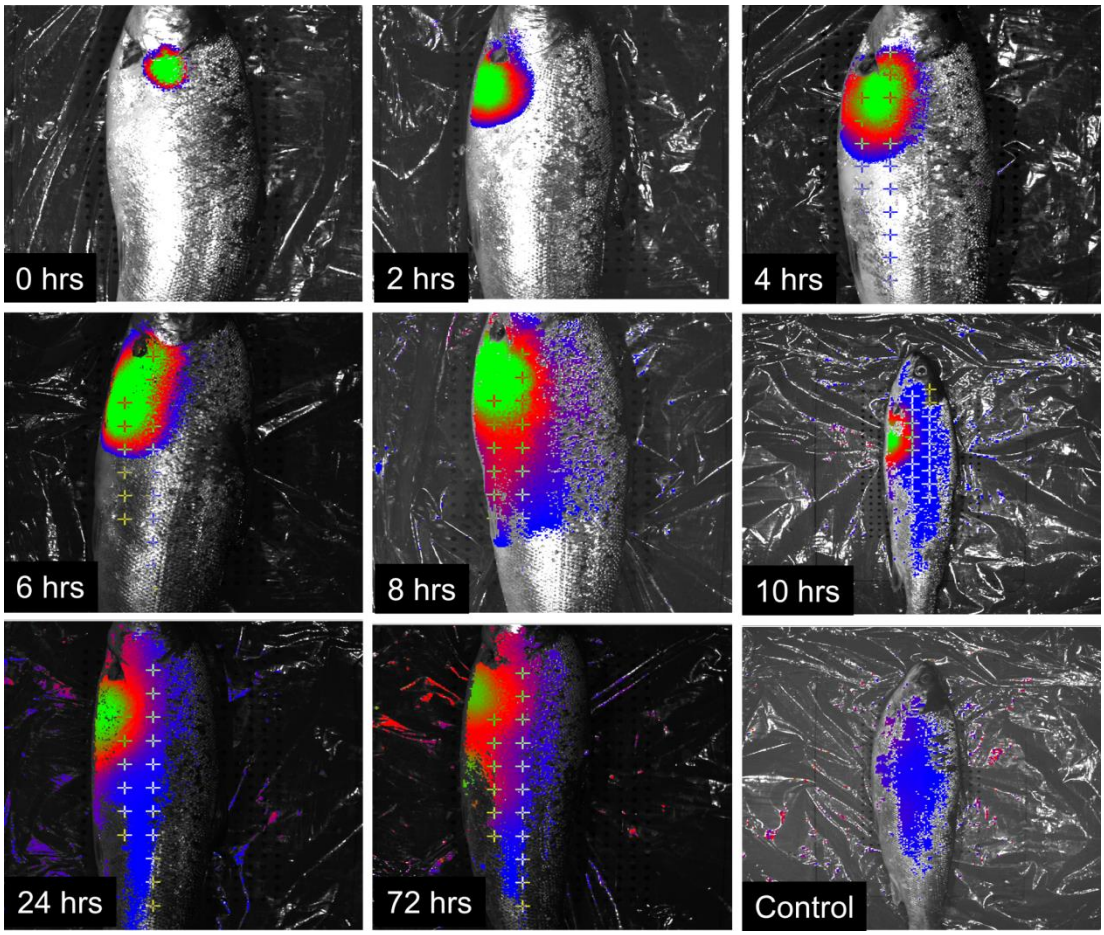

Figure 4.5: Visualisation of alginate beads loaded with cardiogreen by an *in vivo* imaging system (I009, Table 2.3). The beads did not move and due to fish not eating after intubation. For this reason, the real place of dissolution could not be determined in this trial.

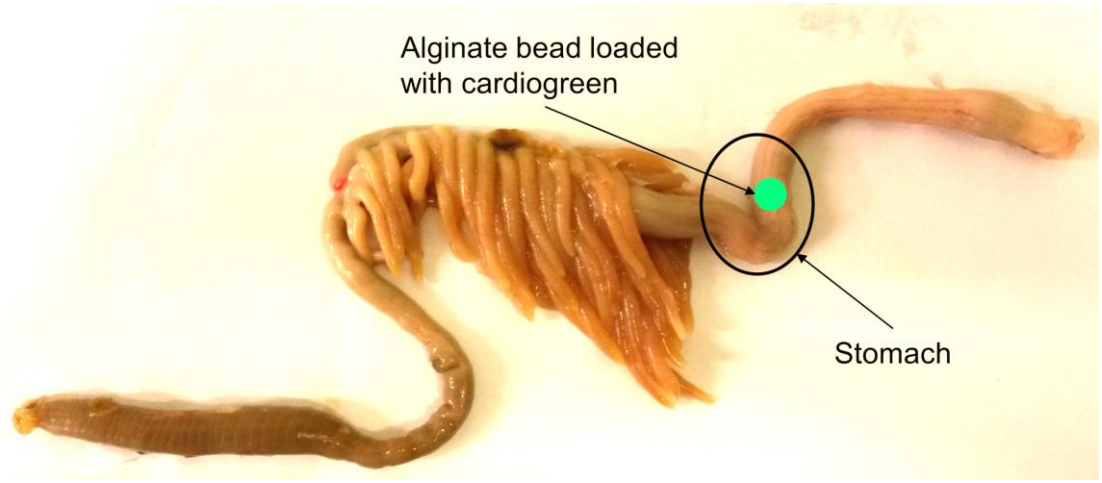

Figure 4.6: Imaginary alginate bead loaded with cardiogreen is shown stuck in the stomach of A. salmon.

4.4 *In vivo* study of HRP release from alginate matrices

This study was conducted with the aim of localising the site of both Ca-alginate and EDA-alginate dissolution in A. salmon using an enzyme assay approach. In accordance with the aim, the fish was voluntary fed with Ca-/EDA-alginate-encapsulated horseradish peroxidase (HRP) infused into feed pellets.

4.4.1 Methods

4.4.1.1 Preparation of alginate microbeads loaded with HRP

Calcium alginate (HRP-Ca-alg) and ethylenediammonium alginate (HRP-EDA-alg) microbeads loaded with HRP were produced according to the general method described in the Section 2.2.1.2 (Chapter 2). Encapsulation was conducted without voltage (U) so the method was an aerodynamically assisted jetting. Process parameters and their respective values are summarised in the Table 4.11. The encapsulation formulation (Item S022, Table 2.4) and cross-linking solutions (Item S003 and S004; Table 2.4) were specific to this process. The HRP-Ca-alg microbeads were formed by processing four batches à 60 ml of encapsulation formulation in combination with crosslinking solution (Item S003, Table 2.4). The HRP-EDA-alg microbeads were generated in the same way but using different crosslinking solution (Item S004, Table 2.4). Later, four and four batches of alginate microbeads were combined into one single batch. The resulting batches were filtered off by suction filtration applying a filter paper (Item T012, Table 2.2). Thus, the obtained mass of HRP-Ca-alg and HRP-EDA-alg microbeads was 81.54 g and 78.29 g respectively. In the end, a laser diffraction system (Item

I007, Table 2.3) was used to measure the size of the generated alginate beads at wavelength λ = 632.8 nm. All steps of the encapsulation process were performed at 4°C. The products (HRP-Ca-alg and HRP-EDA-alg) were store at -20°C until they were used in the feed preparation.

Table 4.11: Air pressure-assisted energised jetting - process variables with their respective values

Distance[i]	Volume[ii]	Voltage	Flow rate	Target volume	Pressure
x	V_{xls}	U	Q	V_{tv}	P
mm	ml	kV	$cm^3\ h^{-1}$	ml	bar
100	500	0	100	60	3

[i]Distance between the jetting head and the surface of crosslinking solution (x)
[ii]Volume of the cross-linking solution (V_{xls})

4.4.1.2 Preparation of the experimental feeds

As the first step, alginate microbeads (d_{median} = 25 – 26 µm) loaded with HRP were suspended in in fish oil (Item C019, Table 2.1). The resulting fish oil suspension was then combined with base pellet (Item C007, Table 2.1) in a vacuum infusion coating process. The coating was performed according to the method described in the Section 2.2.4. Three batches of feed (5.0 kg each) were produced according to the mixing ratios shown in the Table 4.12.

Table 4.12: Composition of the experimental feeds HRP-Ca-feed, HRP-EDA-feed and Ctrl-feed.

Feed name	Oil mixture			BP[iii] [g]	Total [g]
	Fish oil [g]	HRP-Ca-alg[i] [g]	HRP-EDA-alg[ii] [g]		
Ctrl-feed	1210.0	0.00	0.00	3790.00	5000.00
HRP-Ca-feed	1210.0	81.54	0.00	3708.46	5000.00
HRP-EDA-feed	1210.0	0.00	78.29	3711.71	5000.00

[i]HRP-Ca-alg – product generated by encapsulating HRP solution into Ca-alginate matrix

[ii]HRP-EDA-alg – product made by encapsulating HRP solution into EDA-alginate matrix

[iii]BP – base pallet is a semi-finished fish feed product, dry extrudate lacking oil mix (Item C007, Table 2.1)

4.4.1.3 Fish trial

The fish trial was performed according to the general method described in the section 2.2.5.2 (Chapter 2) at Lab G (EWOS Innovation AS, Dirdal, Norway). In addition, feed intake was measured. All Parameters relevant to this trial are listed in the Table 4.13.

The three groups of fish were named as Ca-alginate, EDA-alginate and Control group. Ca-alginate and EDA-alginate group were treated with HRP-Ca-feed and HRP-EDA-feed respectively. The Control group was fed with Ctrl-feed. The health status of the fish was good during the 11 weeks long span of the trial.

The following samples were collected 1) Stomach, 2) Pyloric Caeca, 3) Mid intestine and 4) Distal intestine (Figure 4.7). Each of the sampled gastrointestinal compartments was opened by longitudinal incision and placed into a container with DI water (10.0 ml, t = 4°C). After vigorous

shaking, the solid content was separated from the liquid phase by gravity filtration. The resulting filtrate (2 ml) from each container was transferred to an eppendorf tube and stored at -20^{o}C until assayed.

Table 4.13: Parameters applied in the fish trial carried out by feeding fish with feed containing alginate microbeads loaded with HRP

Parameter	Symbol	Quantity
Average weight of fish	m	394 g
Oxygen saturation in water	O_2	95%
Water temperature	t	5°C
Diameter of a tank	d	1.0 m
Volume of a tank	V	0.5 m^3
Number of tanks	n_{tanks}	9
Total number of fish	n_{fish}	495
Number of groups	n_{groups}	3
Length of the acclimatisation period	t_{accl}	9 weeks
Length of the treatment period	t_{treat}	2 weeks
Number of sampled fish per tank per sampling point	$n_{sf/t}$	15
Number of sampling points	n_{SP}	1
Length of the time intervals from the end of treatment to sampling	t_{SP}	0
Total number of sampled fish	$n_{sampled}$	135

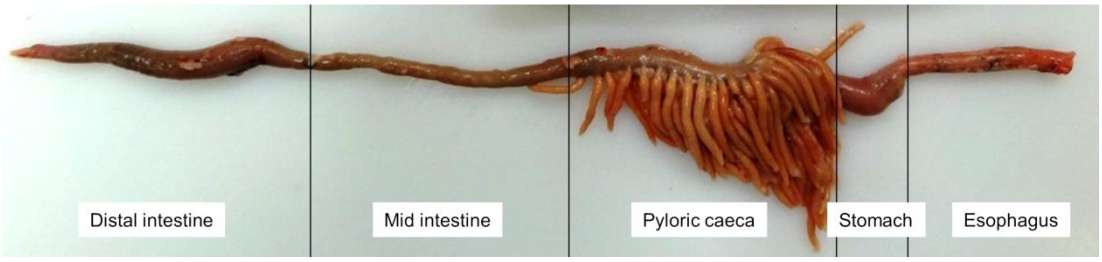

Figure 4.7: Gastrointestinal tract of A. salmon. Sampled compartments: stomach, pyloric caeca, mid and distal intestine are marked off with division lines.

4.4.1.4 Sample analysis

The samples were thawed and spun down at 4000 rpm for four minutes prior to use. Stomach and pyloric caeca samples were applied undiluted while mid and distal intestine samples were diluted 1:200 with DI water (4°C; Item C022, Table 2.1) before assaying. For diluted mid and distal intestine samples (1:200) below quantification limit (0.391 ng ml^{-1}), lower dilutions like 1:10 and 1:100 or no dilution were used to increase sensitivity. Kinetic assay was carried out by pipetting aliquots of samples (50 µl) onto 96-well polystyrene plates (Item T006, Table 2.2). Reaction was initiated by adding 50 µl per well of liquid substrate (Item C018, Table 2.1) at 37°C. Absorbance measurements were conducted by using a microplate reader (Item I003, Table 2.3) at 655 nm. Kinetic rates were recorded every 20 seconds for a total of 10 minutes at 37°C. HRP concentration of the samples was determined by using standard curve as a quantification tool in the range of 0.391 to 200 ng ml^{-1}. The standard curve was generated by plotting HRP concentrations of 10 two-fold serial dilutions of HRP solution (200 ng ml^{-1}; Item S020, Table 2.4) against their kinetic rates (slope of the absorbance versus time curves).

Finally, statistical analysis of the obtained data was performed according to the description in the Section 2.2.6.3 (Chapter 2).

4.4.2 Results

In the current trial, a fish consumed 12-13 g feed on average during the weeklong treatment with feed containing alginate encapsulated HRP. As a result, the treated fish (m_{avg} = 490 – 500 g) received between 230 and 240 µg of HRP in the period (Table 4.14).

Table 4.14: HRP dose related to the fish size in unit of mass and the weekly feed intake (FI) per fish. The dose is shown as a weekly HRP dose per fish (µg fish^{-1} week^{-1}) and a weekly HRP dose per unit of fish mass (µg fish^{-1} week^{-1})

Group[i]	Feed	Fish size (g) ±SD	FI (g fish^{-1} week^{-1}) ±SD	HRP dose[ii] (µg fish^{-1} week^{-1}) ±SD	HRP dose (µg kg^{-1} week^{-1}) ±SD
Control	Ctrl-feed	492 ±121	12.7 ±1.7	0.00	0.00
Ca-alginate	HRP-Ca-feed	495 ±95	12.5 ±1.4	239 ±26	483 ±46
EDA-alginate	HRP-EDA-feed	499 ±108	12.1 ±0.9	232 ±17	465 ±50

[i]Groups were treated with following feeds: feed without HRP (Ctrl-feed), feed with calcium alginate encapsulated HRP (HRP-Ca-feed) and feed with ethylenediammonium alginate encapsulated HRP (HRP-EDA-feed)
[ii]HRP dose is theoretical and assumes very little loss due to processing.

Group of fish (Ca-alginate) fed with HRP-Ca-feed showed significantly higher concentration of HRP in the distal intestine compared to the other gastrointestinal (GI) compartments (Figure 4.8). On the other hand, fish served HRP-EDA-feed had significantly higher concentration of HRP in the mid intestine than in the other GI sections. Additionally, this group had also notably high HRP concentration in the distal intestine. In contrast to the HRP treated groups, peroxidase activity was quite low in the control group.

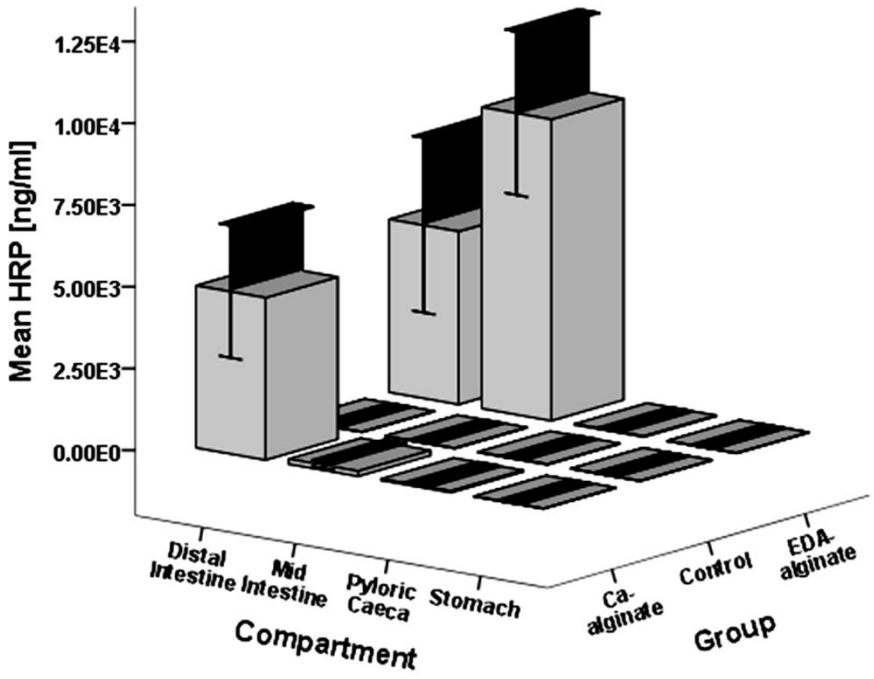

Figure 4.8: HRP concentration in four GI compartments (stomach, pyloric caeca, mid and distal intestine) of three groups of A. salmon (Ca-alginate, EDA-alginate and Control). The error bars represent 95% confidence intervals. Ca-alginate group were treated with calcium alginate encapsulated HRP (HRP-Ca-alg). EDA-alginate group was treated with ethylenediammonium alginate encapsulated HRP (HRP-EDA-alg). Control group did not receive any HRP.

4.5 Discussion

From the present *in vitro* study it could be seen that both Ca-alginate and EDA-alginate matrix are poorly soluble in buffers with pH 1.2 at 37°C, pH 6.8 at 37°C, pH 8.0 at 18°C and pH 8.6 at 18°C within a time frame of 60 minutes. Drug, which is encapsulated in alginate matrices, is released by two mechanisms: 1) diffusion of the drug through the pores of the polymer network and 2) degradation of the polymer network (Wee et al., 2012). Unlike the low molecular weight drugs, BD (M.W. = 2,000,000) is so large that it cannot diffuse through the pores of an alginate matrix without their further expansion (Kim and Lee, 1992).

According to Kikuchi et al. (1999), the lag stage of initial release was longer with an increasing molecular weight of dextran (M.W. = 9,400 –145,000). It was observed very low release rate of FITC-dextran (M.W. = 145,000) at pH 7.4 during the first hour. As a result, most of the BD release from alginate matrices presumably happens due to degradation of polymer network. Accordingly, very little of this degradation is expected to occur at pH < 7.6 in case of EDA-alginate (pKa 1 = 7.56 and pKa 2 = 10.71). This is due to the fact that most of the ethylenediamine (uncharged form) will exist as ethylenediammonium (positively charged, 2+) at pH < 7.6.

However, in Mumper et al 1993, Ca-alginate previously exposed to low pH, degraded faster in pH 7.4 solution than Ca-algnate exposed solely to solution of pH 7.4.Therefore, an effective way to weaken the cross-linked structure of an alginate matrix would be to use an acidic dissolution medium (pH < 3.5) before applying an alkaline medium (pH > 7.6). At pH below 3.5 (alginic acid,

pKa = 1.5 – 3.5), hydrogen ions (H^+) replace cations (+) in alginate networks yielding an unlinked structure of alginic acid. Although alginic acid is poorly water soluble it may ease subsequent conversion to sodium alginate, which is aqueous soluble form of alginate at higher pH. As it can be anticipated, foregoing treatment with acidic medium (pH < 3.5) may give much faster release rate then direct treatment with alkaline medium (pH > 7.6). Taking this into account, it can also be concluded that direct treatment with pH < 7.6 will be ineffective in dissolving EDA-alginate. In other words, applying standard conditions (pH = 1.2 and 6.8 at 37°C) in two separate dissolution tests will most likely result in very slow dissolution rates producing inconclusive results.

This reasoning is in agreement with the results in the current study where pH = 3.0 was combined with pH = 8.0 to generate successful results shown in the Figure 4.4. Putting alginate beads in an acidic buffer (pH = 3.0) for a short period of time would convert some EDA-alginate to alginic acid. Consequently, alginic acid and any remaining EDA-alginate are readily dissolved when acidic buffer is replaced with alkaline one (pH = 8.0). In the same manner, disintegration rate of Ca-alginate matrix is accelerating with increasing pH of the dissolution medium. At the same time, attraction of charged sodium (Na^+) towards carboxylic groups of alginate is increasing when pH is greater than 8 (Oberyukhtina et al., 2001). On the other hand, calcium phosphate may already start precipitating from a system containing Ca_2^+ and phosphate buffer at pH > 6.7 (Feenstra and De Bruyn, 1979).

For the above reasons and for the reason that pH of the stomach is 2.7 - 4.9 and pH of the intestine is 7.5 - 8.5, the dissolution test strategy pH 3.0/8.0 was selected. According to Shi et al. (2011), dissolution of cross-linked alginate is pH- and temperature-responsive. However, from the Figure 4.4, it may be concluded that dissolution of EDA-alginate is pH-responsive but not temperature-responsive in the range of 4 – 18°C.

Contrary to EDA-alginate, dissolution of Ca-alginate is in compliance with the previous study. Release rate of BD from Ca-alginate matrix is significantly lower than release rate from EDA-alginate matrix at 4°C. This observation is in agreement with the results from the *in vivo* trial which was carried out at 5°C. From the Figure 4.8, it can be seen that HRP release *in vivo* is significantly faster from EDA-alginate than from Ca-alginate beads.

According to the observations in this study, it is not expected that drug release from the EDA-alginate is affected by seasonal temperature changes in the habitat of A. salmon. These attributes make delivery system based on EDA-alginate very interesting with respect to salmonid fish.

Chapter Five: Size adaptation of alginate beads for improved integration with fish feed pellets

During recent years, the use of functional ingredients in aquaculture industry has increased dramatically and a broad range of functional feeds are now widely available for use in fish farming. In connection with that, there is ongoing research which deals with developing oral delivery systems for delivering of sensitive bioactive compounds to fish. A variety of products (nutrients, medicines and vaccines) can be incorporated into alginate matrices to avoid damage from the low pH and proteolytic enzymes encountered in the digestive tract of fish. However, there has been very little research reported on the effectiveness of those oral delivery systems in terms of their performance within feed pellets, in a vacuum infusion coating process. Furthermore, the reported sizes of alginate delivery systems, which are generated by an extrusion method, require further reduction to be suitable for effective association within feed pellets. As a result, the main objective of this study is to develop a technology capable of providing an economical and high throughput method for producing fine alginate beads containing a wide range of small molecules capable of lodging themselves in fish feed pellets during their production. The results of these investigative studies significantly improve understanding of the issues regarding incorporation of delivery systems into fish feed in the current manufacturing process and have unearthed a novel approach for functionalizing fish feed

5.1 Introduction

Fish feed has evolved into a fairly advanced product that will most likely go towards increasingly sophisticated for each year to come (Pandey, 2013). Because of the fish farmer's growing demand for ever increasing weight gain and food safety authorities pursuit for healthy farmed fish (Thorud et al., 2007), feed industry has responded with enhancing focus on functional feeds. To put things into perspective, EWOS AS (Norway), which is a fish feed company, has experienced a dramatic increase in sale of functional feeds. Share of functional feeds rose from 16% in 2008 to 47% in 2011 (Cermaq, 2012). Functional feeds are diets that improve both health and growth of the animals, by providing additional bioactive compounds apart from the basic nutritional requirements for growth alone (Martinez-Rubio et al., 2012; Olmos et al., 2011; Tacchi et al., 2011).

Some of the bio-actives (e.g. proteinous compounds) are thermos-sensitive and prone to acidic and proteolytic degradation in the gastro intestinal tract. One way to come around this problem is to entrap/encapsulate these compounds into some sort of protective delivery system ahead of incorporating them into feed pellet (Bernkop-Schnurch, 2009; Bruno et al., 2013; Rosenmayr-Templeton, 2013). Although getting the delivery system into feed pellet remains a formidable challenge, options are few, if any.

Delivery systems could be incorporated into the extruded feeds by so called oil infusion coating process (Goeritz et al., 2014; Ljungqvist et al., 2012). Success of coating depends both on size of delivery system and pore size of

the feed pellet. On the other hand, Eldridge et al. (1990) demonstrate that particles smaller than 10 µm can cross the epithelial barrier.

From the gut lumen, micro-/submicro-particles are taken by micro-fold (M) cells across the epithelial layer. Afterwards, these particles are delivered to antigen presenting cells such as macrophages (van der Lubben et al., 2002). Time-course studies on the fate of the poly(DL-lactide-co-glycolide) microspheres within the gut-associated lymphoid tissue shows that the majority of the microspheres (diameter, $d < 5$ µm) are transported through the efferent lymphatics within macrophages, while the majority of those with $5 < d < 10$ µm remains fixed in the Peyer's patches. In another study Petrie & Ellis (2006) provides evidence for uptake of particles $d < 3$µm by the distal intestine of A. salmon following anal intubation of inert polystyrene microspheres. Given this, it can be concluded that generation of very fine microbeads $d < 10$ µm is essential for both efficient post-extrusional incorporation into feed pellet and successful uptake by distal intestine.

This study was commissioned to assess an alginate based delivery system. Alginates are polysaccharides isolated from brown algae such as *Ascophyllum sp., Durvillaea sp., Ecklonia sp., Laminaria sp., Lessonia sp.*, *Sargassum sp.* and *Macrocystis pyrifera* found in coastal waters around the globe (McHugh et al., 2003). Marine alginates are composed of two forms of uronic acid: mannuronic (M) and guluronic (G). Two blocks of adjacent polymer chains can be cross-linked with multivalent cations (e.g., Ca^{2+} or Ba^{2+}) through interactions with the carboxylic groups in the uronic acid, which leads to the formation of a gel network (Augst et al., 2006) The resulting cross-linked alginate beads have excellent biocompatibility within host

tissues and are able to biodegrade in a controlled manner. These attributes make alginate an ideal compound for use as oral delivery system (Adelmann et al., 2008; Joosten et al., 1997; Maurice et al., 2004; Polk et al., 1994). Alginate beads are stable at low pH and dissolves at high pH. As a result, a faster release from alginate beads occurs in the intestine (alkaline conditions), after the beads have passed through the proteolytic and acidic environment of the stomach (Yu et al., 2008).

The crosslinking properties of alginate form the basis for various encapsulation techniques including both extrusion and emulsion processes (Vemmer and Patel, 2013). Extrusion processes could be further subdivided into electric and non-electric driven methods. Typical electric driven approaches are electromagnetic laminar jet breakup (Martinez et al., 2004), inkjet printing technology (Xu et al., 2008) and electrostatic driven encapsulation process which is also called electrospraying (Gomez and Tang, 1994). General non-electric driven approaches are coaxial air flow induced dripping (Koch et al., 2003) and aerodynamically assisted jetting (Jayasinghe and Suter, 2006). Most common emulsion techniques frequently used are coacervation (de Kruif et al., 2004; Veis, 2011), internal and external gelation (Quong et al., 1998).

Among the aforementioned techniques, aerodynamically assisted jetting (AAJ) distinguishes itself with characteristics such as being fairly inexpensive, easy up-scalable, gentle and high-throughput encapsulation process. These features make this process very well-suited for industrial application where effective large batch processes are favourable (Arumuganathar and Jayasinghe, 2008; Jayasinghe, 2011).

In general, there has been very little research reported on the behaviour of alginate particles and oral delivery systems in a vacuum infusion coating process. This process is the standard industrial method for adding formulated sensitive substances to fish feed. In our view, the reported sizes of alginate delivery systems (Table 5.8), which are generated by an extrusion method, are too large to be suitable for effective association with feed pellet. To check this assertion, a vacuum infusion coating test was performed in the first phase of this study. As a part of this test, we analysed pore size of feed pellets and examine morphology of the pellet pores. This is to determine the particle size suitable for sufficient incorporation into large feed pellets ($d \geq 10$ mm) in the vacuum coater. To evaluate the outcome of the test, we looked for barium alginate (Ba-alginate) particles inside a pellet using an X-ray computed tomography technique.

In the second phase, the present study aims to produce the smallest calcium alginate (Ca-alginate) particles attainable with the APAEJ conjointly supported by electrostatic force. To achieve this goal, the APAEJ was optimised in a controlled experiment. This is to increase chance of getting alginate beads both inside smaller feed pellets ($d < 10$ mm) and inside the intestinal epithelial layer. Finally, morphology of calcium alginate particles was examined by the imaging-based particle analysis system.

In the large perspective, this study contributes much to the effort of creating a successful oral delivery system for delivering of sensitive bioactive compounds to fish which in turn contributes to improved health and welfare of cultured animals.

5.2 Assessment of association of alginate microbeads with fish feed pellets

High level of incorporation of alginate microbeads into feed pellets is the key factor for successful delivery of encapsulated therapeutics to fish. Therefore, as the first step in this study, pore sizes of feed pellets were measured by mercury intrusion porosimetry. This is performed with the aim of determining a suitable particle size for sufficient incorporation into feed pellets by the vacuum infusion coating method. Thereafter, vacuum infusion coating test was carried out with barium alginate microbeads adequately sized for incorporation into feed pellet with diameter around 10 mm. The results of coating test were examined by micro-CT (computed tomography) scanning. In the end, morphology of alginate microbeads was analysed by a fluid imaging-based particle analysis system.

5.2.1 Methods

5.2.1.1 Characterisation of feed pellet pores by mercury intrusion porosimetry and scanning electron microscopy

The pore size distributions of three base pellets: BP1 (d=10 mm, m = 0.4908 g, V = 0.6708 cm^3), BP2 (d = 10 mm, m = 0.4111 g, V = 0.6494 cm^3) and BP3 (d =10 mm, m = 0.4895 g, V =0.5948 cm^3) were determined by mercury intrusion porosimetry. The analysis was carried out by a porosimeter (Item I004 Table 2.3) at low and high pressure ranging from 0.2 to 50 psi and from 20 to 60,000 psi respectively. Specimens were placed in the long cell with internal diameter of 4 mm. Mercury (Hg) volume was recorded at each pressure point and normalised by the sample weight. The output data was generated in the scan mode (Autospeed). Both extrusion and intrusion Hg

contact angles were set to 130°. In addition, surface tension of Hg was adjusted to 470 erg cm^{-2}. Determination range of low-pressure and high-pressure porosimetry was 4.3 –1000 µm and 0.0035 – 7 µm respectively. Pellet pores were also examined by SEM (Item I005, Table 2.3) with the aim of getting insight into the shape and size of the entry pores.

5.2.1.2 Preparation of barium alginate microbeads

Barium alginate (Ba-alginate) microbeads were produced according to the general method described in the Section 2.2.1.2 (Chapter 2). Encapsulation was conducted with the aid of voltage so the method was an aerodynamically assisted energised jetting. Process parameters and their respective values are summarised in the Table 5.1. The following items were specific to this process: encapsulation formulation (Item S027, Table 2.4), jetting head (Item T018, Table 2.2) and cross-linking solution (Item S023, Table 2.4).

The generated Ba-alginate beads were washed three times DI water (10 ml; Item C022, Table 2.1) and then filtered off by suction filtration ahead of vacuum infusion coating step. An amount of 7.24 g Ba-alginate microbeads was recovered.

Table 5.1: Aerodynamically assisted energised jetting – process parameters applied in producing Ba-alginate microbeads for the vacuum coating experiment.

Distance[i]	Volume[ii]	Voltage	Flow rate	Target volume	Pressure
x	V_{xls}	U	Q	V_{tv}	P
mm	ml	kV	$cm^3\ h^{-1}$	ml	bar
85	100	10	50	20	1.75

[i]Distance between the jetting head and the surface of crosslinking solution (x)
[ii]Volume of the cross-linking solution (V_{xls})

5.2.1.3 Incorporation of Ba-alginate microbeads into feed pellets by the vacuum infusion coating method

Firstly, fish oil (Item C019, Table 2.1) was triple filtered using three different filter papers. There were used: coffee filter (Item T010, Table 2.2), qualitative filter paper grade 1 (Item T011, Table 2.2) and grade 6 (Item T012, Table 2.2) in the given order. Thereafter, Ba-alginate microbeads (d_{median} = 25 µm, 7.24 g) were suspended in the triple filtered fish oil (m_{oil} = 250g). The resulting fish oil suspension was then combined with base pellet (m_{BP} = 742.76 g; d_{avg} = 10 mm; Item C007, Table 2.1) in a vacuum infusion coating process. The coating was performed according to the method described in the Section 2.2.4. Finally, feed (m_{feed} = 1000 g) containing Ba-alginate microbeads was produced and one random pellet was taken out of the final batch for micro-CT (computed tomography) scanning.

5.2.1.4 Micro-CT scanning of a feed pellet infused with Ba-alginate beads

One fish feed pellet infused with Ba-alginate microbeads was scanned by high-resolution micro-CT (Item I006, Table 2.3) at RJL Micro and Analytic GmbH (Karlsdorf-Neuthard, Germany). The micro-CT scanning was performed with the purpose of detecting Ba-alginate particles inside a coated pellet. In addition, size distribution of the detected Ba-alginate particles inside pellet was measured. Size distribution of Ba-alginate particles before the infusion coating was determined by laser diffraction equipment (Item I007, Table 2.3).

5.2.2 Results and discussion

5.2.2.1 Characterisation of feed pellet pores

It is challenging to determine the pore size distribution of an extruded pellet and relate it to the size of a delivery system. It is primarily due to the highly irregular shape of pores. The pores have properties dependent on the degree of expansion along with the size, shape and the way the constituent particles are packed together. The largest number of pore sizes is around 100 µm in three analysed pellets (Figure 5.1). There is also another smaller peak at around 400 µm. In general, the most pore sizes are in the range from 10 µm to 500 µm in all three pellets. Draganovic et al. (2013) reported that most pore sizes in the fish feed pellet (d_{avg}=8.7 mm) were below 330 µm. This measurement is a result of micro-CT scanning that produces a visualization of pore space and solid material in a cross-sectional plane. This technique provides very little information about the surface pores and their size distribution. Furthermore, it struggles with recognising pore sizes below 11 µm. These are highly relevant factors for successful incorporation of delivery

systems into feed pellet. Based on this reasoning, measurement of surface pore size distribution by the mercury intrusion porosimetery would presumably be more suitable analytical method (León y León, 1998; Nimmo, 2004; P. Rigby et al., 2004). This presumption is further strengthened by careful examination of SEM images (Figure 5.2).

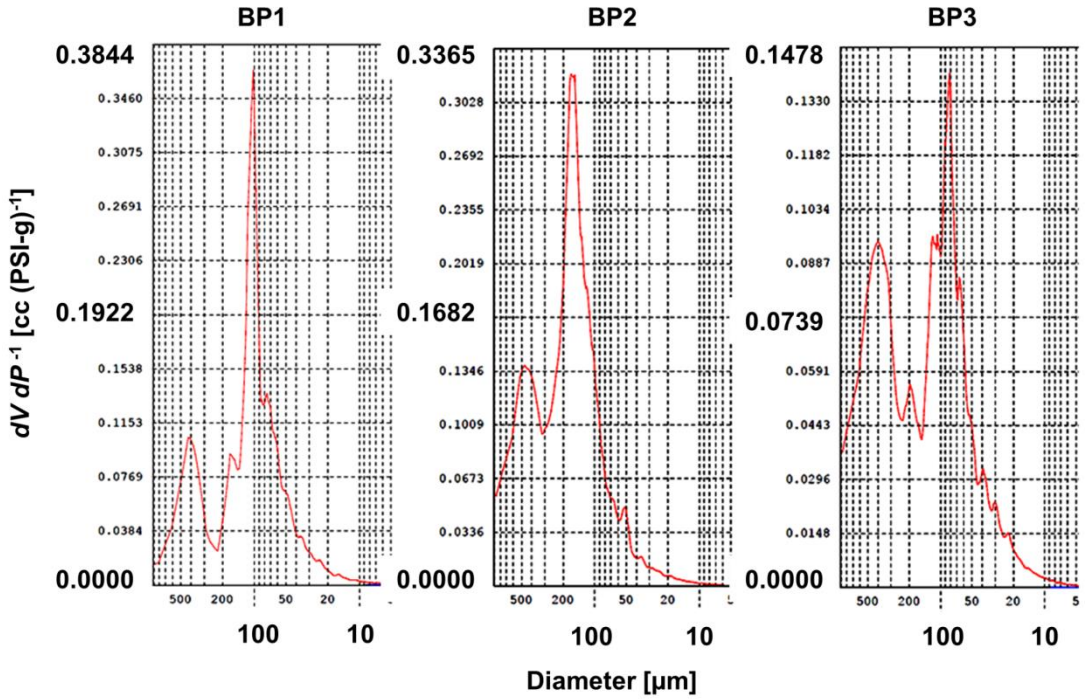

Figure 5.1: Pore size distribution by mercury intrusion porosimetry. Results expressed as difference in mercury volumes intruded between the pressures P2 and P1 (dV/dP) as function of pore diameter. Most of the pores are around 100 µm ranging from 10 to 500 µm. BP – base pellet.

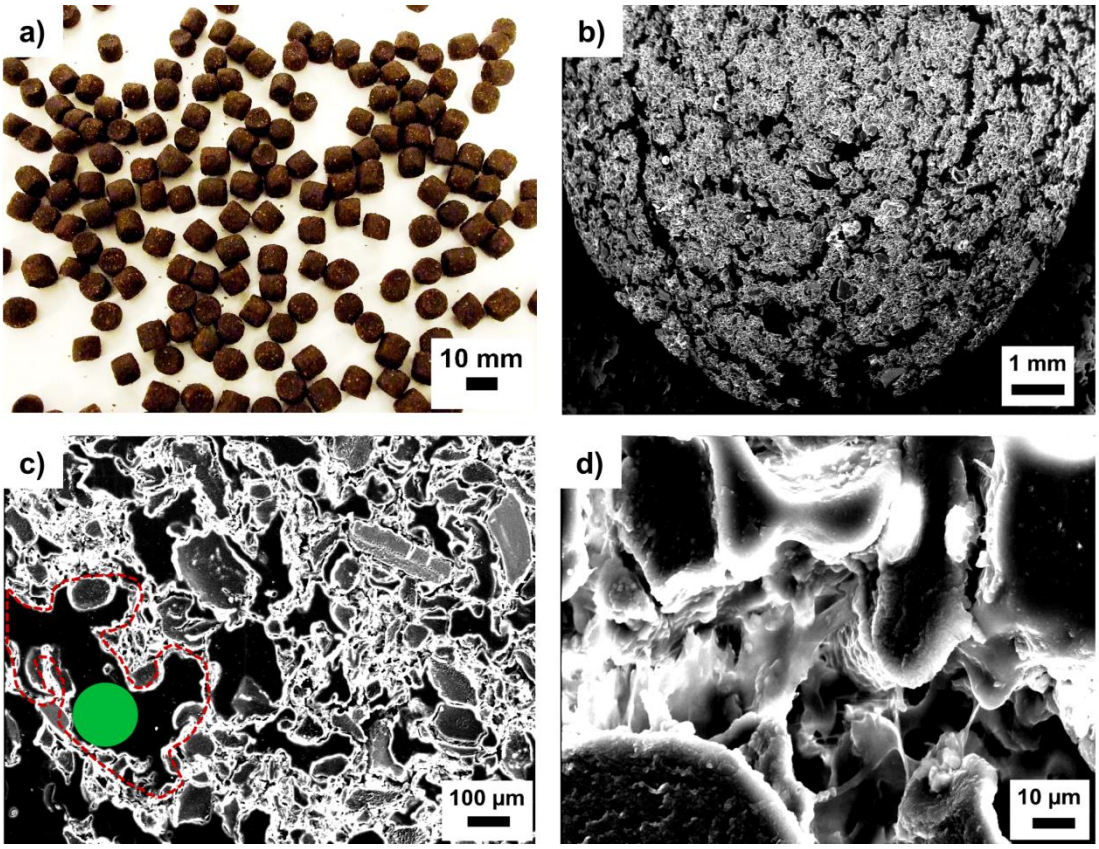

Figure 5.2: SEM images of a typical 10 mm fish feed pellet. A typical-10 mm pellet is shown in the image (a). Characteristic SEM micrographs of the surface of a fish feed pellet, scale bar represents b) 1 mm, c) 100 µm and d) 10 µm showing the variation of pore size. The green circle and the closed red curve are added to the image (c) in order to depict the largest diameter which can fit into the indicated pore. This pore opening is areally four times larger than an imaginary circular area representing a spherical alginate bead.

In the Figure 5.2, the dark area, which is located within the closed red curve, indicates the void space inside a feed pellet. This void space is identified as a pore. The entry hole of that pore is irregularly shaped. Most of the porosimeters will mathematically convert this irregularly shaped entrance to a circular one. For instance, the mercury porosimeter will assume the cylindrical shape of a pore (Quantachrome Instruments, 2009). As a consequence of the assumption, the estimated pore diameter may be much larger than the widest gap in the original shape. It implies that the spherical

objects, which are approximately of the same size as the estimated diameter of a pore, will not be able to enter into that specific pore. In this particular case, the encircled dark area is four times larger than the area of the blue spot. The blue spot is apparently the largest diameter which can fit into the indicated pore. It means that the diameter of a spherical object to go in needs to be at least two times smaller than the estimated pore diameter.

The above discussion is based on one pinpointed pore. It is true that the other pores may have entry holes with higher degree of circularity which brings the estimated diameter of a pore closer to a diameter of a circle/sphere. On the other hand, there are other factors that contribute to estimating the size of surface pores to be larger than what they actually are.

Based on the results of the present study and supported by the previously reported research which we referred to above, it may be assumed that the size of inner pores (air pockets) is larger than the size of entry holes (surface pores). This suggests that the overall pore size distribution is not directly transferrable to the size distribution of the surface pores alone. The actual surface pore sizes are expected to be smaller than the overall pore size distribution measured by an instrument. Therefore, it is important to ensure that the actual alginate beads are able to access feed pellets of interest through the outer openings of the pellet pores. One of the options to check whether alginate beads of a certain size go inside feed pellets is to carry out a vacuum coating test. Afterward, amount of alginate beads inside the coated pellet can be measured by X-ray computed tomography.

5.2.2.2 High resolution micro-CT scanning of fish feed pellet infused with Ba-alginate particles

Based on the results discussed in the previous section, it can be assumed that a great number of surface pore sizes on a fish feed pellet (d = 10 mm) are smaller than 100 µm. It implies that delivery systems with d > 100 µm could not enter into the pellet pores in large numbers. A significant number of particles larger than 100 µm would lie on the surface of a pellet exposed to external conditions. The micro-CT scan revealed large number of white objects inside a feed pellet coated with Ba-alginate particles (Figure 5.3). Based on the size distribution it may be concluded that these objects are Ba-alginate beads. The results show that roughly, 82% of bright objects are below 50 µm, while half of them are below 23 µm (Figure 5.4). This corresponds very well to the median size of Ba-alginate particles which was 25 µm right after preparation. In addition, very large proportion (98%) of these Ba-alginate particles was smaller than 50 µm. Alginate particles of this size could apparently be coated in larger quantities, withstand the mechanical force encountered in feeding systems at fish farm and remain within the feed pellet whilst exposed to the aqueous environment. Though smaller Ba-alginate particles could be incorporated even more effectively, we opted for slightly larger particles (d_{median} = 25 µm) to ensure better detectability at micro-CT scanning. Smaller particles are also useful for associating with smaller feed pellets (d_{avg} < 10 mm) and uptake by distal intestine.

In brief, to enable high degree of inclusion, a reasonable target size of delivery systems could be in the region of one quarter of the estimated pellet

pore size. Some additional research could be done to identify the largest suitable particle size in relation to a given pore size of feed pellet.

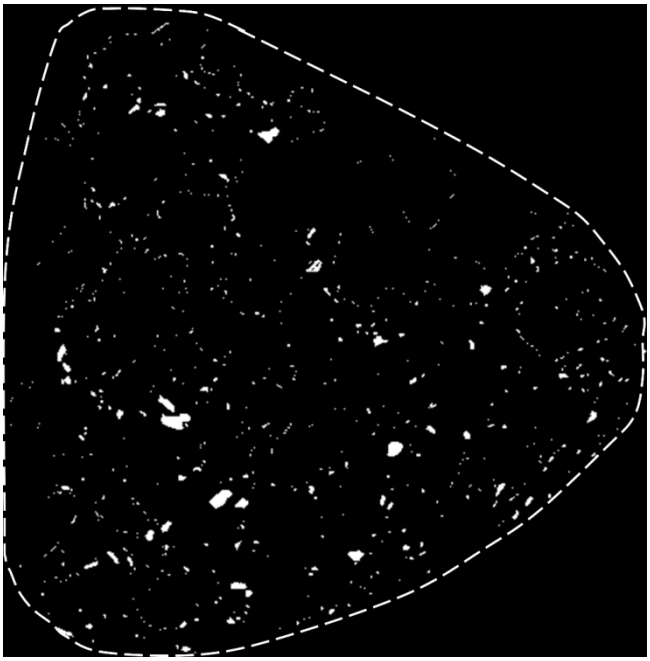

Figure 5.3: Micro-CT scan image of one quarter of a pellet (d=10 mm), which is cut along its central axis. The white objects represent barium alginate particles.

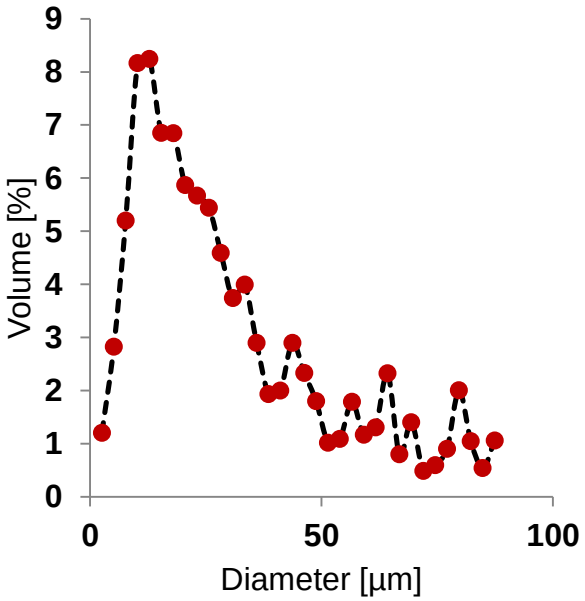

Figure 5.4: Volume percentage of barium alginate particles expressed as function of particle diameter. From the graph it can be seen that 82% of the particles are smaller than 50 µm while 50% are below 23 µm.

5.3 Optimisation of the encapsulation process

For optimal incorporation into feed pellets, small-sized alginate beads are preferable. In addition to associating very well with feed pellet, sufficiently small oral delivery systems are capable of crossing the intestinal epithelial layers as well. Therefore, the encapsulation process was optimised for producing the smallest possible calcium alginate microbeads in a controlled experiment.

5.3.1 Methods

5.3.1.1 Experimental design and statistical analysis

With the aim of optimising the APAEJ encapsulation process for production of minimal Ca-alginate beads, several general types of variables were considered: uncontrollable, background, constant, primary and response variables. As a result, five primary variables were identified: flow rate of alginate solution (Q), alginate concentration (C), distance between spray head and cross-linking solution (x), air pressure (P) and voltage (U). The ranges of the levels of the variables used in the experiment are shown in the Table 5.2.

Internal diameter of the nozzle (350 µm), diameter of exit orifice (350 µm), volume of crosslinking solution (80 ml), concentration of cross-linker (0.25M), volume of extruded alginate solution per sample (6.0 ml), and conductivity of alginate solvent (DI water, $\kappa \leq 0.05$ µS/cm) were kept constant. Background variables which included temperature (18^{o}C) and relative humidity (56%) were measured but not treated as covariates in the model because they remained unchanged during the entire experiment. Ambient concentration of

particulates was singled out as an uncontrollable variable. The median particle size (d_{median}) was used as a response variable.

In order to meet the objective of producing alginate beads of the smallest size, a three-stage experimental approach following the response surface methodology (Box and Draper, 2007) was selected as the most suitable design.

In stage 1, the primary variables were screened to identify the active ones with a 2^5 factorial design with five centre points. In stage 2, the response surface around the minimal particle size was mapped with the help of a central composite design (CCD) on the active factors identified in stage 1. In stage 3, the results were verified by performing some runs around the stationary point, i.e. conditions resulting in the minimal particle size. Bayesian model discrimination (Box and Meyer 1993) was applied to the data set generated in stage 1.

This screening method identified the most probable model among all possible combinations of factors. After identifying the most probable active factors a first-order response surface model with these factors was fitted to the data from stage 1 with the help of generalised linear models. The importance of first-order interactions between the factors was studied with the help of a likelihood ratio test between two nested models (with and without the interactions). In stage 2, the original first-order design from stage 1 was augmented by adding six star points (assuming the experimental space is a cube) and four centre points to achieve a complete CCD design. A block

effect was added to the model in order to account for any effect of conducting the runs in two different steps.

Modelling was conducted with the help of nested general linear models of increasing complexity: first order model with main effects only, first-order model with first-order interactions and second order model with squared terms. Likelihood ratio tests were used to decide upon the most parsimonious but sufficient model. Modelling of stage 2 revealed the stationary point. In stage 3, nine runs around stationary point without any special design and one run at the stationary point were performed for the sake of verifying the results. All statistical modelling was conducted with the R language (R Development Core Team, 2012) and its corresponding packages (R version 2.15.3).

Table 5.2: Primary variables and their experimental levels applied in optimising the encapsulation process (aerodynamically assisted energised jetting).

Variable	Symbol	Low	Centre	High	Unit
Flow rate	Q	5.00	50.50	105.00	$cm^3\ hr^{-1}$
Alginate	C	1.50	2.25	3.00	%
Distance	x	65	85	105	Mm
Pressure	P	0.50	1.75	3.00	bar
Voltage	U	0.0	10.0	20.0	kV

5.3.1.2 Conduct of experimental runs – sample preparation

Samples of alginate microbeads were produced in experimental runs conducted according to the general method described in the Section 2.2.1.2 (Chapter 2). Generally, all solutions along with water used in this experiment were filtered by syringe filter (Item T009, Table 2.2) prior to use. As

previously described in the Section 5.3.1.1, important process parameters such as flow rate (Q), alginate concentration (C), distance (x), pressure (P) and voltage (U) were varied according to the experimental design. The experimental range of values for the variables C, Q, P, x and U are shown in Table 5.2. Volume of the crosslinking solution (Vxls = 80 ml) and target volume (Vtv = 6.0 ml) were kept constant throughout the entire experiment. All performed runs and the applied levels of variables are listed in the Tables 4.3, 4.4 and 4.5.

The following items were specific to this process: alginate solution with 1.5% alginate (Item S024, Table 2.4), alginate solution with 2.25% alginate (Item S025, Table 2.4), alginate solution with 3.0% alginate (Item S026, Table 2.4) and cross-linking solution (Item S003, Table 2.4).

5.3.1.3 Particle size measurement

Size of the generated alginate beads was measured by a laser diffraction instrument (Item I007, Table 2.3). The instrument was equipped with laser diffraction sensor (HELOS BR) and cuvette (CUV-50ML/US). Optical module (R5) with laser beam (d = 13 mm) was used to illuminate the sample at wavelength λ = 632.8 nm. This configuration was specially designed for the analysis of particles which are sized from 0.5 to 875 µm and suspended in volumes lower than 50 ml. The system was specified to perform with accuracy of δ < 2% and repeatability of δ < 0.04%.

Sample with suspended alginate beads was added to the cuvette containing filtered DI water (40 ml; Item C023, Table 2.1) under stirring (100 rpm) until optical concentration (C_{opt} > 11%) was reached. Calculations were performed

in the Fraunhofer enhanced evaluation (FREE) mode which is based on the Fraunhofer theory (Bertero et al., 1985). Particle size was recorded as the average of three consecutive measurements. The instrument was controlled by the software package WINDOX 5 (Version 5.8.0.0).

5.3.2 Results and Discussion

In the first phase, 37 runs were carried out as a part of a 2^5 factorial experiment (Table 5.3). The applied Bayesian model discrimination technique suggested a model including three factors concentration (C), distance (x) and pressure (P) as the most probable model (Probability = 0.998). The most likely model was then fitted using the first-order response surface methodology. A model with two-way interactions proved to be the best option, based upon a likelihood-ratio test.

The residuals of the interaction model plotted against each of the factors indicated a nonlinear response within the experimental region. This suggests the stationary point (i.e. the minimum particle size) may be located within the experimental region. Therefore, the usual next step in the response surface methodology, finding the path of the steepest ascent, was skipped and the full response surface model was sought directly. This was achieved by expending the design with the star points of the central composite design (CCD) involving only three most probable factors (C, x and P). As a result, the additional 10 runs linked to the expended central composite design (CCD), were performed in the second phase (Table 5.4).

The results suggested that the particle size was minimised at the stationary point C = 1.60%, x = 105 mm and P = 3.00 bar (Figure 5.5). In the last

phase, nine runs around stationary point and one run at the stationary point itself confirmed the theory and demonstrated that the median particle size (15.9 µm) was in fact smallest at the stationary point (Table 5.5).

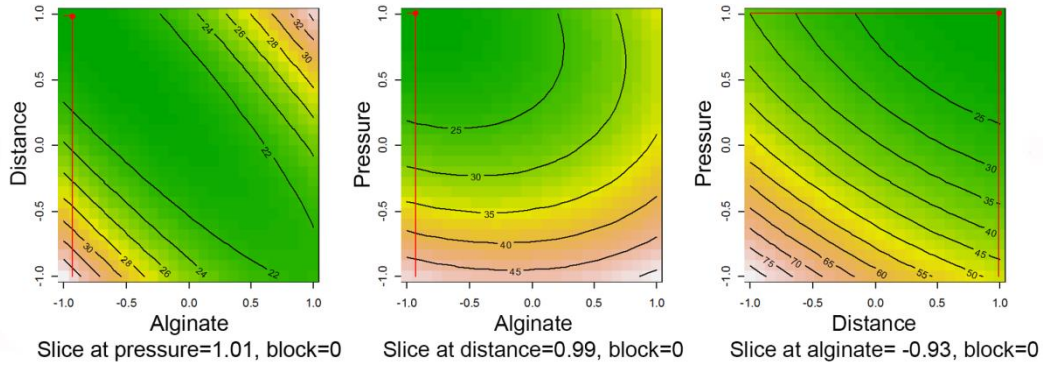

Figure 5.5: Response surface slices of the second-order model showing the stationary point (red dot).

As previously mentioned, it has been concluded that concentration (C), distance (x) and pressure (P) are significant process variables. The inference made on the effect of concentration is supported by the observations of other researchers. According to Watthanaphanit & Saito (2013) concentration of sodium alginate in solution is directly proportional to the viscosity of the solution. Furthermore, Paine et al. (2007) states that for liquids having higher viscosity, more energy is required to draw liquid out of a nozzle. For this reason, the droplets are formed with lower frequency than for liquids of low viscosity. According to the Jaworek et al. (2000) the size of the droplets could be controlled by the frequency of formation.

In the present study, it was observed that too short distance could cause the crosslinking solution to splash back towards the jetting head. Such conditions lead to agglomeration of alginate droplets and even to the blockage of the

exit orifice. Another reason, why too short distance is not desirable, is that it may cause a short circuit in the system when high voltage is applied. It was also noticed that too long distance led to dispersion of very small droplets in such a way that they could hardly reach the crosslinking solution. In other words, they would become airborne or land elsewhere than onto the surface of the crosslinking solution. Given this, it can be concluded that the adequate distance is essential for the optimal performance of this encapsulation process.

Since both distance and sodium alginate concentration are normally adjusted before the process start, pressure remains the only variable that could be used to control size of alginate particles while encapsulating. Changyuan et al. (2012) came to the same conclusion in their study where effect of pressure on droplet size in an air-assisted spraying process was investigated.

Output from the Bayesian model screening indicated that the voltage and flow rate were statistically insignificant variables for the function of adjusting process to produce minimal particle size. It is arguable whether or not these variables are producing any effect at all. When it comes to the voltage, limiting factor may be the measuring range of HELOS BR instrument with R5 lens. Measuring range of this configuration is quoted to be 0.5/4.5-875 µm. According to Sympatec, this system is not extremely accurate below 4.5 µm.

As already stated, primary goal with introducing voltage to the current encapsulation process was to bring down possible hovering alginate droplets generated at the exit orifice of the jetting head. The main reason for the

ineffectiveness of voltage could be found in the size of these airborne droplets which presumably may be smaller than 4.5 µm. Such presumption suggests that the voltage could have an effect but it is not measurable with the applied lens. With reference to the first and ninth run in the Table 5.5, it can be seen that the changes, which were made to the stationary point run in terms of voltage and flow rate, did not notably affect median particle size. Thus, it may be concluded that the inference made by the Bayesian model screening was correct. On the other hand, it would not be unreasonable to expect the median particle size to increase with a large upturn of flow rate while the other parameters are kept at the same level. This assumption is not very strong counterargument since the objective is to minimise, not to maximise the particle size. All things considered, the applied statistical models figured out the stationary point with good accuracy.

Droplets diameter may also depend on the liquid (alginate solution) properties like density, viscosity, conductivity, gas-liquid surface tension, and relative permittivity (Gañán-Calvo et al., 1997). However, we have chosen not to vary these factors in this experiment because they are more related to encapsulation material properties than to the encapsulation process itself. Although concentration of sodium alginate was included in the experimental design, primarily, we wanted to optimise only variables which could be adjusted while running the process. Another advantage of limiting the experimental design to fewer variables is that the complexity and size of the experiment stays at manageable levels. Now, as the effects of process variables are identified it is easier to optimise the liquid variables in a separate design when the encapsulation material is known.

In the next section, the main topic is morphology characterisation of Ca-alginate particles but we use Na-alginate solution with higher conductivity than the Na-alginate solution used in this experiment. This is to test whether the liquid properties affect the size of the final product.

Table 5.3: Stage 1 – results from the 2^5 factorial experiment with five centre points (cp01 to cp05). Constitutive letters in the run name express which factor was at high level in the run.

Run order	Run name	Flow rate Q [ml/h]	Alginate C [%]	Distance x [mm]	Pressure P [bar]	Voltage U [kV]	Response d_{median} [µm]
1	QxP	105.0	1.50	105	3.00	0.0	25.8
2	CPU	5.0	3.00	65	3.00	20.0	27.1
3	Q	105.0	1.50	65	0.50	0.0	103.3
4	QCU	105.0	3.00	65	0.50	20.0	46.5
5	cp03	50.5	2.25	85	1.75	10.0	25.9
6	P	5.0	1.50	65	3.00	0.0	19.3
7	QPU	105.0	1.50	65	3.00	20.0	24.9
8	C	5.0	3.00	65	0.50	0.0	50.3
9	U	5.0	1.50	65	0.50	20.0	78.8
10	cp01	50.5	2.25	85	1.75	10.0	26.1
11	QCP	105.0	3.00	65	3.00	0.0	24.0
12	cp02	50.5	2.25	85	1.75	10.0	25.8
13	QCx	105.0	3.00	105	0.50	0.0	51.6
14	CxP	5.0	3.00	105	3.00	0.0	24.6
15	QCxPU	105.0	3.00	105	3.00	20.0	23.6
16	xPU	5.0	1.50	105	3.00	20.0	19.6
17	CxU	5.0	3.00	105	0.50	20.0	55.3
18	x	5.0	1.50	105	0.50	0.0	38.5
19	QxU	105.0	1.50	105	0.50	20.0	41.2
20	cp04	50.5	2.25	85	1.75	10.0	25.5
21	cp05	50.5	2.25	85	1.75	10.0	25.9
22	CU	5.0	3.00	65	0.50	20.0	50.6
23	Qx	105.0	1.50	10	0.50	0.0	42.2
24	CxPU	5.0	3.00	105	3.00	20.0	24.0
25	xP	5.0	1.50	105	3.00	0.0	20.7
26	QCxU	105.0	3.00	105	0.50	20.0	49.0
27	Cx	5.0	3.00	105	0.50	0.0	62.4
28	QxPU	105.0	1.50	105	3.00	20.0	26.2
29	QCxP	105.0	3.00	105	3.00	0.0	23.5
30	xU	5.0	1.50	105	0.50	20.0	37.5

Run order	Run name	Flow rate Q [ml/h]	Alginate C [%]	Distance x [mm]	Pressure P [bar]	Voltage U [kV]	Response d_{median} [µm]
31	PU	5.0	1.50	65	3.00	20.0	36.7
32	QU	105.0	1.50	65	0.50	20.0	76.3
33	0	5.0	1.50	65	0.50	0.0	97.7
34	QC	105.0	3.00	65	0.50	0.0	48.6
35	QP	105.0	1.50	65	3.00	0.0	25.7
36	QCPU	105.0	3.00	65	3.00	20.0	24.0
37	CP	5.0	3.00	65	3.00	0.0	25.7

Table 5.4: Stage 2 – six star points of the full central composite design (CCD) and four additional centre points with three factors: alginate, distance and pressure. Flow rate and voltage are kept constant at centre levels. Constitutive letters in the run name express which one of the other three factors was at high level in the run.

Run order	Run name	Flow rate Q [$cm^3\ h^{-1}$]	Voltage U [kV]	Alginate C [%]	Distance x [mm]	Pressure P [bar]	Response d_{median} [µm]
1	x	50.5	10	2.25	105	1.75	25.5
2	-P	50.5	10	2.25	85	0.50	38.3
3	P	50.5	10	2.25	85	3.00	19.4
4	C	50.5	10	3.00	85	1.75	26.7
5	cp	50.5	10	2.25	85	1.75	26.2
6	-x	50.5	10	2.25	65	1.75	25.5
7	cp	50.5	10	2.25	85	1.75	26.5
8	cp	50.5	10	2.25	85	1.75	25.8
9	-C	50.5	10	1.50	85	1.75	24.3
10	cp	50.5	10	2.25	85	1.75	25.7

Table 5.5: Stage 3 – stationary point run and nine runs around the stationary point are shown. Alginate, distance and pressure are varied while flow rate and voltage are kept constant except from the last run where voltage and flow rate were reduced.

Run name	Flow rate Q [$cm^3\ h^{-1}$]	Voltage U [kV]	Alginate C [%]	Distance x [mm]	Pressure P [bar]	Response d_{median} [µm]
Stationary point (SP)	50.5	10	1.6	105	3.00	15.9
1. Around SP	50.5	10	1.6	95	3.00	16.2
2. Around SP	50.5	10	1.6	105	2.38	19.3
3. Around SP	50.5	10	1.6	95	2.38	18.9
4. Around SP	50.5	10	1.9	105	3.00	20.1
5. Around SP	50.5	10	1.9	95	3.00	17.9
6. Around SP	50.5	10	1.9	105	2.38	20.7
7. Around SP	50.5	10	1.9	95	2.38	23.9
8. Around SP	50.5	10	1.9	75	3.00	18.3
9. Around SP	28.0	0	1.6	105	3.00	16.0

5.4 Morphology characterisation of alginate particles

From the previous section (Section 5.2), it can be concluded that sphere-like shape is the most preferable form of alginate microbeads. However, alginate particles produced by air pressure-assisted energised jetting (Section 5.3) are so small that their shape can hardly be defined by an ordinary stereo microscope. Therefore, morphology of alginate microbeads were characterised by a fluid imaging particle analysis system (Item I008, Table 2.3) in this study.

5.4.1 Methods

5.4.1.1 Preparation of alginate microbeads

Two samples of alginate microbeads were produced according to the general method described in the Section 2.2.1.2 (Chapter 2). Encapsulation was conducted with the aid of voltage so the method was an aerodynamically assisted energised jetting. Process parameters and their respective values are summarised in the Table 5.6. The following items were specific to this process: alginate solution (Item S028, Table 2.4), jetting head (Item T019, Table 2.2) and cross-linking solution (Item S003, Table 2.4). It is important to note that the alginate solvent used in this experiment was PBS (Item C005, Table 2.1). PBS is different from DI water (Item C023, Table 2.1) which was applied in the previous section (Section 5.3) in terms of conductivity (κ).

Table 5.6: Aerodynamically assisted energised jetting – process parameters applied in producing alginate particles for the study of their morphology.

Distance[i]	Volume[ii]	Voltage	Flow rate	Target volume	Pressure
x	V_{xls}	U	Q	V_{tv}	P
mm	ml	kV	$cm^3\ h^{-1}$	ml	bar
100	80	10	50	6.0	3.00

[i]Distance between the jetting head and the surface of crosslinking solution (x)
[ii]Volume of the cross-linking solution (V_{xls})

5.4.1.2 Morphology measurements of alginate microbeads

The morphology and size of alginate microbeads were studied by the imaging-based particle analysis system (Item I008, Table 2.3). Two samples were analysed at Fluid Imaging Technologies Inc., (Scarborough, ME, USA). Images of individual particle (n = 50,000) were captured, allowing visual detection and measurement of multiple shape parameters. These shape measurements formed the basis for generation of data shown in the Table 5.7.

5.4.2 Results and Discussion

The shape of the alginate particles made of alginate dissolved in PBS was characterised with five parameters: length, width, aspect ratio, circularity, convexity and diameter (Table 5.7). Aspect ratio (mean = 0.8, median = 0.8-0.9) suggests that the shape of alginate particles is fairly close to circular. This observation is also supported by the circularity parameter (mean = 0.9, median = 0.9 – 1.0). A selection of the FlowCAM® images further supports the claim of circularity (Figure 5.6). Maximum convexity score (1.0) indicates that, in addition to being circular, particles were smoothly shaped as well.

The most fascinating is that the mean diameter (d_{avg}) of the particles was 10µm while the median (d_{median}) was only 8 µm. Despite the factum that the levels of process parameters (Q, C, x, P and U) were almost identical to the levels set at the stationary point, the resulting d_{median} was half of the size previously achieved at the stationary point (Table 5.5). The main reason for this large reduction could be a significant difference in conductivity between the two alginate solvents. The indicated conductivity of DI water and PBS was $\kappa \leq 0.05$ µS cm^{-1} and $\kappa = 1.6\times10^{4}$ µS cm^{-1} respectively. This difference suggests that the conductivity probably has a synergistic effect with voltage on minimising alginate particle size. Therefore, the question arises as to whether the conductivity of alginate solvent could enhance the effect of voltage. Study by Jaworek & Sobczyk (2008) points in that direction as it demonstrates that droplet size can be decreased by increasing liquid conductivity in an electrospraying process.

One of the reasons for replacing water with PBS in this experiment was to simulate the usual situation where biological material to be encapsulated is suspended in PBS. It was also assumed that this conductivity change would not affect other shape parameters then size. In the previous section we discussed optimisation of process variables for generating the smallest possible alginate beads from sodium alginate dissolved in DI water. This section confirms that particle size can be further decreased by optimising variables related to liquid properties as well. However, It can be claimed that the obtained mean particle size of 10 µm with 50% of particles smaller than 8 µm is probably the smallest generated alginate particle size with an extrusion method.

Table 5.7: Morphology measurements by the imaging-based particle analysis system (I008, Table 2.3). Measured diameter is equivalent to the spherical diameter (ESD), median particle size is denoted by d_{median} and SD stands for standard deviation.

Sample	Parameter	Diameter [µm]	Length [µm]	Width [µm]	Aspect ratio	Convexity	Circularity
	Mean	10	11	8	0.8	1.0	0.9
1	SD	9	10	7	0.2	0.1	0.1
	d_{median}	8	9	7	0.8	1.0	0.9
	Mean	10	11	8	0.8	1.0	0.9
2	SD	7	8	6	0.1	0.1	0.1
	d_{median}	8	9	7	0.9	1.0	1.0

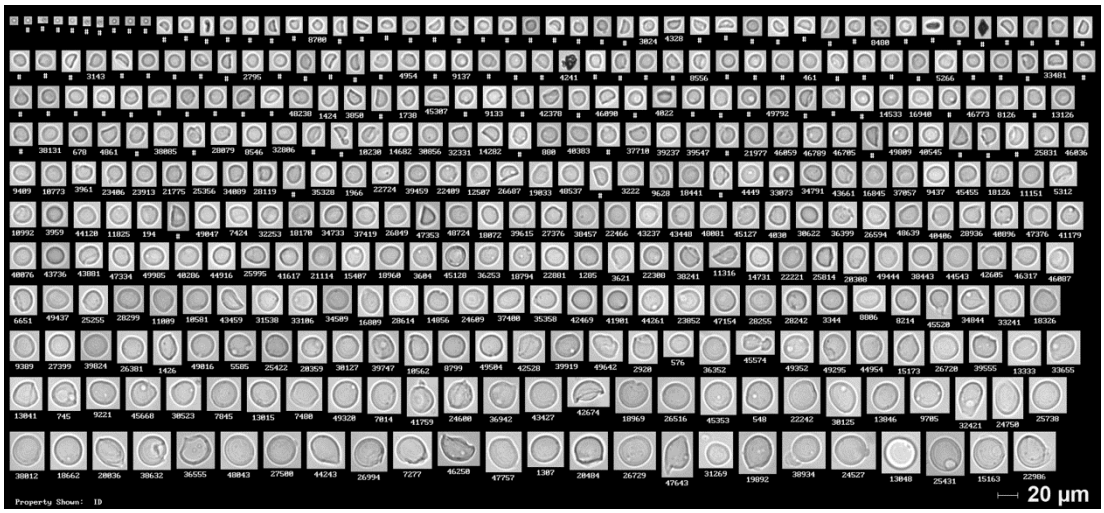

Figure 5.6: A small selection of the 50,000 alginate particles photographed by the imaging-based particle analysis system (I008, Table 2.3). The particles are small (d_{median} = 8 µm) and possess high degree of circularity.

Although there is some reports on optimization of encapsulation processes for drug release characteristics, there is a very few reports on process optimization for the smallest particle size in a controlled experiment (Caballero et al. 2014). As a result, it is only possible to compare our particle size to the sizes which other researchers usually obtain when using this or other encapsulation techniques. For instance, in a study by Arumuganathar et al. (2007), the average droplets size observed in the jet formed by the same aerodynamically assisted jetting device were between 55 and 87 μm (Table 5.8). Reported average alginate particle sizes using methods mentioned in the Introduction section and shown in the Table 5.8 vary from 7 nm to 1000 μm. In addition, Lian et al. (2012) demonstrate that a three-dimensional microfluidic droplet generator which is rather unconventional technique, is able to produce monodisperse alginate microbeads with d_{avg}= 15 μm (SD = 1). In recent years, there has also been increased activity in the field of printing technologies where various printing techniques of use for development of drug delivery systems have been explored (Kolakovic et al., 2013).

Table 5.8: An overview of alginate encapsulation methods and reported particle sizes. Particle diameter is represented by lowercase "d". Mean diameter is designated by "$\overline{d}$". Particle size varies from 7 nm – 1000 µm. The smallest extruded particle size is 13 µm (Inkjet printing). Abbreviations: BCA - Bicinchoninic acid, PASMC cells - pulmonary artery smooth muscle cells, FITC - Fluorescein isothiocyanate.

Encapsulation method	Active compound	Particle size	Reference
Coacervation	None	$\overline{d}$=339.8 nm (SD=0.2)	Sahu & Prusty (2010)
	BCA	$\overline{d}$=474 nm (SD=19)	
	Eugenol	$\overline{d}$=425 µm	Shinde & Nagarsenker (2011)
Emulsification/external gelation	Congo red	$\overline{d}$=1 µm	Paques et al. (2013)
	None	$\overline{d}$=7 nm (SD=2)	Nesamony et al. (2012)
Emulsification/internal gelation	Insulin	$\overline{d}$=60 µm	Silva et al. (2006)
	Yeast cells	$\overline{d}$=151 µm (SD=77)	Song et al. (2013)
Electromagnetic laminar jet breakup	None	d<750 µm	Del Gaudio et al. (2005)
	None	$\overline{d}$=490 µm	Rodríguez-Rivero et al. (2011)
Coaxial air flow induced dripping	None	$\overline{d}$=1000 µm	Ribeiro et al. (2004)
	Maltodextrin and trehalose	400<$\overline{d}$<1800 µm	Semyonov et al. (2010)
Electrospraying	Adenovirus	$\overline{d}$=150 µm	Park et al. (2012)
	None	$\overline{d}$=170±100 µm	Bugarski et al. (1994)
Inkjet printing	FITC-labelled nanoparticles	$\overline{d}$=13 µm	Iwanaga et al. (2013)
Microfluidic droplet generator	None	$\overline{d}$=15 µm (SD=1)	Lian et al. (2012)
Aerodynamically assisted jetting	PASMC cells	55<$\overline{d}$<87 µm	Arumuganathar et al. (2007)

5.5 Conclusion

Air pressure-assisted energised jetting was optimised to produce alginate beads with median size of 16 µm using DI water as sodium alginate solvent. This was done with the conclusion that sodium alginate concentration, pressure and distance are significant variables while the opposite is true for voltage and flow rate.

Furthermore, it was demonstrated that the median particle size dropped down to 8 µm when alginate solvent was changed to PBS, indicating a possible effect of conductivity. In comparison with the particle sizes previously reported, we believe that, the size in the current study is probably the smallest reported size of alginate beads generated by an extrusion method. Therefore it can be concluded that, air pressure-assisted energised jetting could be used to produce alginate beads of a size which can readily be integrated into the fish feed pellet with a size of d_{avg} = 10 mm and probably smaller. In addition to associating very well with feed pellet, oral delivery systems of the size d ≤ 10 µm are reported to be capable of crossing the intestinal epithelial layers as well.

The practical implication of the results of the porosimetry and SEM image analysis is the suggestion that the spherical particles should preferably be at least four times smaller than the estimated pore size of a feed pellet. This is to ensure easy passage of a greater number of beads through the entry holes of the surface pores which appear to be rather irregular.

From the outcome of the micro-CT scan it can be seen that micro-particles with d_{median} = 25 µm are readily able to access the pellet with predominant

pore sizes of 100 µm. Since the significance of voltage for minimising particle size remained unclear, future research should either assess the effect of voltage coupled with an increasing conductivity of alginate solution, or should assess the effect of liquid properties on particle size at the stationary point.

Chapter Six: Stability of antigens in fish feed production process

Fish feed is normally produced by extrusion cooking these days. This technology is converting feed mash into a compact, cylindrical form, called pellet. This process achieves high degree of starch gelatinisation, denatures undesirable enzymes, inactivates some anti-nutritional factors, sterilises and expends the finished product. In short, the extrusion cooking is a high temperature, high pressure short time process. For this reason, it is an open question whether the protein antigens are capable of surviving conditions which can be encountered in fish feed production. Survival of both alginate-encapsulated and free IPNV antigen was assessed in a trial arranged according to a 2^2 factorial design of experiment. Additionally, the specific amount of heat added in to the process runs was described by enthalpy. The findings suggest that IPNV antigen may survive throughout fish feed production machinery at temperature ≤108°C.

6.1 Introduction

Currently, most of the fish feed is produced by extrusion cooking. The extrusion cooking is often called the high temperature short time (HTST) process (de-Oliveira et al., 2012). This kind of processes tends to maximise the beneficial of heating feeds while minimising the detrimental effects.

According to Morken et al. (2012), an increasing extrusion temperature significantly improves digestibility of major nutrients and amino acids in A. salmon. However, most biological proteins will lose their higher-order structure after being exposed to heat treatment. They first coagulate and then become denatured (Eronina et al., 2011; Kilara and Sharkasi, 1986). Loss of three-dimensional structure usually produces a loss of biological activity (Privalle et al., 2011). This is the major concern when it comes to processing protein antigen using the current fish feed manufacturing technology. Proteins show a very wide range of extrusion behavior that is probably related to large differences in their association properties (Arêas, 1992).

Interestingly, some proteins like Glutamate dehydrogenase present is certain type of prokaryotes (e.g. *Pyrococcus furiosus*) may be stable at 100°C (Pavesi, 2014). Regarding IPN virus, Mortensen et al. (1998) observe reduction of IPNV virus already at temperature above 20°C. Tu et al. (1975) stats that half-life of IPN virus is 5-6 days at 15°C. According to MacKelvie and Desautels (1975), IPNV (10^7 $TCID_{50}$ ml^{-1}) was reduced by 99.9% in the first 30 min of exposure to 60° at neutral pH and 0.0001% of the virus was still viable after five hours.

The main objective of this study was to assess stability of IPNV antigen in the current fish feed production process. Additionally, effect of factors (encapsulation state and process temperature) on antigen survival were studied.

6.2 Methods

6.2.1 Experimental design

Survival of both encapsulated and free IPNV antigen was assessed through both “standard/hot” and "mild" process setup. Basically, only two factors were varied, A: encapsulation state (yes/no) and B: feed production conditions (hot/mild). Because there were only two levels for each factor we assumed that the response (ELISA OD = antigen survival) was approximately linear over the range of the factor levels selected. Based on that assumption the 2^2 factorial design with both positive and negative control was chosen (Figure 6.1). All runs that are product of the experimental design are summarised in the Table 6.1.

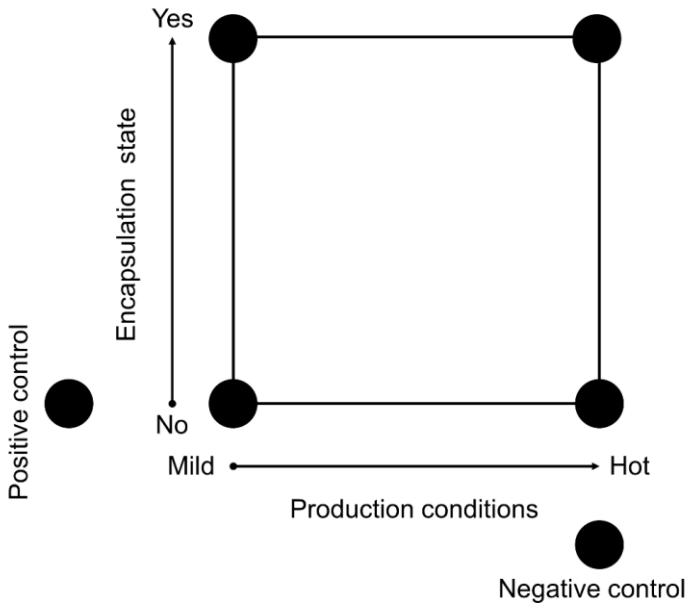

Figure 6.1: Combination of feed production runs in the 2^2 factorial design including two control runs (positive and negative). Two factors were varied: encapsulation state of IPNV antigen (yes/no) and feed production conditions (hot/mild). Hot conditions are standard conditions which would normally be applied for that type of feed. Mild conditions are normally not applied in everyday production.

Table 6.1: Description of the four runs suggested by the 2^2 factorial design in the antigen stability study. As a result of the 2^2 factorial design, four runs should be performed. Four runs with dry mix containing IPNV antigen in either encapsulated or free state and one run (negative control) without any antigen. Positive control is unprocessed dry mix with free antigen.

Run	Name	Encapsulation state	Process conditions
1	Unencap-Mild	No	Mild
2	Encap-Mild	Yes	Mild
3	Unencap-Std	No	Standard/hot
4	Encap-Std	Yes	Standard/hot
Control negative	Ctrl-negative	n.a.	Standard/hot
Control positive	Ctrl+positive	n.a.	n.a.

n.a. – not available

6.2.2 Preparation of alginate beads loaded with IPNV antigen

Alginate beads loaded with IPNV antigen were prepared according to the common encapsulation method. This method (electrospraying) is described in the section 2.2.1.1 (Chapter 2). Process parameters and their respective values are summarised in the Table 6.2. The following items were specific to this encapsulation process: needle (Item T019, Table 2.2), encapsulation formulation (Item S001, Table 2.4) and crosslinking solution (Item S003, Table 2.4). Encapsulation formulation (2000 ml) was extruded in small portions of 50 ml due to the maximum capacity of the available syringe (Item T002, Table 2.2). Later, two batches of alginate beads were formed. Each batch was formed of encapsulation formulation corresponding to 1000 ml.

The resulting alginate beads loaded with IPNV Ag were dried under reduced pressure for 48 hours before being weighed and antigen concentration calculated. Batch 1 was reduced to 44.82 g resulting in an IPNV antigen

concentration of 2.19 x 10^{10} $TCID_{50}$ g^{-1}. Batch 2 weighed 45.77 g which gave an IPNV antigen concentration of 2.14 x 10^{10} $TCID_{50}$ g^{-1}. The size of the beads was then be reduced to below 150 µm by grinding with mortar and pestle followed by sifting. The resulting alginate particles were suspended in PBS just before mixing with feed material (dry mix).

Table 6.2: Electrospraying - process parameters applied in the antigen stability study.

Internal diameter (needle)	Flow rate	Target volume	Voltage	Distance[i]	Volume[ii]
ID	Q	V_{tv}	U	x	V_{xls}
µm	cm^3 h^{-1}	ml	kV	mm	ml
1200	200	50	7.0	30	50

[i]Distance between the needle tip and the surface of crosslinking solution (x)
[ii]Volume of the cross-linking solution (V_{xls})

6.2.3 Preparation of dry mixes for feed trial

For the purpose of feed trial, six dry mixes were prepared. The dry mixes are named “Unencap-Mild”, “Unencap-Std”, “Encap-Mild”, “Encap-Std”, “Ctrl-negative” and “Ctrl+positive”. The dry mixes with free antigen (“Unencap-Mild” and “Unencap-Std”) were prepared by mixing free suspended IPNV antigen (900 g; 10^9 $TCID_{50}$ g^{-1}; Item C003, Table 2.1) with meal mix (89.1 kg; C026, Table 2.1). Furthermore, “Encap-Mild” and “Encap-Std” were prepared by mixing dry mix (89.0 kg) with encapsulated IPNV antigen suspended in PBS (Item C005, Table 2.1). Encapsulated IPNV antigen (42.03 g; Batch 2, Section 6.2.2) was suspended in PBS (957.97 g) for “Encap-Mild” dry mix.

On the other hand, encapsulated IPNV antigen (41.16 g; Batch 1, Section 6.2.2) was suspended in PBS (958.84 g) for “Encap-Std” dry mix.

Dry mix which served as a positive control (Ctrl+positive) was prepared by mixing meal mix (99.00 g) with IPNV antigen suspension (1.00 g,10^9 $TCID_{50}$ g^{-1}). This small reference sample was used “as is” and thus it was not processed. Dry mix of the feed named “Ctrl-negative” was not added any IPNV antigen but it was processed under standard conditions. As a result, the final IPNV antigen concentration in all five dry mixes with antigen was 10^7 $TCID_{50}$ g^{-1}. Compositions of dry mixes are summarised in the Table 6.3.

Table 6.3: Compositions of the dry mixes. Their relation to the extruder runs is shown in the Table 6.1

Feed name	PBS suspension		Free IPNV Ag susp. [g]	Meal mix [kg]	Dry mix [kg]
	PBS [g]	Encapsulated IPNV Ag [g]			
Unencap-Mild	0	0	900	89.1	90
Encap-Mild	957,97	42.03	0	89	90
Unencap-Std	0	0	900	89.1	90
Encap-Std	958,84	41.16	0	89	90
Ctrl-negative	0	0	0	100	100
Ctrl+positive	0	0	1.00	9.9×10^{-4}	1.0×10^{-3}

6.2.4 Feed trial

Feed trial was performed according to the method described in the section 2.2.3 (Chapter 2) at Technology Centre of EWOS Innovation AS (Dirdal, Norway). All produced feeds were 5 mm in size. Standard runs/feeds (Run 3 and 4) were produced in a production process which was defined as hot. On

the other hand, the “mild” runs (Run 1 and 2) were performed under more moderate conditions. All the runs were compared to the Control run (Ctrl-negative, Table 6.1) which was conducted under standard conditions. In addition to some other parameters, these runs were characterised by temperature and pressure measured in different compartments of the process (Table 6.4, 6.5 and 6.6). Temperature and pressure were measured at eight different places in the extrusion process. The first measurement point was at the outlet of the preconditioner. The following seven measurement points were distributed over the seven zones in the extruder barrel. The last zone which was called “spacer” is positioned at the end of an extruder barrel (Table 6.5).

In order to describe the process in terms of applied heat per kilogram of the feed material, the specific enthalpy of the process (liquid part) was calculated. The calculation was performed using the Equation 6.1 and 6.2. Specific heat of the water and “dry mix” mixture was unknown. Since the same feed recipe was used for all five runs, the change of enthalpy of water was applied in calculating the ratio between experimental runs and the control run.

Equation 6.1: Change in enthalpy of a system (Δh)

$$\Delta h = \Delta u + v\,\Delta p$$

h – specific enthalpy of a system [kJ kg^{-1}]

u – specific internal energy of a system [kJ kg^{-1}]

v – specific volume [l kg^{-1}]. This is a tabulated value.

p – absolute pressure [MPa]

Equation 6.2: Change in internal energy of a system (Δu)

$$\Delta u = c\ \Delta T$$

u – specific internal energy of a system [kJ kg^{-1}]

T – temperature [K]

c – specific heat of an incompressible substance [kJ kg^{-1} K^{-1}]. It is equal to specific heat capacity (Cp) in this equation. This is a tabulated value.

Table 6.4: An overview of the process conditions in the preconditioner

Preconditioner							
	Parameters	Unit	Run 1	Run 2	Run 3	Run 4	Control
Meal	Feed rate (dry mix)	kg/h	106.00	104.00	106.00	108.00	104.00
	Temperature (dry mix)	°C	22.20	24.70	23.09	25.20	26.00
Water	Water flow rate	kg/h	21.20	23.00	20.00	21.00	20.80
	Water flow rate (dry mixture)	%	20.06	22.02	18.86	19.55	19.98
	Water temperature	°C	70.40	70.20	70.03	70.10	70.40
Steam	Steam flow rate	kg/h	2.60	2.30	12.60	11.60	11.60
	Steam flow rate (dry mixture)	%	2.45	2.18	11.88	10.80	11.12
Total	Total liquid addition	kg/h	60.00	60.00	68.00	67.00	67.00
	Total liquid addition	%	56.60	57.30	64.10	62.20	64.20

Table 6.5: An overview of the process conditions in the extruder

Extruder							
	Parameters	Unit	Run 1	Run 2	Run 3	Run 4	Control
Engine	Extruder screw speed	rpm	309	309	417	368	407
	Extruder motor load	kW	11.30	11.80	9.10	8.20	8.60
	Current	A	16.30	17,10	13.20	11.80	12.50
	Specific mechanical energy (SME)	kW ton^{-1} h^{-1}	83.04	88.21	63.98	56.46	60.63
Temperature	Zone 1 (precond. outlet temp.)	°C	51.20	54.00	89.90	90.20	90.30
	Zone 2	°C	33.20	36.70	76.40	71.50	88.00
	Zone 3	°C	38.30	38.90	86.80	82.70	94.50
	Zone 4	°C	41.40	43.30	108.70	104.00	114.40
	Zone 5	°C	54.30	55.10	95.80	94.60	101.80
	Zone 6	°C	36.50	38.40	90.10	88.00	98.70
	Zone 7	°C	27.80	28.40	92.80	88.40	105.10
	Spacer	°C	77.10	81.80	94.10	91.10	87.10
Pressure (gauge)	Zone 1 (precond. outlet temp.)	bar	0	0	0	0	0
	Zone 2	bar	0.40	0.40	0.60	0.50	0.70
	Zone 3	bar	4.70	3.60	3.60	3.70	3.70
	Zone 4	bar	14,70	12,90	9,40	9,10	9.10
	Zone 5	bar	0.00	0.00	0.10	0.20	0.20
	Zone 6	bar	0.52	0.00	1.93	1.51	2.21
	Zone 7	bar	13.11	15.70	10.48	10.96	8.40
	spacer	bar	17.88	22.94	19.36	18.72	14.42
Mass flow	Total die area	mm^2	34.02	34.02	34.02	34.02	34.02
	Total cylinder area	mm^2	250.70	250.70	250.70	250.70	250.70
	Extruder discharge rate	kg/h	164.90	164.07	173.81	174.41	171.30

Table 6.6: An overview of the process conditions in the dryer

Dryer							
	Parameters	Unit	Run 1	Run 2	Run 3	Run 4	Control
Temp.	Zone 1	°C	78.10	76.10	75.00	77.80	70.20
	Zone 2	°C	75.30	74.60	75.00	75.00	64.50
	Zone 3	°C	74.10	75.50	75.00	75.20	60.10

6.2.5 Sampling

Sampling was performed at five different stages in the production process: mixing (dry mix, dm), conditioning (wet mix, wm), extrusion (extrudate, ext), drying (base pellet, bp) and coating (final feed, ff). It was taken five samples with 10 seconds time intervals at each point of production stage.

6.2.6 Sample preparation

Initially, pulverised feed sample (2.00 g) was dispersed in hexane (6.0 ml). Afterwards, this dispersion was span down (4000 rpm for 10 min) and then supernatant was transferred to 10 ml separation funnel. The formed precipitate was saved for later use. Subsequently, supernatant (hexane solution) was washed two times with saturated sodium bicarbonate (1 ml, Item S005, Table 2.4). The aqueous fraction was collected and then used to disperse the spared precipitate. The resulting dispersion was left overnight at 4°C. The following day, dichloromethane (4.0 ml) was added and the sample container was shaken thoroughly. Thereafter, the content was span down (4000 rpm for 10 min) yielding supernatant consisting of two fractions (organic on the bottom and aqueous on the top). This new supernatant was transferred to a 10 ml separation funnel and combined with hexane (3.0 ml). This operation changed the order of the fractions.

Finally, the aqueous fraction was collected and stored at 4°C for the later ELISA assay. ELISA was performed as previously described by Munang'andu et al. (2012) with minor modifications at Norwegian School of Veterinary Science (Oslo, Norway). Statistical analysis was conducted according to the method described in the Section (2.2.6.4).

6.3 Results and Discussion

6.3.1 Experimental conditions of the feed production runs

From the results in the Table 6.7, it can be seen that the mean enthalpy of the first two runs is double as low as the enthalpy of the control run. Furthermore, there was no statistically significant difference between the standard runs and the control run at the 5% significance level. This also indicates that the enthalpy of the mild runs is approximately 50% lower than the enthalpy of the standard runs. In conclusion, the amount of heat added in the mild runs was only half of the amount of heat added per kilogram of feed material in the standard runs. This is also graphically illustrated in the Figure 6.2.

The enthalpy calculations were based only on the properties of water in the system. It was justified by the fact that the feed material was of constant composition. In addition, the changes in specific enthalpy of the experimental runs were expressed as the percent ratio to the specific enthalpy of the control run.

Table 6.7: Mean enthalpies with their upper and lower levels of the 95% confidence intervals in the antigen stability study. The mean values were calculated out of eight different measurements (preconditioner, zone 2-7 and spacer; Table 6.5). The measured quantities were gauge pressure and temperature. Calculations were performed using the Equations 6.1 and 6.2. The mean values of Runs 1-4 were compared to the mean value of the control run in the last column.

Run	Upper level	Lower level	Mean Enthalpy (kJ/kg)	Ratio to Control (%)
Control[i, ii]	446	370	408	100
Run 1[iii]	244	136	190	47
Run 2[iii]	256	137	196	48
Run 3[i]	419	352	386	94
Run 4[i]	411	342	377	92

[i]Standard (hot) process conditions
[ii]Control run is the same run as the Ctrl-negative (Table 6.1)
[iii]Mild process conditions

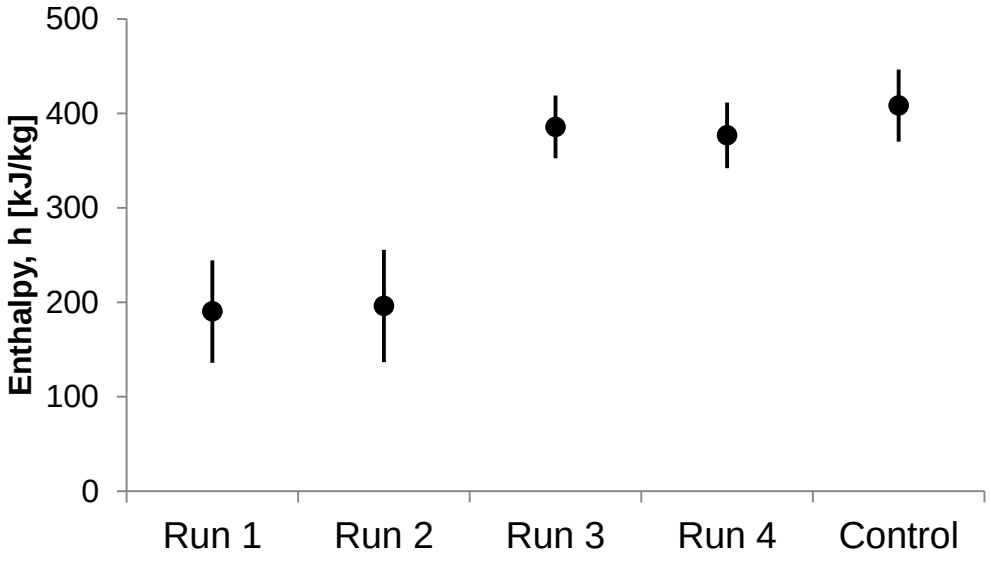

Figure 6.2: Average enthalpies of the four extruder runs along with one control run Enthalpies of the Runs 1 and 2 are significantly lower than the enthalpies of the Runs 3 and 4 and the control run at 5% significance level. It suggest that, the amount of heat applied per kilogram of feed material is approximately 50% lower in the first two runs (mild runs) than in the other runs performed under standard conditions (Table 6.7). Error bars represent 95% confidence intervals.

6.3.2 Survival of the IPNV antigen throughout fish feed production process

From the Figure 6.3, it can be concluded that IPNV was detected in all four groups of the final feed samples. This observation suggests that IPNV antigen may survive throughout fish feed production process conducted at temperature ≤109°C. There is also an indication for both un-encapsulated and encapsulated IPNV antigen surviving throughout extrusion, drying and infusion coating process. It suggest that IPN virus is relatively withstand temperature around 100°C in a short period of time (15 s).This observation is also consistent with the investigation by Dixon et al. (2012) where IPN virus was not completely inactivated within one hour at 60°C.

Low response of encapsulated antigen (Encap-Std and Encap-Mild) in both dry and wet mix could be due to ineffective antigen extraction method. In all, it seems easier to extract antigen from the samples after the extrusion. It could be explained by additional effect of moisture, temperature and shear force on dissolution of alginate matrix. However, the maximum achieved temperature in the standard extrusion process is much lower than the operating extrusion temperature (>150°C) at the factories. Due to this difference, capability of IPNV antigen to retain its viability and integrity could be assessed throughout more extreme process conditions.

From the results it can be seen that the encapsulation has rather negative effect on antigen survival at all stages of production process except form the final feed where it is insignificant (Figure 6.4). This could also be due to an ineffective antigen extraction method. Dissolution of alginate beads requires

alkaline conditions but too high pH may hydrolyse antigen. Another challenge is the high buffer capacity of feed material which may in turn consume hydroxide anions needed for dissolution of alginate matrix.

Responses of samples 1 to 5 were decreasing towards the higher sample number on 96-well plate. We tried to relate position of the samples on ELISA plate to this variability but it proved to be unsupported by data.

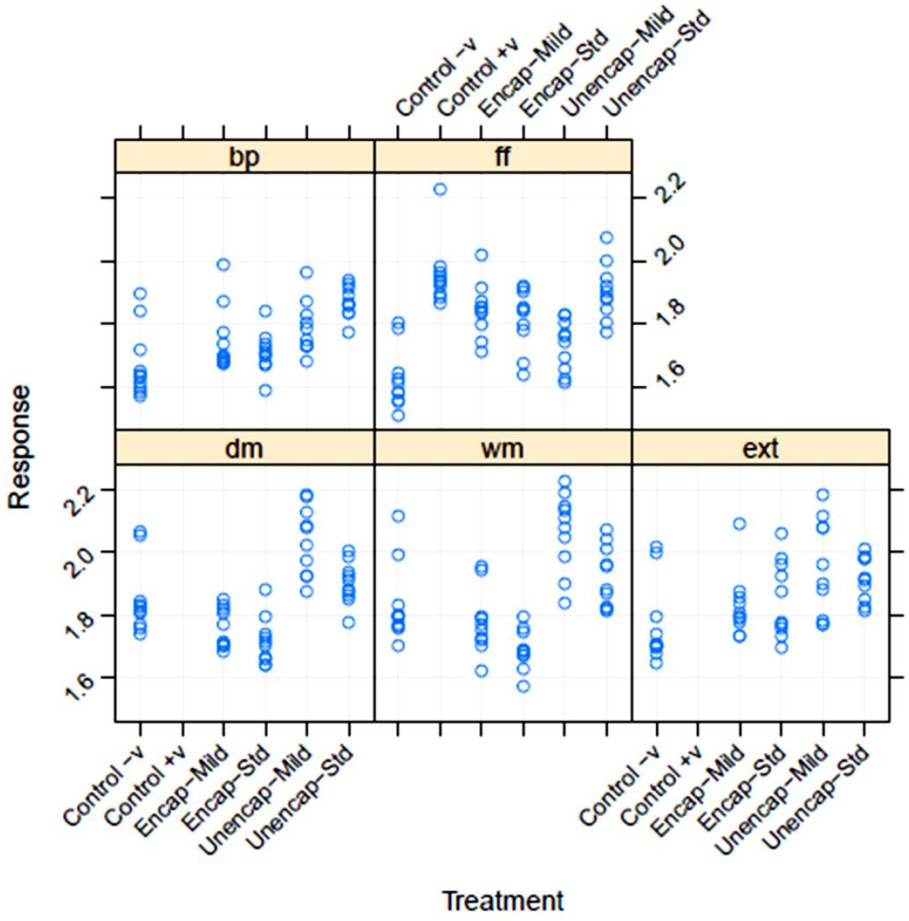

Figure 6.3: Observed responses by treatments at different steps in the feed production process. dm – dry mix (initial meal mix), wm – wet mix (after preconditioning), ext – extrudate (after extruding), bp – base pellet (after drying), ff – final feed (after applying oil), response – optical density.

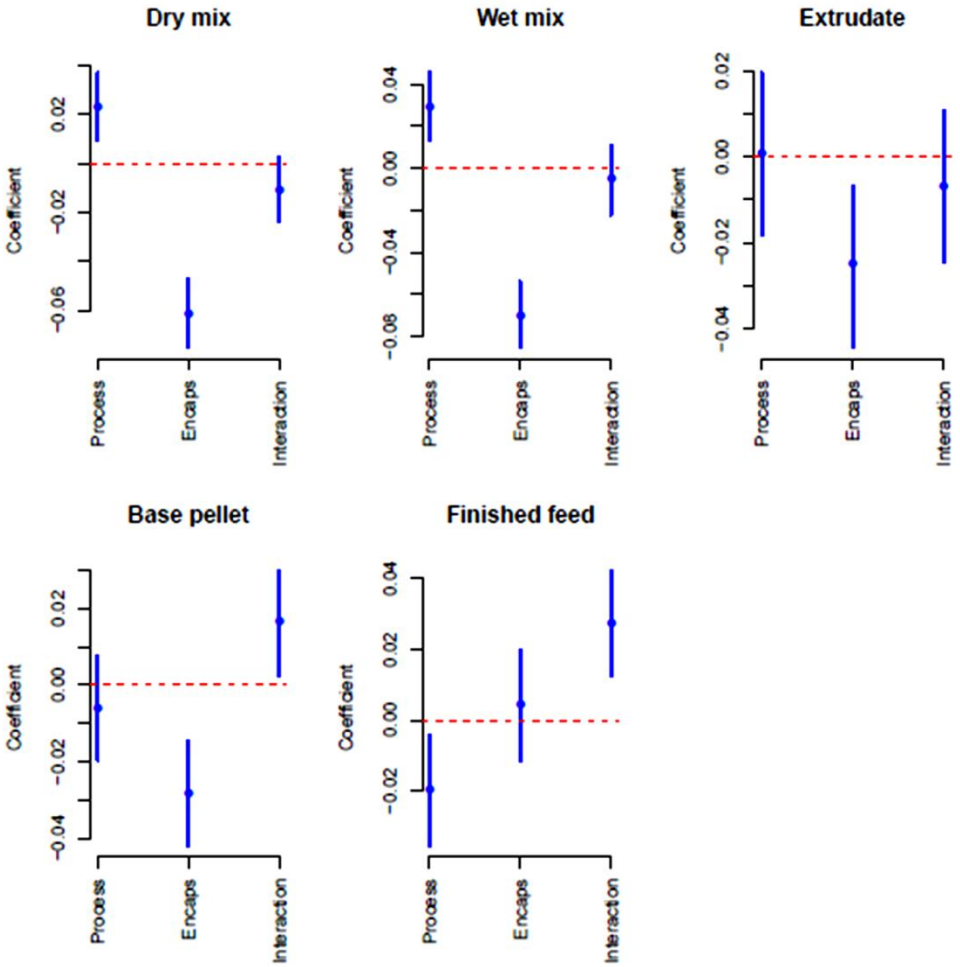

Figure 6.4: Estimated coefficients for process factors, encapsulation factors and their interaction. The coefficients are shown in the same order on the horizontal axes. The actual effect is twice the coefficients because coding [-1, +1] was used. All coefficients are on the logarithmic scale because logarithmic transformation was applied before analysis.

Chapter Seven:General Discussion and Conclusion

This chapter summarises major findings of the thesis and presents an overall conclusion. The conclusion was drawn on the basis of all work carried out. This work includes: *in vitro* trials (dissolutions tests), *in vivo* trial (A. salmon), *in situ* trials (fish feed production trial) and several benchtop experiments (optimisation of encapsulation process). A great number of samples were taken in these trials. In sample analysis, large variety of methods was applied. Data were processed by diverse statistical software generating large amount of results.

The results suggest that protein antigens can be entrapped into alginate beads that are sufficiently small for being effectively incorporated into feed pellets. The antigen will most likely be released in the mid and distal compartment of A. salmon intestine. The results also indicate that the antigen can be absorbed in those compartments. Furthermore, there is evidence to suggest that the absorbed antigen is able to induce specific immune response in A. salmon.

According to the results of study on antigen stability in fish feed production process, we could purpose pre-extrusional addition of IPNV antigen to be considered under mild process conditions.

7.1 Major findings

7.1.1 Very fine alginate beads

Optimisation of encapsulation process air pressure-assisted energised jetting) resulted in very fine alginate beads (d_{median}= 8 µm). In comparison to previous studies the current results were amongst the smallest reported sizes of alginate beads generated by an extrusion method (Table 5.8). The optimised encapsulation process could be used to produce alginate particles which can readily be integrated into the feed pellet with a size of 10 mm and probably smaller. In short, the achieved mean particle size of 10 µm with a half of the particles smaller than 8 µm meets the objectives of producing suitably sized alginate beads for effective association with feed pellet. Finally, it can be said that the outcome of this study improves understanding of the issues regarding incorporation of delivery systems into fish feed in the current manufacturing process.

7.1.2 A new dissolution test strategy

This study developed a new dissolution test strategy with respect to chemical properties of alginate and physiological conditions for A. salmon. The new strategy is based on one single dissolution test combining pH 3.0 for 15 min with pH 8.0 for 50 min performed at two different temperatures (4°C and 18°C). This is in contrast to common practice were release of an active pharmaceutical ingredient from a cross-linked alginate is assessed in a dual dissolution test. The dual dissolution test applies one acidic dissolution medium (pH 1 – 2) and another nearly neutral medium (pH 6.8 – 7.4). The

test temperature, which is adapted to humans, is normally maintained constant at 37°C (Azarmi et al., 2007).

We demonstrated that the results generated in the redesigned dissolution test are in strong correlation with the results produced in the *in vivo* study. This is promising considering the previously reported difficulties experienced in dissolution testing of extended release products (Zahirul and Khan, 1996). Release from ethylenediammonium alginate was both pH- and temperature-independent. Furthermore, encapsulation efficiency of protein antigens in the ethylenediammonium alginate matrix is very high (> 97%). In conclusion, ethylenediammonium alginate proved to be an excellent oral delivery system for macromolecular drugs to A. salmon.

7.1.3 Oral vaccination strategy

On the whole, this study shed light on the opportunities and issues related to i.p. priming/oral boost strategy involving an inactivated IPN virus. Oral delivery of the encapsulated antigens elicited the immune response in A. salmon in the first oral boost period. Although the OD values (ELISA) of the groups fed with oral boost feeds rose from the 1.OB to the 2.OB, there was no significant difference between them and control feed. According to qPCR results, this inefficiency was most likely caused by the immune tolerance which is a common issue in immunising via oral route (Jump and Levine, 2004; Siewert et al., 2008; Weiner et al., 2011).

7.1.4 Survival of IPNV antigen through fish feed production

From the trial related to stability of IPNV antigen in fish feed production process, it can be concluded that IPNV was present in all four groups of the samples. This suggests that IPNV antigen may survive throughout fish feed production process conducted at temperature ≤108°C. Survival of IPNV antigen at elevated temperatures was previously reported as well but this is most likely the harshest tested conditions so far (MacKelvie and Desautels, 1975). Although the temperatures below 108°C are far lower than what commercial reality is, they are not unrealistic. There is also an indication for both un-encapsulated and encapsulated IPNV antigen surviving throughout extrusion, drying and infusion coating process.

7.2 Future directions

Additional studies are required to optimise the alginate formulations further as well as to characterise release profiles of the relevant antigens from alginate matrices both *in vitro* and *in vivo*. Since the dose-response of the oral IPNV Ag in A. salmon is very little known, additional research should address this issue. There are also questions regarding duration of an oral IPNV antigen dose action which could be answered in a future study. Since the significance of voltage for minimising particle size remained unclear, future research should either assess the effect of voltage coupled with an increasing conductivity of alginate solution, or should assess the effect of liquid properties on particle size at stationary point. In future studies, efficacy of alginate-encapsulated antigens could be tested in a challenge trial. In addition to immunohistochemistry tools and ELISA, DNA microarray techniques and multiplex PCR could be used to measure the expression levels of relevant genes.

7.3 General conclusion

According to the results in this study, ethylenediammonium alginate proved superior to calcium alginate in the encapsulation efficiency test. On the other hand, calcium alginate in return performed much better in immunising the fish. This was observed in the second oral boost interval where IPNV antigen entrapped in calcium alginate matrix demonstrated the ability to boost immune response. However, multi-boosting with high antigen doses was not advantageous for immune response. This inefficiency was most likely caused by the immune tolerance which is a common issue in immunising via oral route.

In short, the findings of the present study can be summarised as follows**:** 1) Parenteral prime with the combination vaccine followed by an oral boost with encapsulated antigens results in a the augmentation of both the systemic and mucosal immune responses; 2) Mucosal (gut) immunity is not primed by parenteral but by oral administration of antigens and 3) Oral prime and subsequent boost with encapsulated antigens results in augmentation of mucosal immune responses.

Furthermore, the findings in this study suggest that there is a delay in uptake of the encapsulated antigens compared to the un-encapsulated ones. This is logical given that antigens are less readily available when encapsulated than in solution.

In conclusion, it can be said that differences do exist between differently cross-linked alginate matrices. Differences between the ethylenediammonium and calcium alginate are evident with respect to

dissolution rate at low temperatures. In order to recognise these characteristics of alginate beads, a new dissolution test strategy is developed. This new strategy makes dissolution test highly representative for gastrointestinal conditions found in fish with stomach. As a consequence, the results generated by the redesigned dissolution test are in strong correlation with the results obtained from the present *in vivo* study.

On the whole, ethylenediammonium alginate is an excellent delivery system for macromolecular drug to ectothermic animal like salmon. There is evidence to suggest that this delivery system is temperature-independent within the temperature range of salmon's life habitat. The practical implication of the results of the present study is that the amount of drug delivered is irrespective of the environmental temperature when using this novel oral delivery system.

In addition, our data indicate that some IPNV antigen may survive through the current fish feed production process. Given this, it may be concluded that this antigen is a highly robust. Other antigen candidates for oral vaccination may be less robust. These and then can be delivered through the vacuum coating system. Because of the progress we have made with encapsulation technology in this study, vacuum infusion coating with alginate-encapsulated antigens can be performed with high yield. It is a result of optimising air pressure-assisted energised jetting to produce alginate beads with median size of 16 μm using DI water as alginate solvent. Sodium alginate concentration, pressure and distance were significant production variables whilst voltage and flow rate exerted little effect upon particle size.

However, it has been demonstrated that the median particle size dropped down to 8 µm when alginate solvent was changed to PBS, indicating a possible effect of conductivity. In comparison to previous studies the current results were amongst the smallest reported sizes of alginate beads generated by an extrusion method. Therefore, it can be concluded that, air pressure-assisted energised jetting could be used to produce alginate beads of a size which can readily be integrated into the fish feed pellet with a size of d_{avg} = 10 mm and smaller. In addition to associating very well within the feed pellet, oral delivery systems of the size d ≤ 10 µm are reported to be capable of crossing the intestinal epithelial layers.

The results of the porosimetry and SEM image analysis suggest that the spherical particles should be at least four times smaller than the estimated pore size of a feed pellet. This is to ensure easy passage of a greater number of beads through the entry holes of the surface pores which appear to be rather irregular.

From the outcome of the micro-CT scan it can be seen that micro-particles with d_{median} = 25 µm are readily able to access the pellet with predominant pore sizes of 100 µm.

In conclusion it can be said that protein antigens can be successfully delivered to A. salmon using the encapsulation technology developed in this study.

Bibliography

Abeyewickreme, A., Kwok, A., McEwan, J.R., Jayasinghe, S.N., 2009. Bio-electrospraying embryonic stem cells: interrogating cellular viability and pluripotency. Integr. Biol. (Camb). 1, 260–266.

Adelmann, M., Köllner, B., Bergmann, S.M., Fischer, U., Lange, B., Weitschies, W., Enzmann, P.-J., Fichtner, D., 2008. Development of an oral vaccine for immunisation of rainbow trout (*Oncorhynchus mykiss*) against viral haemorrhagic septicaemia. Vaccine 26, 837–844.

Ainsley Reid, A., Vuillemard, J.C., Britten, M., Arcand, Y., Farnworth, E., Champagne, C.P., 2005. Microentrapment of probiotic bacteria in a Ca(2+)-induced whey protein gel and effects on their viability in a dynamic gastro-intestinal model. J. Microencapsul. 22, 603–619.

Akdis, C.A., Akdis, M., 2014. Mechanisms of immune tolerance to allergens: role of IL-10 and Tregs. J. Clin. Invest. 124, 4678–4680.

Akdogan, H., 1999. High moisture food extrusion. Int. J. Food Sci. Technol. 34, 195–207.

Alam, M.S., Kaur, J., Khaira, H., Gupta, K., 2015. Extrusion and Extruded Products: Changes in Quality Attributes as Affected by Extrusion Process Parameters: A Review. Crit. Rev. Food Sci. Nutr. In Press.

Aldrin, M., Storvik, B., Kristoffersen, A.B., Jansen, P.A., 2013. Space-time modelling of the spread of salmon lice between and within Norwegian marine salmon farms. PLoS One 8, 64039.

Allnutt, F.C.T., Bowers, R.M., Rowe, C.G., Vakharia, V.N., LaPatra, S.E., Dhar, A.K., 2007. Antigenicity of infectious pancreatic necrosis virus VP2 subviral particles expressed in yeast. Vaccine 25, 4880–4888.

Amalia Kartika, I., Pontalier, P.Y., Rigal, L., 2006. Extraction of sunflower oil by twin screw extruder: screw configuration and operating condition effects. Bioresour. Technol. 97, 2302–2310.

Anand, O., Yu, L.X., Conner, D.P., Davit, B.M., 2011. Dissolution testing for generic drugs: an FDA perspective. AAPS J. 13, 328–335.

Anjani, K., Kailasapathy, K., Phillips, M., 2007. Microencapsulation of enzymes for potential application in acceleration of cheese ripening. Int. Dairy J. 17, 79–86.

Arêas, J.A., 1992. Extrusion of food proteins. Crit. Rev. Food Sci. Nutr. 32, 365–392.

Arumuganathar, S., Irvine, S., McEwan, J.R., Jayasinghe, S.N., 2007. Aerodynamically assisted bio-jets: the development of a novel and direct

non-electric field-driven methodology for engineering living organisms. Biomed. Mater. 2, 158–168.

Arumuganathar, S., Jayasinghe, S.N., 2008. A versatile pressure assisted jet-fabrication by coating approach for forming biocompatible constructs for tissue engineering. Mater. Lett. 62, 2574-2577.

Augst, A.D., Kong, H.J., Mooney, D.J., 2006. Alginate hydrogels as biomaterials. Macromol. Biosci. 6, 623–633.

Azarmi, S., Roa, W., Löbenberg, R., 2007. Current perspectives in dissolution testing of conventional and novel dosage forms. Int. J. Pharm. 328, 12-21.

Bain, N., Gregory, A., Raynard, R.S., 2008. Genetic analysis of infectious pancreatic necrosis virus from Scotland. J. Fish Dis. 31, 37–47.

Ballesteros, N.A., Saint-Jean, S.S.R., Perez-Prieto, S.I., Coll, J.M., 2012. Trout oral VP2 DNA vaccination mimics transcriptional responses occurring after infection with infectious pancreatic necrosis virus (IPNV). Fish Shellfish Immunol. 33, 1249–1257.

Bashir, S., Asad, M., Qamar, S., ul Hassnain, F., Karim, S., Nazir, I., 2014. Development of sustained-release microbeads of nifedipine and *in vitro* characterization. Trop. J. Pharm. Res. 13, 505–510.

Belkaid, Y., 2007. Regulatory T cells and infection: a dangerous necessity. Nat. Rev. Immunol. 7, 875–888.

Bernkop-Schnurch, A., 2009. Oral Delivery of Macromolecular Drugs. Springer US, New York, NY, 153-167.

Bertero, M., Boccacci, P., Pike, E.R., 1985. Particle-size distributions from Fraunhofer diffraction: the singular-value spectrum. Inverse Probl. 1, 111–126.

Biology-Online.org, 2014. Digestion [WWW Document]. Dictionary. URL http://www.biology-online.org/dictionary/Digestion (accessed 5.25.14).

Bixler, H.J., Porse, H., 2011. A decade of change in the seaweed hydrocolloids industry. J. Appl. Phycol. 23, 321-335.

Bock, N., Dargaville, T.R., Woodruff, M.A., 2012. Electrospraying of polymers with therapeutic molecules: State of the art. Prog. Polym. Sci. 37, 1510–1551.

Bock, N., Woodruff, M.A., Steck, R., Hutmacher, D.W., Farrugia, B.L., Dargaville, T.R., 2014. Composites for delivery of therapeutics: combining melt electrospun scaffolds with loaded electrosprayed microparticles. Macromol. Biosci. 14, 202–214.

Bowen, J.C., Nair, S.K., Reddy, R., Rouse, B.T., 1994. Cholera toxin acts as a potent adjuvant for the induction of cytotoxic T-lymphocyte responses with non-replicating antigens. Immunology 81, 338–342.

Boxus, M., Lockman, L., Fochesato, M., Lorin, C., Thomas, F., Giannini, S.L., 2014. Antibody avidity measurements in recipients of Cervarix vaccine following a two-dose schedule or a three-dose schedule. Vaccine 32, 3232–3236.

Braghirolli, D.I., Zamboni, F., Chagastelles, P.C., Moura, D.J., Saffi, J., Henriques, J.A.P., Pilger, D.A., Pranke, P., 2013. Bio-electrospraying of human mesenchymal stem cells: An alternative for tissue engineering. Biomicrofluidics 7, 44130.

Brudeseth, B.E., Wiulsrød, R., Fredriksen, B.N., Lindmo, K., Løkling, K.-E., Bordevik, M., Steine, N., Klevan, A., Gravningen, K., 2013. Status and future perspectives of vaccines for industrialised fin-fish farming. Fish Shellfish Immunol. 35, 1759–1768.

Bruno, B.J., Miller, G.D., Lim, C.S., 2013. Basics and recent advances in peptide and protein drug delivery. Ther. Deliv. 4, 1443–1467.

Bucking, C., Wood, C.M.M., 2009. The effect of postprandial changes in pH along the gastrointestinal tract on the distribution of ions between the solid and fluid phases of chyme in rainbow trout . Aquac. Nutr. 15, 282–296.

Bugarski, B., Li, Q., Goosen, M.F.A., Poncelet, D., Neufeld, R.J., Vunjak, G., Mattheus, F., Goosen, A., 1994. Electrostatic Droplet Generation: Mechanism of Polymer Droplet Formation . AICHE J. 40, 1026–1031.

Caballero, F., Foradada, M., Miñarro, M., Pérez-Lozano, P., García-Montoya, E., Ticó, J.R., Suñé-Negre, J.M., 2014. Characterization of alginate beads loaded with ibuprofen lysine salt and optimization of the preparation method. Int. J. Pharm. 460, 181–188.

Carrier, Y., Yuan, J., Kuchroo, V.K., Weiner, H.L., 2007. Th3 cells in peripheral tolerance. II. TGF-beta-transgenic Th3 cells rescue IL-2-deficient mice from autoimmunity. J. Immunol. 178, 172–178.

Castro-Sánchez, P., Martín-Villa, J.M., 2013. Gut immune system and oral tolerance. Br. J. Nutr. 109, 3–11.

Cecere, T.E., Todd, S.M., LeRoith, T., 2012. Regulatory T cells in arterivirus and coronavirus infections: Do they protect against disease or enhance it? Viruses 4, 833-846.

Cepeda, V., Cofre, C., Gonzalez, R., MacKenzie, S., Vidal, R., González, R., MacKenzie, S., Vidal, R., 2011. Identification of genes involved in

immune response of Atlantic salmon (*Salmo salar*) to IPN virus infection, using expressed sequence tag (EST) analysis. Aquaculture 318, 54–60.

Cermaq, 2012. Cermaq annual report 2011. Oslo.

Chang, R.-K., Raw, A., Lionberger, R., Yu, L., 2013. Generic development of topical dermatologic products: formulation development, process development, and testing of topical dermatologic products. AAPS J. 15, 41–52.

Changyuan, Z., Xiu, W., Jishuai, G., 2012. Design of droplet size measuring system of air-assisted spraying and experiment on its influencing factors. Trans. Chinese Soc. Agric. Eng. 28, 1–6.

Chen, L., Evensen, O., Mutoloki, S., 2013. Delayed protein shut down and cytopathic changes lead to high yields of infectious pancreatic necrosis virus cultured in Asian grouper cells. J. Virol. Methods 195, 228-235.

Chen, W., Jin, W., Hardegen, N., Lei, K.-J., Li, L., Marinos, N., McGrady, G., Wahl, S.M., 2003. Conversion of peripheral CD4+CD25- naive T cells to CD4+CD25+ regulatory T cells by TGF-beta induction of transcription factor Foxp3. J. Exp. Med. 198, 1875–1886.

Chen, Y., Inobe, J., Kuchroo, V.K., Baron, J.L., Janeway, C.A., Weiner, H.L., 1996. Oral tolerance in myelin basic protein T-cell receptor transgenic mice: suppression of autoimmune encephalomyelitis and dose-dependent induction of regulatory cells. Proc. Natl. Acad. Sci. U. S. A. 93, 388–391.

Ciofani, G., Raffa, V., Menciassi, A., Dario, P., 2008. Alginate and chitosan particles are drug delivery system for cell therapy. Biomed. Microdevices 10, 597–600.

Collet, B., 2014. Innate immune responses of salmonid fish to viral infections. Dev. Comp. Immunol. 43, 160–173.

Cooper, C.A., 2008. Post-prandial alkaline tide in freshwater rainbow trout: effects of meal anticipation on recovery from acid-base and ion regulatory disturbances. J. Exp. Biol. 211, 2542.

Cooper, R.E., Upadhyay, J., Wassermann, A., 1962. Molecular size and shape of the ethylenediammonium salt of a polycarboxylic acid. J. Chem. Soc. (Resumed), 2705-2708.

Costa, P., Sousa Lobo, J.M., 2001. Modeling and comparison of dissolution profiles. Eur. J. Pharm. Sci. 13, 123–133.

Coulibaly, F., Chevalier, C., Delmas, B., Rey, F.A., 2010. Crystal structure of an *Aquabirnavirus* particle: insights into antigenic diversity and virulence determinism. J. Virol. 84, 1792–1799.

D'Arcy, D.M., Liu, B., Bradley, G., Healy, A.M., Corrigan, O.I., 2010. Hydrodynamic and species transfer simulations in the USP 4 dissolution apparatus: considerations for dissolution in a low velocity pulsing flow. Pharm. Res. 27, 246–258.

Damask, C., 2015. Update on eosinophilic esophagitis. Curr. Opin. Otolaryngol. Head Neck Surg. 23, 240–246.

Dashevsky, A., 1998. Protein loss by the microencapsulation of an enzyme (lactase) in alginate beads. Int. J. Pharm. 161, 1–5.

De Kruif, C.G., Weinbreck, F., de Vries, R., 2004. Complex coacervation of proteins and anionic polysaccharides. Curr. Opin. Colloid Interface Sci. 9, 340–349.

Del Gaudio, P., Colombo, P., Colombo, G., Russo, P., Sonvico, F., 2005. Mechanisms of formation and disintegration of alginate beads obtained by prilling. Int. J. Pharm. 302, 1–9.

de-Oliveira, L.D., de Carvalho Picinato, M.A., Kawauchi, I.M., Sakomura, N.K., Carciofi, A.C., 2012. Digestibility for dogs and cats of meat and bone meal processed at two different temperature and pressure levels*. J. Anim. Physiol. Anim. Nutr. (Berl). 96, 1136–1146.

Dhar, A.K., 2013. Challenges and Opportunities in Developing Oral Vaccines against Viral Diseases of Fish. J. Mar. Sci. Res. Dev. 3, 1-6.

Dhar, A.K., Manna, S.K., Thomas Allnutt, F.C., 2014. Viral vaccines for farmed finfish. Virusdisease 25, 1–17.

Dixon, P.F., Smail, D.A., Algoët, M., Hastings, T.S., Bayley, A., Byrne, H., Dodge, M., Garden, A., Joiner, C., Roberts, E., Verner-Jeffreys, D., Thompson, F., 2012. Studies on the effect of temperature and pH on the inactivation of fish viral and bacterial pathogens. J. Fish Dis. 35, 51–64.

Douce, G., Giannelli, V., Pizza, M., Lewis, D., Everest, P., Rappuoli, R., Dougan, G., 1999. Genetically detoxified mutants of heat-labile toxin from *Escherichia coli* are able to act as oral adjuvants. Infect. Immun. 67, 4400–4406.

Draganovic, V., van der Goot, a. J., Boom, R., Jonkers, J., 2013. Wheat gluten in extruded fish feed: effects on morphology and on physical and functional properties. Aquac. Nutr. 19, 845–859.

Dunn, S., 2011. The modern food industry and public health: a Galbraithian perspective. J. Post Keynes. Econ. 33, 491–516.

Eddaoudi, A., Townsend-Nicholson, A., Timms, J.F., Schorge, S., Jayasinghe, S.N., 2010. Molecular characterisation of post-bio-electrosprayed human brain astrocytoma cells. Analyst 135, 2600–2612.

Einarsson, S., Davies, P.S., Talbot, C., 1996. The effect of feeding on the secretion of pepsin, trypsin and chymotrypsin in the Atlantic salmon, *Salmo salar L*. Fish Physiol. Biochem. 15, 439–446.

El-Attar, L.M., Anstaett, O., Thomas, C., Luke, J., Williams, J., Brownlie, J., 2013. Enhanced Neutralising Antibody Response to Bovine Viral Diarrhoea Virus (BVDV) Induced by BVDV DNA Vaccine Co-Expressing RIG-I Agonist in Cattle. Mol. Ther. 21, 72.

Eldridge, J.H., Hammond, C.J., Meulbroek, J.A., Staas, J.K., Gilley, R.M., Tice, T.R., Eldridge, Hammond, Meulbroek, Staas, Gilley, Tice, T.R., 1990. Controlled vaccine release in the gut-associated lymphoid tissues. I. Orally administered biodegradable microspheres target the peyer's patches. J. Control. Release 11, 205–214.

Ellis, A.E., Cavaco, A., Petrie, A., Lockhart, K., Snow, M., Collet, B., 2010. Histology, immunocytochemistry and qRT-PCR analysis of Atlantic salmon, *Salmo salar L.*, post-smolts following infection with infectious pancreatic necrosis virus (IPNV). J. Fish Dis. 33, 803–818.

Eronina, T., Borzova, V., Maloletkina, O., Kleymenov, S., Asryants, R., Markossian, K., Kurganov, B., 2011. A protein aggregation based test for screening of the agents affecting thermostability of proteins. PLoS One 6, 22154.

Evensen, Ø., Leong, J.-A.C., 2013. DNA vaccines against viral diseases of farmed fish. Fish Shellfish Immunol. 35, 1751–1758.

FAO, 2012. Global Aquaculture Production 1950-2012, in: FishStat Plus: Universal Software for Fishery Statistical Time Service. Food and Agriculture Organisation of the United Nation, Rome.

Feenstra, T.P., De Bruyn, P.L., 1979. Formation of calcium phosphates in moderately supersaturated solutions. J. Phys. Chem. 83, 475–479.

Fellows, P., 2000. Extrusion, in: Food Processing Technology: Principles and Practice. Woodhead Publishing Ltd, Cambridge, UK, 294–308.

Ferreira Almeida, P., Almeida, A.J., 2004. Cross-linked alginate-gelatine beads: a new matrix for controlled release of pindolol. J. Control. Release 97, 431–439.

Fox, N., 1997. Empowering research: statistical power in general practice research. Fam. Pract. 14, 324–329.

Fuglem, B., Jirillo, E., Bjerkås, I., Kiyono, H., Nochi, T., Yuki, Y., Raida, M., Fischer, U., Koppang, E.O., 2010. Antigen-sampling cells in the salmonid intestinal epithelium. Dev. Comp. Immunol. 34, 768–774.

Gadan, K., Sandtrø, A., Marjara, I.S., Santi, N., Munang'andu, H.M., Evensen, Ø., 2013. Stress-induced reversion to virulence of infectious pancreatic necrosis virus in naïve fry of Atlantic salmon (*Salmo salar L.*). PLoS One 8, 54656.

Gañán-Calvo, A.M., Dávila, J., Barrero, A., 1997. Current and droplet size in the electrospraying of liquids. Scaling laws. J. Aerosol Sci. 28, 249–275.

Ganjyal, G.M., Hanna, M.A., Jones, D.D., 2003. Modeling Selected Properties of Extruded Waxy Maize Cross-Linked Starches with Neural Networks. J. Food Sci. 68, 1384–1388.

Gasperini, L., Maniglio, D., Migliaresi, C., 2013. Microencapsulation of cells in alginate through an electrohydrodynamic process. J. Bioact. Compat. Polym. 28, 413–425.

George, M., Abraham, T.E., 2006. Polyionic hydrocolloids for the intestinal delivery of protein drugs: alginate and chitosan--a review. J. Control. Release 114, 1–14.

Georgopoulou, U., Dabrowski, K., Sire, M.F., Vernier, J.M., 1988. Absorption of intact proteins by the intestinal epithelium of trout, *Salmo gairdneri*. A luminescence enzyme immunoassay and cytochemical study. Cell Tissue Res. 251, 145–152.

Goeritz, I., Atorf, C., Whalley, P., Seymour, P., Klein, M., Schlechtriem, C., 2014. Investigation into feed preparation for regulatory fish metabolism studies. J. Sci. Food Agric. 94, 438–444.

Gol-Ara, M., Jadidi-Niaragh, F., Sadria, R., Azizi, G., Mirshafiey, A., 2012. The Role of Different Subsets of Regulatory T Cells in Immunopathogenesis of Rheumatoid Arthritis. Arthritis 2012, 1-16.

Gomez, A., Tang, K., 1994. Charge and fission of droplets in electrostatic sprays. Phys. Fluids 6, 404.

Gonnella, P.A., Chen, Y., Inobe, J., Komagata, Y., Quartulli, M., Weiner, H.L., 1998. In situ immune response in gut-associated lymphoid tissue (GALT) following oral antigen in TCR-transgenic mice. J. Immunol. 160, 4708–4718.

Gray, M., 1879. Supplying plastic compounds of india rubber and Gutta percha to molding or shaping. British Patent Office, Pat. No. 5056.

Gray, V., Kelly, G., Xia, M., Butler, C., Thomas, S., Mayock, S., 2009. The science of USP 1 and 2 dissolution: present challenges and future relevance. Pharm. Res. 26, 1289–1302.

Gregory, G.D., Bickford, A., Robbie-Ryan, M., Tanzola, M., Brown, M.A., 2005. MASTering the Immune Response: Mast Cells in Autoimmunity,

in: Mast Cells and Basophils: Development, Activation and Roles in Allergic/Autoimmune Disease: Novartis Foundation Symposium 271, 215–231.

Griessinger, E., Jayasinghe, S.N., Bonnet, D., 2012. Aerodynamically assisted bio-jetting of hematopoietic stem cells. Analyst 137, 1329–1333.

Gudding, R., Van Muiswinkel, W.B., 2013. A history of fish vaccination: science-based disease prevention in aquaculture. Fish Shellfish Immunol. 35, 1683–1688.

Harper, J.M., 1989. Food Extrusion, in: Singh, R.P., Medina, A.G. (Eds.), Food Properties and Computer-Aided Engineering of Food Processing Systems. Springer Netherlands, Dordrecht, 271–297.

Harper, J.M., 1978. Food extrusion. CRC Crit. Rev. Food Sci. Nutr. 11, 155–215.

Haug, A., Larsen, B., Smidsrød, O., Møller, J., Brunvoll, J., Bunnenberg, E., Djerassi, C., Records, R., 1966. A Study of the Constitution of Alginic Acid by Partial Acid Hydrolysis. Acta Chem. Scand. 20, 183–190.

Haugland, Mikalsen, A.B., Nilsen, P., Lindmo, K., Thu, B.J., Eliassen, T.M., Roos, N., Rode, M., Evensen, 2011. Cardiomyopathy syndrome of Atlantic salmon (*Salmo salar L.*) is caused by a double-stranded RNA virus of the Totiviridae family. J. Virol. 85, 5275-5286.

Hernandez-Blazquez, F.J., Silva, J.R.M.C. Da, 1998. Absorption of macromolecular proteins by the rectal epithelium of the Antarctic fish Notothenia neglecta. Can. J. Zool. 76, 1247-1253.

Hevrøy, E.M., Waagbø, R., Torstensen, B.E., Takle, H., Stubhaug, I., Jørgensen, S.M., Torgersen, T., Tvenning, L., Susort, S., Breck, O., Hansen, T., 2012. Ghrelin is involved in voluntary anorexia in Atlantic salmon raised at elevated sea temperatures. Gen. Comp. Endocrinol. 175, 118–134.

Hohlweg, U., Doerfler, W., 2001. On the fate of plant or other foreign genes upon the uptake in food or after intramuscular injection in mice. Mol. Genet. Genomics 265, 225–33.

Hordvik, I., 2015. Immunoglobulin Isotypes in Atlantic Salmon, *Salmo Salar*. Biomolecules 5, 166–177.

Hori, S., Nomura, T., Sakaguchi, S., 2003. Control of regulatory T cell development by the transcription factor Foxp3. Science 299, 1057–1061.

Hølvold, L.B., Myhr, A.I., Dalmo, R.A., 2014. Strategies and hurdles using DNA vaccines to fish. Vet. Res. 45, 21.

Iwanaga, S., Saito, N., Sanae, H., Nakamura, M., 2013. Facile fabrication of uniform size-controlled microparticles and potentiality for tandem drug delivery system of micro/nanoparticles. Colloids Surf. B. Biointerfaces 109, 301–326.

Jansen, M.D., Jensen, B.B., Brun, E., 2015. Clinical manifestations of pancreas disease outbreaks in Norwegian marine salmon farming - variations due to salmonid alphavirus subtype. J. Fish Dis.38, 343-353.

Jarp, J., GJEVRE, A.G., OLSEN, A.B., BRUHEIM, T., 1995. Risk factors for furunculosis, infectious pancreatic necrosis and mortality in post-smolt of Atlantic salmon, *Salmo solar L*. J. Fish Dis. 18, 67–78.

Jaworek, A., 2007. Electrospray droplet sources for thin film deposition. J. Mater. Sci. 42, 266–297. doi:10.1007/s10853-006-0842-9

Jaworek, A., Machowski, W., Krupa, A., Balachandran, W., 2000. Viscosity effect on EHD spraying using AC superimposed on DC electric field, in: Conference Record of the 2000 IEEE Industry Applications Conference. Thirty-Fifth IAS Annual Meeting and World Conference on Industrial Applications of Electrical Energy (Cat. No.00CH37129). IEEE, 770–776.

Jaworek, A., Sobczyk, A.T., 2008. Electrospraying route to nanotechnology: An overview. J. Electrostat. 66, 197–219.

Jayasinghe, S.N., 2011. Bio-electrosprays and Aerodynamically Assisted Bio-jets, Flow Cytometry Concepts for Interrogating Living Cells and Whole Organisms. MRS Proc. 1239, 01–06.

Jayasinghe, S.N., Suter, N., 2006. Aerodynamically assisted jetting: a pressure driven approach for processing nanomaterials. Micro Nano Lett. 1, 35.

Jiménez-Pranteda, M.L., Poncelet, D., Náder-Macías, M.E., Arcos, A., Aguilera, M., Monteoliva-Sánchez, M., Ramos-Cormenzana, A., 2012. Stability of lactobacilli encapsulated in various microbial polymers. J. Biosci. Bioeng. 113, 179–84.

Johansen, L.-H., Eggset, G., Sommer, A.-I., 2009. Experimental IPN virus infection of Atlantic salmon parr; recurrence of IPN and effects on secondary bacterial infections in post-smolts. Aquac. 290, 9-14.

Johansen, L.-H., Sommer, A.-I., 2001. Infectious pancreatic necrosis virus infection in Atlantic salmon *Salmo salar* post-smolts affects the outcome of secondary infections with infectious salmon anaemia virus or *Vibrio salmonicida*. Dis. Aquat. Org. 47, 109-117.

Johansen, R., 2013. Fish Health Report 2012. Oslo.

Joosten, P.H.M., Tiemersma, E., Threels, A., Caumartin-Dhieux, C., Rombout, J.H.W.M., 1997. Oral vaccination of fish against *Vibrio anguillarum* using alginate microparticles. Fish Shellfish Immunol. 7, 471-485.

Joshi, A., Pund, S., Nivsarkar, M., Vasu, K., Shishoo, C., 2008. Dissolution test for site-specific release isoniazid pellets in USP apparatus 3 (reciprocating cylinder): optimization using response surface methodology. Eur. J. Pharm. Biopharm. 69, 769–775.

Jump, R.L., Levine, A.D., 2004. Mechanisms of Natural Tolerance in the Intestine. Inflamm. Bowel Dis. 10, 462–478.

Jung, J.H., Lee, J.E., Kim, S.S., 2009. Generation of nonagglomerated airborne bacteriophage particles using an electrospray technique. Anal. Chem. 81, 2985–2990.

Karwe, M. V, 2003. Food Engineering, in: Barbosa-Conovas, G.V., Juliano, P. (Eds.), Encyclopedia of Life Support Systems. Eolss Publishers Co Ltd., Oxford, UK, 545–563.

Kaushik K., Chaurasia, D., Chaurasia, H., Mishra, S.K., Bhardwaj, P., 2011. Development and characterization of floating alginate beads for Gastroretentive drug delivery system. Acta Pharm. Sci. 53, 551–562.

Kikuchi, A., Kawabuchi, M., Watanabe, A., Sugihara, M., Sakurai, Y., Okano, T., 1999. Effect of Ca2+-alginate gel dissolution on release of dextran with different molecular weights. J. Control. Release 58, 21–28.

Kilara, A., Sharkasi, T.Y., 1986. Effects of temperature on food proteins and its implications on functional properties. Crit. Rev. Food Sci. Nutr. 23, 323–395.

Kim, C., Lee, E., 1992. The controlled release of blue dextran from alginate beads. Int. J. Pharm. 79, 11–19.

Koch, S., Schwinger, C., Kressler, J., Heinzen, C., Rainov, N.G., 2003. Alginate encapsulation of genetically engineered mammalian cells: comparison of production devices, methods and microcapsule characteristics. J. Microencapsul. 20, 303–316.

Kolakovic, R., Viitala, T., Ihalainen, P., Genina, N., Peltonen, J., Sandler, N., 2013. Printing technologies in fabrication of drug delivery systems. Expert Opin. Drug Deliv. 10, 1711–1723.

Kongtorp, R.T., Halse, M., Taksdal, T., Falk, K., 2006. Longitudinal study of a natural outbreak of heart and skeletal muscle inflammation in Atlantic salmon, *Salmo salar L.* J. Fish Dis. 29, 233–244.

Kraugerud, O.F., Jørgensen, H.Y., Svihus, B., 2011. Physical properties of extruded fish feed with inclusion of different plant (legumes, oilseeds, or cereals) meals. Anim. Feed Sci. Technol. 163, 244–254.

Kristoffersen, A.B., Bang Jensen, B., Jansen, P.A., 2013. Risk mapping of heart and skeletal muscle inflammation in salmon farming. Prev. Vet. Med. 109, 136–143.

Krogdahl, A., Bakke-McKellep, A.M., 2005. Fasting and refeeding cause rapid changes in intestinal tissue mass and digestive enzyme capacities of Atlantic salmon (*Salmo salar L.*). Comp. Biochem. Physiol. A. Mol. Integr. Physiol. 141, 450-460.

Krogdahl, Å., Nordrum, S., Sørensen, M., Brudeseth, L., Røsjø, C., 1999. Effects of diet composition on apparent nutrient absorption along the intestinal tract and of subsequent fasting on mucosal disaccharidase activities and plasma nutrient concentration in Atlantic salmon *Salmo salar L.* Aquac. Nutr. 5, 121–133.

Kumari, J., Bogwald, J., Dalmo, R.A., 2009. Transcription factor GATA-3 in Atlantic salmon (*Salmo salar*): Molecular characterization, promoter activity and expression analysis. Mol. Immunol. 46, 3099–3107.

Kumari, J., Bøgwald, J., Dalmo, R.A., 2013. Vaccination of Atlantic salmon, *Salmo salar L.*, with Aeromonas salmonicida and infectious pancreatic necrosis virus (IPNV) showed a mixed Th1/Th2/Treg response. J. Fish Dis. 36, 881–886.

Kytariolos, J., Dokoumetzidis, A., Macheras, P., 2010. Power law IVIVC: an application of fractional kinetics for drug release and absorption. Eur. J. Pharm. Sci. 41, 299–304.

Köksel, H., Ryu, G.-H., Başman, A., Demiralp, H., Ng, P.K.W., 2004. Effects of extrusion variables on the properties of waxy hulless barley extrudates. Nahrung 48, 19–24.

Lauterslager, T.G.., Stok, W., Hilgers, L.A.., 2003. Improvement of the systemic prime/oral boost strategy for systemic and local responses. Vaccine 21, 1391–1399.

Lavelle, E.C., Grant, G., Pusztai, A., Pfuller, U., O'Hagan, D.T., 2000. Mucosal immunogenicity of plant lectins in mice. Immunology 99, 30–37.

Lavelle, E.C., O'Hagan, D.T., 2006. Delivery systems and adjuvants for oral vaccines. Expert Opin. Drug Deliv. 3, 747–62.

Lee, B.-B., Chan, E.-S., Ravindra, P., Khan, T.A., 2012. Surface tension of viscous biopolymer solutions measured using the du Nouy ring method and the drop weight methods. Polym. Bull. 69, 471–489.

Lee, B.-J., Min, G.-H., 1996. Oral controlled release of melatonin using polymer-reinforced and coated alginate beads. Int. J. Pharm. 144, 37–46.

León y León, C.A., 1998. New perspectives in mercury porosimetry. Adv. Colloid Interface Sci. 76-77, 341–372.

Letterio, J.J., Roberts, A.B., 1998. Regulation of immune responses by TGF-beta. Annu. Rev. Immunol. 16, 137–161.

Li, M.O., Flavell, R.A., 2008. TGF-beta: A Master of All T Cell Trades. Cell 134, 392-404.

Lian, M., Collier, C.P., Doktycz, M.J., Retterer, S.T., 2012. Monodisperse alginate microgel formation in a three-dimensional microfluidic droplet generator. Biomicrofluidics 6, 44108.

Lillehaug, A., 1997. Vaccination strategies in seawater cage culture of salmonids. Dev. Biol. Stand. 90, 401–408.

Liu, Y., Olaf Olaussen, J., Skonhoft, A., 2011. Wild and farmed salmon in Norway-A review . Mar. Policy 35, 413-418.

Ljungqvist, M.G., Ersboll, B.K., Kobayashi, K., Nakauchi, S., Frosch, S., Nielsen, M.E., 2012. Near-infrared hyper-spectral image analysis of astaxanthin concentration in fish feed coating, in: 2012 IEEE International Conference on Imaging Systems and Techniques Proceedings. IEEE, 136–141.

Ljungqvist, M.G., Frosch, S., Nielsen, M.E., Ersbøll, B.K., 2013. Multispectral image analysis for robust prediction of astaxanthin coating. Appl. Spectrosc. 67, 738–746.

Lorenzen, N., LaPatra, S.E., 2005. DNA vaccines for aquacultured fish. Rev. Sci. Tech. 24, 201–213.

Lyngstad, T.M., Jansen, P.A., Sindre, H., Jonassen, C.M., Hjortaas, M.J., Johnsen, S., Brun, E., 2008. Epidemiological investigation of infectious salmon anaemia (ISA) outbreaks in Norway 2003-2005. Prev. Vet. Med. 84, 213–227.

Løkka, G., Austbø, L., Falk, K., Bjerkås, I., Koppang, E.O., 2013. Intestinal morphology of the wild Atlantic salmon (*Salmo salar*). J. Morphol. 274, 859–876.

Løkka, G., Austbø, L., Falk, K., Bromage, E., Fjelldal, P.G., Hansen, T., Hordvik, I., Koppang, E.O., 2014a. Immune parameters in the intestine of wild and reared unvaccinated and vaccinated Atlantic salmon (*Salmo salar L.*). Dev. Comp. Immunol. 47, 6–16.

Løkka, G., Falk, K., Austbø, L., Koppang, E.O., 2014b. Uptake of yeast cells in the Atlantic salmon (*Salmo salar L.*) intestine. Dev. Comp. Immunol. 47, 77–80.

MacKelvie, R.M., Desautels, D., 1975. Fish Viruses — Survival and Inactivation of Infectious Pancreatic Necrosis Virus. J. Fish. Res. Board Canada 32, 1267–1273.

Makki, F., 2002. Extrusion Cooking: Technologies and Applications. Food Res. Int. 35, 897–898.

Marrella, V., Lo Iacono, N., Fontana, E., Sobacchi, C., Sic, H., Schena, F., Sereni, L., Castiello, M.C., Poliani, P.L., Vezzoni, P., Cassani, B., Traggiai, E., Villa, A., 2015. IL-10 Critically Modulates B Cell Responsiveness in Rankl-/- Mice. J. Immunol. 194, 4144-4153.

Martinez, L., Agnely, F., Bettini, R., Besnard, M., Colombo, P., Couarraze, G., 2004. Preparation and characterization of chitosan based micro networks: Transposition to a prilling process. J. Appl. Polym. Sci. 93, 2550–2558.

Martinez-Rubio, L., Morais, S., Evensen, Ø., Wadsworth, S., Ruohonen, K., Vecino, J.L.G., Bell, J.G., Tocher, D.R., 2012. Functional feeds reduce heart inflammation and pathology in Atlantic salmon (*Salmo salar L.*) following experimental challenge with Atlantic salmon reovirus (ASRV). PLoS One 7, 40266.

Maurice, S., Nussinovitch, A., Jaffe, N., Shoseyov, O., Gertler, A., 2004. Oral immunization of *Carassius auratus* with modified recombinant A-layer proteins entrapped in alginate beads. Vaccine 23, 450–459.

McHugh, D.J., Fisheries, F.A.O., Paper, T., 2003. A guide to the seaweed industry, in: FAO Fisheries Technical Paper. FAO of the United Nations, Rome, 27–37.

McKenzie, G.J., Bancroft, A., Grencis, R.K., McKenzie, A.N., 1998. A distinct role for interleukin-13 in Th2-cell-mediated immune responses. Curr. Biol. 8, 339–342.

Min, L., Li-Li, Z., Jun-Wei, G., Xin-Yuan, Q., Yi-Jing, L., Di-Qiu, L., 2012. Immunogenicity of Lactobacillus-expressing VP2 and VP3 of the infectious pancreatic necrosis virus (IPNV) in rainbow trout. Fish Shellfish Immunol. 32, 196–203.

Minghou, J., Yujun, W., Zuhong, X., Yucai, G., 1984. Studies on the M:G ratios in alginate. Hydrobiologia 116-117, 554–556.

Moen, T., Baranski, M., Sonesson, A.K., Kjøglum, S., 2009. Confirmation and fine-mapping of a major QTL for resistance to infectious pancreatic

necrosis in Atlantic salmon (*Salmo salar*): population-level associations between markers and trait. BMC Genomics 10, 368.

Moher, D., 1994. Statistical Power, Sample Size, and Their Reporting in Randomized Controlled Trials. JAMA J. Am. Med. Assoc. 272, 122.

Moore, J.W., Flanner, H.H., 1996. Mathematical comparison of dissolution profiles. Pharm. Technol. 20, 64–74.

Morken, T., Kragerud, O.F., Sørensen, M., Storbakken, T., Hillestad, M., Christiansen, R., Øverland, M., 2012. Effects of feed processing conditions and acid salts on nutrient digestibility and physical quality of soy-based diets for Atlantic salmon (*Salmo salar*). Aquac. Nutr. 18, 21–34.

Mortensen, S.H., Nilsen, R.K., Hjeltnes, B., 1998. Stability of an infectious pancreatic necrosis virus (IPNV) isolate stored under different laboratory conditions. Dis. Aquat. Organ. 33, 67–71.

Moyer, H.R., Kinney, R.C., Singh, K.A., Williams, J.K., Schwartz, Z., Boyan, B.D., 2010. Alginate microencapsulation technology for the percutaneous delivery of adipose-derived stem cells. Ann. Plast. Surg. 65, 497–503.

Mukhopadhyay, N., Sarkar, S., Bandyopadhyay, S., 2007. Effect of extrusion cooking on anti-nutritional factor tannin in linseed (*Linum usitatissimum*) meal. Int. J. Food Sci. Nutr. 58, 588–594.

Munang'andu, H.M., Fredriksen, B.N., Mutoloki, S., Brudeseth, B., Kuo, T.-Y., Marjara, I.S., Dalmo, R.A., Evensen, Ø., 2012. Comparison of vaccine efficacy for different antigen delivery systems for infectious pancreatic necrosis virus vaccines in Atlantic salmon (*Salmo salar L.*) in a cohabitation challenge model. Vaccine 30, 4007–4016.

Munang'Andu, H.M., Fredriksen, B.N., Mutoloki, S., Dalmo, R.A., Evensen, Ø., 2013. Antigen dose and humoral immune response correspond with protection for inactivated infectious pancreatic necrosis virus vaccines in Atlantic salmon (*Salmo salar L*). Vet. Res. 44, 7.

Munang'andu, H.M., Mutoloki, S., Evensen, Ø., 2014. Acquired immunity and vaccination against infectious pancreatic necrosis virus of salmon. Dev. Comp. Immunol. 43, 184–196.

Mutwiri, G., Bowersock, T., Kidane, A., Sanchez, M., Gerdts, V., Babiuk, L.A., Griebel, P., 2002. Induction of mucosal immune responses following enteric immunization with antigen delivered in alginate microspheres, in: Veterinary Immunology and Immunopathology 87. 269–276.

Möbs, C., Slotosch, C., Löffler, H., Pfützner, W., Hertl, M., 2008. Cellular and humoral mechanisms of immune tolerance in immediate-type allergy

induced by specific immunotherapy. Int. Arch. Allergy Immunol. 147, 171-178.

National Research Council, 2011. Digestive physiology of fish and shrimp, in: Whitacre, P.T. (Ed.), Nutrient Requirements of Fish and Shrimp. The National Academies Press, Washington DC, p. 22.

Nesamony, J., Singh, P.R., Nada, S.E., Shah, Z.A., Kolling, W.M., 2012. Calcium alginate nanoparticles synthesized through a novel interfacial cross-linking method as a potential protein drug delivery system. J. Pharm. Sci. 101, 2177–2184.

Nichols, W.W., Ledwith, B.J., Manam, S. V, Troilo, P.J., 1995. Potential DNA vaccine integration into host cell genome. Ann. N. Y. Acad. Sci. 772, 30–39.

Nimmo, J., 2004. Porosity and pore size distribution. Encycl. Soils Environ. 3, 295–303.

Noyes, A.A., Whitney, W.R., 1897. The rate or solution of solid substances in their own solutions. J. Am. Chem. Soc. 19, 930–934.

Oberyukhtina, I., Bogolitsyn, K., Popova, N., 2001. Physicochemical properties of solutions of sodium alginate extracted from brown algae *Laminaria digitata*. Russ. J. Appl. 74, 1645–1649.

Oke, M.O., Awonorin, S.O., Sanni, L.O., Asiedu, R., Aiyedun, P.O., 2012. Effect of extrusion variables on extrudates propeties of water yam flour - a response surface analysis. J. Food Process. Preserv. 37, 456-473.

Olmos, J., Ochoa, L., Paniagua-Michel, J., Contreras, R., 2011. Functional feed assessment on Litopenaeus vannamei using 100% fish meal replacement by soybean meal, high levels of complex carbohydrates and Bacillus probiotic strains. Mar. Drugs 9, 1119–32.

Owen, R.D., 1945. Immunogenetic Consequences of Vascular Anastomoses between Bovine Twins. Science 102, 400–401.

P. Rigby, S., S. Fletcher, R., N. Riley, S., 2004. Characterisation of porous solids using integrated nitrogen sorption and mercury porosimetry. Chem. Eng. Sci. 59, 41–51.

Pabst, O., Mowat, A.M., 2012. Oral tolerance to food protein. Mucosal Immunol. 5, 232–239.

Paine, M.D., Alexander, M.S., Stark, J.P.W., 2007. Nozzle and liquid effects on the spray modes in nanoelectrospray. J. Colloid Interface Sci. 305, 111–123.

Palacios, G., Lovoll, M., Tengs, T., Hornig, M., Hutchison, S., Hui, J., Kongtorp, R.-T., Savji, N., Bussetti, A. V, Solovyov, A., Kristoffersen, A.B., Celone, C., Street, C., Trifonov, V., Hirschberg, D.L., Rabadan, R., Egholm, M., Rimstad, E., Lipkin, W.I., 2010. Heart and Skeletal Muscle Inflammation of Farmed Salmon Is Associated with Infection with a Novel Reovirus. PLoS One 5, 11487.

Pandey, G., 2013. Feed Formulation and Feeding Technology for Fishes. Int. Res. J. Pharm. 4, 23–30.

Paques, J.P., van der Linden, E., van Rijn, C.J.M., Sagis, L.M.C., 2013. Alginate submicron beads prepared through w/o emulsification and gelation with CaCl2 nanoparticles. Food Hydrocoll. 31, 428–434.

Park, H., Kim, P.-H., Hwang, T., Kwon, O.-J., Park, T.-J., Choi, S.-W., Yun, C.-O., Kim, J.H., 2012. Fabrication of cross-linked alginate beads using electrospraying for adenovirus delivery. Int. J. Pharm. 427, 417–425.

Pathak, T.S., Yun, J.-H., Lee, J., Paeng, K.-J., 2010. Effect of calcium ion (cross-linker) concentration on porosity, surface morphology and thermal behavior of calcium alginates prepared from algae (*Undaria pinnatifida*). Carbohydr. Polym. 81, 633–639.

Pavesi, A., 2014. Prediction of the determinants of thermal stability by linear discriminant analysis: The case of the glutamate dehydrogenase protein family. J. Theor. Biol. 357, 160-168.

Pedersen, T., 2007. VP3, a structural protein of infectious pancreatic necrosis virus, interacts with RNA-dependent RNA polymerase VP1 and with double-stranded RNA. J. Virol. 81, 6652.

Petrie, A.G., Ellis, A.E., 2006. Evidence of particulate uptake by the gut of Atlantic salmon (*Salmo salar L.*). Fish Shellfish Immunol. 20, 660–664.

Pinto Reis, C., Silva, C., Martinho, N., Rosado, C., 2013. Drug carriers for oral delivery of peptides and proteins: accomplishments and future perspectives. Ther. Deliv. 4, 251–265.

Pipa, F., Frank, G., 1989. High-pressure conditioning with annular gap expander, in: A New Way of Feed Processing: Advances in Feed Technology. Verlag Moritz Schäfer, Detmold, 22–30.

Plant, K.P., Lapatra, S.E., 2011. Advances in fish vaccine delivery. Dev. Comp. Immunol. 35, 1256–1262.

Polk, A., Amsden, B., De Yao, K., Peng, T., Goosen, M.F.A., 1994. Controlled release of albumin from chitosan—alginate microcapsules. J. Pharm. Sci. 83, 178–185.

Privalle, L., Bannon, G., Herman, R., Ladics, G., McClain, S., Stagg, N., Ward, J., Herouet-Guicheney, C., 2011. Heat stability, its measurement, and its lack of utility in the assessment of the potential allergenicity of novel proteins. Regul. Toxicol. Pharmacol. 61, 292–295.

Prodduturi, S., Smith, G.J., Wokovich, A.M., Doub, W.H., Westenberger, B.J., Buhse, L., 2009. Reservoir based fentanyl transdermal drug delivery systems: effect of patch age on drug release and skin permeation. Pharm. Res. 26, 1344–1352.

Pugh, H.L.D., Watkins, M.T., 1961. Experimental investigation of the extrusion of metals. Prod. Eng. 40, 256 – 282.

Quantachrome Instruments, 2009. PoreMaster GT Operating Manual. Quantachrome Corporation, Boynton Beach (USA), 118–140.

Quentel, C., Vigneulle, M., 1997. Antigen uptake and immune responses after oral vaccination. Dev. Biol. Stand. 90, 69–78.

Quong, D., Neufeld, R.J., Skjåk-Braek, G., Poncelet, D., 1998. External versus internal source of calcium during the gelation of alginate beads for DNA encapsulation. Biotechnol. Bioeng. 57, 438–446.

R Development Core Team, 2012. R: A Language and Environment for Statistical Computing.

Ramstad, A., Romstad, A.B., Knappskog, D.H., Midtlyng, P.J., 2007. Field validation of experimental challenge models for IPN vaccines. J. Fish Dis. 30, 723-731.

Rayleigh, Lord, 1882. XX. On the equilibrium of liquid conducting masses charged with electricity. Philos. Mag. Ser. 5 14, 184–186.

Ribeiro, C.C., Barrias, C.C., Barbosa, M.A., 2004. Calcium phosphate-alginate microspheres as enzyme delivery matrices. Biomater. 25, 4363–4373.

Roberts, R.J., Pearson, M.D., 2005. Infectious pancreatic necrosis in Atlantic salmon, *Salmo salar L*. J. Fish Dis. 28, 383–390.

Robertsen, B., 2011. Can we get the upper hand on viral diseases in aquaculture of Atlantic salmon? Aquac. Res. 42, 125–131.

Rodger, H., Mitchell, S., 2007. Epidemiological observations of pancreas disease of farmed Atlantic salmon, *Salmo salar L*., in Ireland. J. Fish Dis. 30, 157–167.

Rodrguez Saint-Jean, S., de las Heras, A.I., Prez Prieto, S.I., 2010. The persistence of infectious pancreatic necrosis virus and its influence on the early immune response. Vet. Immunol. Immunopathol. 136, 81-91.

Rodríguez-Rivero, C., Del Valle, E.M.M., Galán, M.A., 2011. Development of a new technique to generate microcapsules from the breakup of non-Newtonian highly viscous fluid jets. AIChE J. 57, 3436–3447.

Romagnani, S., 2000. T-cell subsets (Th1 versus Th2). Ann. Allergy. Asthma Immunol. 85, 9–18.

Romalde, J.L.J.L., Luzardo-Alvárez, A., Ravelo, C., Toranzo, A.E., Blanco-Méndez, J., Luzardo-Alvarez, A., Ravelo, C., Toranzo, A.E., Blanco-Mendez, J., 2004. Oral immunization using alginate microparticles as a useful strategy for booster vaccination against fish lactoccocosis. Aquaculture 236, 119–129.

Romarheim, O.H., Aslaksen, M.A., Storebakken, T., Krogdahl, A., Skrede, A., 2005. Effect of extrusion on trypsin inhibitor activity and nutrient digestibility of diets based on fish meal, soybean meal and white flakes. Arch. Anim. Nutr. 59, 365–375.

Rombout, J.H.W.M., Abelli, L., Picchietti, S., Scapigliati, G., Kiron, V., 2011. Teleost intestinal immunology. Fish Shellfish Immunol. 31, 616–626.

Rosenmayr-Templeton, L., 2013. The oral delivery of peptides and proteins: established versus recently patented approaches. Pharm. Pat. Anal. 2, 125–145.

Rote, N.S., 2007. Adaptive Immunity, in: McCance, K.L., Huether, S.E. (Eds.), Understanding Pathophysiology. Elsevier - Health Sciences Division, 143–165.

Sahoo, S., Lee, W.C., Goh, J.C.H., Toh, S.L., 2010. Bio-electrospraying: A potentially safe technique for delivering progenitor cells. Biotechnol. Bioeng. 106, 690–698.

Sahu, K.S., Prusty, K.A., 2010. Design and evaluation of a nanoparticulate system prepared by biodegradable polymers for oral administration of protein drugs. Pharmazie 65, 824.

Sakaguchi, S., Yamaguchi, T., Nomura, T., Ono, M., 2008. Regulatory T Cells and Immune Tolerance. Cell 133, 775-787.

Salomonsen, T., Jensen, H.M., Larsen, F.H., Steuernagel, S., Engelsen, S.B., 2009. Direct quantification of M/G ratio from (13)C CP-MAS NMR spectra of alginate powders by multivariate curve resolution. Carbohydr. Res. 344, 2014–2022.

Salvador, A., Igartua, M., Hernández, R.M., Pedraz, J.L., 2012. Combination of immune stimulating adjuvants with poly(lactide-co-glycolide) microspheres enhances the immune response of vaccines. Vaccine 30, 589–596.

Samuelsen, T.A., Mjøs, S.A., Oterhals, Å., 2014. Influence of type of raw material on fishmeal physicochemical properties, the extrusion process, starch gelatinization and physical quality of fish feed. Aquac. Nutr. 20, 410-420.

Santos, Y., García-Marquez, S., Pereira, P.G., Pazos, F., Riaza, A., Silva, R., El Morabit, A., Ubeira, F.M., 2005. Efficacy of furunculosis vaccines in turbot, Scophthalmus maximus (L.): evaluation of immersion, oral and injection delivery. J. Fish Dis. 28, 165–172.

Sarei, F., Dounighi, N.M., Zolfagharian, H., Khaki, P., Bidhendi, S.M., 2013. Alginate nanoparticles as a promising adjuvant and vaccine delivery system. Indian J. Pharm. Sci. 75, 442–9.

Schoeff, W.R., 1994. History of the formula feed industry, in: McEllhiney, R.R. (Ed.), Feed Manufacturing Technology IV. American Feed Industry Association Inc., Arlington, 2–11.

Schwartz, C., Eberle, J.U., Voehringer, D., 2015. Basophils in inflammation. Eur. J. Pharmacol. In Press.

Semyonov, D., Ramon, O., Kaplun, Z., Levin-Brener, L., Gurevich, N., Shimoni, E., 2010. Microencapsulation of Lactobacillus paracasei by spray freeze drying. Food Res. Int. 43, 193–202.

Shah, V.P., Tsong, Y., Sathe, P., Liu, J.P., 1998. *In vitro* dissolution profile comparison--statistics and analysis of the similarity factor, f2. Pharm. Res. 15, 889–896.

Shaji, J., Patole, V., 2008. Protein and Peptide drug delivery: oral approaches. Indian J. Pharm. Sci. 70, 269–277.

Shi, J., Zhang, Z., Li, G., Cao, S., 2011. Biomimetic fabrication of alginate/CaCO3 hybrid beads for dual-responsive drug delivery under compressed CO2. J. Mater. Chem. 21, 16028.

Shinde, U., Nagarsenker, M., 2011. Microencapsulation of eugenol by gelatin-sodium alginate complex coacervation. Indian J. Pharm. Sci. 73, 311–5.

Siewert, C., Lauer, U., Cording, S., Bopp, T., Schmitt, E., Hamann, A., Huehn, J., 2008. Experience-driven development: effector/memory-like alphaE+Foxp3+ regulatory T cells originate from both naive T cells and naturally occurring naive-like regulatory T cells. J. Immunol. 180, 146–155.

Sigler, J.W., Sigler, W.F., 1986. History of fish hatchery development in the Great Basin states of Utah and Nevada. West. north Am. Nat. 46, 583–594.

Silva, C.M., Ribeiro, A.J., Figueiredo, I.V., Gonçalves, A.R., Veiga, F., 2006. Alginate microspheres prepared by internal gelation: development and effect on insulin stability. Int. J. Pharm. 311, 1–10.

Singh, M., O'Hagan, D., 1998. The preparation and characterization of polymeric antigen delivery systems for oral administration. Adv. Drug Deliv. Rev. 34, 285–304.

Singh, S., Gamlath, S., Wakeling, L., 2007. Nutritional aspects of food extrusion: a review. Int. J. Food Sci. Technol. 42, 916-929.

Sjolander, A., 1998. Uptake and adjuvant activity of orally delivered saponin and ISCOM? vaccines. Adv. Drug Deliv. Rev. 34, 321–338.

Skjelstad, B., FHL, VESO, 2003. IPN in salmonids : a review. FHL, Fiskeri- og havbruksnæringens landsforening, Trondheim, Norway.

Skjesol, A., Skjæveland, I., Elnæs, M., Timmerhaus, G., Fredriksen, B.N., Jørgensen, S.M., Krasnov, A., Jørgensen, J.B., 2011. IPNV with high and low virulence: host immune responses and viral mutations during infection. Virol. J. 8, 396.

Skugor, S., Glover, K.A., Nilsen, F., Krasnov, A., 2008. Local and systemic gene expression responses of Atlantic salmon (*Salmo salar L*.) to infection with the salmon louse (*Lepeophtheirus salmonis*). BMC Genomics 9, 498.

Smail, D.A., McFarlane, L., Bruno, D.W., McVicar, A.H., 1995. The pathology of an IPN-Sp sub-type (Sh) in farmed Atlantic salmon, *Salmo solar L.*, post-smolts in the Shetland Isles, Scotland. J. Fish Dis. 18, 631–638.

Smidsrød, O., Glover, R.M., Whittington, S.G., 1973. The relative extension of alginates having different chemical composition. Carbohydr. Res. 27, 107–118.

Smith, H.A., Klinman, D.M., 2001. The regulation of DNA vaccines. Curr. Opin. Biotechnol. 12, 299–303.

Sommerset, I., Krossøy, B., Biering, E., Frost, P., 2005. Vaccines for fish in aquaculture . Expert Rev. Vaccines 4, 89–101.

Song, H., Yu, W., Gao, M., Liu, X., Ma, X., 2013. Microencapsulated probiotics using emulsification technique coupled with internal or external gelation process. Carbohydr. Polym. 96, 181–189.

Song, H., Yu, W., Meng, G., Liu, X., Ma, X., 2005. Molecular determinants of infectious pancreatic necrosis virus virulence and cell culture adaptation. J. Virol. 79, 10289–10299.

Sonmez, M., Sonmez, B., Eren, N., Yilmaz, M., Karti, S.S., Ovali, E., 2004. Effects of interferon-alpha-2a on Th3 cytokine response in multiple myeloma patients. Tumori 90, 387–389.

Sperger, D.M., Fu, S., Block, L.H., Munson, E.J., 2011. Analysis of composition, molecular weight, and water content variations in sodium alginate using solid-state NMR spectroscopy. J. Pharm. Sci. 100, 3441–3452.

Stanford, E.C.C., 1886. Manufacture of useful products from seaweed. US Patent 341,072.

Storebakken, T., 1985. Binders in fish feeds. Aquaculture 47, 11–26.

Strober, W., Kelsall, B., Fuss, I., Marth, T., Ludviksson, B., Ehrhardt, R., Neurath, M., 1997. Reciprocal IFN-gamma and TGF-beta responses regulate the occurrence of mucosal inflammation. Immunol. Today 18, 61–64.

Sugiura, S., Oda, T., Izumida, Y., Aoyagi, Y., Satake, M., Ochiai, A., Ohkohchi, N., Nakajima, M., 2005. Size control of calcium alginate beads containing living cells using micro-nozzle array. Biomater. 26, 3327-3331.

Suksamran, T., Opanasopit, P., Rojanarata, T., Ngawhirunpat, T., Ruktanonchai, U., Supaphol, P., 2009. Biodegradable alginate microparticles developed by electrohydrodynamic spraying techniques for oral delivery of protein. J. Microencapsul. 26, 563–570.

Tacchi, L., Bickerdike, R., Douglas, A., Secombes, C.J., Martin, S.A.M., 2011. Transcriptomic responses to functional feeds in Atlantic salmon (*Salmo salar*). Fish Shellfish Immunol. 31, 704–715.

Tec, S., Morita, H., 2015. IL-10 – overexpressing B cells regulate innate and adaptive immune responses. J. Allergy Clin. Immunol. 135, 771–780.

Thamotharan, M., Gomme, J., Zonno, V., Maffia, M., Storelli, C., Ahearn, G.A., 1996. Electrogenic, proton-coupled, intestinal dipeptide transport in herbivorous and carnivorous teleosts. Am. J. Physiol. 270, 939–947.

Thinh, N.H., Kuo, T.Y., Hung, L.T., Loc, T.H., Chen, S.C., Evensen, O., Schuurman, H.J., 2009. Combined immersion and oral vaccination of Vietnamese catfish (*Pangasianodon hypophthalmus*) confers protection against mortality caused by *Edwardsiella ictaluri*. Fish Shellfish Immunol. 27, 773–776.

Thorud, K., Brun, E., Lillehaug, A., Almklov, M., Romstad, S., Binde, M., 2007. A new system for monitoring health status in Norwegian aquaculture. Dev. Biol. (Basel).129, 65–69.

Tian, J.-Y., Sun, X.-Q., Chen, X.-G., 2008. Formation and oral administration of alginate microspheres loaded with pDNA coding for lymphocystis disease virus (LCDV) to Japanese flounder. Fish Shellfish Immunol. 24, 592–599.

Tilseth, S., Hansen, T., Møller, D., 1991. Historical development of salmon culture. Aquaculture 98, 1–9.

Tobar, J.A., Jerez, S., Caruffo, M., Bravo, C., Contreras, F., Bucarey, S.A., Harel, M., 2011. Oral vaccination of Atlantic salmon (*Salmo salar*) against salmonid rickettsial septicaemia. Vaccine 29, 2336–40.

Toennessen, R., Lauscher, A., Rimstad, E., 2010. Comparative aspects of infectious salmon anemia virus, an orthomyxovirus of fish, to influenza viruses. Indian J. Microbiol. 49, 308-314.

Tonheim, T.C., Bøgwald, J., Dalmo, R.A., 2008. What happens to the DNA vaccine in fish? A review of current knowledge. Fish Shellfish Immunol. 25, 1–18.

Trifunović, J., Miller, L., Debeljak, Ž., Horvat, V., 2015. Pathologic patterns of interleukin 10 expression – A review. Biochem. Medica 36–48.

Tu, K.C., Spendlove, R.S., Goede, R.W., 1975. Effect of temperature on survival and growth of infectious pancreatic necrosis virus. Infect. Immun. 11, 1409–1412.

Tumuluru, J.S., 2014. Effect of process variables on the density and durability of the pellets made from high moisture corn stover. Biosyst. Eng. 119, 44–57.

Urabe, Y., Shiomi, T., Itoh, T., Kawai, A., Tsunoda, T., Mizukami, F., Sakaguchi, K., 2007. Encapsulation of hemoglobin in mesoporous silica (FSM)-enhanced thermal stability and resistance to denaturants. Chembiochem 8, 668–674.

Urban, J.F., Noben-Trauth, N., Donaldson, D.D., Madden, K.B., Morris, S.C., Collins, M., Finkelman, F.D., 1998. IL-13, IL-4Rα, and Stat6 are required for the expulsion of the gastrointestinal nematode parasite *Nippostrongylus brasiliensis*. Immunity 8, 255–264.

USP, 2012a. <711> Dissolution, in: U. S. Pharmacopoeia National Formulary: USP36 NF31. United States Pharmacopeial.

USP, 2012b. <725> Topical and transdermal drug products – Product performance test, in: U. S. Pharmacopoeia National Formulary: USP36 NF31. United States Pharmacopeial.

USP, 2012c. <1092> The dissolution procedure: development and validation, in: U. S. Pharmacopoeia National Formulary: USP36 NF31. United States Pharmacopeial.

USP, 2012d. <1088> *In vitro* and *in vivo* evaluation of dosage forms, in: U. S. Pharmacopoeia National Formulary: USP36 NF31. United States Pharmacopeial.

Valle, A.Z.D., Iriti, M., Faoro, F., Berti, C., Ciappellano, S., Dalla Valle, A.Z., Iriti, M., Faoro, F., Berti, C., Ciappellano, S., 2008. *In vivo* prion protein intestinal uptake in fish. APMIS 116, 173–180.

Van Buskirk, G.A., Asotra, S., Balducci, C., Basu, P., DiDonato, G., Dorantes, A., Eickhoff, W.M., Ghosh, T., González, M.A., Henry, T., Howard, M., Kamm, J., Laurenz, S., MacKenzie, R., Mannion, R., Noonan, P.K., Ocheltree, T., Pai, U., Poska, R.P., Putnam, M.L., Raghavan, R.R., Ruegger, C., Sánchez, E., Shah, V.P., Shao, Z.J., Somma, R., Tammara, V., Thombre, A.G., Thompson, B., Timko, R.J., Upadrashta, S., Vaithiyalingam, S., 2014. Best practices for the development, scale-up, and post-approval change control of IR and MR dosage forms in the current quality-by-design paradigm. AAPS PharmSciTech 15, 665–693.

Van der Lubben, I.M., van Opdorp, F.A.C., Hengeveld, M.R., Onderwater, J.J.M., Koerten, H.K., Verhoef, J.C., Borchard, G., Junginger, H.E., 2002. Transport of chitosan microparticles for mucosal vaccine delivery in a human intestinal M-cell model. J. Drug Target. 10, 449–456.

Vandenberg, G.W., 2007. Oral vaccines for finfish: academic theory or commercial reality? Anim. Heal. Res. Rev. 5, 301–304.

Veis, A., 2011. A review of the early development of the thermodynamics of the complex coacervation phase separation. Adv. Colloid Interface Sci. 167, 2–11.

Vemmer, M., Patel, A. V, 2013. Review of encapsulation methods suitable for microbial biological control agents. Biol. Control 67, 380–389.

Villumsen, K.R., Neumann, L., Ohtani, M., Strøm, H.K., Raida, M.K., 2014. Oral and anal vaccination confers full protection against enteric redmouth disease (ERM) in rainbow trout. PLoS One 9, 93845.

Volkoff, H., 2010. Influence of intrinsic signals and environmental cues on the endocrine control of feeding in fish: potential application in aquaculture. Gen. Comp. Endocrinol. 167, 352.

Wan, Y.Y., Flavell, R.A., 2008. TGF-beta and regulatory T cell in immunity and autoimmunity. J. Clin. Immunol. 28, 647–659.

Wang, R.-L., Bencic, D.C., Garcia-Reyero, N., Perkins, E.J., Villeneuve, D.L., Ankley, G.T., Biales, A.D., 2014. Natural Variation in Fish Transcriptomes: Comparative Analysis of the Fathead Minnow (Pimephales promelas) and Zebrafish (Danio rerio). PLoS One 9, 114178.

Wang, T., Husain, M., 2014. The expanding repertoire of the IL-12 cytokine family in teleost fish: Identification of three paralogues each of the p35 and p40 genes in salmonids, and comparative analysis of their expression and modulation in Atlantic salmon *Salmo salar*. Dev. Comp. Immunol. 46, 194–207.

Watthanaphanit, A., Saito, N., 2013. Effect of polymer concentration on the depolymerization of sodium alginate by the solution plasma process. Polym. Degrad. Stab. 98, 1072–1080.

Wee, S.F., Gombotz, W.R.W., Wee, S.F., 2012. Protein release from alginate matrices. Adv. Drug Deliv. Rev. 31, 267–285.

Weiner, H.L., 2001. Oral tolerance: Immune mechanisms and the generation of Th3-type TGF-beta-secreting regulatory cells. Microbes Infect. 3, 947-954.

Weiner, H.L., da Cunha, A.P., Quintana, F., Wu, H., 2011. Oral tolerance. Immunol. Rev. 241, 241–259.

Whitmire, J.K., 2014. Editorial: Not all roads to T cell memory go through STAT4 and T-bet. J. Leukoc. Biol. 95, 699–701.

Wilson, C.B., Rowell, E., Sekimata, M., 2009. Epigenetic control of T-helper-cell differentiation. Nat. Rev. Immunol. 9, 91–105.

Xu, T., Kincaid, H., Atala, A., Yoo, J.J., 2008. High-Throughput Production of Single-Cell Microparticles Using an Inkjet Printing Technology. J. Manuf. Sci. Eng. 130, 021017.

Yu, C.-Y., Zhang, X.-C., Zhou, F.-Z., Zhang, X.-Z., Cheng, S.-X., Zhuo, R.-X., 2008. Sustained release of antineoplastic drugs from chitosan-reinforced alginate microparticle drug delivery systems. Int. J. Pharm. 357, 15–21.

Yuksel, N., Kanık, A., Baykara, T., 2000. Comparison of *in vitro* dissolution profiles by ANOVA-based, model-dependent and-independent methods. Int. J. Pharm. 209, 57–67.

Zahirul, M., Khan, I., 1996. Dissolution testing for sustained or controlled release oral dosage forms and correlation with *in vivo* data: Challenges and opportunities. Int. J. Pharm. 140, 131-143.

Zhang, Z.-H., Wu, H.-Z., Xiao, J.-F., Wang, Q.-Y., Liu, Q., Zhang, Y.-X., 2014. Booster vaccination with live attenuated *Vibrio anguillarum* elicits

strong protection despite weak specific antibody response in zebrafish. J. Appl. Ichthyol. 30, 117–120.

Zhou, M.X., Shoudt, D., Calderon, G., Feng, M., 2007. Application of USP Apparatus 7 to *in vitro* Drug Release in Scopolamine Transdermal Systems. Dissolution Technol. 14, 25–30.

Zimonja, O., Svihus, B., 2009. Effects of processing of wheat or oats starch on physical pellet quality and nutritional value for broilers. Anim. Feed Sci. Technol. 149, 287–297.

Zouali, M., 2014. Immunological Tolerance: Mechanisms, in: eLS. John Wiley & Sons, Ltd, Chichester, UK, 1–13.